# The remaining capacity of the timber foundation of a historical quay wall with relieving platform

## A case study of the Maaskade

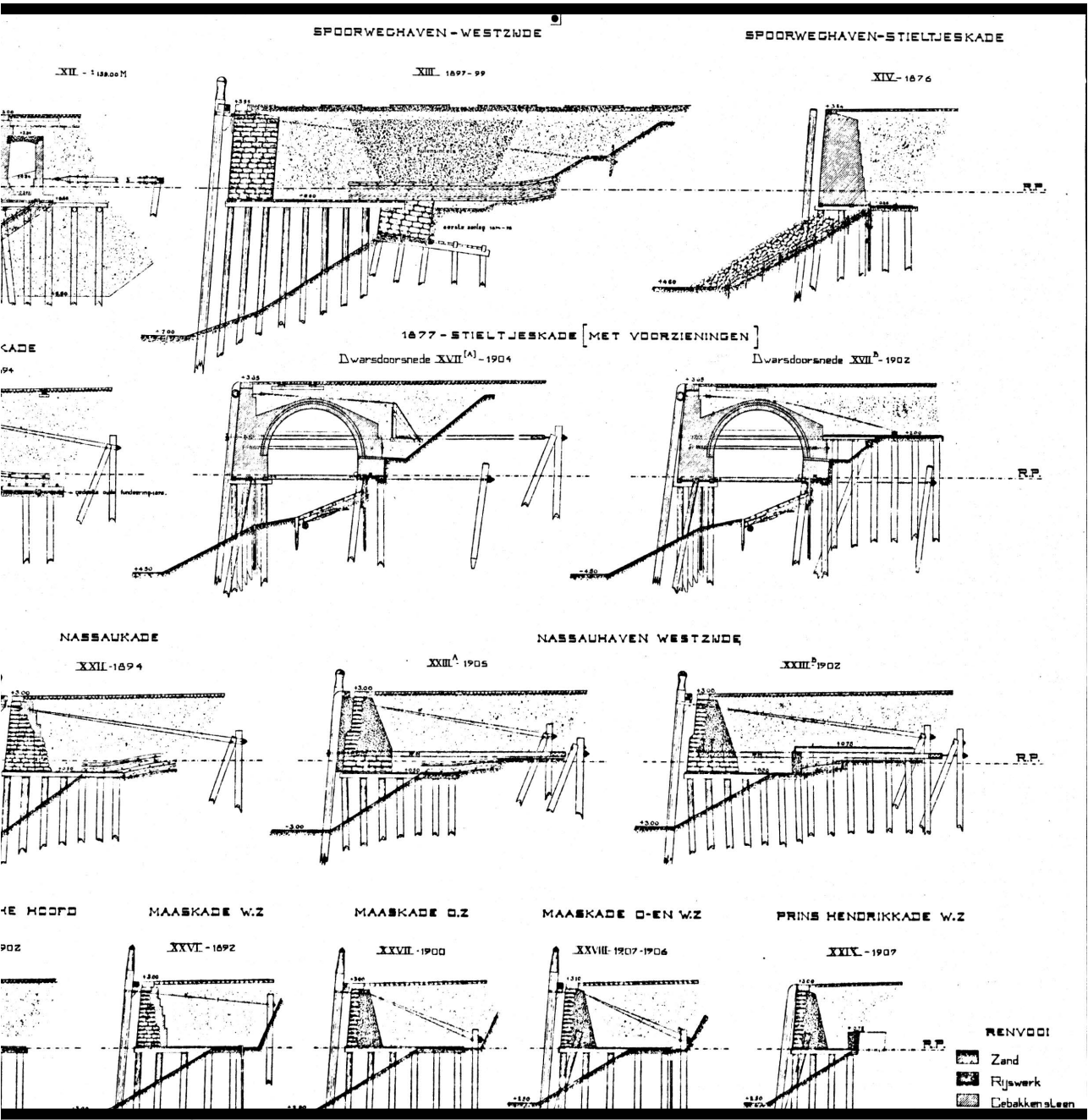


TU Delft Delft University of Technology

Master of Science Thesis M.P. Schilder

# THE REMAINING CAPACITY OF THE TIMBER FOUNDATION OF A HISTORICAL QUAY WALL WITH RELIEVING PLATFORM

A CASE STUDY OF THE MAASKADE

**Master Thesis**

in partial fulfilment of the requirements for the degree of
**Master of Science**
in Civil Engineering: Building Engineering - Structural Design
at the Delft University of Technology
to be defended publicly online on Monday September 7, 2020 at 15:00

by

**Mark Petrus SCHILDER**

Composition thesis committee:

| | |
|---|---|
| Prof. dr. ir. J.W.G. van de Kuilen, | TU Delft (chair) |
| Dr. ir. G.J.P. Ravenshorst, | TU Delft |
| Drs. W.F. Gard, | TU Delft |
| Dr. ir. M. Korff, | TU Delft |
| Dr. ir. H.R. Schipper, | TU Delft |


*Front & Back:* Overview of quays on the southern Nieuwe Maas riverbank. Unknown author, retreived from the Rotterdam city archives.

An electronic version of this dissertation is available at
http://repository.tudelft.nl/.

# CONTENTS

# SUMMARY

The increased loading and decreasing strength of historical quay walls calls for remedy and has drawn the attention of many Dutch municipalities, Rotterdam being one of those. In order to set up proper assessment methods that result in an economical and ecological policy for renovation or replacement of these structures the Port of Rotterdam has asked Delft University of Technology to assist them. This thesis focusses on the elements perhaps most prone to decay and hardest to inspect: the timber foundations implemented in quay walls with relieving platforms from the late $19^{th}$ and early $20^{th}$ century. The main research question of this thesis is *What is the (remaining) capacity of the timber foundation of a quay wall with relieving platform?* and focusses on the Maaskade case. The aim is the provision of a structural analysis and appointment of weakspots on a representative quay section build-up using measured material characteristics. This quay has partially collapsed and has been replaced as of May 2020. 45 Timber piles from the site have been investigated in the Rotterdam harbour to derive density and (dynamic) Young's modulus measured by a Timber Grader MTG. A selection of these piles was then further tested in pieces (21) at the TU Delft structural laboratory (Stevin II) to derive the Young's modulus and compressive strength. Using the correlation found between the compressive strength parallel to the fibre ($f_{c,0}$) and the dynamic Young's modulus parallel to the fibre ($E_0$) the compressive strength values of the entire 45 pile group have been derived. This results in $f_{c,0,k}$ = 12.64 MPa and $E_{0,mean}$ = 11.3 GPa under 50% moisture content, the saturated state the wood is expected to be in in the quay. The resulting design strength $f_{c,0,d}$ = 10.7 MPa is very much in line with the advised strength of 10.8 MPa in NEN 8707 [1]. Missing characteristics necessary for structural assessment are used from bending class C22 (sawn timber) from EN 338 [2]. A FEM model of section 4-1 of the Maaskade under different historical build ups has been set up in Plaxis 2D, and an Ultimate Limit State computation has been carried out on the final build-up before replacement under four load cases. The found normative location that can be seen as the weakspot is the joint between the raking pile and the adjacent capping beam. A structural assessment based on sectional forces results in a negative outcome of the structure even on self weight governed loadcase as unity checks > 3 are given for the capping beam. These results do have the shortcomings due to simplifications from 3D to 2D and a modelling with linear elements with no volume in the model and no allowance for further load distribution beyond elasticity. A definite answer on the capacity in terms of additional external loads cannot be given and the need for a model that incorporates the exact lay out and positioning of the loads is stressed. Further recommendations for practice are to find out if the capping beam - pile connections are expected to be able to take tension and to name their state after an inspection.

# PREFACE

This thesis is written to complete my Master in Building Engineering at the TU Delft.

I would like to use this preface to thank my committee members for their help, ideas and tips throughout the process. Especially in the last months, during the Covid-19 pandemic, their guidance from a distance was much appreciated.

In the selection and measurement of the timber pieces John Hermsen and Ruben Kunz showed me how this works in practice and they were there, often for days in a row, to complete the tasks necessary for the material testing. A great thank you to them.

Other contributors I am grateful to are Jarit de Gijt who told me about the construction stages of the historical walls, Theo de Bruin from the city archive that provided useful drawings and documents, Ronald Brinkgreve who explained the tougher parts in Plaxis modelling and of course Eric Knibbeler from the port of Rotterdam who showed the works on the Maaskade and made the material available for testing.

Lastly I would like to thank my family and friends for their support, for the breaks and sport trainings that pulled me through this year.

*Mark Petrus Schilder*
*Delft, August 2020*

# 1

# INTRODUCTION

*THE introductory chapter includes the indirect and direct motive for the need of this study on quay wall foundations, discusses its relevance, states the research questions and leads the reader through further build up of the report.*

1

## 1.1. MOTIVE

Quay walls are a man made structure on the waterside, making berthing of ships possible and ensuring a sharp border between land and seaside, which can provide safety during high waters and retains the soil behind it [3]. They have existed for millennia throughout the world and are often altered and expanded to facilitate berthing and unloading of larger ships or retain higher water levels for safety. A possible set up of quay walls often chosen in the Netherlands in the past is a retaining wall made of masonry or concrete placed on top of a timber floor which reaches deep towards the landside and is supported itself by timber piling. This combination is called a soil retaining wall on a timber relieving platform (see figure 1.1).

Timber stems have been used often in these structures whenever a deeper soil layer had to be reached, which is deemed too hard to achieve by soil removal and placement of stony material elements [4]. Only since 1925 use of steel and mostly concrete columns in the soil is common. Since 1970, timber has not been used as foundation material anymore in the Netherlands, with exceptions for sewer and greenhouse foundations [5].

Since timber is a natural material, it can deteriorate and degrade in the outside environment. The foundation elements are hard to reach when this happens, but also for inspection to find out *if* this happens. In addition, the exact set up and reach of these structures is often unknown due to missing documents or inconsistent placement during construction e.g. due to imperfect construction technologies. Next to the unknown capacity, the loading of the historical quay walls has an increasing trend in time due to use of motorised traffic and the growth of berthing ships and their cargo. Hence, this makes a problematic combination. This is the indirect motive for the dissertation topic.

Quite possibly one result of this combination is the partial collapse of the Maaskade in the centre of Rotterdam in December 2015. Over a width of approximately 40 metres, the wall broke and the soil behind it was able to flush away (see figure 1.1). The conclusions of the inspection afterwards included a poor to very poor connection of the piles with the timber floor structure, broken timber capping beams and fungal decay on the horizontally placed timber elements [6]. This has been the direct motive of the research in this thesis.

In a broader field, the study of remaining safety in timber foundations is necessary for economical and ecological reasons, to ensure an optimised service life [7], to develop strategies for conservation and restoration and prohibition of unnecessary demolition or replacement of foundations [8].

Figure 1.1: A quay wall with relieving platform (left), inspection of the failure of the Maaskade (right) [6] .

## 1.2. PROBLEM STATEMENT

The result of the Maaskade accident was removal of the quay wall structure and replacement with a modern anchored steel sheet pile wall. But the curator of the wall, the Port of Rotterdam (PoR), remains in charge of a lot of similar structures and is in search of long term solutions.

This is why TU Delft was contacted. Its assignment is a structural analysis of the structure under current and original loading situations, a weakspot analysis of the structure, a way to handle degradation and ageing in a remaining strength model and improved inspection and assessment methods of timber elements in quay wall foundations. To fulfil this request, TU Delft has been given material from the collapsed Maaskade. The overall research is not to be based on this case only, though.

## 1.3. AIM

The main aim of this report is referring to the first and second part of the request of the PoR : a structural analysis and search for weakspots in current and original loading situations for the Maaskade case.

The main research question is : ***What is the (remaining) capacity of the timber foundation of a quay wall with relieving platform?***

By comparing the force distribution on different set ups of the wall together with the possible loading and material state, weakspots can be found that are dominant for the remaining capacity calculation. Applying a safety philosophy can afterwards make

1

statements on remaining safety and need for replacement possible for quay curators.

## 1.4. SCOPE

Many different quay walls with timber relieving platforms are situated in the Netherlands in general or Rotterdam in particular. The choice has been made to set the focus of this report on the Maaskade only, as material of it is present. Even within the Maaskade, a lot of alterations in build-up are present, as will be explained later on in the report. Corresponding to the choice of the Port of Rotterdam to renovate the western side (500 m west of the Willemsbrug bridge), this is the part to be examined as collapse has taken place here.

A quay wall collapse can have many reasons. It consists of many elements and can be loaded by many different loads. The choice has been made to focus on one part of the wall: the timber foundation. The other elements of the wall will be incorporated in the load cases only. The wall can also collapse in many different ways, as described in EN 9997-1, section 2.4.7.1 [9] "Geotechnical design" (see figure 1.2). Since the focus of the study is on the material timber, the ultimate limit state 'STR' (subfigures 5 and 6) will be tested. This incorporates collapse or extreme deformation of the structure or its parts, where the strength of the construction materials is giving the main contribution to the resistance (citation from [9]). It leaves behind the failure through instabilities, uplift, soil failure or hydraulic fracture.

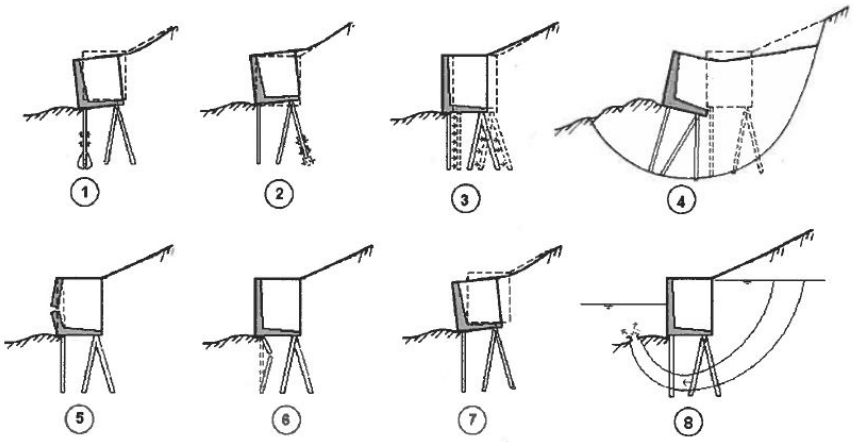


Figure 1.2: Failure modes according to EN 9997-1, STR (structural failure) can be found on pictures 5 and 6 [10].

## 1.5. GUIDE TO THE REPORT

To come to the answer of the main question, the following chapter structure has been chosen.

Chapter 2 incorporates a literature review on capacity related topics and the state of art of historical timber foundation calculations in Dutch practice. Next, chapter 3 elaborates on the experimental plan. The first sub-question will be elaborated on in chapter 4: *What is the build up of the Maaskade and what are the loads exerted on it?* The report will then continue with chapter 5, which answers the second sub-question: *What is the state and strength of the timber components?*. Chapter 6 puts the found information together in a computational model and answers *What are the load distribution, resulting stresses and weakpoints in the quay?*. The last chapters will then conclude on the main question with a discussion. Recommendations will be given too.

Afterwards, one will find the appendices. These include elaboration on chapters 5 and 6, which consist of procedures and graphs on obtainment of material characteristics and elaboration of computational modelling in- and output.

# 2

# LITERATURE REVIEW ON CAPACITY RELATED TOPICS

*THIS chapter will give a literary overview of capacity related topics. The first part includes an introduction into timber, foundations and quay walls to provide the reader with basic understanding of the aspects that have an impact on the capacity. These are the sections 'Backgrounds of timber in foundations', 'The material timber', 'Durability and weakening' and 'Soil structure interaction'. The second part then focusses on assessment, safety philosophy and service life modelling to find the ins & outs of capacity calculations, remaining lifetimes and the philosophy behind them. These sections are 'Assessment of ecisting structures according to current norms', 'Service life estimation and modelling' and 'Investigation, inspection and implementation'.*

## 2.1. BACKGROUNDS OF TIMBER IN FOUNDATIONS

Timber foundations can be found in many structures built before 1970. The reason for building these is elaborated on to show the use and scale of piled foundations in combination with timber.



### 2.1.1. PILED FOUNDATIONS

Deep foundations are necessary if the highest soil layer is not stiff enough to bear the load of the above structure before large settlements occur. If removal or substitution of this weak layer is not an option, the use of piles to reach the stable layer is the best option. Alternatively, structures on water also required a pile foundation [4].

Piled foundations are therefore used for a long time in areas with either unstable upper soil layers or in the case of building on water.

Timber stems proved to be a good source for foundation construction material due to its availability in nature (a renewable resource), easy processing (possiblitity of on-site adjustments, repairs and recycling) and possession of a useful shape to penetrate the soil. Its compressive and tensile strength characteristics ensure integrity during the driving process (with exception of splitting issues at the place of hammer impact), while its low weight gives it a high strength to weight ratio.

Some of the earliest notions of the use of timber piled foundations are from the alpine pile-dwellings, mainly to be found in Switzerland. These origin from the neolithic and bronze age, from 5000 to 500 years BC [11]. Keller and Lee [12] report "driven piles with platform beams and cross timbers to keep the piles together" (see figure 2.1), as well as fascine mattresses (bundled branches topped on top of each other) in between piles as an alternative to reach the bottom of the lake the dwellings are built on.

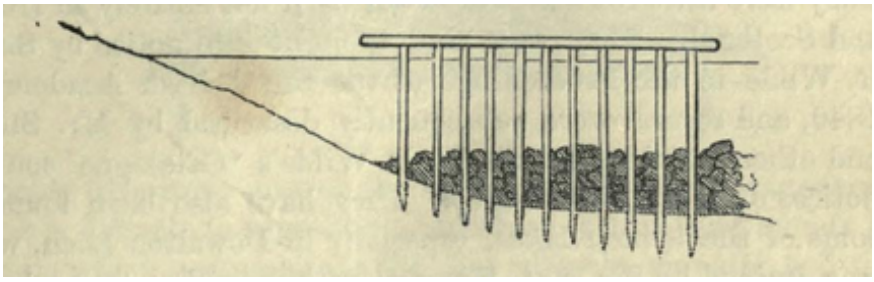

Figure 2.1: An ancient alpine pile-dwelling foundation as drawn by Keller & Lee in 1878 [12].

The Romans too made use of piled foundations [13] [5]. During the dark ages, most of the buildings were made of timber, which resulted in relatively light structures. With the increment in stone building construction, the need for reach to a sturdy soil layer reintroduced itself [5].

The first deeper foundations in the Netherlands consisted of so called *slietpalen*, which are relatively short (1m) and thin. They were placed close to each other and reinforced the ground. As tip diameter and length increased, the number of piles necessary to bear

the load decreased. The final form of timber piled foundations reach all the way to the load bearing soil layer [13].

### 2.1.2. QUAY WALL FOUNDATIONS



Quay walls are always in contact with the ground, therefore per definition they form or need some kind of a foundation. The foundation must ensure loads from water- and landside are distributed into the ground and needs to ensure its stability. A deep foundation solution may be deemed necessary when the loads or geometry in combination with the soil do not give a stable solution or if it results in a cheaper solution [3].

The choice of type of quay wall has firstly to do with of the possibility of building from the landside or from the waterside only. The types include a simple slope, jetties or platforms (ancient history), retaining walls on shallow foundations ($17^{th}$ century) or fascine mattresses, walls with a deep foundation or a whole relieving platform ($19^{th}$ century), reinforced concrete caissons (early $20^{th}$ century), steel sheet pile based solutions (1927) and post war steel & concrete combinations [3]. Timber can be found in these either as a pile, but also as foundation beams or fascine mattresses that consist of branches.

Timber use in quay walls often results in an open structure, which can be a reason of application due to the advantage of having a low impact on natural movement of sediments[14]. The placement of timber on a few meters below groundlevel in quay wall structures with retaining walls is twofold. Firstly, the timber can be placed entirely under the waterlevel, preventing decay of the pilehead (see section 2.3). Secondly, a slope that reduces the necessary earth retaining wall height can be hidden under street level which saves a lot of space aboveground.

A study by René Klaassen in 2014 shows the difference in use of timber in quay walls in comparison to buildings. The study consisted of a large database of timber piles from Haarlem, Den Haag, Rotterdam and Amsterdam. It proved quay wall piles have on average a larger diameter and came from older trees. As quay wall projects need very large numbers of piles, less spruce has been used as it was more expensive. The reason for this is that spruce needed to be imported. Also, less decay has been found on average in comparison with buildings, and more often limited to the outer 20 mm of the cross section [15].

Differences in the environment of timber in quay wall foundations with respect to timber underneath buildings is twofold: before placement from regional or national timber sources the timber was more often immediately placed after transport by rafting (meaning it stayed wet all along transport) and - secondly- the environment after placement is, at least partially, in a full water environment for the upper parts of the piles in contrast with the soil underneath buildings[15].

### 2.1.3. TIMBER FOUNDATIONS IN PRESENT TIMES

Timber was the only material used for deep foundations until 1925, when concrete was introduced in this market. Both were applied, also in composite forms often including concrete close to the water table, until the use of timber was practically banished around 1970.



Timber proved to have not enough capacity for truly heavy projects (due to the restriction in section size or long lengths), unless used in huge numbers (like the *Paleis op de Dam* in Amsterdam - a building that incorporates over 14 000 piles [5]). It also deemed sensitive to deterioration by biological activity. The use of timber underground got a negative image and is often seen as old-fashioned[5]. Its flaws and variability due to the natural formation are also seen as a drawback in comparison with other foundation materials [14].

The only projects timber piles are used for nowadays are greenhouses, sewerage systems or small projects. It has been estimated 25 million piles are still in use, of which 50% underneath buildings and the other half underneath quay walls and bridge heads [5].

It is quite possible timber foundations will make a reintroduction, as timber as a material is praised for its sustainable aspects. It captures $CO_2$ and with a sustainable silvicultural plan the harvest does not harm nature. It is mentioned though, that most species used in engineering applications are renewable over a relatively long timescale, making it difficult to demonstrate the sustainability aspect[14].

Timber is still extensively used in marine and fluvial applications as groynes, dune protection, wave screens, jetties, support trestles, mooring dolphins, lock gates, bed and bank protection and earth retaining structures. Some of these also include the use of piling, with e.g. the addition of a steel shoe at the pile tip as a reinforcement. Crossman mentions an additional reason for the choice of this material in these applications is its high tolerance to short duration (shock) loads [14].

## 2.2. THE MATERIAL TIMBER

This section discusses timber material characteristics to provide the reader from outside of the field with basic knowledge that is necessary to understand the strong- and weak-points related to it. Since this report focusses on capacity, the elaboration is on the tree elements that influence the strength of the timber: Anatomy, Formation and Physics. Next to this, elaboration is given on the grading process and the property assignment. The first three subsections are based on 'Timber Engineering, Principles for design' from Hans Joachim Blaß and Carmen Sandhaas [16], which on itself refers to article A4 by P. Hoffmeyer and Article A19 by L.D. Andriamitantsoa in STEP:2 [17]. The last subsection (Grading and Property Assignment) is based on an article by Ridley-Ellis , Stapel and Baño [18]. Other sources used are named within the text.

### 2.2.1. ANATOMY

Wood is a natural and organic material, made of cells. It consists of the chemical compounds cellulose, hemicellulose and lignin together with other constituents. The term 'Timber' is used for wood that is used for building or wood that is originating from trees that are grown for this purpose as defined by Blass & Sandhaas [16].

Special about this material is the fact that it consists of a structure of elongated cells. This makes it orthotropic and its orthotropy is a function of variation in cell size and type but also its orientation preferences during growth. The directions considered are longitudinal (along the stem direction), radial (from the heart towards the bark of the tree) and tangential (on a tangent to the growth ring).

There are tree main factors in the structure of the wood that impact its properties are:

1. Fine cell wall structure
2. Collection of cells in clear wood
3. Growth irregularities (see subsection 2.2.2)

These largely depend on species. There are two main groups a tree can be part of: coniferous and deciduous trees. Timber from the first group is called softwood, while timber from the second group is called hardwood.

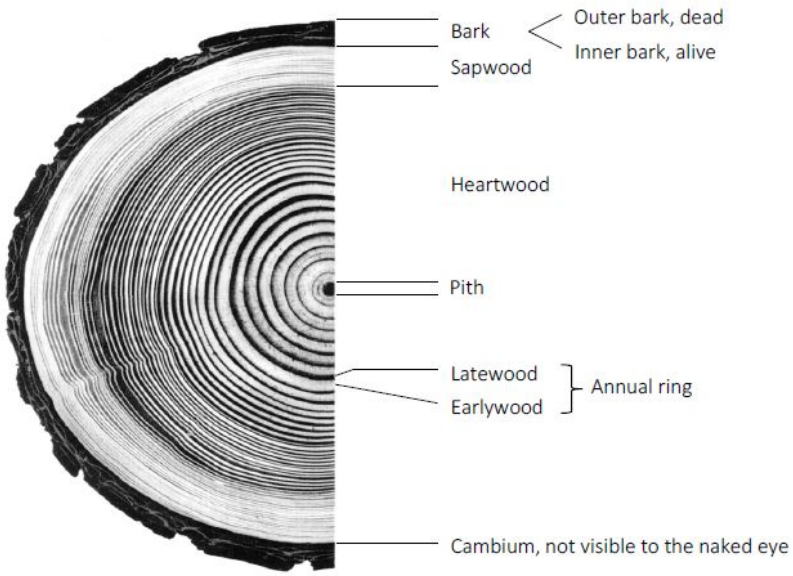


Figure 2.2: The cross section of a stem with its elements, Douglas fir. From Grosser (1971), retrieved from 'Timber Engineering' [16] page 23.

On the macroscopic scale, the main element that affects strength is the stem layout. But next to the structural function it must also ensure transport of nutrients downwards by the bark and transport of water upwards by the wood.
If one zooms in (see figure 2.2), one would distinguish the pith (centre of stem, supplies the young plant with water), heartwood and sapwood (older and younger wood respectively with vertical cell orientation for water transport), rays (cells in horizontal direction for water and nutrient transport throughout the section), cambium (the cell layer providing secondary tree growth), the bark (nutrient transport and protection) and resin canals (placed parallel and perpendicular to the stem axis and include resin that protects the wood from invaders).

From engineering perspective, the heart- and sapwood includes the elongated tracheid cells that include the strength properties that are of most interest to engineers. It must be noted that sapwood is physiologically active, while the heartwood has died, the piths (openings) between its cells closed making transport between them impossible and its starch has been consumed. This in general makes it much less attractive for biological invaders and therefore more durable. The border between sap- and heartwood can be more or less evidently visible.

Moving on to the mesoscopic scale, one would see the annual rings that indicate the secondary growth. It is closely linked to the climatic conditions. In spring the main function is water supply which results in large open cells, while in late summer and autumn the focus is on strength and stability which results in small cells packed closely together. From engineering perspective, it is clear that the climatic conditions therefore strongly affect the density and regularity of the material by means of annual ring formation.

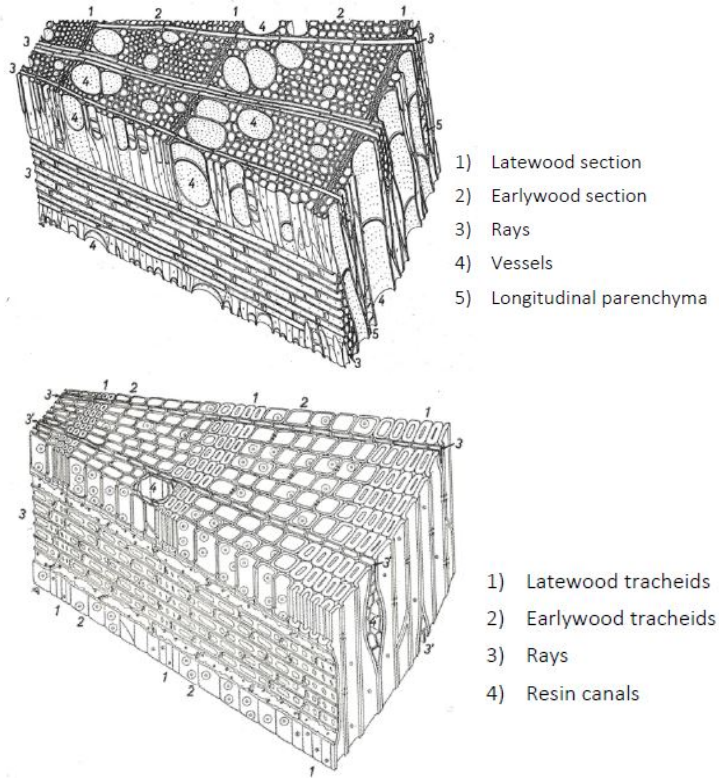


Figure 2.3: The structure of wood on a mesoscopic scale: hardwood (top) and softwood (bottom). From Nardi-Berti (1993), retrieved from 'Timber Engineering' [16] page 29.

On the microscopic scale, cell types can be distinguished. Softwoods mainly consist of tracheids and parenchyma. The longitudinal tracheid cells take about 95% of the total volume. Hardwoods are clearly more evolved and have a more extensive division of function. More rays and vessels can be found. The main cell types stay tracheids and parenchyma. Piths between the longitudinal cells prevent collapse of the water column during tree growth. When the sapwood dies and converts into heartwood they close, but can also close by drying.
For engineers the pith closure is important for impregnation with chemicals or for durability reasons as fungi and bacteria can not travel as easily between closed cells.

Finally, on submicroscopic scale one can describe the chemical compounds and the cell wall structure. The compounds will be elaborated on first: the main ones are cellulose, hemicellulose and lignin. Cellulose is a polysaccharide chain with a very high (tensile) strength. It is hydrophilic due to free hydroxyl groups. Hemicellulose is also a polysaccharide but with a spacious 3D structure and functions as matrix. It is highly reactive and controls the permeability and can be used as sealant. Lignin is a 3D macromolecule from alcohols. It is pressure resistant and hydrophobic. Next to the three main

compounds, constituents are found that have a high impact on chemical, biological and physical behaviour. The percentage of constituents grows from temperate to tropical climate species.
Then the set up of layers is as follows (see figure 2.4): the space in between the cells is called the middle lamella and is mainly composed of lignin. Next, the primary wall consists of diffuse orientated cellulose fibres. The secondary wall has a 3 layer set up on its own, with the middle 'S2' layer consisting of fibres with a straight orientation (parallel to the cell axis) and the S1 and S3 layers reinforcing the S2 layer by having a different fibre orientation angle. Finally, the tertiary wall is mostly composed of lignin as well. It forms the perimeter of the cell lumen, that is an empty space possibly to be filled by water.
Of interest is the cooperation of the compounds and the orientation of them within a layer and inbetween the layers. Not only do the S1 and S3 layer within the secondary wall prevent the S2 layer with high tensile strength from buckling, so does the middle lamella and tertiary wall by making use of the lignin that stables the fibres and gives the wood its compressive strength.

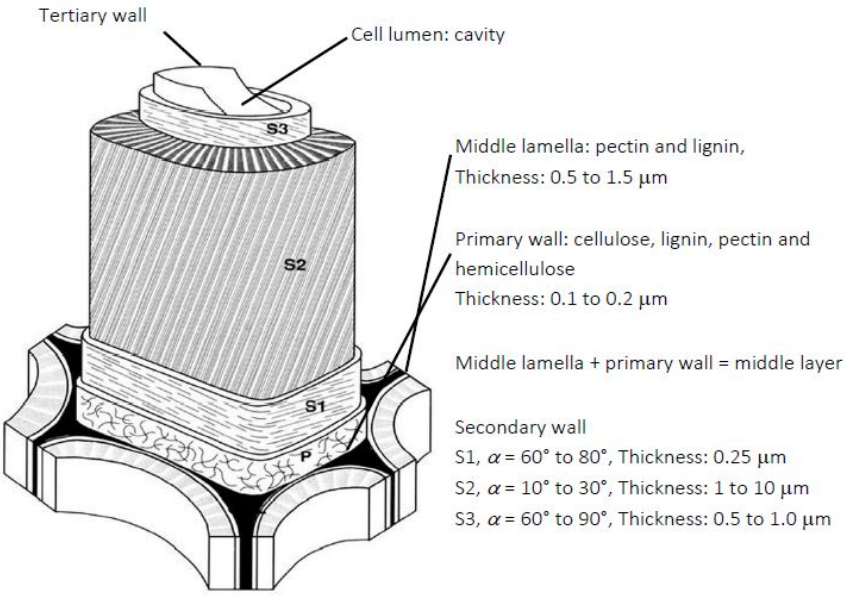


Figure 2.4: Lay out of layers in the cell structure (submicroscopic scale). From Booker & Sell (1998), retrieved from 'Timber Engineering'[16] page 31.

### 2.2.2. FORMATION

The quality of both the micro as the macro structure is dependant on the formation procedure. The growth is on its turn dependant on climatic conditions - therefore the origin of the wood changes its structural capabilities. There are three reasons formation can influence the strength:

1. Deviation from ideal stem shape. The ideal stem is straight and cylindrical with perfectly parallel grains. It can however show increased tapering, a spiral grain, an oval section, fork growth (splitting of the stem into smaller stems) or fluting (recesses along the stem resulting in a flower shaped cross section).

2. Deviation from average wood formation. The more homogeneous the wood, the higher the finally assigned strength properties to the element. Unwanted are: knots (size and their orientation), lack of bonding between layers, reaction wood (wood with specific properties, such as higher tensile or compressive strength at the sacrifice of its counterpart), heterogeneity in annual rings, growth stress cracks (due to longitudinal growth and self-weight of the tree), pitch pockets (overgrowth due to cambium damage) and false heartwood (irregularly shaped and coloured heartwood formation).

3. Unwanted subsequent changes. These can occur during growth or after felling. The unwanted subsequent changes include cracks, fractures, holes, discolorations and biological destruction. The reason for occurrence are forestry operations, extreme weathering or biodegredation.

### 2.2.3. PHYSICS

This subsection deals with the physical phenomena Moisture Content, Density, Temperature and Rheological Activities. These phenomena influence strength but also appropriate use of timber.
There are three remarkable points of timber with regard to **moisture content (M.C.)**: oven dry (0% M.C.), fibre saturation point (25 to 35 %, 28% on average) where the cell walls are completely saturated, and water saturation where no more water can enter since the lumen too have been filled (numbers of more than 100% M.C. are possible). The definition of moisture content is as stated in equation B.3. The moisture in wood can therefore either be bound (in the cell wall) or free (in the cell lumen, which has a porosity of 50 to 70 %).

$$\omega = 100 * \frac{m_{wet} - m_{dry}}{m_{dry}} \tag{2.1}$$

with
$\omega$ = moisture content %
$m_{wet}$ = wet mass $[kg]$
$m_{dry}$ = dry mass $[kg]$

An increase in moisture content results in a decrease in strength and stiffness, more creep deformation, rising thermal conductivity and an increased sensitivity to fungal infection (especially above a moisture content of 20 %). As Blaß & Sandhaas state, "it lowers the forces of attraction between the cellulose chains, and the hydrogen bonds holding the cell wall are weakened." Only an increase till fibre saturation point makes a large difference, and most properties are constant afterwards.

A change in M.C. will result in swelling and shrinking movements, which can cause internal stresses if restricted and eventually cracking. The movement varies in all three directions, but the change in volume is often perceived as 0% longitudinal (very small), 50% tangential and 50% radial. The key parameters are S2 layer fibre orientation since it dictates the swelling direction and the lignin content, since it is hydrophobic.

The M.C. will go to equilibrium if the surrounding climate remains constant. This is called the equilibrium moisture content. Relative humidity is more important than temperature for this. The adsorption and desorption curves differ (hysteresis), so the previous climatic conditions are of importance to assess the present state. It is found that moisture content is a key variable when assessing vulnerability to pests and durability.

The **density** depends on moisture content, which therefore always needs to be specified. Often $\rho_{12}$ is used, which indicates a M.C. of 12% under a relative humidity of 65%. The density of the cell wall itself is 1500 $\frac{kg}{m^3}$, and dependant on the void volume proportion the oven dry density of wood is about 300 to 550 $\frac{kg}{m^3}$. The density varies between and within wood species and is correlated to the annual ring width, since the proportion of early to late wood dictates the average density. The density is one of the three main properties used for class assignment.

**Temperature** influences volume change indirectly by the Moisture Content but has a direct influence on strength and stiffness. Compression characteristics are more influenced by a rise in temperature than tension ones.

Creep and relaxation regard the **rheological** or **'flow' properties** of wood. Creep regards the increase of deformation under constant stress. From plastic deformations in the timber one can observe a damage in the cell structure. The behaviour is therefore viscoelastic-plastic. Creep is primarily influenced by M.C. or changes in M.C. and the duration of the load and secondarily temperature and level of stress. The primary influencers are incorporated in the eurocode by a factor $k_{def}$ that incorporates M.C. and a load duration class for the calculation of deformations, and a factor $k_{mod}$ for the calculation of strength. The increased creep during drying is called mechano-absorptive creep. Relaxation is the process of stress decrease under a constant deformation. Sometimes however, the deformation does change e.g. due to shrinkage in the drying phase. Understandably, this increases the relaxation. For prestressed members, relaxation means frequent re-tensioning is necessary.

### 2.2.4. GRADING AND PROPERTY ASSIGNMENT

Since properties depend on so many factors, they vary between species, between trees and even within one stem. For the sake of safe and economic design, it is necessary to segregate the different qualities within one population or group of felled stems. This process is called 'Grading', and can be done for either strength properties or aesthetics. The former is called 'Strength Grading'. To able to make a design, it is necessary to link numbers to every selected grade. These are put together in the classes with set properties in EN 1995 and EN 338. These are the so called 'Strength Classes'. Alternatively,

grading of entire logs is also a possibility, with placement in log classes [18]. The standard classes are based either on bending (C and D classes for coniferous and deciduous species respectively) or tension (T classes). The properties used as a base during grading procedures are bending strength, bending stiffness and density for the C and D classes, or alternatively tensile strength, tensile stiffness and density for the T classes. For both, they are determined for a reference moisture of 12% content. Choosing the right grading method and criteria will result in an optimised system for a certain use, as stated by Ridley-Ellis & al. [18]. Therefore, it is allowed to create one's own classes after a check by the European Committee for Standardization.

The process of grading can be done either visually or mechanically. A combination would suffice in theory as well. Origin and species must be known for both methods, to set the grading criteria. A choice of grades must be made for assignment into them ('grading combinations'). Usually 1,2 or 3 groups are chosen together with a 'reject' class. Some destructive testing is also needed to set the limits in the criteria, which is described in EN 384. Sampling is often done on whole stems but every single piece that is to be assigned into classes will have to be checked. The parameters used for grading can be combined to achieve higher correlation coefficients [16]. The choice of grading method is however important, because the outcome will be affected. This because of different parameters to set the criteria and different normative requirements.[18]

**Visual grading** is the older method and usually based on knot area. It also incorporates a check for defects, grain angle, reaction wood, fungal-, bacterial- or insect attack, mechanical damage and discolouration [16]. Because of the low coefficients of correlation, it is not a powerful prediction method but it does require less destructive testing than machine grading.

**Machine grading** can be further distributed into machine controlled grading with pre-set criteria based on destructive testing of the graded population, or output controlled grading that uses post processing of collected data to adjust the limits for criteria (criteria for the process described in EN 14081). The methods are usually based on Modulus of Elasticity (MoE) from either static 4-point bending tests or dynamic measurements that use longitudinal oscillations [16].

The grading process comes with consequences. It is important to understand that classes describe populations and not individual parts [18]. One cannot know for sure certain numbers for properties are met because of use of a $95^{th}$ percentile characteristic value and because of application of extra factors as $k_v$ (human involvement), $k_h$ & $k_l$ (size factors) and a 0.95 factor on MoE that is applied for adaptation to previous standards that used measurement on different positions [18]. If different grading combinations are used, the assignment of a single piece can change. Since the variation within one class cannot be narrowed down completely, overlap exists between classes too. Additionally, regrading is necessary if substantial changes are made to the cross section. This is because defects as knots in large pieces are averaged into 1 class the large piece can be assigned to, but a much larger variety occurs after downsizing this large piece

into smaller ones [18]. Lastly, it is important to notice that current standards are based on the knowledge and data obtained so far. With more research being done, and more data being collected with every graded timber piece, the classes in EN 338 are subjected to change with every update of the code.



For research use, it is not always handy to use the standard procedure for class assignment, since the exact properties of the timber can deviate from the classes in EN 338 [2]. It is advised to test the parts more extensively, which is possible with the same methods used for class assignment. These are stated in NEN 408 [19]. This code describes:

- Stiffness
  - MoE in bending (local and global)
  - MoE in tension parallel to the grain
  - MoE in compression parallel to the grain
  - MoE perpendicular to the grain
  - Shear modulus
- Strength
  - Tension strength parallel and perpendicular to the grain
  - Compressive strength parallel and perpendicular to the grain
  - Bending strength parallel to the grain
  - Shear strength parallel to the grain

## 2.3. DURABILITY AND WEAKENING

This section describes the natural durability of timber and what this depends on. Next, the ways it can deteriorate is elaborated on including the way it occurs, when it occurs and how it can be signalled. Lastly, in short other factors that can weaken the foundation or increase the load on it are named. The words, 'degradation', 'deterioration' and 'decay' will further be used as equal terms for weakening or its results.

### 2.3.1. NATURAL DURABILITY

This subsection is based on 'Timber Engineering, Principles for Design' by Hans Joachim Blaß and Carmen Sandhaas[16].

The natural durability of timber depends on a few important factors. Firstly, the constituents. They posses qualities that can stop biodegradors. Since biological activity is higher in warmer climates, the percentage of constituents in wood is higher in tropical hardwoods (2-30% opposed to 1-10% in temperate climates). Next: heartwood. During the process of heartwood formation from sapwood, piths close and starch is consumed. As it also stores constituents, this part is the most durable part of the tree. Furthermore, the occurrence of cracks and openings is important since they make it easier for insects,

fungi and bacteria to penetrate the cross section. Moisture content is important to fungi as well: no fungi will grow with a M.C. of less than 20%. Lastly, environmental conditions have an impact as they correspond to a M.C. and the formation of cracks, as well as the availability of oxygen, insects or marine borers, which will be elaborated on later on in this section.



Durability is assessed by the prescribed rules in EN350-2 'Natural durability of solid wood'. The classes for fungi are class 1 to 5 (with timber with class 1 having a good durability of heartwood - sapwood is always class 5 unless specified), while the classes against insects and wood pests have classes D - Sh (with D being the most durable) - see EN 350-2 for a full elaboration [16]. The classes are prescribed per species, not per batch or population. Environmental conditions are then coupled to this by Use classes in EN 335.

Increasing natural durability is possible however. The first step is silviculture: wood felled in timber has no active water transportation going on and will also not contain insect eggs. Then comes conservation until spring. If it is in water, there is excessive moisture for fungi and insects, and the timber will also not have drying cracks. After this, one can try to increase durability artificially. An option are chemical preservatives like paintings and coatings. Since water transport is taking place behind the bark in a direction parallel to the grain, it is of largest importance to cover the end grain section. For some species like spruce the paints do not want to impregnate, since the piths between the cell lumen can be closed due to the drying process. Another option is wood modification, this reduces hygroscopy (the phenomenon of attracting and holding water). With this process, the hydroxyl groups at the cellulose chains are either cross linked or occupied by chemicals. If heat is used, these groups are broken. The equilibrium moisture content is altered downwards by this procedure, which makes it less attractive to fungi and reduces swelling and shrinking. If a heat treatment is decided on, one has to bear in mind there will be a reduction in strength of about 30% and for impact energy by 60% depending on the exact specifications of the treatment, which means this is not an option for structural timber. Measures can also be taken in construction design: smart locational placement, or placement under expected equilibrium moisture content which prevents cracking, swelling and shrinking. Covering of the end grain is of importance as well. Lastly, there is need for correct drying. If the drying procedure happens too fast, case hardening can occur that results in residual stresses as the timber dries faster at the outside compared to the inside.

### 2.3.2. DEGRADATION TYPES

The type of degradation discussed for the Maaskade situation are:

1. Fungal
2. Bacterial
3. Insects and marine borers
4. Metal induced
5. Mechanical

**Fungal degredation** can take place when the M.C. of the timber is at least 20%, and is strongly related to it. This is because it needs free water, which is assured for moisture contents above the saturation point. Fungi also need oxygen (aerobic conditions)[16], Daniel 2016], and dislike salt water [14]. Therefore, it depends on ground water table height and the water capacity of the soil layers if fungal deterioration takes place. If it takes place, it will be only on the part that is exposed to air, which for foundations is usually the upper part. For this reason it is important to monitor the water table and sewer systems or temporary local evaporation due to plant growth in spring [8]. Softrot however, can live in near-anaerobic conditions but deteriorates in rates of 0.05 $\frac{mm}{year}$ which is negligible [10].
The process of degredation looks as follows [20]. The infestation starts if contacted with loose spores or the ones in the ground. The start of colonization is through open cells (cut-offs) or through the rays, the latter supplying the fungi with starch and being often poorly lignified. Afterwards, fungi can penetrate through piths or bore holes in cell walls. The fungi live in the lumen, from where they can attack by (biologically based) erosion. If the fungi is not capable of penetrating lignin, it forms a barrier and the invader can only consume unprotected cellulose, which binds it to the cell lumen (mold & blue stain). Other fungi make holes or thin the cell wall from the inside to the outside (soft rot, white rot), preferentially remove lignin and hemicellulose (preferential white rot), attack the middle lamella (certain white rots) or depolymerise cellulose and hemicellulose (brown rot), as explained by Geoffrey Daniel [20]. The susceptibility of the wood piece depends on the concentration of constituents and extractives.
The speed of fungal attack differs per species. Soft rot can degrade up to 10 $\frac{mm}{year}$ in water saturated wood, while white and brown rot can degrade with a tempo of 100 $\frac{mm}{year}$ in drier wood (M.C. of 25 - 100 %). The degradation takes place radially, from the outside in. The velocity depends on the time that the parts are above the ground water [5].
Prevention of degredation can take place in the form of water table management, copper concentration increase or wood modification, as discussed in the previous subsection [20].

**Bacterial degradation** takes place when waterflow is present; this is necessary as the different bacteria species need to follow a sequence to properly erode the cell walls and cannot move themselves without a waterflow [8]. For the case of foundation piles,

watermovement is either stimulated by direct flow, changing waterlevels or pressure differences between soil layers[15].
Bacteria can degrade wood under water because of their ability to survive in near-anaerobic conditions. The elements attacked are the pith membranes, which increases permeability and thus enables waterflow. This has been known for a long time, but since the 1980s it has been found out that the woody cell wall is also attacked [8]. The S2 layer is mostly affected. The bacteria use enzymes to break up the cell wall and need a succession of species to effectively do so[15]. As with fungi, the infestation takes places in radial direction outside-in [8].
The speed is significantly lower than that of fungi with a maximum of 1.1 $\frac{mm}{year}$, but this can add up to heavy strength loss over the years as foundations are usually placed for long periods. Difference can be made between 'invasive' and 'severe decay', as used in the study of Klaassen [15]. The severe decay is here a loss of >70% of strength. If both penetration depths are equal, no more decay can take place. This shows clear boundaries in the wood between permeable and non-permeable parts, like the sapwood-heartwood boundary. Bacterial activity in heartwood is considerably lower.
It was already known decay takes place over full pile height (though the dynamics are to be further studied [5]), and the 2014 study showed a few additional conclusions. The decay is more likely to take place in a soil environment in comparison to a water environment (buildings vs. quay walls), with two reasons: the path of lowest waterflow resistance is the pile in soil, but not in free water and secondly the soil houses more bacteria in the first place. Next, spruce piles more often show partial decay of the sapwood, while pine pile sapwood is more often totally decayed. The reason for faster decay can be found in a higher radial permeability. In 2012 Klaassen and Creemers also found out that the bacterial decay velocities were higher in Amsterdam than in Rotterdam. This could be due to use of different tree species (relatively higher spruce presence) which in its turn can be explained by deeper stable layers in this town, which requires higher tree species [5].
Bacterial deterioration is blocked if watermovement is prevented. This can happen due to pith closure (e.g. drying), blue stain fungus that fills the cell lumen, watertight soil layers or increased mineral content like pyrite[15]. Other methods are being developed.

**Insect invasion** is another possible decay mechanism and usually takes place under warm circumstances, as heat is appreciated by insects ans especially by their eggs and larvae. They use lignocellullose for food, shelter and breeding. As insects do not travel through cells, cracks and openings are necessary to let them in. Heartwood is not on the menu and is not affected. [16]. **Marine borers** can threaten harbour structures. Amongst them are the shipworms (Teredinidae), their distribution depends on salt content and temperature of the water. They require a salt content of 0,9 to 3,5% and can be found in almost all European areas. The worms bore holes 6-8 mm in diameter and affect both sap- and heartwood. The resulting circular section looks like a sieve [21]. Another borer is the gribble from the Limnoriidae family. These flattened isopod creatures need cold waters with a maximum of 20 degrees Celsius and 1.5% salinity. They use the wood as a food source and as a breeding shelter. It creates a borehole of about 1.5 - 2 mm and does not penetrate more than 20 mm into the wood. The degradation speed is up to 6-12 mm

a year, from the outside to the inside [21].

Metals can trigger a **chemical decay** in wood in its proximity. This can take place after placement of metal fasteners in wet wood, in the crevice between the two materials. The fastener can loosen and black stains are formed. It is often referred to as 'nail sickness'. The following is based on the article of Baker [22].
An acid-base reaction can take place. The use of two different wood species can speed up the process due to increased oxygen concentrations at the border of the two due to a difference in permeability. Either way, concentrations of oxygen and certain ions must occur and no degradation will take place if these are washed away directly.
If the material of the fasteners is ferrous, galvanic erosion can occur where the head is the anode and the shank the cathode. If two metals are used, one of them forms the anode and the other the cathode. The reason for the formation of this process with a single metal is the natural alkalinity of wood (ph = 4 to 6). Reaction 2.2 will take place at the cathode, while reaction 2.3 will take place at the anode.

$$O_2 + 2H_2O + 4e^- \rightarrow 4OH^- \tag{2.2}$$

$$Fe \rightarrow Fe^{++} + 2e^- \tag{2.3}$$

The $OH^-$ (hydroxyl) can cause hydrolisation of the adjacent cellulose chains, weakening the connection. If the hydroxyl group binds, the remaining environment will turn relatively more acidic which fastens the corrosion. The unstable $Fe^{++}$ will react to $Fe^{+++}$ which forms the black dyes visible on timber and catalyses cellulose weakening reactions.

The protection for fasteners in timber is stated in Eurocode 5 and can prevent loosening[16]. When inspecting fasteners, it is important to bear in mind that the head is often in good shape, whilst the anodic shank can have a severe loss in cross section [14].

**Mechanical degradation** can take place in the form of abrasion, impact and creep. This paragraph is based on Crossman, 2004 [14].
Abrasion takes place due to sediment transport in wind and water. It is stated 'a major factor in determining the life of a timber structure' and is most clear in areas with a small tidal range. A general rule is that the higher the density, the smaller the wear due to abrasion will be. It is clear that softening due to e.g. fungi will have a negative impact on the resistance to abrasion. The result is a decrease in the cross section which can have a large impact the smaller the original section was, such like decking.

Impact on the other hand, due to e.g. boats, can result in compressive failure of the fibres.

Creep is in its way also a form of mechanical degradation. It is defined by Crossman as a loss in strength with time under a load [14] and is incorporated in the design with a load endurance factor, part of $k_{mod}$ in Eurocode 5.

### 2.3.3. OTHER WEAKENING MECHANISMS

Next to deteriorating mechanisms there are more reasons why a timber piled foundation could be weakened. One of those is **scour**: soil removal by waterflow around the piles can cause reduced embedment depth of up to 1.5 - 2 times the pile diamater [23]. Alternatively soil in between fascine mattresses can be washed away as well, decreasing embedment and increasing the chance of buckling.



Next to a reduced capacity, (unexpected) **additional loading** can take place as well. This does not immediately reduce the strength, but does reduce the redundancy in the structure or indirectly reduces the timber strength by long term loading. Next to the obvious case of application of additional external loading, the following can be noted down on soil-related problems:

- Relocation of soil on top of the quay wall may weaken the soil anchor and increase horizontal loading on the piles;
- Negative skin friction as a consequence of subsiding layers: downward drag by the weight of soil layers that move downwards with respect to the pile shaft increase the load on the pile;
- Differential settlements that induce loads.
- Consequences of geotechnical instabilities.

The soil related topic will be further elaborated on in the following section.

## 2.4. SOIL STRUCTURE INTERACTION

Since the capacity of a foundation depends on both structural components as well as on the soil characteristics, the interaction of the two is of utmost importance. This chapter describes the working of a foundation in soil, attributes of timber foundations from a geotechnical perspective and current calculation methods.
Since timber piled foundations use closed, soil-displacing piles that have been driven, no information is given on other types.

### 2.4.1. WORKING OF A PILED FOUNDATION

A foundation needs to transfer all its loads to the underground, therefore the capacity of the whole structure is dictated by the weaker of the two. The way both are loaded depends on the interaction of the two.
A single pile consists of head, shaft and tip. For vertical loading, forces from the above structure are applied at the head. The top force on the pilehead can be enlarged if soil along the pile shaft has a relative downward movement with respect to the pile, the so called 'negative friction'. The soil counter reacts with an (upward) reaction force along the shaft ('positive friction') and with a base reaction on the tip of the pile. With two components to the reaction force, there are two types of piled foundations applied. The first method relies on the shaft friction, its pile is called a cohesion pile or *Kleefpaal* in

Dutch, while the other method relies mostly on the tip resistance, these piles are called end-bearing piles or *Stuitpalen* in Dutch [24].
Although foundation beams or a foundation footing is often present on top of the piles, EN 9997-1 'Geotechnical design of structures Part 1' states that if a deep foundation is applied, the piled part needs to be able to take all the forces [9]. The failure modes according to the same norm are a general loss of stability, exceeding the geotechnical capacity or the structural capacity of the pile, simultaneous collapse of both, collapse of the soil due to horizontal loading, excessive uplift or settlement of the structure, excessive horizontal deformations or unacceptable vibrations.

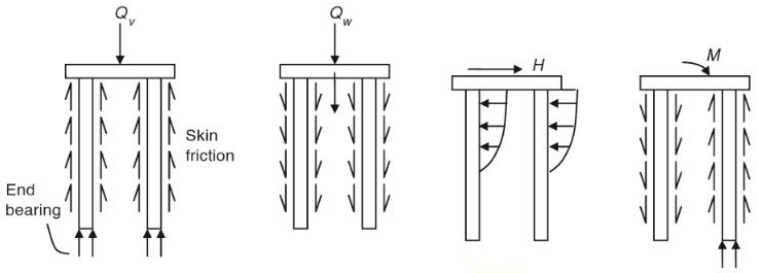


Figure 2.5: Load transfer mechanisms in piled foundations, where picture (b) is for an uplift situation. From the Geotechnical Engineering Handbook, page p4-63. [25]

### 2.4.2. TIMBER FROM GEOTECHNICAL PERSPECTIVE

The vast use of timber foundations have resulted in some conclusions from geotechnical perspective, as described by A.F. van Tol [24].

- The pile is placed with the taper downwards: the tip has a smaller diameter (often 13-15 cm) than the pilehead (often 26 to 28 cm). This downward taper has a positive effect on the positive skin friction and a negative effect on the negative skin friction. However, no substantial decrease in negative skin friction can be concluded;

- The circumference of the shaft is larger in higher layers, which on its turn increases the effects of negative skin friction.

- Timber piles have a small tip which can fail during driving into dense sand layers. Therefore usually the penetration into the sand layer is no more than 1 or 2 metres. Consequently, timber piled foundations often have to rely on shaft friction rather than end-bearing capacity;

- As the driving force is directly applied to the head and radial tensile strength of timber has its limits, splitting of the head can occur during driving. A placement of a ring from steel around the pilehead forms a countermeasure. This can be seen on The Maaskade piles too, see chapter

- Driving piles is mentioned to be harder than piles of concrete or steel, as timber absorbs more energy. To reduce the need for excessively hard driving, the working loads on piles are often limited to e.g. 300 kN for a square 300x300 mm pile [14].
- Crossman [14] states that for piling purposes, the grain should be as straight as possible to prevent damage during driving;



### 2.4.3. CALCULATION METHODS FOR PILED FOUNDATIONS

Piled foundation calculations can be made for vertical loading in vertical load driven designs or use can be made of lateral load models that include pile group behaviour for lateral load driven designs. Both will be discussed. The former is based on the foundation techniques handbook by A.F. van Tol [24] ; other sources are indicated.

The maximum pile capacity under **vertical loading** is given by equations 2.4 to 2.6. The numbers for $p_{r,max}$ can be based on Cone Penetration Test (CPT) cone resistance or on shear resistance and friction properties of the soil. Since the CPT uses direct data from the site itself, it is the method preferred in the Netherlands. The CPT measurement device is a small soil displacement pile on its own, and needs adaptive factors for other pile types.

$$F_{r,max,pile} = F_{r,max,tip} + F_{r,max,shaft} \tag{2.4}$$

$$F_{r,max,tip} = A_{tip} * p_{r,max,tip} \tag{2.5}$$

$$F_{r,max,pile} = O * \Delta L * p_{r,max,shaft} \tag{2.6}$$

With:
$F_{r,max,pile}$ = Maximum geotechnical pile resistance $[N]$
$F_{r,max,tip}$ = Maximum geotechnical end bearing resistance $[N]$
$F_{r,max,shaft}$ = Maximum geotechnical shaft friction resistance $[N]$
$A_{tip}$ = Tip area $[m^2]$
$O$ = shaft perimeter $[m]$
$\Delta L$ = positive shaft friction height $[m]$
$p_{r,max,tip}$ = Maximum geotechnical end bearing resistance pressure $[\frac{N}{m^2}]$
$p_{r,max,shaft}$ = Maximum geotechnical shaft friction resistance pressure $[\frac{N}{m^2}]$

For **pile tip** capacity, the method of Koppejan is used. It is based on the theory of Prandtl, giving maximum capacity following soil fracture along a logarithmically curved failure plane, where the soil below but also above the tip contributes. The depth below the pile contributing is 0.7 to 4 times the tip diameter and has to be chosen conservatively (zone I and II), while the depth above is 8 times the diameter (zone III)(see figure 2.6, left). Both parts have an equal contribution to the resistance. Using the method one bears in mind that the soil always starts failing along the weakest layer, which means that after choosing a value of the CPT cone resistance ($q_c$) in zone I can never be topped as one progresses to zone II and zone III (see figure 2.6, right). The final average cone resistance number (in MPa) is adjusted by factors for that account for the difference with

the CPT measurement process: installation method ($\alpha_p$), tip to shaft diameter ratio ($\beta$), and a factor for asymmetrical piles (s). See equation 2.7. It seems factor $\beta$ for tapered piles should in theory not reduce but increase the cone friction because of further soil densification after the pile tip has passed the layer, but this is not accounted for.

$$p_{r,max,tip} = \alpha_p * \beta * s * (\frac{1}{4} q_{c,I,ave} + \frac{1}{4} q_{c,II,ave} + \frac{1}{2} q_{c,III,ave}) \tag{2.7}$$

With:
$p_{r,max,tip}$ = maximum tip resistance [$\frac{N}{m^2}$]
$\alpha_p$,$\beta$,$s$ = reduction factors for installation method, tip geometry, asymmetrical piles [−]
$q_{c,N,ave}$ = average cone resistance over trajectory 'N', for N in I, II or III [$\frac{N}{m^2}$]

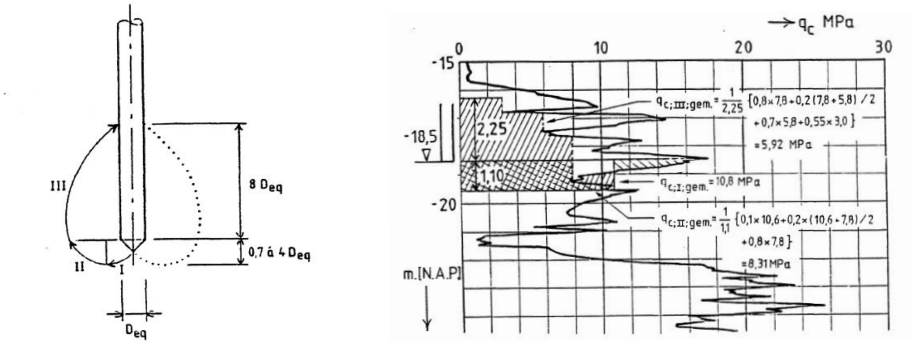


Figure 2.6: Influence zones according to the Koppejan method (left), example of averaging resistances with this method (right) From 'Funderingstechnieken', section 3.11 [24].

Shaft friction is as named before either negative or positive. The **positive shaft friction** gives resistance but can only be accounted for layers that do not or barely subside. This is why generally only sand layers are given this property, or stiff clay and silt layers with $q_c$> 2 MPa (see figure 2.7). However, if the pile is a friction pile larger settlements will occur meaning soft layers will also produce positive shaft friction. The magnitude of the friction depends on two factors: the horizontal contact pressure on the surface and the friction angle between shaft and soil. The former depends on the pressure in the original situation but even more on the installation method (due to densification or relaxation), where driving increases the horizontal pressures. The latter depends mainly on the roughness of the pile, with the surface angle '$\delta$' as a limit which is a portion of $\frac{2}{3}$ to $\frac{3}{4}$ of friction angle '$\phi$'.
Just as with the pile tip end bearing resistance, the (maximum) shaft friction resistance can be based on either in situ tests (e.g. CPT) or on (theoretical) shear strength characteristics of the soil layer. Again, the first method is preferred in Dutch practice and incorporates both the dependencies described above, see equation 2.8. Though sleeve friction is also often directly measured in CPT measurements, but the method using a

percentage factor $\alpha_s$ in combination with the cone resistance $q_c$ was deemed more accurate.

$$p_{r,max,shaft} = \alpha_s * q_c \tag{2.8}$$



With:
$p_{r,max,shaft}$ = maximum shaft resistance $[\frac{N}{m^2}]$
$\alpha_s$ = factor dependant on pile type roughness [%]
$q_c$ = cone resistance over trajectory where positive friction is expected $[\frac{N}{m^2}]$

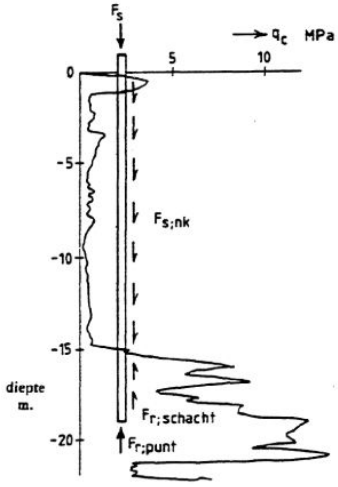


Figure 2.7: Shaft friction visualised. From 'Funderingstechnieken', section 3.1 [24].

On the other hand, **negative friction** should be added as a load on the pile. Its magnitude can become as large as the force on the pilehead. The occurrence is after settlement of layers along the pile due to surcharge loads or lowering of the watertable that results in consolidation. It can also occuring after pile driving because of re-settling of the soil due to its self-weight. Negative friction has not been taken into account before the 1930s, resulting in under-performing foundation designs for some cases in the years before. Another source mentions 1950 as the turning point for including negative friction [10]. The magnitude and location depend on relative movements between soil and pile and therefore is dependant on the equilibrium situation. Generally, it is taken into account for ground level settlements of more than 20 mm. Since settlement of the weak layers is smaller the deeper along the pile one goes, the negative friction can turn into positive friction in the weak layer as well. However, with a ground level settlement of 100 mm the practice tells that the entire top layer generates negative friction along the shaft. For values between 20 and 100 mm an equilibrium calculation can be made.

The surcharge load on the soil per ground surface area taken by the pile can be taken as maximum value, because no further settlement will occur if the pile takes this whole force. But other methods are preferred due to the uncertainty about other driving factors for settlement. One of them is the *slipmethod* that is an upper bound method that assumes slip and therefore full downward friction (as described in equation 2.6). Due to this assumption it is mostly used for single piles or piles at the edge of pile groups. For group behaviour, the downward force is distributed over multiple piles and the negative shaft friction is less likely to be fully mobilised. The method *Zeevaert & de Beer* uses the horizontal stress as a result of vertical effective stress deducted with the stress taken by shaft friction, since the soil reacts to the shaft friction generated at the pile surface. A differential equation is the result and it shows a large difference for closely placed piles and a smaller difference with the maximum friction by the slipmethod for piles placed further apart (see figure 2.8).

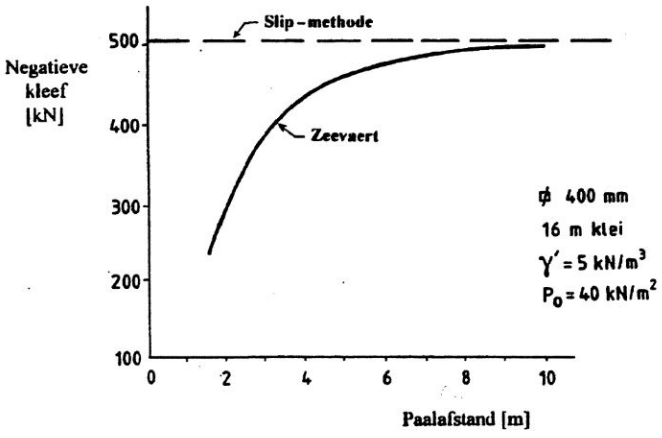


Figure 2.8: Comparison of the activated negative friction (y-axis) between the slip- and Zeevaert & de Beer methods for increasing pile to pile distance (x-axis). From 'Funderingstechnieken', section 3.28 [24].

**Settlements** are due to instantaneous deformation, negative friction (new equilibrium) or compression of deep layers. The settlement of a single pile depends on:

1. Elastic shortening of the pile (with a variable normal force);
2. Necessary deformation to provide tip bearing resistance;
3. Necessary deformation to provide shaft resistance.

The interaction of these will determine the way the force is distributed along the pile into the underground. Force-displacement diagrams are made from numerous samples to show a relative number for 2 and 3 of the above dependencies.
For the elastic shortening, the axial force distribution must be known. A loading experiment for a typical West-Netherlands soil profile (see figure 2.9) with clay and peat shows

us that the ratio of force taken by the pile tip and pile shaft varies largely as the pile is loaded, where shaft friction is mobilised faster than end-bearing. After waiting for consolidation of the weaker layers due to surcharge load shows us the final force in the pile can be larger than the original force applied at the head. It is of importance to find the normative cross section (curve 6 in figure 2.9).

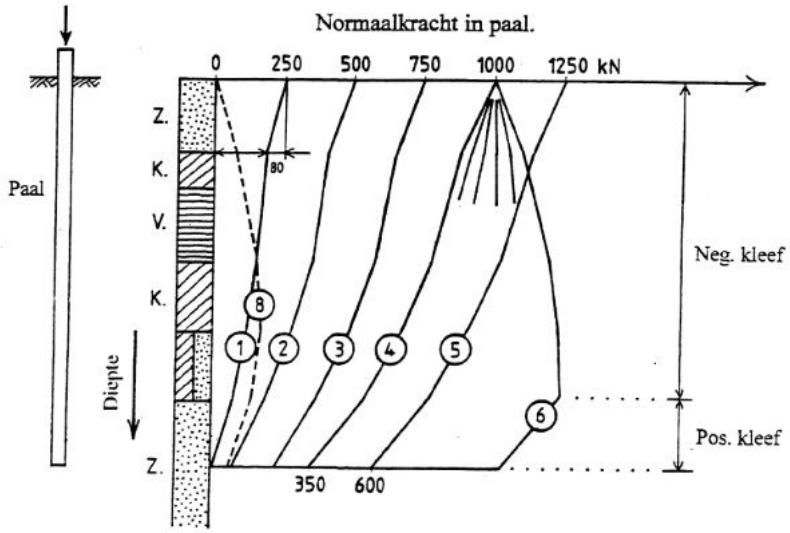


Figure 2.9: Proof loading of a pile in a soil profile typical for the west of the Netherlands. Plotted on the x-axis is the axial force in the pile, over the y-axis is depth: 'Z' = sand, 'K' = clay, 'V' = peat. The curves in between 4 and 6 show a time increment in which settlement of soft layers due to a surcharge load occurs [24].

Pilegroup effects under compressive axial loading are positive for driven piles as they densify the soil, and are negative for bored piles as the loosening reduces the ground pressure along the piles.

**Lateral loading** can result in rotation for short and bulky piles or in bending failure or local soil fracture near the pile head for long and slender piles. The loading occurs due to moving soil (load along the entire pile) or by external loading (load occuring at the head). According to EN 9997-1 [9], group effect needs to be taken into account and the resulting force distributions. The interaction in groups is through the pile cap (attention needs to be given to the support conditions) and the deformable soil medium. The eurocode states resistance can be obtained through destructive or non-destructive testing or with soil & pile characteristics [9], but no further detailing is given.

The group effect for lateral loaded piles is in negative: the sum of the capacities of the piles in a group is smaller than the capacity of a single standing pile multiplied with the amount of piles in the group; this is called the efficiency. The reason for this is the shadow effect; the second pilerow is in the way of the soil that gives the horizontal bearing resistance to the first pilerow. See figure 2.10.

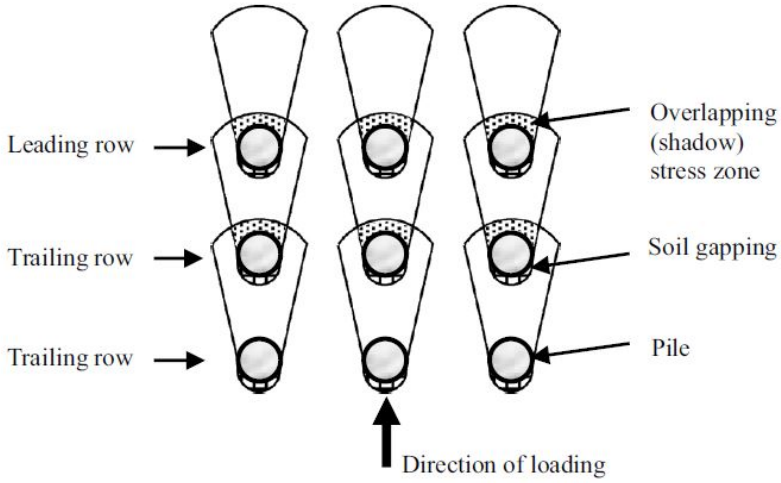


Figure 2.10: The shadoweffect. Original picture from [26]

Ultimate bearing resistance can be estimated by the Brinch-Hansen equations, that take into consideration a rigid pile and a resultant soil pressure (passive minus active). The failure lines it uses are straight and inclined towards the ground level at small and moderate depths, but horizontal at larger depths. The basic equation has effective stress, angle of friction and cohesion as input parameters (see equation 2.9) [27].

$$e_{(D)} = q * K_q^D + c * K_c^D \tag{2.9}$$

With:
$e_{(D)}$ = ultimate bearing pressure at depth D $[\frac{kN}{m^2}]$
$q$ = Effective overburden pressure at depth D $[\frac{kN}{m^2}]$
$c$ = cohesion $[\frac{kN}{m^2}]$
$K_c, K_q$ = Factors dependant on soil strength, pile diameter and depth $[-]$

Calculation models for lateral loading can be distributed into three groups [28].

1. Spring models (e.g. Cap interaction, Mindlin, various Spring reduction models);
2. Continuum models (Poulos model, Koch model);
3. Finite Element Models (FEM's).

The outcome of all models shows a certain distribution in efficiency factors (utilisation of the pilerow), where an unsymmetrical solution is most reliable. The front pilerow will take up more force than the ones behind, certainly if the pilerows are placed close together and the their soil influence zones overlap [28].

The **spring models** makes use of discrete spring stiffnesses to model the soil restraint. Next to this, interaction is possible through the cap (or only through the cap in the Cap model). The limitation in this approach are difficulties in choosing correct force-displacement curves for a combination in pile size and soil type [25]. Pile group behaviour is modelled better if the interaction through the soil layers is implemented (e.g. Mindlin model).

**Continuum models** are analytical as well and use various constitutive models to characterise the continuous soil medium [25]. The Poulos model models the soil as an elastic medium, while the Koch model enables local plasticity (usually near the pile head)[28] which corresponds to the local soil fracture as described in EN 9997-1 [9].

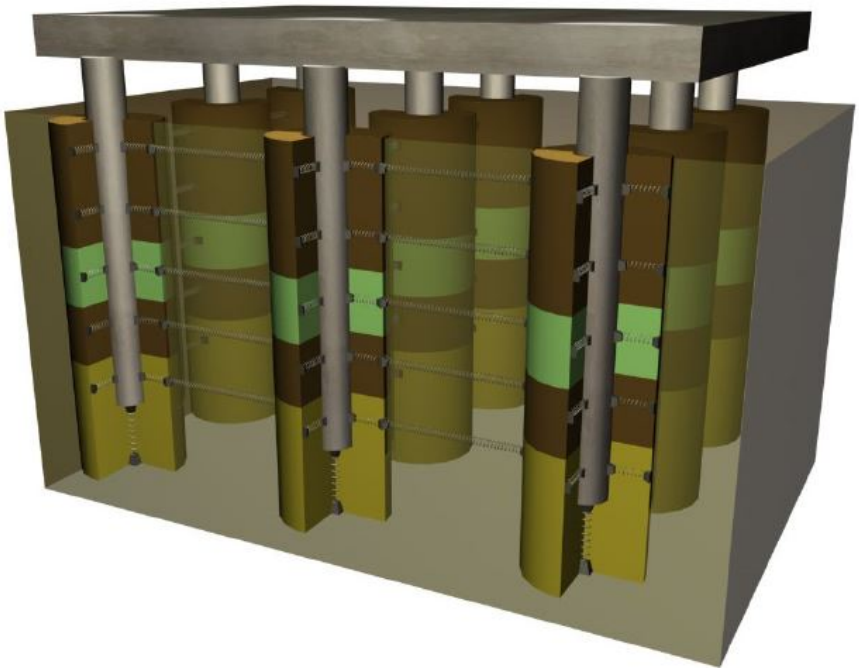

Figure 2.11: Example of a spring model (Mindlin). Interaction takes place through the cap and through the soil layers [28].

**FEM Models** use discretization of the soil layers and the pile elements with a numerical solution to the displacement field problem. Modelling of piles in 2 dimensions can only be done for a single pile (cylindrical coordinates) or with an equivalent embedded beam row, where it is made sure that the pile row is not modelled as a wall with the use of spacing factors (which would be the result if the 2D analysis would be extruded). This results in a "2.5D modelling" where the embedded beam is connected to -but not present in- the mesh. This allows for soil movement in between the pilerows. A 3D analysis is a good option but requires more computational cost. Piles can be modelled as a volume pile (the 'classic' solution of a volume with given properties of the pile it represents and an interface with the soil) or an embedded beam (a one dimensional beam element that

needs an extended interaction surface for correct modelling). The volume pile requires larger computational costs but performs better in ULS calculations and lateral load situations [29]. Unfortunately, both models have the drawback of not including installation effects. This is a topic of research.



For the software programme of Plaxis 2D, Sluis [30] has researched the embedded beam element and concluded on interface spacing factors that link the elements with the mesh behind it by stiffnesses. His study was based on axial loading. He recalls Plaxis does not take into account loading effects and therefore bases the stiffnesses on bored pile characteristics from NEN9997-1. Sluis mentions the large differences in reaction of piles at the head and the base when loaded laterally and concludes this is modelled correctly in Plaxis 2D only for close spacing, up to 4 times pile diameter. At larger spacings, either the differences between soil and pile movement are too large, or when the default factors are adapted, the difference at the bottom becomes incorrect [30].
The Plaxis 2D 2019 manual stresses the embedded beam element is more realistic in modelling horizontal forces along its shaft than at its top, which seems in correspondence with the conclusions of Sluis [31].

*Now that the base of design aspects is given in the form of a historical use overview, material knowledge and characteristics of placement in soil, the focus of the literature study shifts towards assessment and modelling of existing structures. These are necessary to make statements on the capacity and if it is sufficient.*



## 2.5. ASSESSMENT OF EXISTING STRUCTURES ACCORDING TO CURRENT CODES

Norms and guidelines are available for assessment of existing quay walls, quay wall foundations and timber foundations in particular. First, the base of the assessment method according to the Eurocode will be given, and differences with regular design of new structures highlighted. For the next step: implementation of these rules on timber foundations, see section 2.7.

### 2.5.1. REASONS AND TYPES OF ASSESSMENT

The reasons for different assessment of existing structures in comparison to new structures are [32]:

1. Larger costs to implement an equal economical and social safety level that follow from changing regulation;

2. Different reference period: the theoretical remaining period of usage is lower and different peak loads are to be expected within the time frame;

3. More certainty of the in-situ structure can be obtained by measurements, in contrast to designing a yet-to-be built one.

The norm series for assessment of existing structures is the EN 8700 to 8709 series, corresponding to the eurocodes 1990 to 1999. Not all are yet ready, including EN 8705 for timber. It makes assessment on two levels possible: *Renovation* (including new objects in the structure) or *Disapproval* (excluding new objects). The latter may sound as if the final decision statement has already been made, but this is not the case. If a check is to be given on the disapproval level, use can be made of lowered load factors or a different use can be incorporated but never both at the same time [32]. If the structure is finally disapproved, no variable loads may be applied till replacement, reinforcement or demolition. Since inland quay walls are neither bridges [32] or primary water-retaining structures [10], they should be assessed according to the rules for buildings. Since this thesis is about the verification of an existing structure and not of a renovation, the 'disapproval level' will be the further focus.

### 2.5.2. REFERENCE PERIODS VERSUS REMAINING LIFETIME

NEN 8700 states that a remaining lifetime is the period in which an existing structure or renovated structure is usable for the chosen function and use. The reference period is the period used for obtainment of statistical calculations and the correct variable and extreme load factors [32]. It is clear that the remaining lifetime follows from present

strength (unchangeable) and wanted use (changeable), where the reference period is chosen by the designer to accommodate correct calculations needed for the remaining lifetime.



Reference periods that are allowed to be used are coupled to the consequence class (CC) of the structure. This class is coupled to economical and sociological (including harm or death to humans) consequences of a collapse. Inland quay walls are in CC2 and need a reference period of at least 15 years for the disapproval level assessment. If however the choice is made to use a (considerably) longer reference period, one should assess according to the new design level (described in the norms EN 1990-1999) [32]. In line with the used reference period of 15 years, the guidelines of F3O (the (Dutch) organisation for independent research on foundations) uses an inspection & assessment period of 10 years.

### 2.5.3. SAFETY PHILOSOPHY

For the standard procedure, use is made of the $\beta$ method. This factor is the reliability index given to a reliability class (RC) and incorporates a yearly failure chance. The reliability class (RC) gives then the reliability that is coupled to a consequence class. For CC2, RC2 a $\beta = 2,5$ holds, which gives a failure chance of $2 * 10^{-4}$ per year . The $\beta$ indeces use accepted or assumed statistical change of resistance & load effects and modelling uncertainties. Further differentiation in EN8700 is made for wind-driven and non-wind driven design (with wind being the normative load) and a statement is made on the allowed use of lower consequence classes for parts of the structure where a lower consequence of collapse can be proven [32].

Next to this, it is allowed to use the *Observational method* which uses measured deformations and derives present stress from this situation. Another method is the *Proven strength* method: if original design is according to old building rules, if all extreme loads are well documented and if these loads are lower or equal to the current loads, the structure is approved [32]. This can be used if [10]:

- Normative loads from the past have been resisted;
- No damage has taken place after extreme situations;
- No degradations have occurred, no disadvantageous changes have been made;
- All the information can be confirmed with sufficient reliability.

However, if not everything is present, the concept of proven strength can still be used by the *correction factor method*. It uses an adapted Factor of Safety (FoS) equation 2.10.

$$FoS_{current,corrected} = \frac{FoS_{current\ norm}}{FoS_{original\ design}} \tag{2.10}$$

Since proven extreme/normative loads are often point loads, this approach can be used for quay walls only if [10]:

- The quay wall has a constant condition;
- Shows similar behaviour throughout history;
- Has a constant soil profile and build-up over its length;
- If a check is made on dredging and scour depths at the embedment location.

Furthermore, an approach must be followed with regard to uncertainties. *Systematic uncertainties* (e.g. the soil profile) are always uncertain but do not change. A choice can be made in three scenarios: optimistic, average or conservative. *Non-systematic uncertainties* (e.g. traffic loads) are uncertain and can change. These should be taken on the conservative side (low value) for resistance related parameters and on the optimistic side (high value) for the loading related parameters. The former is often forgotten, where a calculation is made in the 'as built' (optimistic) scenario. The uncertainties for historical quay walls in resistance are pile tip level, pile configuration, racking pile angle, diameter piles over length (taper). The uncertainties in loading are the level of drainage and placement of non-structural elements in the vicinity like trees, cable pipes and structural elements as e.g. mooring objects [10].

### 2.5.4. FACTORS AND ASSESSMENT

The final assessment can be made on three levels [10]:

1. Simple: A scheme that requires no calculations, but a statement that everything has been done by the book and no degradation has taken place.
2. Detailed: Calculations show that the critical parts are safe and that the stability can be ensured.
3. Advanced: A Finite Element Analysis (FEA), probabilistic calculations for exact safety factors, changing chance of failure based on inspections. using proof-loading or a combination of those.

Any uncertainties in assessment or models can be checked by comparison of advanced to simple models and test or proof-loading, or the choice is made to accept the uncertainties by applying conservative assumptions [32].

When the assessment calculation is made on the detailed and advanced level, the adapted $\beta$-index results in different load factors '$\gamma_F$' factors (equation 2.12). The adapted reference period also changes the value of the variable loads (equation 2.11)[32].

$$\gamma = 1 + \alpha * \beta * V \tag{2.11}$$

With:
$\alpha$ = An influence factor (usually 0.7) [−]
$\beta$ = The required reliability index [−]
$V$ = The coefficient of variation of the load [−]

$$F_t = F_{t0} * \left(1 + \frac{1-\psi_0}{9} * ln(\frac{t}{t_0})\right) \tag{2.12}$$



With:
$F_t$ = The adapted extreme value of the distributed variable load at chosen reference period $[kN/m]$
$F_{t0}$ = The extreme value of the distributed variable load at base reference period (often 50 years) $[kN/m]$
$\psi_0$ = The $\psi_0$ value from table A1.1 or A2.1 from NEN 8700 $[-]$
$t$ = the reference period chosen $[years]$
$t_0$ = The base reference period (often 50 years) $[years]$

The reason of reduction in loads from the design reference periods of 50 or 100 years to 15 years are [32]:

- Future trends are not of interest;
- Chance on extreme loading gets lower;
- Change in loads for fatigue gets smaller (steel structures).

On the material resistance side, the $\gamma_M$ partial factor can also be adapted. The elements can be tested and proof loading can take place in order to conclude on a certain material quality. In theory, proof loading and testing can lower $\gamma_M$ to 1.0, but if a single characteristic is tested the exact influence on the partial factor that also includes aspects as eccentricities is hard to predict. NEN-ISO13822 And the JCSS (Joint Committee on Structural Safety) give guidelines for this, but often the partial factors on the loading side are the only ones adapted[32].

If the structure is disapproved, one can either choose to demolish and replace it, or choose from the following [10]:

- Change the use class and thereby lower the Reliability Class and required safety level;
- Lower the loading, which inquires a quantitative change in use;
- Lower the reference period, by taking the end-of-use date closer. Shorter use means lower peak loads.

## 2.6. SERVICE LIFE ESTIMATION AND MODELLING

All structures have a certain remaining service life that depends on residual capacity, past & present loading and planned future use. This section goes deeper into the possibilities of service life modelling for timber structures.

### 2.6.1. CURRENT MODELS

Modelling service life comes from the need of (current) safety assessment, the need for possible interventions (strategic maintenance planning) and to asses the possibilities for future use [33]. Moreover, for timber the fact that its failure occurs within a very short timeframe and that creep decay is not visible to the naked eye adds up to these arguments [34]. A specific reason for foundations is that any damage prevented to it also prevents damage to the upper structure resulting from it [33].

A standard way of applying creep degradation is use of the $k_{mod}$ factor as described in EN 1995. This factor does not take into account the load history of the structure and will therefore lead to inaccurate estimations. Models have been developed that do include the load history and creep decay (such as the model of Gerhards [35]). An important factor they still miss however, is the impact of other degradation modes than creep only [34].

### 2.6.2. IMPLEMENTATION OF DECAY

Implementation of timber specific decay mechanisms that alter the service life can make the estimations more accurate. The influence of cross section modification to the remaining capacity over time becomes clear as well, a factor that is assumed to be constant in current codes. An example is crack development. Furthermore, implementation of timber-specific decay is needed because relationships between density and strength cannot be used for decayed materials [36].

Before decay can be modelled, it has to be measured. This is possible with inspection methods combining visual assessment and sharp tools. Pilodyn hammers can be used or their blow type counterparts that penetrate a steel needle into the specimen. Drilling and testing of bore cores have proven to give a high correlation for compression strength - an important parameter for timber foundation piles. For dry conditions, drilling methods based on torque resistance are an option too. Another possibility is making use of non-destructive techniques like the ultrasound stress wave technique [33].

Important to point out that the outcome of decay in terms of loss of mass per time are not handy for engineers. Much more preferred are strength values and their distribution over the cross section [36].

### 2.6.3. THE MECHANICAL & DECAY INCLUDING DAMAGE ACCUMULATION MODEL

The estimation of the residual lifetime as stated by van de Kuilen [33] includes a historical situation analysis, together with a measured decay state and planned future use. The model is a damage accumulation model based on the one of Gerhards [35], see equation 2.13 that states the rate of damage. A relative load level is placed in its formula that includes mechanical decrease in strength, biological and physical degradation by decrease in strength and an increase in load (stress) due to a changing cross section. All factors are time dependant.

$$\frac{d\alpha}{dt} = exp\left(-C_1 + C_2 \frac{\sigma(t)}{f(t,T,\omega,\lambda,\mu,...)}\right) \tag{2.13}$$

With:
$\alpha$ = Damage $(0 \leq \alpha \leq 1)$ $[-]$
$C_1, C_2$ = Time-to-failure parameters obtained from tests on fresh wood $[-]$
$\sigma(t)$ = Time dependant occurring stress $[Pa]$
$f$ = Variable strength $[Pa]$
$t, T, \omega, \lambda, \mu$ = Time, Temperature, Moisture Content, Cross section reduction parameter, Strength degradation parameter

$$Z(t) = R(t) - S(t) = 1 - \alpha \tag{2.14}$$

With:
$Z$ = Residual capacity , e.g. $[kN]$
$R$ = Resistance , e.g. $[kN]$
$S$ = Load , e.g. $[kN]$
$\alpha$ = Damage $(0 \leq \alpha \leq 1)$ $[-]$

The limit state function (equation 2.14) shows the dependency of the residual capacity on the damage. Damage accumulation models can be compared to fatigue models in steel (stress and blow count numbers versus stress and loading time for timber). The output is time dependant safety due to time dependant loads and time dependant material properties [36]. A visual representation can be seen in figure 2.12.

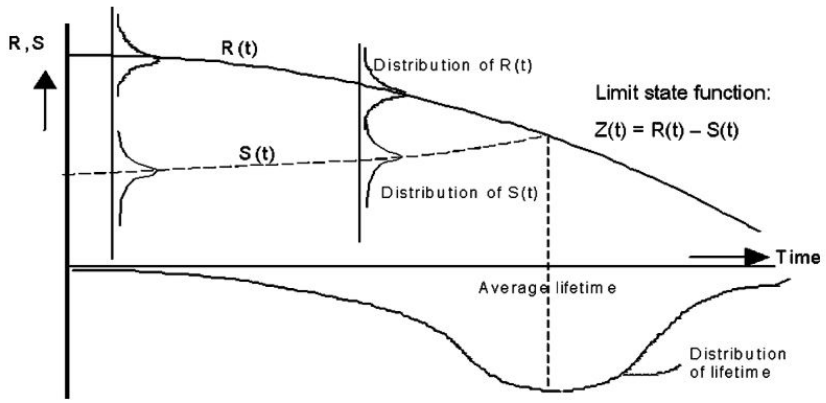


Figure 2.12: The limit state function visualised over time. Original from Siemes, as placed in (van de Kuilen, 2006) [33].

Input for the damage accumulation function from the loading side (S(t) / $\sigma(t)$) is an estimation of loads and moisture contents, temperatures. This is to be done by archival

research, where it is especially hard to estimate peak loads. The load model suggested by van de Kuilen & Gard is from Ferry, Borges and Castanheta, which divides the year into blocks with several load levels [34]. The variable load values are based on the $95^{th}$ percentile for a return period chosen by the user. From the resistance side (R(t) / $f(t,T,\omega,\lambda,\mu,...)$), an important input parameter is the original strength, which must be assumed with a certain spread if unknown. Then as with loads, the moisture content and temperature are to be found through archival research. For the decay parameters $\lambda$ and $\mu$, a degradation development or damage pattern needs to be implemented: how will the cross sectional area decrease or how will the strength be influenced? The time-to-failure parameters $C_1$ and $C_2$ are obtained with fresh timber tests, and a steeper failure curve is to be expected for decayed wood. However, decay is now incorporated in the strength function in equation 2.13 which also has an influence on the curve. Lastly, an intervention level is to be stated that incorporates the minimum safety level expected [34].

For building or formation of the function a stepwise time integration is needed. The output is a time dependant safety that can, next to assessment, also be used for a sensitivity analysis of different load sets or material parameters. Studies from van de Kuilen & Gard showed that high peak loads, even for short timespans, can lower the residual load capacity immensely [36] and that timber failure is initiated in a very short timeframe [34]. Possible cases for this model are e.g. drying cracks in beams, radial decay in foundation piles and delamination due to weathering in glulam [33][36][34]. See figure 2.13 for an implementation example by van de Kuilen & Gard [34].

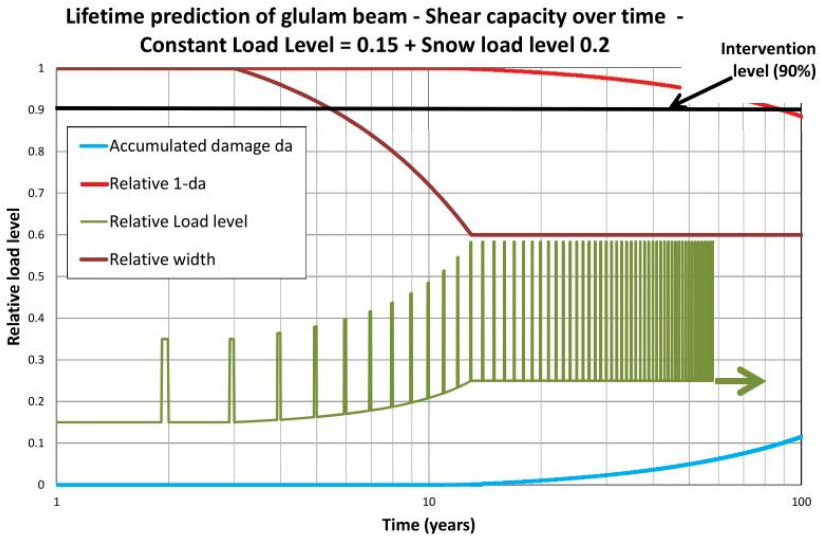


Figure 2.13: Damage evolution of a delaminating glulam beam, where the intervention level is reached after approximately 87 years. Figure from (van de Kuilen, Gard, 2013) [34].

Missing for wider use of this model is the residual strength in decayed wood and the exact rate at which decay reduces the cross section [33], though research is in progress. The obtainment of time-to-failure properties (incorporated in constants $C_1$ and $C_2$) for decayed wood are also missing [36].



## 2.7. INVESTIGATION, INSPECTION AND IMPLEMENTATION

Norms and guidelines describe research and inspection to be implemented and a calculation method. Since these are quite extensive and well-described, an overview is given on the general method and important details for Historical quay walls (as described in 'Binnenstedelijke Kademuren' by Roubos, de Gijt and Grotegoed [10] and the norm NEN 8707), for existing timber piled foundations (as described in the F3O guideline for deep foundations [37] and NEN 8707 as well). As stated in section 2.6, no elaborate service life modelling is incorporated in the current norms.

### 2.7.1. HISTORICAL QUAY WALLS

The norm for existing quay walls is EN 8707 (from the EN 8700 series for existing structures) which is based on EN 9997-1. The corresponding Dutch guideline for historical inner-city quay walls is the book 'Binnenstedelijke Kademuren' or 'BiKa'. Any details on timber foundations, though also described in these two documents, are skipped in this subsection and provided in the next.

The aim of the *'BiKa' guideline* is to build onwards on the general guideline for (new) quay walls, 'Handbook quay walls, $2^{nd}$ edition', and to make a uniform assessment possible for existing inner-city quay walls as they have proven to be problematic. Next to age related problems, a shift in the function is mentioned. Where it used to be an industrial, waterside dominated function it shifted to a recreational, landside dominated one for most of the inner-city historical quay walls. Next to this current codes and norms would often result in a negative judgement, as described in paragraph 2.5. The guideline also names a management approach including maintenance and inspection, which will be omitted, except the fact that next to a *preventive* approach a *corrective* approach is a possibility too for elements that are easy and quick to repair. A 10-yearly check for remaining lifetime is advised, which is also the timespan for large maintenance as it greatly affects functionality and liveability of the quay and the neighbourhood.

Assessment is performed on safety, functionality and aesthetics [10]. The following is based on EN 8707 unless stated differently; it mentions the next verification steps [1]:

1. (Archival) Data assimilation of the assessed structure;
2. Inspection;
3. Calculation of the geotechnical capacity;
4. Check of the resulting present material stresses;
5. Assessment of the Remaining Lifetime.

The **archival study** includes structure (build-up), soil layers & water levels, adjoining structures [1] and load history [10]. Additionally, for the piled foundation part, installation and placement data, pile level and dimensions and changes to the foundation are named. For soil retaining structures and anchors consulting the original calculations is stressed. The allowed CEMT class for berthing is also mentioned.

Next, the **inspection** should include a visual elaboration of the out- & inside of the structure and measurements of dimensions, deviations, deflections and rotations. A check must be made of the situation and dimensions with the original drawings and data from the archival study, also regarding the soil build-up and water level state. Additionally, for piled foundations at least 3% of the piles or a minimum of 3 pieces for the Rotterdam-type foundation system should be inspected and if the groundwater table is 0.05 m or less above the timber a yearly monitoring program is to be set up. Additionally, Roubos & al name the check for washed soil due to scour around the pile base at embedment depth [10]. For soil retaining structures a measurement of the soil level under water (on the wet side) is to be done until twice the retaining height, as well as the sludge thickness. The state of steel walls is to be checked with regard to corrosion and remaining thickness. A check of the quay wall furniture (e.g. boulders and ladders), cables and a check for placement of additional concrete behind the retaining wall are named too [1]. BiKa names three levels of inspection, each with their own return period: Base geometry (type 0), Deformation measurements (type 1a), Visual deviation search (type 1b), Technical inspection with possible sampling (type 2/3).

The **calculations** on structural and geotechnical capacity is the following step. For soil, the parameters $phi'$,$c'$ and $c_u$ are to be taken from the peak value of triaxial and DSS (Direct Simple Shear) tests. For piled foundations, a change in pile tip level of +-0.25 m is to be taken into account. Pile factors are to be taken as in annex G: $\alpha_p$ = 1.0, $\alpha_s$ = 0.010 (straight) or 0.012 (tapered) and $\alpha_t$ = 0,007, *if* the structure is build before 2003 or has a building certificate from before 2017. From the loading perspective, a reference is made to the guideline 'Binnenstedelijke Kademuren' as it has an elaborative description. As a calculation is made in chapter 4 , the elaboration is given there. Partial load factors to be used are also named in EN 8707.

**Assessment** can be made on three levels, as described in section 2.5.4. Maximum settlements and rotations for each specific reference period are given in EN 8707, annex C. Named Ultimate Limit State failure modes, coupled to their abbreviation in EN 9997-1: vertical compressive pile pressure (GEO), vertical tensile capacity of piles (GEO/UPL), horizontal soil fracture (GEO), overall stability loss (GEO/EQU), structural failure of retaining wall or piles (STR), failure due to imposed very large deformations (STR) and failure by erosion or piping (HYD). Named Serviceability Limit States are: functionality loss, aesthetical loss, out of bounds deformations in the surrounding, leakage by transport of elements (soil) and unwanted $2^{nd}$ order effects for slender elements [10].

### 2.7.2. EXISTING TIMBER DEEP FOUNDATIONS

The guideline that has been set up for assessment of existing piled foundations in the Netherlands is written by the F3O group and is called *'Richtlijn Houten Paalfunderingen onder gebouwen'* [37]. It is referred to by the EN 8700 series in the Dutch version. Like the guideline for historical quay walls, its aim is to give one standardized assess-

ment method, but specializes on timber foundations under buildings. It could prevent collapse, demolition or unnecessary repairs and gives the management of a structure an indication of a maintenance free period. The reason for the start of this project is the bad suitability of assessment methods by the Bouwbesluit of 2012 for old structures that often result in a rejection. The reason of this rejection for timber piled foundations specifically is an empirical approach using blow count for the last 30 cm of penetration and the negligence of negative skin friction before 1950, next to disadvantageous factors for timber in norms: for geoengineering the partial uncertainty factor went from 1.25 to 1.4 for timber in NEN6740,6743 and 6744 in 1991 and for timber structures the change of the partial material factor from 1.2 to 1.3 and the lowest modification factor $k_{mod}$ for sawn timberfrom 0.6 to 0.5 [37]. The information in this subsection will be from the F3O guideline unless otherwise stated.

The following are timber-specific additions to the inspection and assessment procedures, as described in the previous subsection [37].

The **archival study** explicitly mentions the levels of timber for comparison with results of earlier inspections and researches.
The **visual inspection** is twofold. If possible, an aboveground and underground inspection should be undertaken. For the case of historical quay walls however, this is often not possible. For the aboveground inspection, a check for signals should be undertaken that could result from foundational failure: settlements, rotations, cracks. The historical building level should be compared and above mentioned deformations measured. Drainage possibilities in the surroundings must be noted down.
The underground measurements should take place in a dug out hole (buildings) of at least 0.4 m underneath pilehead level, where a description is to be given of the removed soil according to NEN5104. The strived waterlevel is at least 20 cm above highest timber level. Pictures must be taken, measurements made of: Pile diameters, centre to centre distances between piles or pilecaps, skew of raking piles, capping-, transverse- and shear beam details and crack notification, embedment of piles into the above laying element, position of the pilehead with respect to a reference point and the national Dutch reference level 'NAP'. If found, a description must be made of discolourations and deformations like the squash of the capping beam perpendicular to the grain.
Specified points of notice for quay walls are described in the BiKa guide. These mention a doubled area that can be degraded in mortise and tenon joints, construction mistakes in the connection between raking piles and adjoining beams, non overlapping pile and cap (reasons are mechanical damage, wrong placement or loss of contact due to deterioration), and a corroded pilehead-ring that supposedly has no influence on remaining strength as it was placed for driving purposes only. The retaining wall is stated to often have the tongue-and-groove connection, and the state of the planks and the joint with the top beam are to be checked. A brittle failure could occur after a wash out of the soil particles if there is a street above due to the membrane action of the street deck [10].

Following is a description of **decay measurement and sample taking**. The quality of the wood is checked by:

1. Visual assessment (as described above);
2. Soft shell measurement;
3. Choice whether to do additional measurements or taking samples;
4. Sample taking;
5. Laboratory research.

Ad 2) Use is made of a calibrated impact hammer. Measurement on the pile is done 15 cm underneath the capping beam and if possible 15 cm below and at different places around the perimeter. For the horizontal timber at least three measurements 10 cm apart have to be taken, at least 20 cm of the end grain. Knots are to be omitted. For quay wall applications, it is stated that impact hammer measurements give large deviations (40%), especially in decayed wood, and that the measurements can only be supportive for laboratory research. Difference in deterioration state are to be expected over the depth of the quay wall and in front versus behind a soil retaining wall [10].

Ad 3) The choice depends on whether the wood is or is not the normative element, the remaining service life is more or less than a year or if the graph seen in figure 2.14 for piles states so. This graph is based on regularly occurring pileloads of 30 kN for a diameter of 100 mm, 60 kN for a diameter of 150 mm and 150 kN for diameters above 250 mm. The conclusions taken from it only regard the outer surface of the pile. If dry timber is found, sampling is advised as decay cannot always be seen or felt. For the quay wall application of timber foundations, it is always necessary to sample since impact hammer measurements are only indicative or as supportive evidence [10].

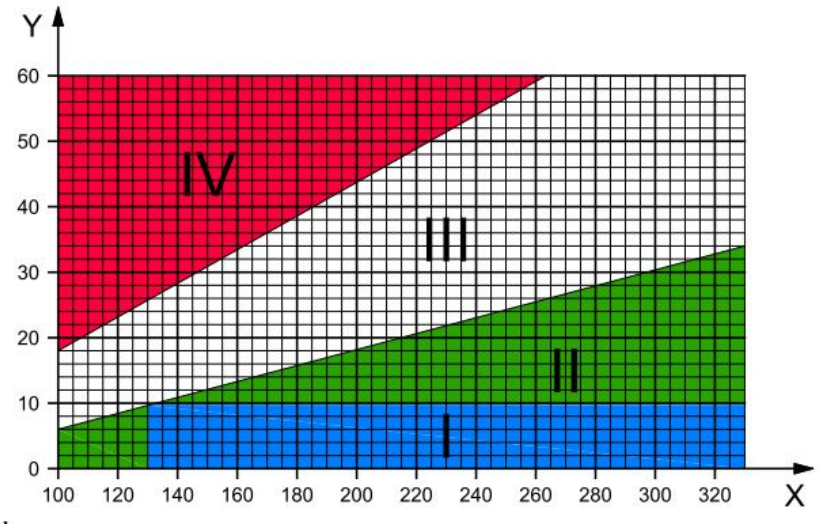


Figure 2.14: Decision making graph for sampling of piles under buildings. Under quay walls, samples are always to be taken. Pile diameter (x-axis) versus the penetration of the impact hammer (y-axis). Zone I: No significant degradation; not necessary to take samples. Zone II: Degradation is limited: taking samples is only necessary to make a statement about the type and future progress of decay. Zone III: Clear decay; it is of importance to take samples for the future perspectives of decay development in the pile. Zone IV: Relatively large deterioration; de shaft resistance is negligible. Taking samples is only necessary if the type of deterioration is of interest. Figure from the F3O guideline [37].

Ad 4) To take the sample, use can be made of a hollow drill with a diameter of at least 10 mm, with at least two samples per element around the impact hammer measurement location. The penetration should be all the way to the heart, and the place of sampling must be noted down. For horizontal timber in quay walls, end grains are of less importance because of the arc effect of the above laying stony wall. Additional sample taking is advised for later use due to the amount of effort to be undertaken for an underwater inspection [10].

Ad 5) A microscopic analysis to find the species, wood structure, constituents, type and level of decay. Measurement of the moisture content gradient and density by means of mass and volume. The strength gradient can be derived according to the model of Klaassen in certain cases, see equation 2.7.2[1]. These strength values can then be used in the remaining cross section approach.

$$f_c = 38,543 * e^{0,6965 * w} \tag{2.15}$$

With:
$f_c$ = compressive strength parallel to the grain $[MPa]$
$w$ = Moisture content at saturation [%]

The formula can be used when the wood is saturated, if the type of decay is bacterial

or if no decay is present at all, if larger samples that the standard 10 mm drilling samples are at hand and if there is not trace of fungal decay.

**Calculation** of the capacity according to the remaining cross section approach is as follows. Equations 2.16 to 2.20 are used.



For all cases:

$$A = \frac{1}{4}\pi d^2 \tag{2.16}$$

For regular cases:

$$d = D - 2(i + 5) \tag{2.17}$$

If the severe decay is local:

$$d = D - 2(i) \tag{2.18}$$

If the decayed wood has a compressive strength of more than 10 MPa:

$$d = D - 2(i - 5) \tag{2.19}$$

With:
$A$ = Remaining cross section $[mm^2]$
$d$ = Remaining diameter $[mm]$
$D$ = Original, or measured diameter $[mm]$
$i$ = Impact hammer penetration $[mm]$

For piles, the strength is to be calculated at two points: at the pilehead level and at the friction turning point along the pile, where the normal load is biggest. The strange thing in personal opinion however, is that even if larger stresses due to pile tapering can be expected below this point, but a piletip assessment is not implemented. The state of decay around this point follows from the type of decay to be expected. Since for (nearly) anaerobic conditions under ground the type of decay that influences the cross section can only be bacterial, only bacterial degradation influence is taken into account at the friction turning point. EN 5491 States a standard taper of 7.5 mm/m of diameter decrease [38], and a bacterial decay of half the thickness of the decay at the pile head is expected at the pile tip (though this is uncertain as of 2016). Following from this:

$$d = D - l * 7.5 - \frac{D - d}{2} * \frac{2 - l}{L} \tag{2.20}$$

With:
$l$ = Distance to the friction turning point $[m]$
$L$ = Total pile length $[m]$

**Assessment** consists of:

1. Stability of the foundation structure;
2. Capacity of the pilewood;

3. Capacity of the capping- and transverse beams;

4. The geotechnical capacity of the soil.



Ad 1) For structures that are coping with (mostly) vertical loads only, a check of the integrity of the joints suffices.

Ad 2) Taking the reference period into account, calculations are made for the current and future scenarios. The piles are assessed on compression perpendicular to the grain, where distinction is made between a load case for normative permanent or variable loads (equations 6.10a versus 6.10b in EN 1991-1). The former case results in $\sigma_{Ed} \leq 10.8$ [MPa] (using $k_{mod} = 0.6$) and the latter in $\sigma_{Ed} \leq 12.6$ [MPa] (using $k_{mod} = 0.7$), where use has been made of the fact a cooperation factor $k_{sys} = 1.1$ has been taken into account. According to EN 8707, decay is to be expected to carry on in the same pace as beforehand, not exceeding the border with heartwood [1].

Ad 3) The normative strength for horizontal timber is compression perpendicular to the grain. Equation 2.7.2 is used. Although EN 338 uses values of 2.5 MPa for the characteristic strength for e.g. class C24, it has been empirically deducted that larger strength values are possible if large deformations and force distribution are allowed - which is the case for foundations. A side note is made that no eccentrical loading or bending is to take place in the capping beam to use this extra plastic capacity. The value raises until 6.0 MPa for small piles in certain cases, as seen in graph 2.15. Again, EN 8707 states an equal decay speed to be taken into account [1].

$$d = D - 2(i-10); (i-10) \geq 5 \tag{2.21}$$

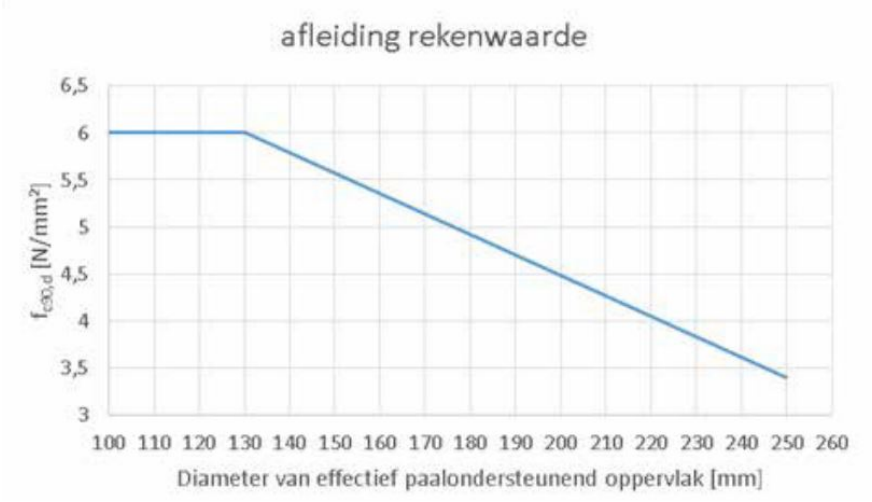


Figure 2.15: Compressive strength perpendicular to the grain in a capping beam at a joint with the pile. Strength on the x-axis, diamater of the effective pilesupporting area on the beam-pile connection on the y-axis. Figure from the F3O guideline, page 50 [37].

Ad 4) Assessment is to be made either according to the proved strength method (if sufficient data is available), or with the EN 9997-1 method described in chapter 7 with either a geotechnical calculation or an in-situ test. For the calculation EN 9997-1 states that for the negative friction value, use should be made of actually occurring settlements rather than calculated settlements, that reduced loads can be used according to the EN 8700 series and that a pile foundation should be able to carry all the loads without using the capacity of the soil underneath the beams for geotechnical category 1 and 2 (including quay walls) (paragraph 3.2.2) [9]. Important to say is that the piletip factors $\alpha_p$ are 0.7 for new and 1.0 for existing timber piles [9] [1].

Assessment is to be done by an expert and will result in **classification** into one of the three codes (with subcategories): Green, Orange or Red. Code green means: The research concludes on sufficient quality for the coming 25 years under equal circumstances. A load increase of 3 to 5% may be applied for the best category within 'Green'. Code orange means: Monitoring is necessary, as inspection and research gives no clear conclusions on the remaining lifetime. Code red means: Repair in short term is necessary and imminent.

The report is valid for 5 years and if the settlement rates and relative settlement have not changed it is valid for another 5 years. This ends up in a maximum validity of 10 years before new assessment.

# 3

# RESEARCH DESIGN

*CHAPTER 3 is all about the further steps in this thesis, that forms an introduction to the Rotterdam-focussed project on timber foundations in quay walls. Included is the methodology for the sub-questions of the coming chapters (stated in the section titles of this chapter) that will all together answer the main question: " What is the (remaining) capacity of a historical quay wall with relieving platform ?".*

## 3.1. CHAPTER 4: WHAT IS THE BUILD UP OF THE MAASKADE AND WHAT ARE THE LOADS EXERTED ON IT?

This chapter focusses on all the background information necessary to use this case for the study. From the physical boundary conditions to timelines, necessary information on build-up details and the lay out of the loads. This gives insight in what the timber elements can be tested on in addition to the stated material characteristics found in the literature review (chapter 2).



The first step in finding the build up will be an archive research on drawings and descriptions of the Maaskade. Next, relevant loading aspects for this quay specifically need to be found. The questions to be answered are:

- When is it built?
- What method was used for installation?
- How has the build up changed and what where the reasons?
- How do the connective details look like?
- Are material details described?
- Is any deterioration noted in archival documents?
- What are the soil conditions and watertables?
- In what way is the Maaskade (and with it this study) comparable to other historical quay walls in the vicinity?
- What relevant loading types are specified in the eurocodes?
- How can these load types be implemented on this case?

The combinations made with these and their quantification are stated in chapter 6 as this is the chapter that will use them as direct input for the FEM calculation.

The chapter should conclude with a series of technical drawings, material statements, environmental conditions and possible load situations for the timber foundation.

## 3.2. CHAPTER 5: WHAT IS THE STATE AND STRENGTH OF THE TIMBER COMPONENTS?

Obtainment of actual material from the Maaskade is a great opportunity to study the material, the differences of quality between different components, within one component and the spread in the population. This information will give the relevant capacity of the components after finding the relevant mechanics in the load distribution described in chapter 6.]

For elements that cannot be studied in detail, a more of a general qualitative check has to be made stating the expected type of deterioration and remaining dimensions.

The assignments to be carried out are:

- Comparison of the components with the components as on archival drawings or descriptions;
- A check for traces of deterioration and remaining component size;
- Search of traces of decay on photographic material (for items not acquired physically);
- Use of destructive and non-destructive testing for obtainment of relevant material characteristics for the expected load effects types found in literature. This is to be done for pile elements only in the scope of this thesis;
- Conversion of the found characteristics into standard reference state of 12% Moisture Content and 65% Relative Humidity, and for the state to be expected in the quay wall;
- Obtainment of missing characteristics by means of empirical formulas or by class assignment, e.g. within EN 384 and EN 338.

The chapter should conclude with directly or indirectly obtained relevant material characteristics for the Maaskade loading case as well as a description of the found state with regard to degradation mechanisms and their location on the element.

## 3.3. CHAPTER 6: WHAT ARE THE LOAD DISTRIBUTION, RESULTING STRESSES AND WEAKPOINTS IN THE QUAY?

Having found the layout, connection types, component size, relevant environmental & material characteristics, the loading types on the timber foundation and relevant assessment level, this chapter makes computation of the load distribution possible under specified safety approach.

The actions that should make this possible are:

- Statement of relevant safety philosophy, factors and loadcases (the general input);
- Set up of a computational model that incorporates the environmental factors for soil and water, proper foundation set up and component sizes, (remaining) strength characteristics found in chapter 5 and load cases from chapter 4;
- Execution of the proper/realistic load cases in a converging run;
- Computation of the resulting stresses from the computational model output;

- Statement of the moment of failure, the type of failure and the weakspot (with a local failure);
- If strength is abundant, the loads can be increased to find out the moment of collapse.

This chapter is of relevance for further computations using damage accumulation models as it states the steady-state loading throughout the years 2.6.3, which are a possible continuation of - but are not included in - this thesis.



## 3.4. CHAPTER 7: DISCUSSION, CONCLUSIONS & RECOMMENDATIONS

These chapters sections are here to provide the reader with a critical view on- and possible interpretations of- the obtained results, before concluding on the answer of the main question by the findings of the report and giving lessons learned. Expected results are comparisons between occurring design stresses and concluded design resisting strengths and pinpointing the weak spots. A capacity can be given in an amount of load that can be taken on the moment of collapse. The end gives guidelines to further research or recommendations for practice.

# 4

# History, Build-up and Loading of the Maaskade

*Chapter 4 describes the necessary archival research to find out about the basics of the quay wall de Maaskade: history (age and use), surroundings (soil layers, water levels), build-up (placement and renovations) and detailing (connections, materials). The focus then shifts towards the most western wall sections named in the scope. When these backgrounds are known, norms and guidelines are used to find the relevant loading on the wall that will be input for computational analysis in chapter 6. Additionally, a comparison is made with other quays to make a statement on applicability of this study on other quays.*

## 4.1. HISTORY & ENVIRONMENT

### 4.1.1. NOORDEREILAND

The Maaskade quay is one of the two main quays of the *Noordereiland*, a man-made island on the edge of the city centre and in the middle of the river *Maas*. It is part of the expansion of the city outside of its $16^{th}$ century walls that took place from 1825 onwards.

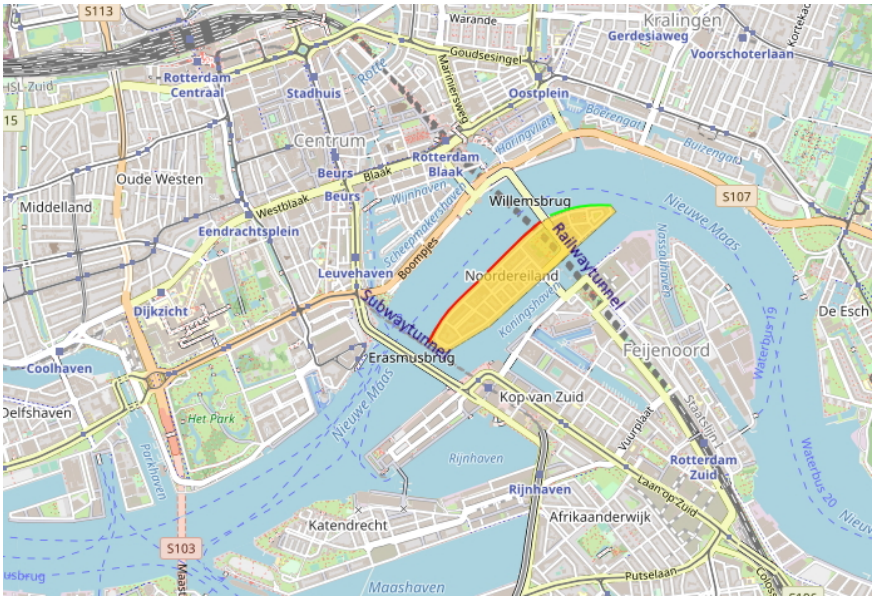


Figure 4.1: Location of the Noordereiland (highlighted in yellow), with the Western side of the Maaskade in red and the Eastern side in green [39].

The first known use of the location is from around 1600; the current island was just a sandbank and used to hang criminals. Later on, a quarantine building for people bearing the plague was placed [40]. In 1820 a slope for a ship repair yard was built, which was later shut down in 1895 [41].

The history of this location as an island starts in 1860, as between this year and 1880 a canal was dug out in the sandbank, forming an artificial island. After placement of 4 bridges (road and railroad ones) in 1878 the island became an important stepping stone between the two shores of the river Maas and an attractive location as it accommodated land- and water based transport alike. Industry started to boom, with many factories including the first lightbulb factory in the Netherlands being placed here. The north-eastern tip became the place of departure for the ferry to Antwerp [40].

The Noordeiland was partly damaged at both tips due to missed bombings of the British RAF and the Dutch airforce on the $10^{th}$ and $11^{th}$ of may 1940 respectively, in an attempt to destroy the bridges and stop the German advance from the south. The con-

sequences noted down were a few destroyed buildings and a fire [42].

Post WWII the island saw a decline in industrial activity and a general pamper is noted. It was flooded during the great flood of 1953 [40], was cut-off at the south-western tip due to placement of a subway tunnel in 1968 [43] and saw placement of a railroad tunnel in 1990 [44]. The inhabitant number fell from 8000 to 3300 [40] [45], but the neighbourhood underwent a change when the art project *Motorschip Noordereiland* started in the year 2000 and is currently revitalising [45]. Throughout the years, its quays have been used for industrial supply, as bridgeheads, swimming pool and ferry 'accesses', and are still in use for mooring and as a parking lot today.

### 4.1.2. SOIL BUILD-UP



As the Noordereiland is originally created with sediments from the river de Maas, and cut from the mainland afterwards, it shows an interesting soil layering. Visible in CPT measurements, clays and sands are both present in the top layer. It seems the term 'sandbank' is correct for at least parts of this island; the characteristic Rotterdam soil profile is not met as the top clay layer is not present in all parts of the island.

Specifically for the Maaskade, an overview has been set up from CPT measurements from the waterside and landside, see figures 4.3 and 4.5. The corresponding 'sections' of the Maaskade are further elaborated on in section 4.2. The west side of the Maaskade has been named in the scope and will be the part elaborated. The soil used directly above the retaining platform has also been investigated; see figure 4.4.

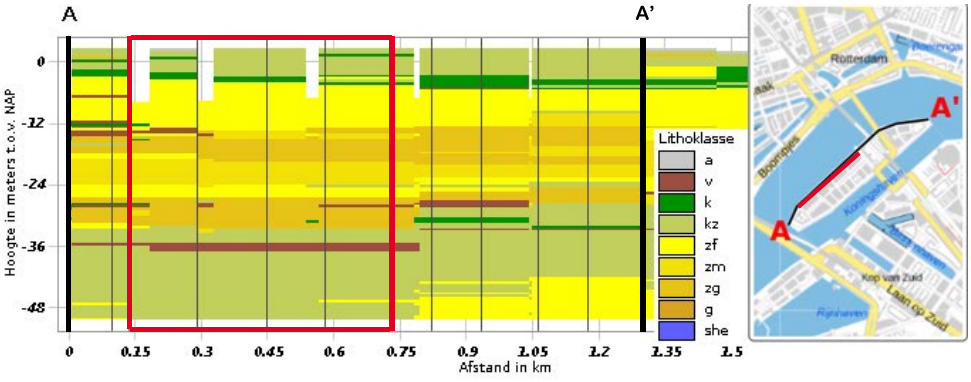


Figure 4.2: Soil profile of the entire Maaskade as produced by the automatised system *BRO GeoTOP v1.3* from Dinoloket.nl. The lately rebuilt area as indicated in figure 4.3 is now in a red contour. Legend: v-peat, k - clay, kz - clayie sand, zf - fine sand, zm - medium sand, zg - coarse sand, g - gravel. [46]

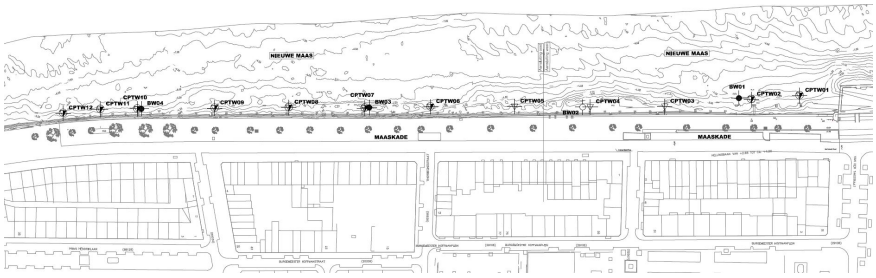


Figure 4.3: Indication of the locations of the taken CPT's used for this study, in correspondence with the profile overview in figure 4.5. [47].



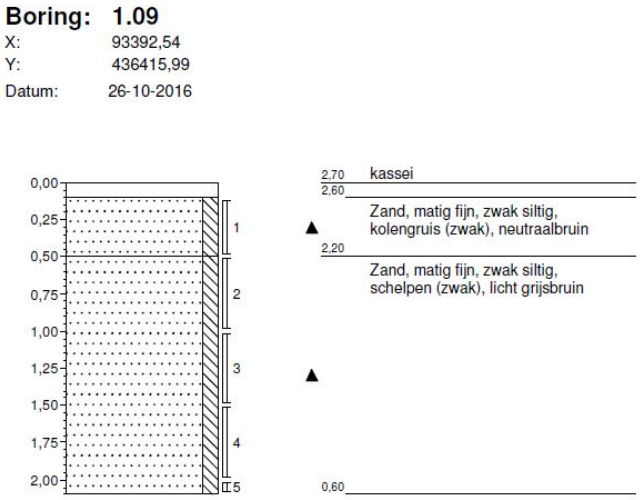


Figure 4.4: Soil build up above the relieving platform within the quay, at wall section 4-1, consisting of silty sand mixed with residues from shells and/or coals. Original figure from ATKB [48].

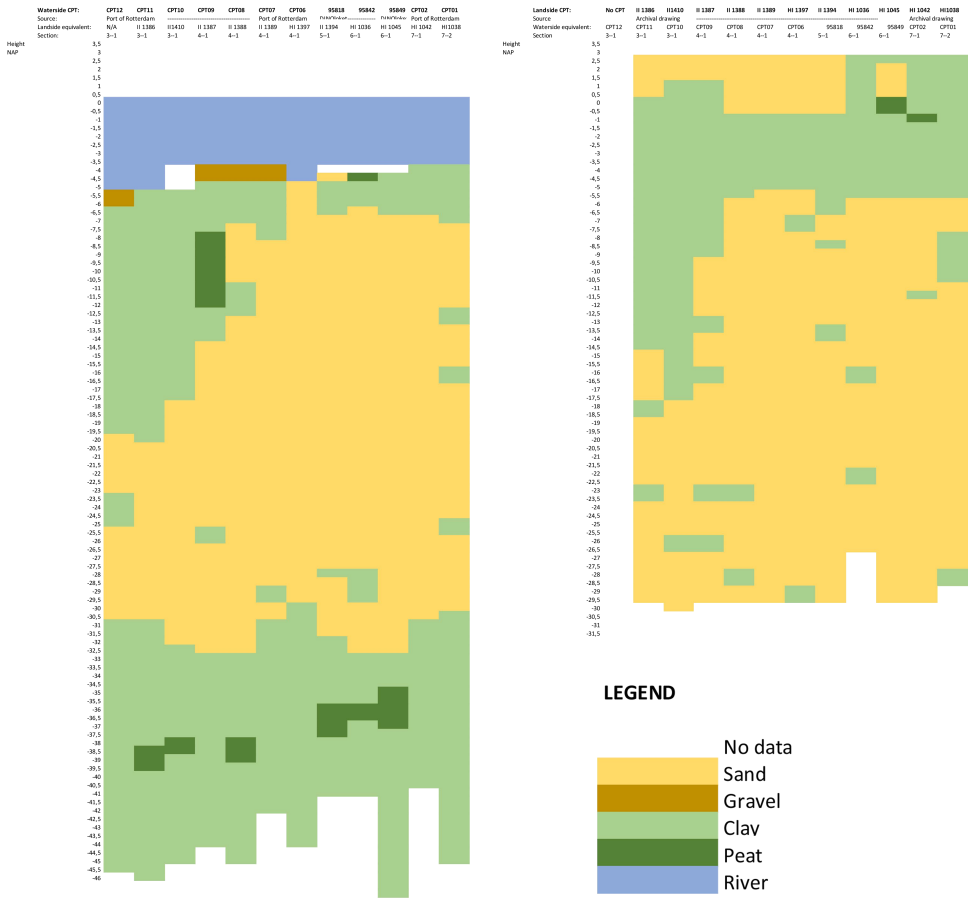


Figure 4.5: Soil profiles along the wall, from the waterside (Left) and the landside (right). The landside CPT's have been taken directly behind the quay and its data have been retracted from a scanned (pixeled) drawing from 2002 (Archive drawings)[49], making the waterside vectorised measurements (2019 PoR[47], 2016 Dinoloket[46]) more clear. Their location can be retrieved from figure 4.3, the section is indicated in the top. Note the different classification of the left (southwest) shallow clay layers to -19 NAP with respect to figure 4.2.

### 4.1.3. WATERLEVELS

The waterbody on one side of the Maaskade is the river de Nieuwe Maas, which largely dictates the groundwatertable on the landside. The reason is simple: porous materials have been used in the creation of the original quay wall. Since the river is influenced by the tides on this trajectory, the level varies between ca. 1 and 2 metres with every ebb and flow depending on the type of cycle and precipitation; see figure 4.6. An average hightide

level and lowtide level are noted down in all drawings, 'GWH' and 'GWL' in Dutch. These are + 1.32 and - 0.39 m respectively for the year of 2015 [50]. Measurements behind the later added steel sheet pile wall (2003; see 4.2)show that the waterlevel behind this structure is not varying with the tidal changes anymore [48].

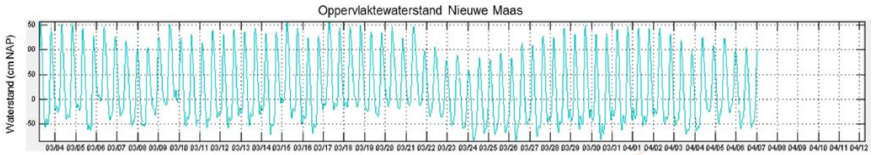


Figure 4.6: Example of changing waterlevels on the river Maas on Maaskade height. The measurements are from march 2017. Original figure from ATKB [48].



The wall has been calculated to withstand floods with a chance of overflow once every year, as stated by the Port of Rotterdam, and has a varying height between + 2.55 to 2.75 m to the reference level N.A.P. [51]. Some suggest the waterlevel was much lower in the past. Stikvoort [52] refers to a historic source that notes down average levels of 4 cm above N.A.P. in 1876. Data from Rijkswaterstaat shows different levels for the year of 1982 (and the decade 1980-1990 in general) as well. These three measurement timestamps build the graph in figure 4.7. Any changes could be described by the changing river trajectory, added canal joints and changes in sea level.

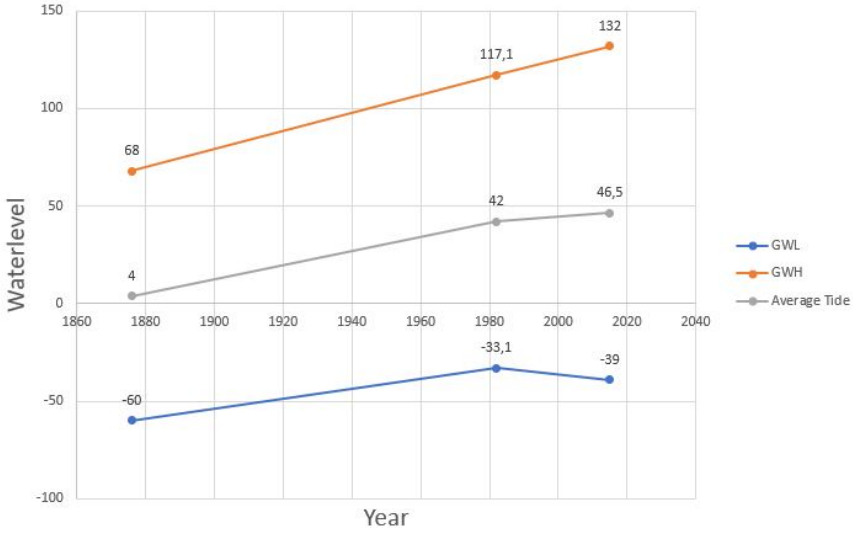


Figure 4.7: Changing waterlevels over the years, in cm above N.A.P. [52] [53]

## 4.2. CONSTRUCTION AND RENOVATIONS

### 4.2.1. ORIGINAL STRUCTURE

The original structure of the Maaskade quay wall was from 1875, and is a simple retaining wall on two rows of piles with an anchor in the form of another pile some meters behind it. Historical documentation notes down that the Maaskade wall at the front side of the island, the Prins Hendrik wall at the back-side of the island, and the Nassau wall across the island have a similar structure. The flooring is 1.6 to 1.8 m wide and includes fir piles. The front pile is raking slightly and between the two pilerows a sheet pile wall is placed. The wall itself is either from masonry or of concrete and could include basalt blocks on the riverfront side as the construction progressed [54]. Noticeable is that throughout its history, the mooring pile structure remains separate and uncoupled of the rest of the quay.



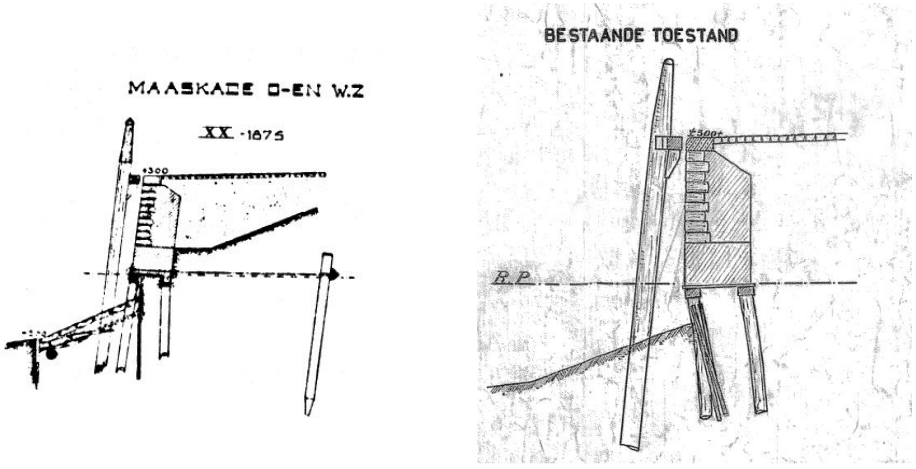


Figure 4.8: The original section according to archival drawings from the municipal archive (left, unknown age), The section according to renovation plans (right, 1922). Note the difference in front row slant and the presence of the anchor (left), and its absence (right). The sheet pile wall at front pilerow height is visible in both drawings [55][56].

As the dieselhammer was not yet invented [4], the piles have most probably been placed with a steam engine based pile driver. In a letter from 1850 stating options for the building of the Willemskade across the river, a remark is made that placement of timber foundations should be lowered to a depth of 20 to 40 inches below the Rotterdam reference level (Rotterdams Peil; R.P. = N.A.P.-0.603 m before 1924 and N.A.P.-0.65 m after 1924), in order to ensure a wet timber flooring [54]. This brings along the problem of placement in wet conditions. The letter underlines the financial consequences of the need of a building pit.

As the timber of the original Maaskade is placed at R.P. exactly, building in dry conditions can still be achieved during low waters (though impractical) and a use of a building pit is uncertain. Use could have been made of large overpressurised diving bells. It is the

question whether the piles for the platform have been placed before or after digging the slope towards the river, but placement after building the slope is easier and more convincing [57]. This for sure is the case if fascine mattresses have been used.

### 4.2.2. CHANGES IN BUILD-UP

The first renovation to the Maaskade on the western side took place in 1892, with unknown reasons. One reason could be the need for larger retaining heights to accommodate the fastly growing ships.
The Prinsenhoofd on the other hand (south-western tip of the Noordereiland) has been built only by 1894 as the quay still had some gaps. Use of fascine mattresses at this location is noted down which distinguishes the spot from the other walls along the Maaskade. These mattresses stabilise the slope and prevent scour and erosion of the embankment. Other than that, the Prinsenhoofd structure uses a 6.0 meter wide relieving platform or 'floor' and fir piles, all vertical. [54].
In 1902 and 1905 settlements become apparent, and it is decided some of the walls of the Noordereiland are to be renovated again. These renovations took place in 1905 to 1907 and include placement of anchors, a 6 m wide floor and sheetpiling behind it. The use of pine raking piles is named from the year 1904 onwards [54]. From drawings, we find this slanted pile is penetrating into the wall. An overview is given by an archival drawing with unknown age; from between 1907 and 1923. The reworked version is to be seen in figure 4.9 [55].

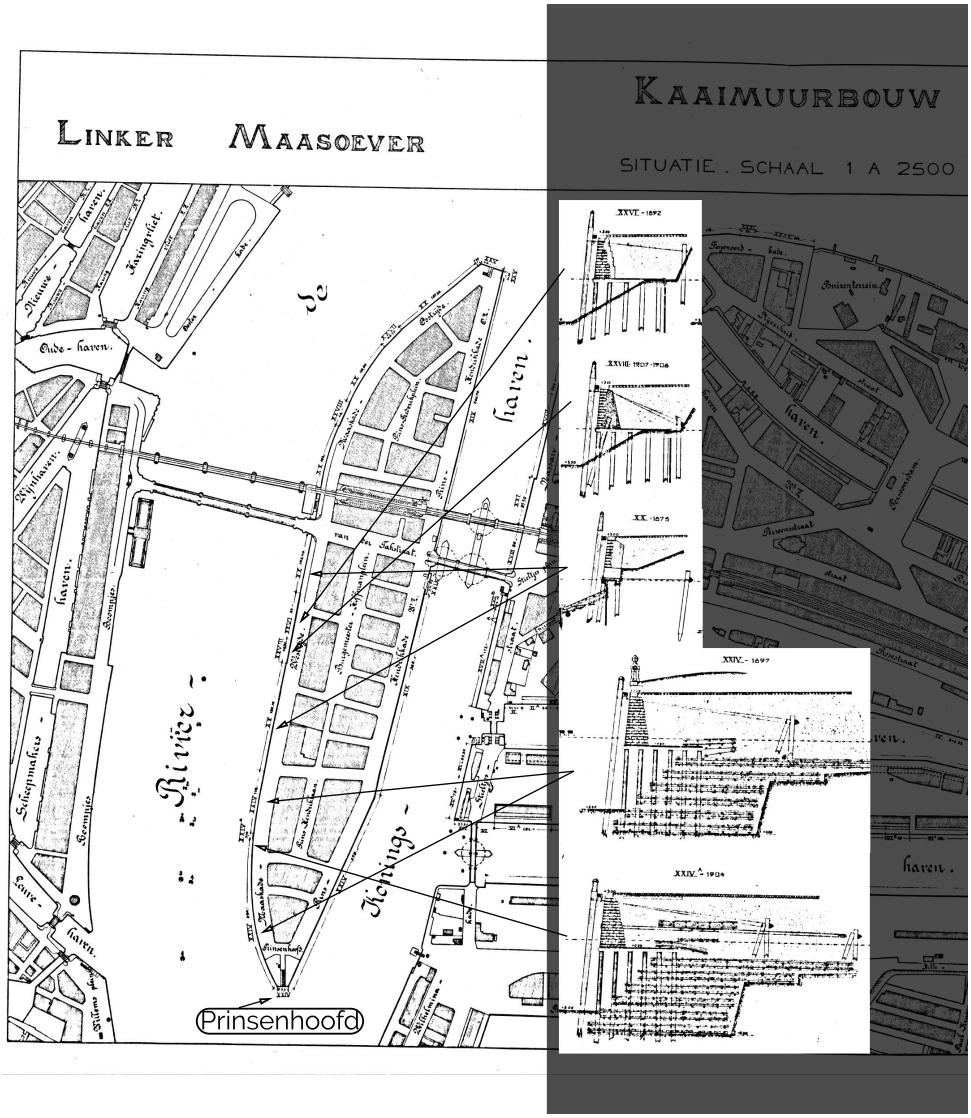


Figure 4.9: Reworked figure from the archive overview drawings, dating between 1907 and 1923. The different sections over the Western side of the Maaskade are shown. Note the location of the Prinsenhoofd. Original from the Rotterdam archives [55].

For the wall section close to the Willemsbrug it is known that the 1875 wall is actually placed *behind* the new structure. It is assumed that for every section along the wall that whenever a major change is made to the quay that includes a new type of the foundation no old elements are used.

Further renovations take place in the period 1920 - 1923 for the yet unreplaced, orig-

inal 1875 quay sections. The newly used design uses a less wide retaining floor than the other sections, with only 4 pilerows though still incorporating the raking pile. This renovation results in much larger parts of the Western side (Westzijde) of the Maaskade to have a raking pile and replaces all 1875 walls.

It is unclear what damages the bombardments and fires of WWII brought to the Maaskade, but a drawing of the Prinsenhoofd from 1947 shows damages and collapsed parts. The use of steel anchor plates, fastened by an H-profile is implemented for the directly *adjacent* quay sections. See figure 4.10.



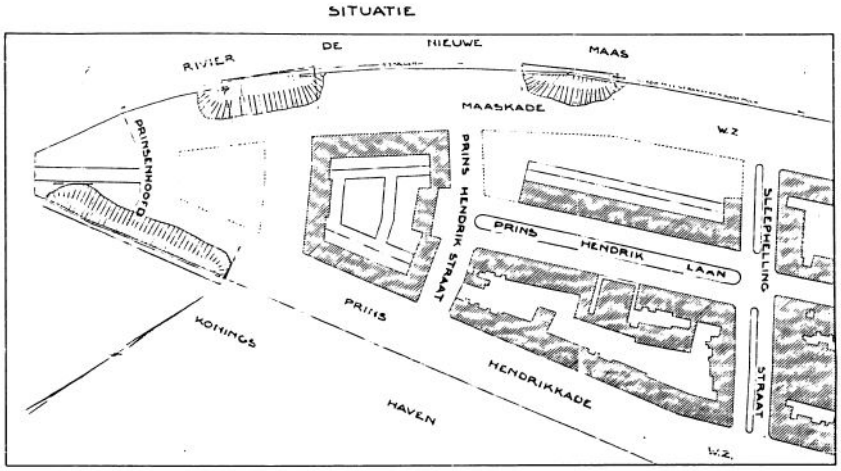


Figure 4.10: Devastation around the Prinsenhoofd, 1947. Original drawing from the Rotterdam Municipal Archive [58].

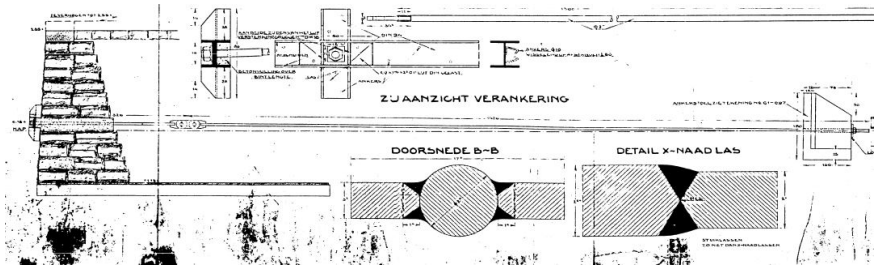


Figure 4.11: Strengthening measure for the nearby located wall, perhaps to prevent further collapse. Nothe the H profile on the waterside of the wall (top). [58]

In 1955, more settlements and partial collapses take place around the Prinsenhoofd. The choice is made to replace the retaining wall on timber flooring with a retaining wall on a concrete floor on concrete piles around this island tip. It is unclear due to incom-

plete documentation if this is a (very late) response to the 1947 collapse or if an intermediate solution has taken place by then.

During the building of a subway tunnel in 1968, part of the island was demolished: the Prinsenhoofd was cut. The Maaskade beyond this southern tip was not changed this year.

In 1982, more settlements are noted along the entire wall; placement of horizontal steel anchors of which 2 or 3 are connected into a single steel anchor plate is the remedy action. Next to horizontal sliding forces that the piles need to take, the pushing of the soil against the wall results in a moment 'couple' that is to be taken as a normal force in the piles. The anchors act as an additional support and lessen the forces on the piles due to the sliding and the tipping 'couple' [59]. See figure 4.12 for the change made.



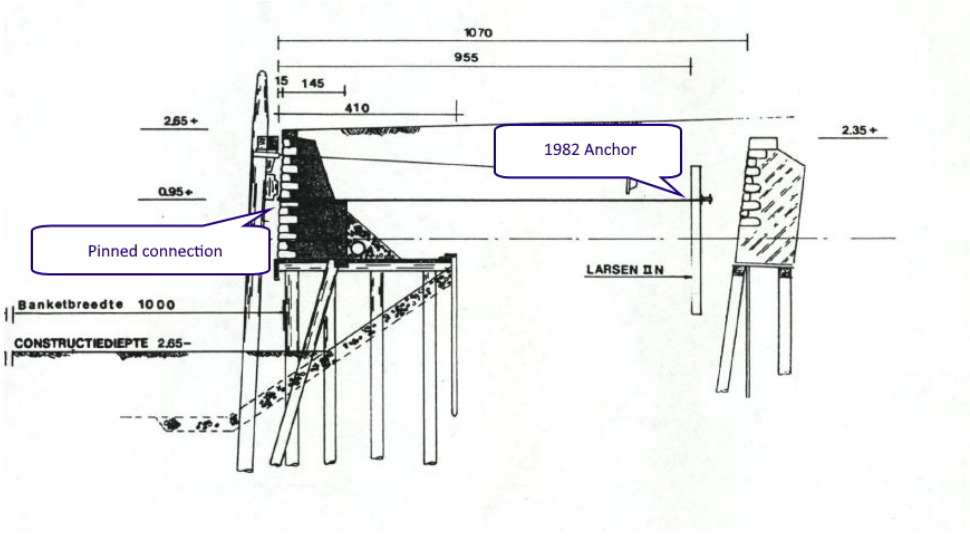


Figure 4.12: Strengthening of the wall in the 500 m directly west of the Willemsbrug with Larsen plates and anchors. Note the location of the original wall from 1875 behind the later wall with relieve platform. [59].

The years 1988-1990 bring along a change of the Maaskade in the direct vicinity of the Willemsbrug bridge. A railroad tunnel is placed which results in a replacement of the quay wall with a steel sheet pile based one. Remnants of the old wall are still in place behind the sheet pile wall, a build up also to be seen on the entire eastern side of the Noordereiland.

With a research on timber foundations going on in 1997 and 2002, the Maaskade was subjected to inspection and analyses. Inspections in situ in 2002 were carried out on the timber foundation with a Frank hardness tester, dimensions noted. Post analyses on the material were anatomical (to find the species), biological (to find deteriorative traces), and computational (calculation on whether the piles could take extra weight) [60]. The

main conclusion is that the timber platform will loose its earth retaining function eventually.

After these measurements and inspections, it is decided to renovate. The main earth retaining function of the historical quay wall is taken away by giving this function to a new steel sheet pile wall behind tubular piles, that was to be built behind the entire timber & masonry/ basalt/ concrete structure. The sheet pile includes diagonal grout anchors and a large concrete beam on top. This capping beam also supports concrete decking, that spans above the historical timber all the way to the masonry/ concrete/ basalt historical wall. This one is then adapted to accommodate supports for the concrete slabs which in turn have geotextile on top that prevents wash of soil in the dilations. During this process, the 1982 horizontally placed anchor rods are cut and the mooring pile anchors are also to be removed .The structure omits most of the timber flooring, and only the piles have been subjected to quantitative structural assessment beforehand, with an axial load computation. See figure 4.13 for the renovation plan. The new final situation of all the sections along the western side of the Maaskade as until 2015 is shown in figure 4.14.

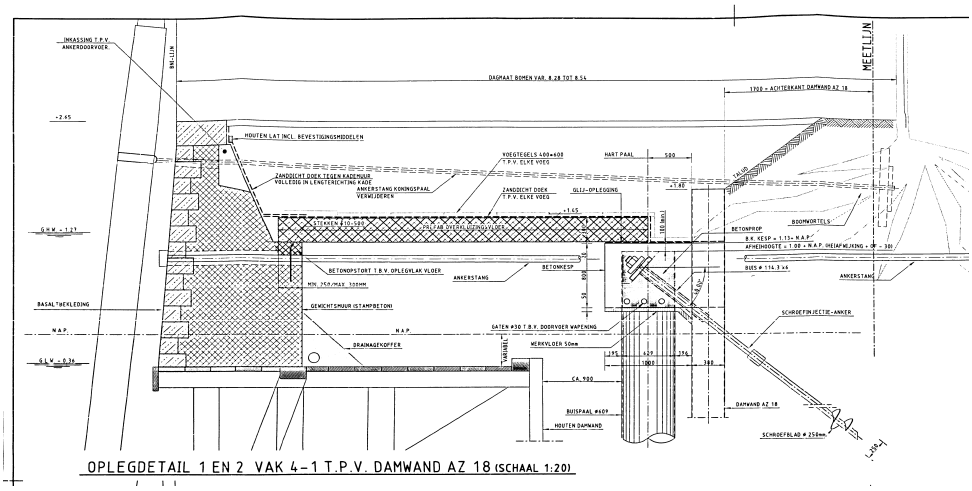


Figure 4.13: Detail of the concrete floorslab (middle), concrete capping beam (right) and anchored steel piling (bottom right) addition of 2002-2004 in relation to the original stoney wall (left) and the timber floor (bottom left). [61].

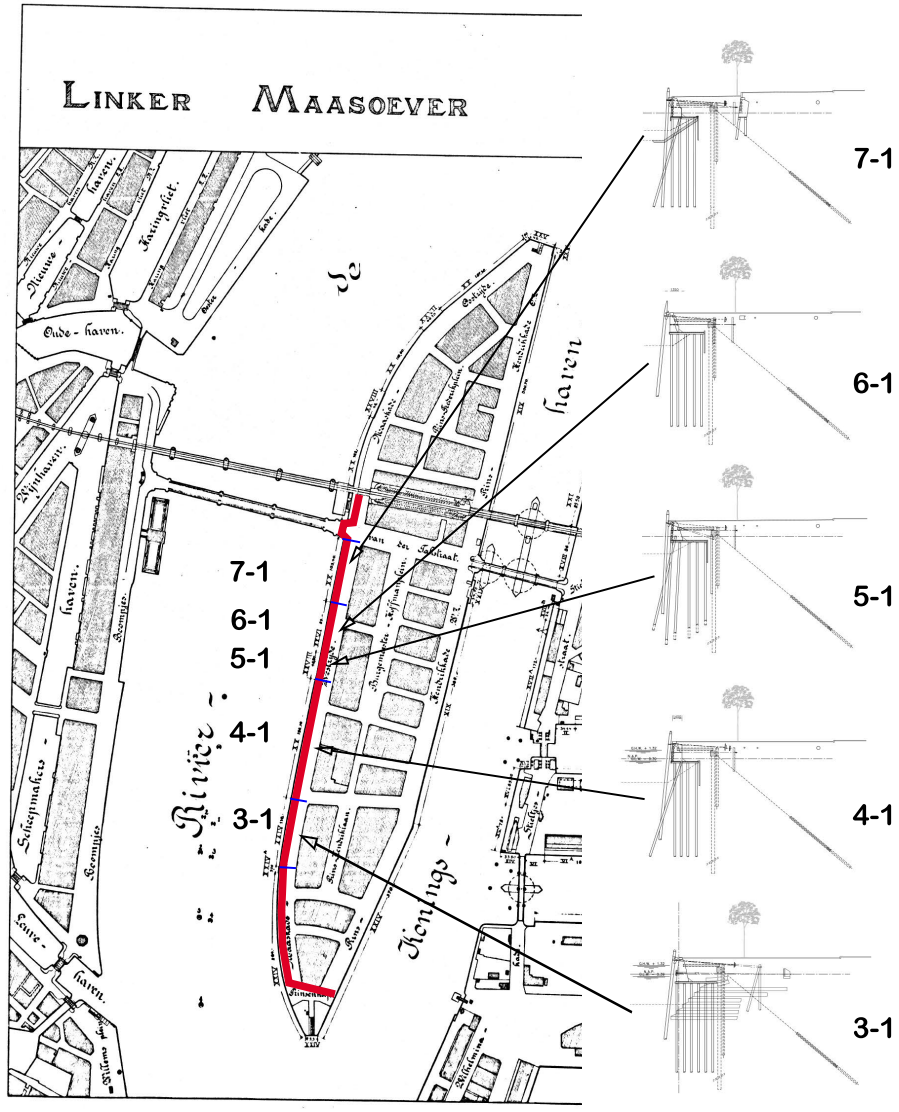


Figure 4.14: Reworked figure from the archive overview drawings, now for the 2015 situation. Te new section names (3-1, 4-1 etc. are indicated). The different sections over the Western side of the Maaskade are shown. Note the new island perimeter in **red**. Original background from [55], original section drawings from [50].

### 4.2.3. COLLAPSE AND FINAL REPLACEMENT

Sadly, a collapse of the Maaskade took place in December 2015 without clear previous signal. Inhabitants noticed a shock 2 days before the severe settlement of the wall [62] over a 40 m wide part in section 6-1 (see figure 4.14) [51]. As a damaged spot was noted on the outer side of the wall, at the berthing beam, it is assumed a ship could have been the direct reason for this collapse. An inspection was called for by the PoR. In the meantime, the collapsed section was reinforced by a dump of stones on the waterside and taken out of its functional use.

The inspection conducted was an inspection on the collapsed wall, an assessment of deformations, loading and a visual and laboratorial check of the timber for degradation [6]. The conclusion states that the ship collision was only the final push that trigger the quay to fail. The overloading of the connection between the piles and the capping beam was the main reason of failure (see section 4.3 for an overview of the elements). The recommendations given in the report are a closing of the entire sections 3-1 and 6-1 since they are particularly vulnerable, and a further elaboration on the structural assessment or calculation of the entire wall [6].
The PoR then concludes on the base of this report, deformations and vulnerability of the unbraced sections on the Maaskade that these similar to the collapsed wall must be relieved of their function on this location. The renovation includes all unbraced and braced sections between the Willemsbrug and the Noordereiland tip alike, finally uniforming the type of wall along the Maaskade. No further calculations are made on the old wall.

The new structure consists of a steel sheet pile wall with grout anchors. See figure 4.15. In the process, the 2003 sheet pile wall is kept in place, with a removal of the concrete slabs and most of the timber structure, with exception of any pilerows behind the first two (seen from the waterside).

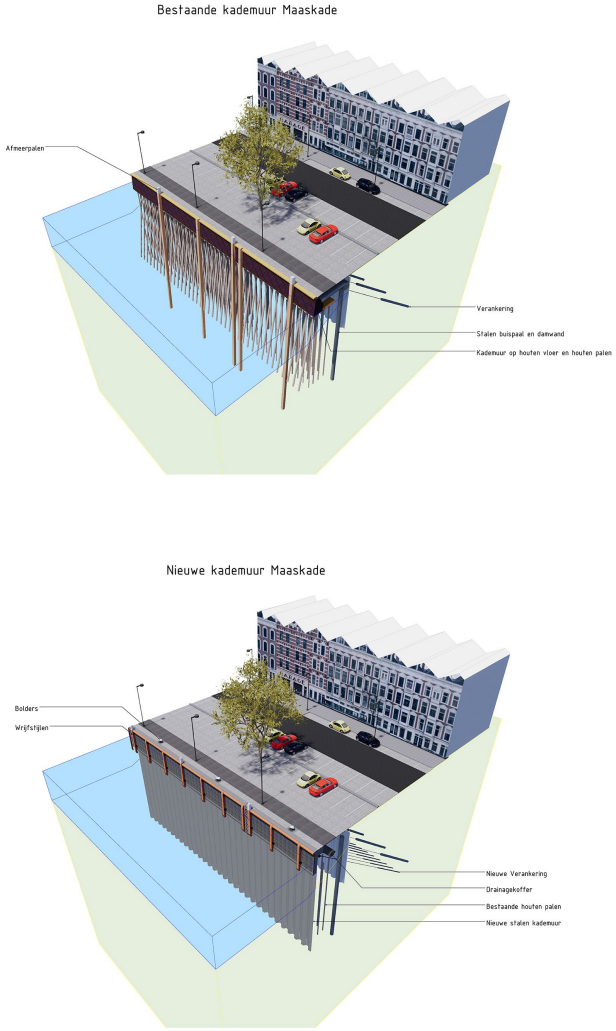


Figure 4.15: Section 4-1. 3D Visual on the situation between 2003 and 2018 (top) and the new design to be implemented from 2019 onwards. Figure from the Port of Rotterdam website [51].

A removal of the historical quay while only adapting the 2003 placed sheet pile seems a tempting option, but one has to bear in mind this wall is not designed to retain soil to the required depth for berthing of ships and valuable public and parking space would be lost.

The overall height of the wall is decided to be + 3.0 m NAP, lowering the chance of flooding from 1:1 year to 1:10 years, and the riverbed is locally deepened to -5.2 meters. Keeping the old-fashioned look is important and designs are altered accordingly: the top concrete cap includes basalt cladding. As of May 2020, the structure is entirely completed [51].

## 4.3. STRUCTURE DETAILING

### 4.3.1. THIRD DIMENSION LAYOUT

Most of the archival drawings contain information about the cross-section only. One exception is a detailed layout drawing from 1923 'as built' (see 4.16). A site investigation during the replacement of the quay in February 2019 showed the detailing in the third dimension that is necessary for true understanding of the forces in each member (see 4.17). The focus of the layout now shifts towards the inspected wall sections 3-1 and 4-1.



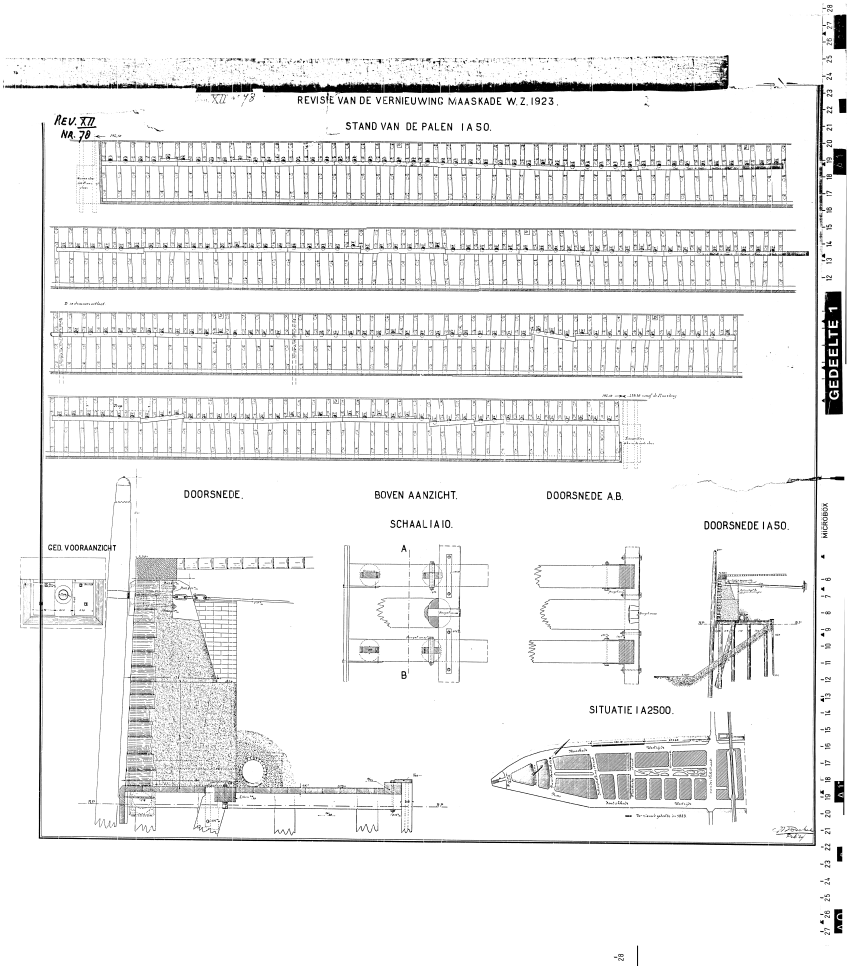


Figure 4.16: Section 4-1, detailed drawing of the pile plan as built (top), cross section and detailing (bottom), placement along the quay (bottom right). Note the presence of a drainage pipe behind the retaining wall (bottom left)) [63].

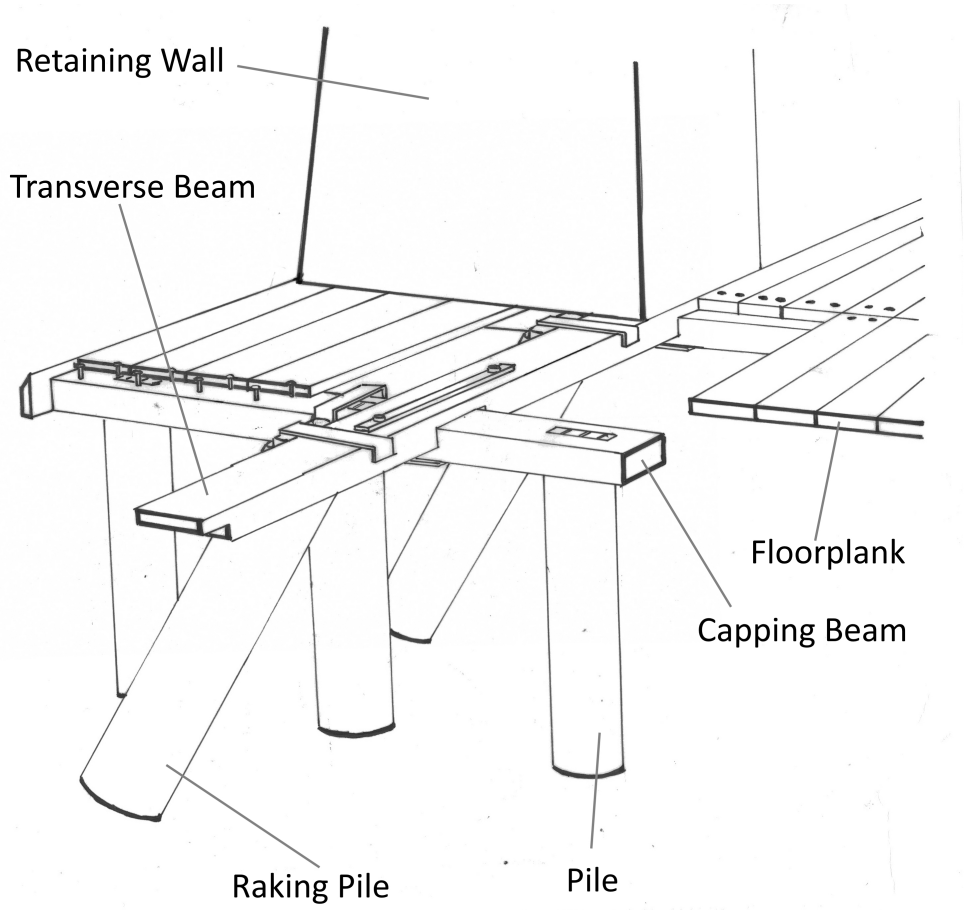


Figure 4.17: Section 4-1, 3D exploded view of all elements within the quay foundation. Based on the site inspection in 2019 (drawing by author).

Comparing the drawing to the findings of the site investigation, we find that the raking pile is connected rather close to the capping beam with the vertical piles, and not halfway as indicated on the archival drawings. This pile is then connected on a transverse beam that is placed on top of the capping beams and has an incision at the contact point.

The floor planks are spanning about 5-7 capping beam distances, which are on average 1.02 m each. Their tight placement should prevent soil wash out. The top level of each plank aligns with the transverse beam top, giving a flat surface for the wall to be placed on.

Figure 4.18 shows that between two types of sections (here between 3-1 and 4-1), an overlap of piles can be seen. For the 'normal' situation without overlap the pile spacing

underneath one capping beam is ranging between 0.9 and 1.2 meter making the Spacing over Diameter factor $\frac{L}{D}$ about 4 in both directions.

Figure 4.18: Start of section 4-1 from the site investigation in 2019. Note the large amount of piles due to overlap of structure in the 2nd and 3rd beam row. It may be possible as well that these piles are even older piles (from the 1875 wall), as the piles from nearby wall section 3-1 are not as high, though sectional drawings of section 7-1 suggest differently: the old wall is behind the quay with relieving platform.

### 4.3.2. CONNECTIONS

In the inspected sections, generally three types of connections between pilehead and beam could be distinguished. The first one is a steel pin driven through the capping beam and into the pile. A ring around the head is visible; it had the function of preventing splitting of the timber cells during the pile driving procedure. The second type is a mortise-and-tenon joint, where a hole is made in the capping beam to accommodate a square section of the pilehead to be fit through. The connection is finished by placing two wedges in at the top of the pilehead for a tight fit between the two structural elements. Both these connections also come in a version with a brace. For section 4-1 these are placed at the second row, where the close to the connection with the transverse beam. See figure 4.19.

Lastly, the connection between raking piles and transverse beams is characterised by being mostly a contact-based joint, where a specially cut raking pile head is placed underneath the beam. Only a steel strip without fasteners around the top of both the transverse beam and the raking pile head makes sure the connection stays in place. It seems the connection can only take compressive loads. The transverse beam itself is connected

to the capping beam by means of two steel strips, wrapping the capping beam and bolted into the transverse beam. See figure 4.20.

The connection between floor planks and the capping beam consists of two steel nails, which continue to be placed on every capping beam the plank crosses, making some diaphragm action and thus (horizontal) force distribution possible in the timber floor.
The connection of the timber sheetpile wall to the capping beams is through a smaller transverse beam that is placed on top of the capping beams. A nail ensures the connection. It is clear that the connection is made in such a way that the downward loads on the floor are not transferred onto the sheetpile wall (a compression only connection).

The wall that stands on top of the floor is usually placed without any extra measures. The plank at the waterside is not in touch of the wall (see figure 4.17 at the very left). The only thing keeping it in place is friction or the bond between the floor as formwork for the wall and the wall itself. A different approach is seen in section 5-1, where the raking pile penetrates the floor and enters the wall, giving it a comparatively rigid connection.



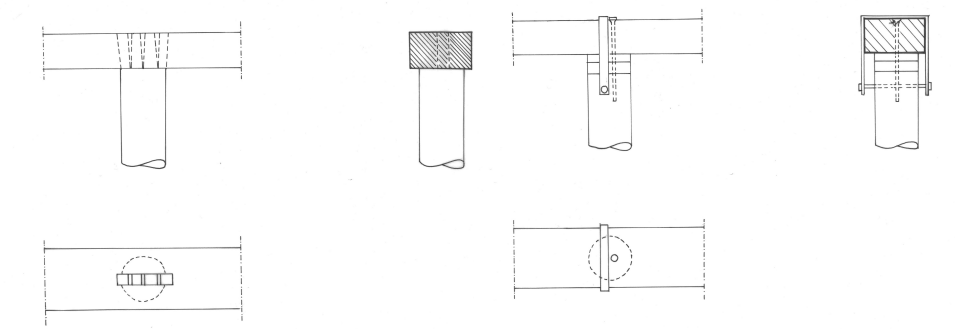

Figure 4.19: Connection type: mortise-tenon joint (left, wall section 4-1), steel pin - braced edition (right, wall section 3-1). Note the absence of the floor planks in this drawing.

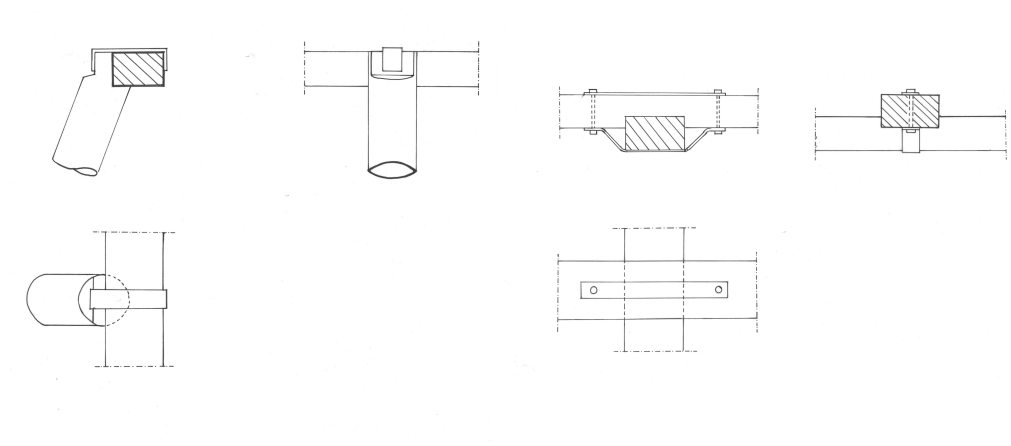

Figure 4.20: Connection type: Raking pile connection in wall section 4-1 (left), transverse beam to capping beam (right). The transverse beam is on top. Again, the floor planks are absent in this drawing.

As for the connection with the mooring piles next to the wall, the case is clear: the mooring piles and their wood fenders are not in direct contact with the wall. Only if a sufficiently large compression force bends the mooring piles they come into contact with the wall via a protruding bufferblock. If in tension, the mooring pile pulls a ground anchor that travels through the wall but is also not in contact with it. It is important to mention that these mooring piles, always indicated in cross sections, are not as numerate as the foundation pilerows. It is only about every 8-10 m that a mooring pile is placed along the quay.

### 4.3.3. MATERIALS

Description of the timber is given only twice. The first is in a document describing the formation of all quays on the southern bank of the Maas in Rotterdam. It mentions in particular the use of 'dennen'(fir) around the Antwerpsche and Prinsenhoofd [54]. Section 3-1, built in 1897, is one of these sections. The second description is in the drawing of 1923 (4.16), but only for some parts; the transverse beam is to be built in 'Eiken' (oak), as are the wedges for the mortise-and-tenon joint.
The steel quality and type used in the foundation is not mentioned at all.
As for the stoney retaining wall, three types are distinguished. Originally, the walls from the 19th century are completely from basalt blocks with mortar, where from 1904 onwards it was chosen to build in concrete with only a basalt finish at the waterside.

Materials for the renovations of 1982 and 2003 are noted down more exactly, as documentation has not been lost. The necessary material descriptions for computations are described in short in appendix C.

From the physically obtained materials it has been found the type of timber for all the transverse beams was hardwood (oak), while capping beams were either soft or hardwood.

### 4.3.4. DIMENSIONS

The dimensions known are the ones from original drawings from 1923 (see figure 4.16). They are presented in table 4.1. Other dimensions available from drawings, such as pile lengths, could only be obtained from other sections. A diameter of '300/150' mm is mentioned and a length of 12.08 to 15.78 m are noted down for section 5-1. Furthermore, different capping beam dimensions and spacings are mentioned which show again the large variety of structures within the Maaskade. They shall not be discussed all in further detail.

Table 4.1: Dimensions known from archival drawings.

| Section | Element | height [m] | width [m] | length [m] |
|---|---|---|---|---|
| 4-1 | Capping Beam | 0.2 | 0.3 | ca. 4.6 |
| 4-1 | Transverse Beam (front) | 0.2 | 0.3 | - |
| 4-1 | Transverse beam (back) | 0.13 | 0.25 | - |
| 4-1 | Floorplank | 0.075 | - | - |
| 4-1 | Sheetpile | 0.15 | - | 4.4 |
| 3-1 | Capping Beam | - | - | ca. 6.0 |

## 4.4. LOADING

### 4.4.1. CHOSEN WALL SECTIONS AND LOAD COMPONENTS

As will be stated in chapter 5, material research could only be conducted on certain parts of the Maaskade due to logistic reasons: section 3-1 and 4-1. To implement the real material characteristics as to be extracted from tests in chapter 5, the best conclusions can be drawn for elements that have undergone the equivalent load history and have been applied in the equivalent set-up. The choice is made to analyse section 4-1, where most of the material is coming from. This section also covers the largest part of the western side of the Maaskade, as section 7-1 is very similar.

The relevant load components extracted from the guidelines for quay walls [3] and historical quays [10]. *It is important to note that relevant loading will only be discussed for the situation right before collapse (2003-2015).* The loads have been split into water oriented and land oriented loads. This means that the load effects in a reaction of the structure towards either the river or the land. The characteristic loads are:

1. Towards the land: Ship Berthing.
   The Nieuwe Maas is used by ship class CEMT I to VI-B. Class I to V is allowed on the Noordereiland according to PoR. However, taking into account the dredging depths and the tide only class I is realistic on wall section 4-1. The relevant loaded ship weight is 400 tonnes. With the approach speed of 0.2 m/s and angle of $10^o$ this results in a to be absorbed energy of 3210 Joules perpendicular to the wall [23]. NEN 1991-7 specifically states ship impact is not to be taken as an accidental loadcase for quays that have this as a primary function [64];

2. Towards the land: Waveloads
   Not enough information on waveloads could be acquired to make accurate statements on the loading by waves;

3. Towards the land: Iceloads
   This part of the river is far enough inland to be classified as sweet water - which influences the maximum icestrength the load is based on. Adding the fact it is a tidal area the load to be taken into account is 100 kN/m [23];

4. Towards the river: Ship Mooring
   Mostly caused by winds, for CEMT class I this is 150 kN [23];

5. Towards the river: Self weight and surcharge loads
   For this class of quay (consequence class 2), at least 10 kN/m$^2$ is to be added. Acoording to PoR however, 20 kN/m$^2$ was to be expected due to the function as parking lot in the years after the last renovation (2003-2015);

6. Towards the river: Traffic loading
   As the street for local traffic is located near the buildings and not above the quay, the only way of accounting for traffic will be by means of surcharge;

7. Towards the river: Raised groundwater table / broken drainage
   A raised groundwater table is always to be taken into account for ULS cases. The

BiKa guideline names 5 kPa overpressure on the landside. Further on, a broken drainage could result in a temporary held high-tide behind the wall. The case of a water table accumulation equivalent to the top of the wall is irrelevant due to the use of porous materials ;

8. Towards the river: Selfweight of trees
   Trees on this quay are placed just behind the relieving platform. The elms are largest at the Prinsenhoofd. At section 4-1 the trees are slender, 11 m tall and estimated to weigh about 6 kN.;

9. Towards either side: Windloads on the quay or elements on the quay (e.g. trees)
   For a low quay such as the Maaskade, the windload on the quay itself is small. The loads on the trees is to be accounted for. For the elms, it is estimated to be 11 kN at a height of 5.2 m, for a drag coefficient of 0,5 and a windspeed of 26 m/s [10][65].



Statements on capacity can also be simplified; we find mainly a concentrated or lineload from the river towards the land (ship, ice) and a distributed load from the land towards the river (self weight, surcharge). The exact specifications however make an assessment on 'rejection' possible (see chapter 2).

## 4.5. COMPARISON WITH OTHER QUAY WALLS

Studies of Stikvoort [52] show that for the Dutch quay wall areal of 1863-1923 most walls do not have the inclusion of a raking pile and are more often built with 2 or 3 pilerows and a sheetpile instead of 4 or more, resulting in a much smaller or absent relieving floor.These structures look much like the 1875 original Maaskade quay. However, the retaining wall is more often from brick masonry.
Technical drawings from Rotterdam itself show us that multiple pile rows and the use of fascine mattresses to replace the sheetpile are indeed quite popular around 1910, together with the use of a single raking pile and later on multiple raking pile (as seen in the Parkkade built in 1940). 7 Or more pilerows are not an exception [60].

A reason for these more heavily built quays in Rotterdam is most probably the river de Nieuwe Maas. Unlike many quay walls along smaller canals in city centres, the historical Rotterdam quays have to do with stronger currents and variations in the waterlevel. The function of ship-berthing would also push towards deeper quays which require longer slopes and therefore more pilerows to build along them. Not astonishingly, most of the 'traditional design' 2 row quays have been replaced on the Noordereiland within 30 years.

One way or the other, any quantitative results of this thesis are only valid for the Maaskade case due to the specific material tested and specific build-up and boundary conditions chosen.

# 5

# STATE AND STRENGTH OF THE TIMBER COMPONENTS

*CHAPTER 5 is where an approximation of the strength of the material is made. For the piles themselves, this has been done by means of physical testing. The other elements are inspected visually. Next to strength and stiffness, dimensions and state are also important: have pieces been chopped off or are they missing? Are the found dimensions the same as in the original structural drawings? Is the wood containing traces of deterioration? To start with, a description is given of what parts of the quay were obtained and in what way they were conserved before testing. The chapter concludes with an overview of characteristics and dimensions to be used in the computational analysis of the capacity of the quay wall.*

*It has been chosen to give a detailed description of the two physical tests in the appendix, in order to keep a good overview in the chapter which only holds the results. The linked appendices are A and B.*

# 5.1. MATERIAL OBTAINMENT, SELECTION AND TRANSPORTATION

## 5.1.1. AVAILABLE MATERIAL FROM THE CONSTRUCTION WORKS

In cooperation with the Port of Rotterdam material was made available. Parts of the Maaskade were stripped of their timber parts beforehand - the southern tip in 1955 and the section east of the Willemsbrug in 1968. As the remaining section (the 500 meters directly west of the old Willemsbrug abutment) underwent renovation in 2019, this was the material that could be acquired by the TU Delft (see figure 5.1). However, restrictions were present on which elements could be taken from the site. Following is a description of the acquisition of the material.




Figure 5.1: Location of the 2019 renovation (orange) and the firstly tackled section (red).[39]

The renovation works required only the horizontal timber elements and the two front pile rows to be removed.

Works on the renovation began at the south-western side of the quay wall, corresponding to Maaskade (streetname) 136 to 154 - or: mooring pile 17 to 40, in February 2019 (see figure 5.1). This was the given moment to decide which elements to choose. Spanning approximately 150 metres, this part consists of two sections: Section 3-1 and section 4-1. Both were in different break down stages. Section 3-1 was stripped of the entire superstructure including the wall as well as its floor planks and beams, while section

4-1 was just in the first stage which included removal of the sand fill and earth retaining wall. For breakdown details, see figure 5.2.

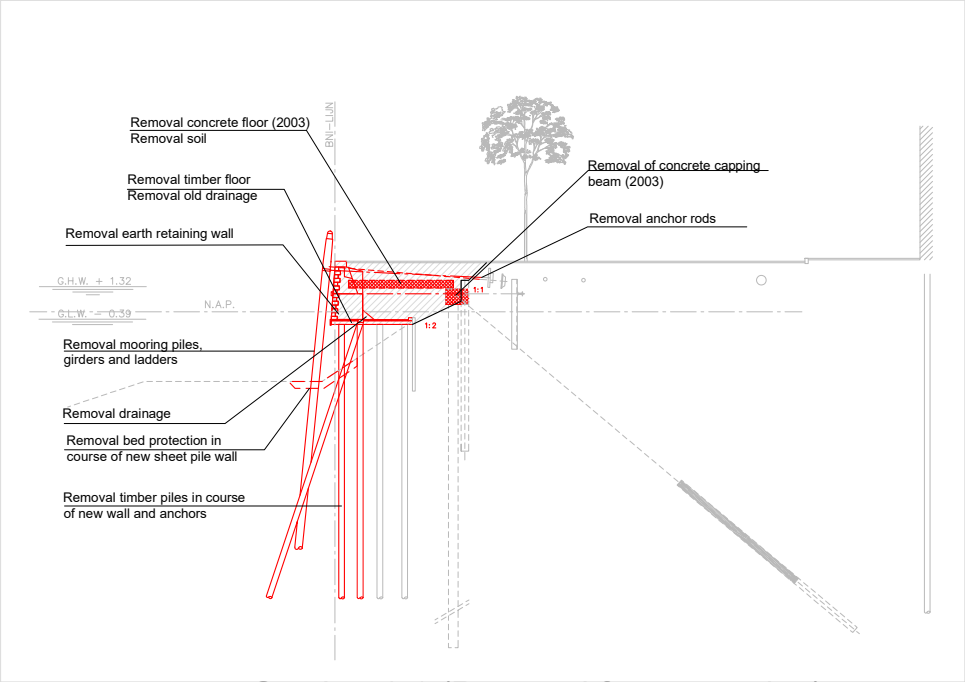


Figure 5.2: Removal of elements of the 2019 renovation. Adapted figure from Royal Haskoning DHV drawing [66].

Therefore, from section 3-1 only piles were retrieved, while from section 4-1 also horizontal timber was requested for. See table 5.1. Surprisingly, a hardwood 6.5 m capping beam from section 3-1 was retrieved anyhow. The material had to be marked for later reference. While information about the exact positioning, which side is facing the water- or landside and the pilerow is of interest, it was deemed impractical by the workforce on site. Only the groupnumber - a Roman letter - was given to the material (third column of table 5.1).

Table 5.1: Requested timber elements from the Maaskade

| Section | Mooring Pile number | Group | Elements from group |
|---|---|---|---|
| 3–1 | 17 | A | 4 piles |
| 3–1 | 20 | B | 4 piles |
| 3–1 | 23 | C | 4 piles |
| 4–1 | 26 | D | 4 piles |
| 4–1 | 28 | E | 4 piles |
| 4–1 | 30 | F | 4 piles |
| 4–1 | 32 | G | 4 piles, 2 capping beams, 2 planks |
| 4–1 | 34 | H | 4 piles, 2 capping beams, 2 planks |
| 4–1 | 36 | I | 4 piles, 2 capping beams, 2 planks, 2 raking piles, 2 transverse beams |
| 4–1 | 38 | J | 4 piles, 2 capping beams, 2 planks, 2 raking piles, 2 transverse beams |
| 4–1 | 40 | K | 4 piles, 2 capping beams, 2 planks, 2 raking piles, 2 transverse beams |

The action of taking the timber from its original placement was done by tracked vehicles from a raft on the river. Planks and beams were taken out by a tracked material handler with grapplers, while the piles were pulled out with a vibratory hammer. See figure 5.3. This action results in damages to the timber, and makes state assessment afterwards harder.




Figure 5.3: Maaskade strip. Removal of timber floor (left) and removal of timber piles (right). Pictures provided by the Port of Rotterdam.

Next, the material was transported on a raft on the river de Nieuwe Maas into a storage some 3.2 km away (as the crow flies) in the Charlois harbour. Both transport and storage was done in an open-air environment. From the moment the first elements got pulled out to the arrival of the last element on storage site took 5 weeks.

### 5.1.2. ACTIVITIES IN THE CHARLOIS HARBOUR

An inventory of the acquired material was made. The present material showed small deviations in the request made beforehand and the markings were partly or totally eroded on some elements. Numbering and naming these was therefore a challenge, and done according to the system in table A.1 of appendix A. In short: Piles got the abbreviation

'P', Raking Piles 'S', Capping beams 'K', Transverse beams 'D' and floorplanks 'V'; due to their Dutch translations.

Selection of the material was necessary due to space limitations of the laboratory climate room in Delft. The aims of the works on site were the following.

1. Measurement of the dynamic E modulus of the piles for selection of a representable group that could be tested further. The later measurements could then be compared to the initial group by means of this dynamic E modulus. To acquire it volume and density must be known - they have been measured accordingly.

2. Measurement of the spacing of joints on transverse and capping beams. This was necessary as those elements were too large for transportation within the Stevin II laboratory.

Appendix A describes the workflow on site. After the actions, chosen parts were marked and put aside. Further storage was again in open air, for a period of approximately 11 weeks. From the other elements (capping beams, floor planks and transverse beams), no further selection was to be made in this stage. Afterwards it proved the TU Delft storage capabilities were lower, and some floor planks and beams had to be left out. For results of the measurements made at the storage site, as well as acquired moisture contents and dynamic E moduli, see table B.1 to B.4 in appendix A.




Figure 5.4: Storage site activites. Measuring (left) and ordening (right).

After comparison of the dynamic E modulys ($E_{dyn}$) was done, 6 piles were selected for transportation to the university laboratory together with all pile heads and horizontal beam elements. The latter were cut on size to fit the container. Before the cut, one piece of each horizontal element was measured in its whole, including spacing of connections still visible on the timber face. As entire piles were retrieved from the Maaskade site, selected piles were cut multiple times resulting in either 3 or 4 pile pieces per pile, each of them around 2 metres in length. Transportation took place in an open container by road. On arrival, further selection was made due to space restrictions in the laboratory. Only part of the pile heads and horizontal elements were left behind, as well as splintered parts. All the remaining timber was then stored in a climatised chamber, under a

temperature of 19.1 degrees. The moisture content in the room was lowered to 30.6% at the moment piles were taken out for testing.

### 5.1.3. SELECTION

Selection of the horizontal wood, being the planks and the beams, has been done purely on variety of elements: it has been made sure a few specimens of all available types of elements are present for further investigation.
Selection of the pilepieces has been done differently. To show the range of strengths present 2 piles with low stiffness, 2 with medium and 2 with high stiffness were selected. These are POC0100 & PJC0100, POC0700 & PGC0100 and PKO0100 & POA0600 respectively. Due to difficulty on site, pile POA0600 was abandoned, while the average-stiff pile POA0100 was picked. In the choice, no distinction is made between raking piles and ordinary piles since no difference between the two is found, assuming the same timber batch has been used for both. See appendix B for the corresponding measurement details.

5

## 5.2. STATE AND DETERIORATION TRACES

### 5.2.1. TIMBER

Sadly, no testing on deterioration traces in the timber could be made as this report is being written. The material is still present in the climate room and future evaluation is possible.

Still, traces of deterioration are visible on all types of materials, albeit in different levels. The **piles** were on average not in the worst state, with an exception of the mortise-and-tenon joint ends at the head. These were heavily tackled due the disassembly procedure during the construction works and as a result sometimes disappeared as a whole. Pictures from before the disassembly however show a bad state too, as can be seen in figure 5.7. In this case the capping beam - pile connection requires a hole to be made in the beam and relies on a tight fit of the two. Wedges ensure this and can also provide a prestress on the interface. In the final material state the tight fit was lost. The other type of pilehead (the one with the steel pin, figure 5.5, right) was often coloured by the corrosion products (orange tan). The pileshafts in general did not show clear deterioration traces, with some exceptions where the shaft was clearly shaped into a wavy pattern. Most probably this is due to erosion by waterflow. On a single pilepiece one could even feel by touch that the outer shell was clearly softer on one side. All shafts showed drying cracks most probably due to the long stay at the storage sites, and some had remnants of Sessilia lobster-like creatures, that do not enter the wood but have an own shell to settle in and rely on the water as their food source.

Figure 5.5: Pileheads; pin (left), mortise-and-tenon (right)

The **hardwood** elements (transverse beams, capping beams for section 3-1) showed extensive cracking that again most probably occured due to drying, though the cracks are deeper than with the piles and continue all the way to the heart of the section. A black staining was visible on the entirety of each hardwood beam, and some brownred corrosion stains at the spots in contact with steel pins and braces. Places in contact with other structural elements clearly stick out of the profile; meaning the face around them have been worn; see figure 5.6. Further, it has to be noted one floorplank was also from hardwood, but was rather an exception than a rule.



Figure 5.6: A hardwood capping beam Note the difference in thickness along the profile and the cracks on the end grain. All hardwood capping beams are from wall section 3-1 and are constant in cross-section, the pins in the picture are from the connections to the piles.

The **softwood** beams (section 4-1) and planks (all sections) were clearly in the worst state of all elements inspected. Assuming all elements had flat surfaces when delivered,

the surface now is uneven and has knots sticking out of it, often together in circular patterns. Since knots have a higher density, they could deteriorate less fast by erosion. Some capping beams were in contact with the mortise-and-tenon jointed pileheads and had therefore even more faces in the joint area that could be deteriorated. As with the hardwood, faces in contact with other structural elements were clearly better preserved and distinguishable from faces in contact with the water.



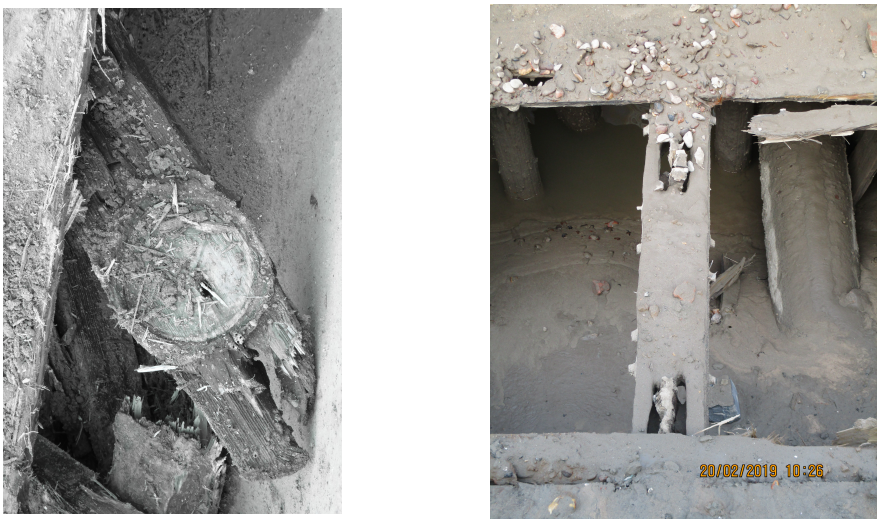


Figure 5.7: State of softwood. Left: clearly visible connection places are less deteriorated. Right: Bad state of mortise and tenon joints.

Figure 5.8: State of a floorplank.

A design evaluation by the engineering department of Rotterdam from 2003 [67] states that the timber floor is prone to failure in the future. The conclusions on the piles was that fungal and bacterial deterioration is taking place, but the speed is low. The state of the capping beams is also named as 'good'. The flooring elements are stated to loose their soil-retaining function and that measurements are to be taken to prevent wash-out. The state of the timber is comparable to the measurements made in 1997 and it has not worsened [67]. The outcome of the pilodyn measurements are available in another report from 2004 used for statistical analysis for other timber foundation inspections in the

neighbourhood [60], but these histograms do not distinguish between floorplanks, capping beams and foundation piles. The design evaluation document (2003) concludes a 25 mm deterioration is found in section 3-1 and a 10 mm deterioration in the other sections along the quay. As they assume a pile sapwood thickness of 10 to 15 mm, they conclude that only in section 3-1 the heartwood could have been degraded [60]. The fact that section 3-1 is one of the older sections (1897) is a possible explanation of why the deterioration is furthest at this place [67].

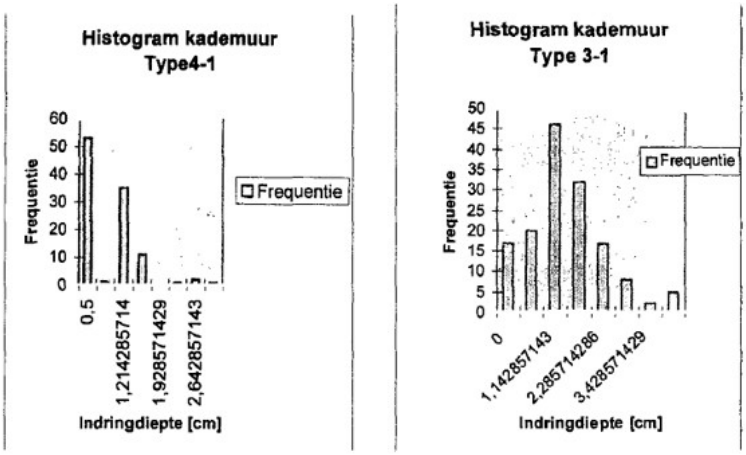


Figure 5.9: Measurements by TNO Bouw of the Maaskade. Sadly, it is only clear that these have been taken in either 1997 or 2003 and that these are measurements of all timber elements; no distinction is made between beams, planks and piles. Original by IGWR Rotterdam [60].

The fact biological degradation could have taken place is not shocking. For section 4-1, the possibility arises it comes in contact with air with every low-water in the tidal cycle that is just 1 cm lower than the average one because of its high placement. Also, it seems that in the past the waterlevels in the Nieuwe Maas river indeed were lower, giving a chance the wood has been in aerial contact more often (see figure 4.7). However for section 3-1, that is located 65 cm lower than section 4-1, this could not describe the reason for deterioration. Even in the past, this section should have been totally under water, suggesting deterioration is of a non-fungal origin.

### 5.2.2. STEEL

The steel pins, bolts and braces all showed severe corrosion, but no clearly broken parts were found. One of the bolts still has a clearly visible thread even when the corrosion reduced the section to half its original diameter. The plates have a surface that flakes off when touched.

Figure 5.10: Overview of 3 different steel parts. Note the poor state of the threaded end of the bolt.

### 5.2.3. ECCENTRICITIES

Next to the material state of the elements, eccentricities and poor placement can also contribute to deviations of intended versus actual stress states and pose a thread to rigidity of the structure. Some of these have been found on site; see figure 5.11.


Figure 5.11: Eccentricities in placement of the beams on the pileheads. On the right even a much wider beam had to be placed to accommodate the poor pile placement

## 5.3. (REMAINING) DIMENSIONS

### 5.3.1. HORIZONTAL ELEMENTS

Only a few elements have actually been measured for comparison with the drawings. The findings have been stated in table 5.2. The denoted dimensions are according to figure 5.12.

| Name | l0 (m) | h0(m) | b0 (m) | l1 (m) | l2 (m) | l3 (m) | l4 (m) | l5 (m) | l6 (m) | h1 (m) |
|---|---|---|---|---|---|---|---|---|---|---|
| KO0200 | 6.48 | 0.17 | 0.25 | 1.95 | 3.15 | 4.4 | 5.5 | 6.15 | N/A | N/A |
| VO0300 | 6.38 | 0.07 | 0.25 | 0.83 | 1.92 | 2.95 | 4.1 | 5.1 | N/A | N/A |
| DH0100 | 4.95* | 0.16 | 0.3 | 0.16 | 0.77 | 1.07 | 1.75 | 2.13 | 2.49 | 0.11 |

Table 5.2: Dimensions retrieved from horizontal timber example pieces. *DH0100 has been broken in two during transport. Measured length is approximately 2/3 of the total length.

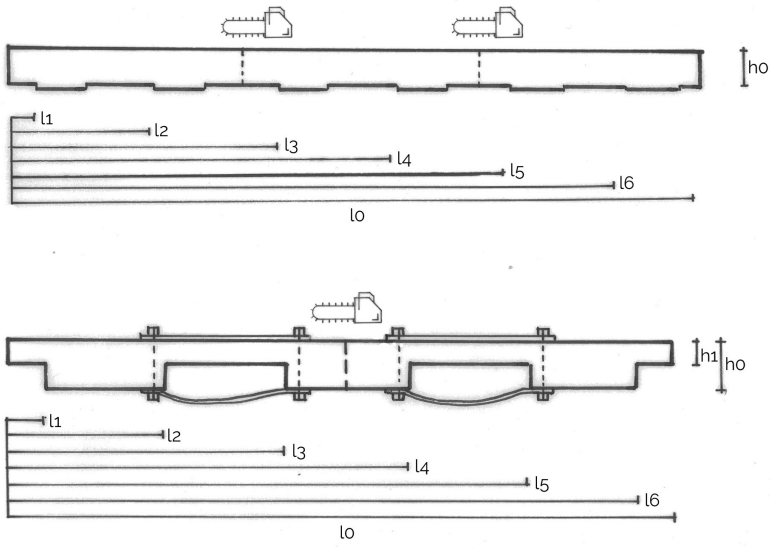


Figure 5.12: Naming and placement of cuts in horizontal parts. Capping beams K and planks V (top), primary transverse beams D (bottom). Lengths measured till former attachment points.

**Cross Section:** The found dimensions do not correspond 1:1 with the original drawings. Since it is only one measurement per type of beam it is hard to draw conclusions, but there is a reduction of 15% and 17% for the height and width of the capping beam, and a reduction of 13% and 0% for the height and width of the transverse beam. The measured floorplank matches its original dimensions perfectly. As traces of cross section reduction are clearly present, the conclusion is that the measurement must have been taken at an unharmed section: at a support spot.

Another topic is that of the effective remaining section: the one that remains if one would peel off the deteriorated shell. The Frankheidsmeter measurements of 2002 [60], see figure 5.9, give some insight into the thickness of the degraded layers, though their accuracy is low (+-5 mm; 50% of the concluded deteriorated shell for section 4-1). It is not entirely possible though to superimpose this degradation with erosion, with the exception if both are measured simultaneously. This is because the erosion is faster with a lower density of the material - an effect of the biological degradation. Some of the degraded material will get eroded as a result. It is clear though that erosion only occurs on the faces that are exposed to flowing water, while the biological degradation is not bound to this; see figure 5.13.



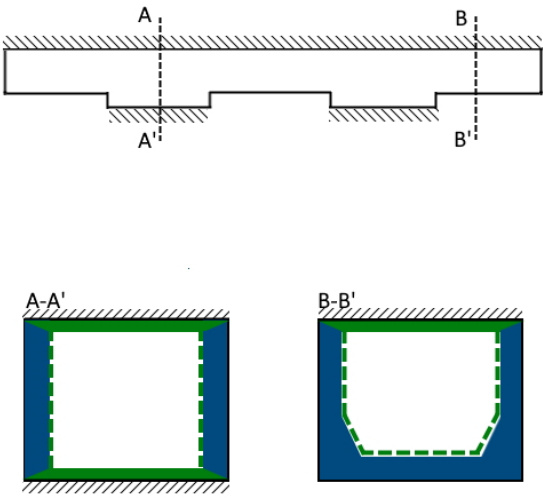


Figure 5.13: The cross section of a capping beam. In blue: erosion, in green: biological degradation. Since erosion hits harder on soft targets, the remaining biologically degraded shell is unknown unless both are determined simultaneously. In case of a mortise-and-tenon joint, section A-A is even smaller due to the joint.

**Length:** The length of the measured capping beam is longer than denoted in the 2019 cross sectional CAD drawings of Royal Haskoning DHV by 68 cm (for the wider section 3-1), suggesting spacing of the piles could be larger and the floor continues deeper into the landside. The spacing between the piles for this measured capping beam is from 1.10 m to 1.25 m, which only slightly exceeds with the 1.08 m in the CAD drawing. For section 4-1 an original drawing is present next to the CAD drawing, mentioning spacing from 0.9 to 1.2 m. It is chosen to use the original drawing for section 4-1.

### 5.3.2. PILES

Since all the piles obtained from the construction site (40 vertical piles and 5 raking piles) have been measured an overview of the dimensions can be given in bar graphs. The P (vertical) piles and S (raking) pile data have been combined, since there were no big differences: Average length for P piles is 12.51 m , for S piles 12.16. The average pilehead diameters are 0.24 and 0.26 m respectively, the piletip diameters 0.20 and 0.21 m respectively.
It is remarkable that the piles are much longer than the depth of the clay layer. Along their shaft we find approximately 6.5 m of clay and 6 m of sandy layers.

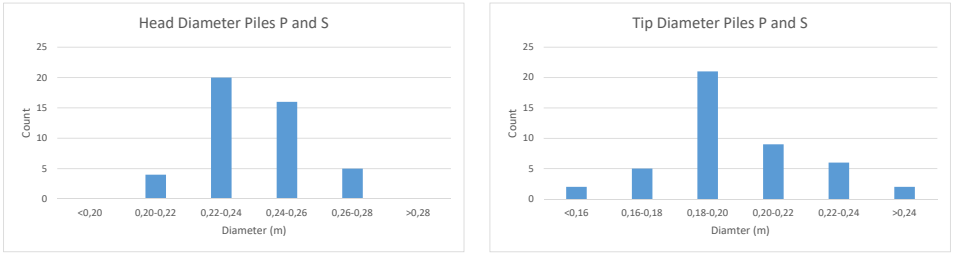


Figure 5.14: Distribution of piledіameters at the head (left) and the tip (right). Average value for the head is 0.24 m and for the tip is 0.20 m.

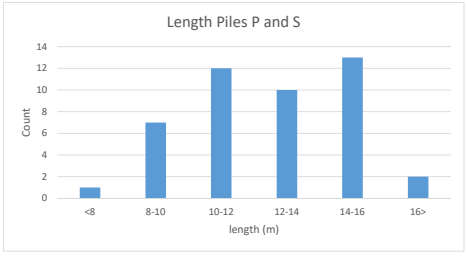


Figure 5.15: Bar graph of the length. Average of both groups is 12.48 m.

No cross section reduction has to be given to the piles, as further measurements are done on the entire section directly obtaining remaining strength and stiffness. Any deterioration is already included in these results.

## 5.4. STRENGTH, STIFFNESS AND DENSITY

As stated before, only the piles were tested on material characteristics. The dynamic E modulus has been tested in the harbour (45 piles). More measurements were taken at the TU Delft (6 piles cut in parts plus unexpected extras; 21 pilepieces). For the full specifics on these tests, the reader should take a look at appendix A and B.
Material characteristics of timber vary with moisture content, relative humidity and temperature. The harbour and laboratory tests have been carried out under different circumstances than the expected state in the quay. The next graph from Aicher & al. [68] shows the change in compressive strength with moisture content (figure 5.16). The change in Young's modulus parallel to the fibre has been added manually in purple (this is an interpolation between the two named values in this research).

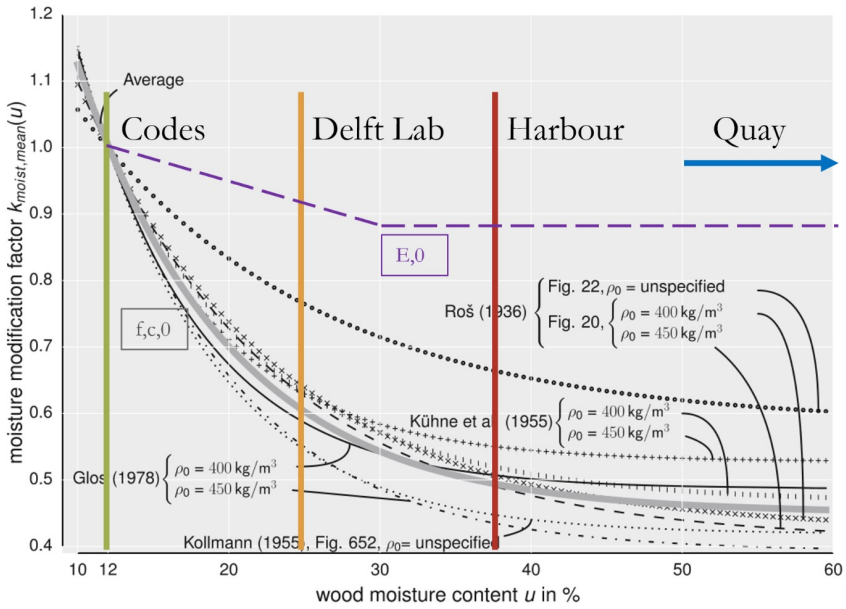


Figure 5.16: The change in compressive strength parallel to the fibre as found from the literature review on small specimen by Aicher & al. [68]. The Young's modulus has been plotted as an interpolation of their own results between 12 and 30% moisture content, keeping it constant afterwards (purple dashed line). The modification factor on the y-axis is to be used as reduction factor with respect to the 12% moisture content of the codes.

The laboratory test findings are changed to 12 and 50 % moisture content. The first for comparison with codes, the second for direct implementation in the quay wall computations. The moisture contents are added in subscript behind the material characteristics.

The laboratory tests carried out concern density, moisture content, *dynamic* E modulus (as a preparation and *comparable to the harbour tests*). Then the pile pieces are tested in a universal testing machine to failure under compression parallel to the fibre.

This concerns the *static* E modulus and compressive strength parallel to the fibre.

The conclusive figures from the Delft lab tests on Young's modulus $E_{0,12}$ and compressive strength $f_{c,0,12}$ are figures 5.17 and 5.18. They exclude outliers or failed tests and therefore have different number of measurements processed.

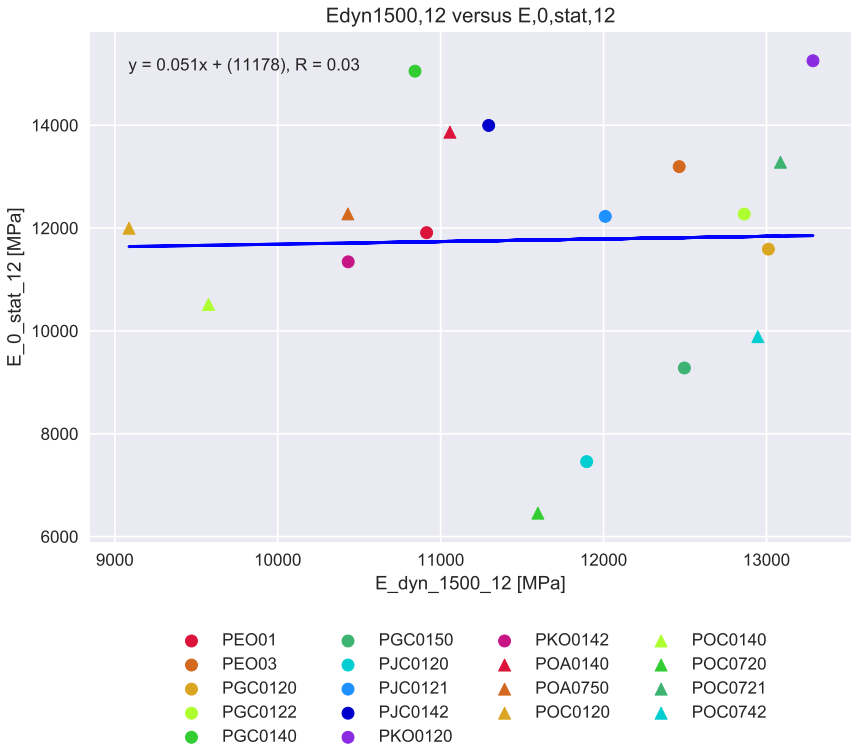


Figure 5.17: Comparison of static to dynamic E moduli for the Fr/B signal, after conversion to 12% M.C.. A Note the low coefficient of correlation R = 0.03. The number of elements tested do not give a good base for the formulation of a formula.

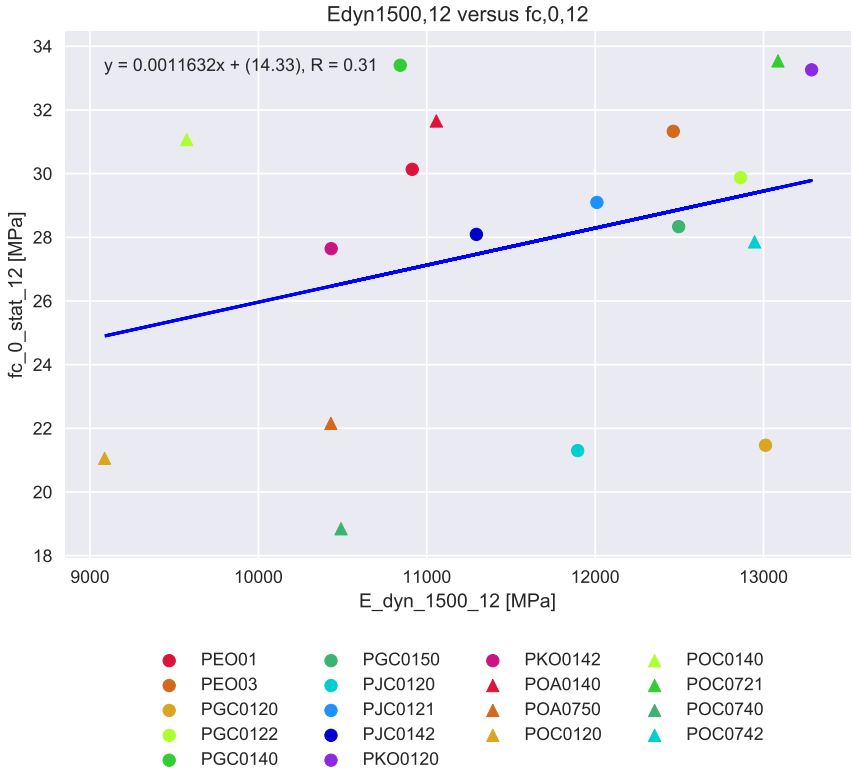


Figure 5.18: Formula for obtaining fc0 out of Edyn. The coefficient of correlation is again low.

The tests of appendix B can be used to find the strength and stiffness of all piles regarded in the harbour (the tests of appendix A). However, the correlation between the static and dynamic Young's modulus is so low that no sensible results would come out. For the obtainment of the static E-modulus it has been chosen to use equation 5.1, from literature [69], which holds for European softwoods only.

$$E_{0,stat} = 0.81 * E_{0,dyn} \tag{5.1}$$

with
$E_{0,stat}$ = Static Young's modulus parallel to the fibre $[N/m^2]$
$E_{0,dyn}$ = Dynamic Young's modulus parallel to the fibre $[N/m^2]$

The compressive strength also has a low correlation coefficient (0.31; see figure 5.18), but it is chosen to use the indicated correlation formula in figure 5.18. This is done as similar values are expected for the larger group because most of the lab-tested pilepieces have been selected to represent this group.

$$f_{c,0,12} = 1.1632 * 10^{-3} * E_{0,dyn,12} + 14.33 \tag{5.2}$$

with
$f_{c,0,12}$ = Compressive strength parallel to to the fibre at 12% moisture content $[N/mm^2]$
$E_{0,dyn,12}$ = Dynamic Young's modulus parallel to the fibre at 12% moisture content$[N/mm^2]$

The strengths and stiffnesses needed for computational modelling are the ones in fully saturated state, as expected on site. The results of the moisture adaptation can be found in table 5.3 and figures 5.19 and 5.20. These are the conclusive numbers for the pilegroup tested in the harbour. The 50% moisture content is chosen as above this percentage the compressive strength is barely influenced by moisture according to Aicher & al. [68]. Their article is also the source of reduction factors for this procedure.
Another aspect used for computation of mean and characteristic values are the methods described in NEN14358 [70]. This accounts for the number of measurements used (see equation 5.3).



$$E_{m(n)} = \overline{E} - k_{mean} * \sigma_{(n-1)} \tag{5.3a}$$

$$f_{k(n)} = \overline{f} - k_{char} * \sigma_{(n-1)} \tag{5.3b}$$

With:
$(n)$ = adaptation for number of measurements made
$\sigma_{(n-1)}$ = standard deviation adapted for measurements made
$\overline{E}, \overline{f}$ = true mean values of Young's modulus and compression strength

| | $E_{dyn,\omega}$ (MPa) | $\omega$ (%) | $E_{dyn,12}$ | $E_{stat,12}$ | $f_{c,0,12}$ (MPa) | $E_{stat,50}$ | $f_{c,0,50}$ |
|---|---|---|---|---|---|---|---|
| Mean | 14354 | 39 | 16128 | 12994 | 32,54 | 11565 | 15,62 |
| StDev (n-1 method) | 3157 | 7,45 | 3547 | 2416 | 3,39 | 2150 | 1,63 |
| $k_{mean}$ NEN14385 | | | | 0,11 | | 0,11 | |
| $k_{char}$ NEN14385 | | | | | 1,84 | | 1,84 |
| Used Mean value | | | | 12724 | | 11324 | |
| Used Characteristic value | | | | | 26,32 | | 12,64 |

Table 5.3: Recalculation of the measurement on 45 piles in the harbour to 50% moisture content and obtainment of the compressive strength.

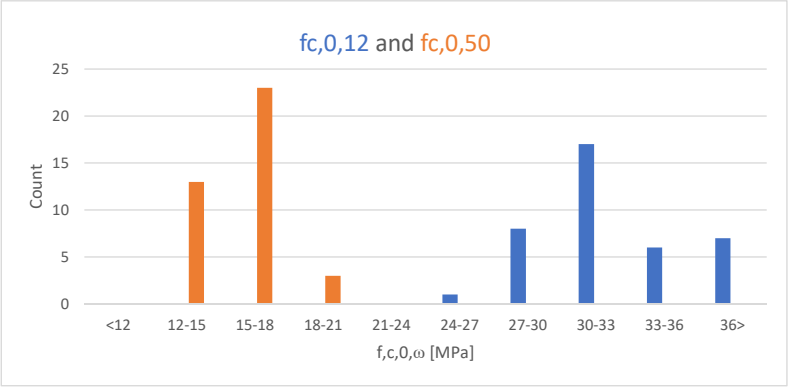




Figure 5.19: Spread of the compressive stress for dry and saturated state. Below the 50% moisture content, the strength is heavily influenced by moisture.

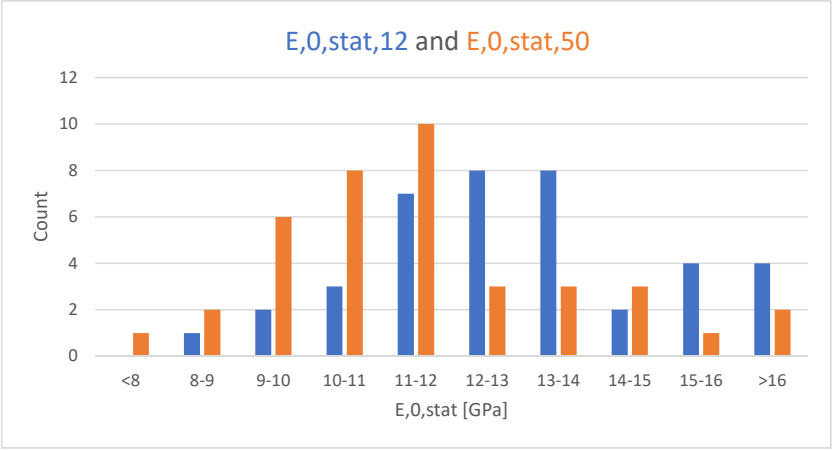


Figure 5.20: Spread of the static Young's moduli for dry and saturated state. Moisture influences the modulus by 11% only between 12% and 30% M.C. according to Aicher & al [68].

Last but not least, the density of the pilegroup looks as shown in 5.21. The equation used to modify the densities is equation A.4. It takes into account an overall shrinkage factor of 0.5% with every % change in M.C., until fibre saturation of 25% M.C. [69]. We find an average and characteristic value of 445 and 342 kg/m$^3$ using the methods of NEN14358 (see equation 5.3) [70].

$$\rho_{12} = \frac{(1+\frac{\Delta V}{100})}{(1+\frac{\Delta G}{100})} * \rho_{\omega} \tag{5.4}$$

with

$\rho_{12}$ = density under 12% moisture content $[kg/m^3]$
$\rho_{\omega}$ = density under current moisture content $[kg/m^3]$
$\omega$ = moisture content [%]
$\Delta V = \beta * (\omega - 12)$ = change in volume [%]
until $\omega$ = 30% at most (fibre saturation corresponding to used borders for the E modulus). $\beta$ =0.5 [%]
$\Delta G$ = change in weight [%]

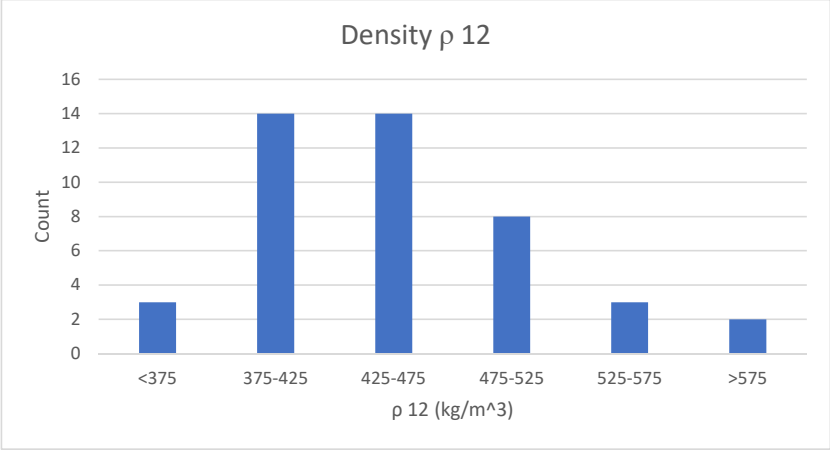


Figure 5.21: Spread of the density, normalised to 12% M.C.

## 5.5. CONCLUDING CHARACTERISTICS

The concluding characteristics are intended for a capacity calculation in the 2015 situation. This means the chosen characteristics are finetuned to the most recent state for the capacity judgement.

### 5.5.1. DIMENSIONS

The software used for the load distribution calculation works with prismatic elements. This means that for *modelling* the force distribution, full sectional sizes as described in the original drawings are used. Average pile diameters are placed into the models.
For *Safety calculations*, reduced cross sections on the horizontal timber and piles alike will be used taking into account erosion. This is based on the executed dimension measurements. For the horizontal timber this is based only on one measurement per element type, although visually it is very apparent erosion is present on all elements which would make the use of full sections non-conservative. This leaves one non-conservative measurement: that of the planks. No section reduction has been measured here due to measurement over a support spot. Since the quay wall's safety is judged in 2D, no attention needs to be given to these elements, but a reduction similar to the capping beams in absolute terms would be sensible. Therefore, no biological degradation effects have been taken into account for the remaining cross sections. The effects are however present indirectly as the material characteristics are obtained on the piles, where no distinction is made between non-deteriorated and deteriorated wood. However, as most pile elements tested were under the water table throughout their lifespan, the chance of (fungal) degradation being more severe on the horizontal timber than on the piles is large. The approach regarding the biological degradation is therefore non-conservative. But as stated before, it is not sensible to superimpose both erosion and biological degradation if they are not measured simultaneously. The finally used dimensions can be seen in tables 5.4 and 5.5.

| Element | Height (m) | Width (m) | Diameter (m) | Length (m) |
|---|---|---|---|---|
| Capping Beam | 0.20 | 0.30 | | 4.60*, 6.00** |
| Pile | | | 0.22 | 12.50 |

Table 5.4: Dimensions to be used for modelling. *Section 4-1, **section 3-1.

| Element | Location | Height (m) | Width (m) | Diameter (m) |
|---|---|---|---|---|
| Capping Beam | At support | 0.20 | 0.25 | |
| | At span | 0.17 | 0.25 | |
| Pile | Head | | | 0.24 |
| | Tip | | | 0.20 |

Table 5.5: Dimensions to be used for capacity and safety judgement.

### 5.5.2. MATERIAL CHARACTERISTICS

Some material characteristics are obtained through testing, but the remaining ones for a safety calculation must be derived. The tested characteristics are therefore compared to EN 338 under 12 % moisture content to find a class which can from then on represent the wood of the Maaskade. It must be noted that the norm is for rectangular timber (in contrast to the tests on logs). Also, the values do not take into account any degradation (which most probably is present on a few pilepieces).
The characteristic *density* would conclude to (bending) class C22. The mean and characteristic *Young's modulus* (//) would end inbetween C30 and C35. The characteristic *compressive strength* (//) leaves the impression of C35 to C40. What immediately is noticed

is the fact that the difference in mean and characteristic value for the Young's modulus is similar in the class and the tested pilegroup, but this does not hold for the density. Although not justifiable without further differentiation into multiple classes, using the Maaskade pilegroup's mean density at 12% MC (445 kg/m$^3$) would result in class C27 to C30 which is two to three classes higher than C22. It is chosen to stick to the lower class of the three groups: C22, for the *remaining characteristics* which are not tested directly. See figure 5.22.

**Table 1 — Strength classes for softwood based on edgewise bending tests – strength, stiffness and density values**

| | Class | C14 | C16 | C18 | C20 | C22 | C24 | C27 | C30 | C35 | C40 | C45 | C50 |
|---|---|---|---|---|---|---|---|---|---|---|---|---|---|
| **Strength properties in N/mm²** | | | | | | | | | | | | | |
| Bending | $f_{m,k}$ | 14 | 16 | 18 | 20 | 22 | 24 | 27 | 30 | 35 | 40 | 45 | 50 |
| Tension parallel | $f_{t,0,k}$ | 7,2 | 8,5 | 10 | 11,5 | 13 | 14,5 | 16,5 | 19 | 22,5 | 26 | 30 | 33,5 |
| Tension perpendicular | $f_{t,90,k}$ | 0,4 | 0,4 | 0,4 | 0,4 | 0,4 | 0,4 | 0,4 | 0,4 | 0,4 | 0,4 | 0,4 | 0,4 |
| Compression parallel | $f_{c,0,k}$ | 16 | 17 | 18 | 19 | 20 | 21 | 22 | 24 | 25 | 27 | 29 | 30 |
| Compression perpendicular | $f_{c,90,k}$ | 2,0 | 2,2 | 2,2 | 2,3 | 2,4 | 2,5 | 2,5 | 2,7 | 2,7 | 2,8 | 2,9 | 3,0 |
| Shear | $f_{v,k}$ | 3,0 | 3,2 | 3,4 | 3,6 | 3,8 | 4,0 | 4,0 | 4,0 | 4,0 | 4,0 | 4,0 | 4,0 |
| **Stiffness properties in kN/mm²** | | | | | | | | | | | | | |
| Mean modulus of elasticity parallel bending | $E_{m,0,mean}$ | 7,0 | 8,0 | 9,0 | 9,5 | 10,0 | 11,0 | 11,5 | 12,0 | 13,0 | 14,0 | 15,0 | 16,0 |
| 5 percentile modulus of elasticity parallel bending | $E_{m,0,k}$ | 4,7 | 5,4 | 6,0 | 6,4 | 6,7 | 7,4 | 7,7 | 8,0 | 8,7 | 9,4 | 10,1 | 10,7 |
| Mean modulus of elasticity perpendicular | $E_{m,90,mean}$ | 0,23 | 0,27 | 0,30 | 0,32 | 0,33 | 0,37 | 0,38 | 0,40 | 0,43 | 0,47 | 0,50 | 0,53 |
| Mean shear modulus | $G_{mean}$ | 0,44 | 0,50 | 0,56 | 0,59 | 0,63 | 0,69 | 0,72 | 0,75 | 0,81 | 0,88 | 0,94 | 1,00 |
| **Density in kg/m³** | | | | | | | | | | | | | |
| 5 percentile density | $\rho_k$ | 290 | 310 | 320 | 330 | 340 | 350 | 360 | 380 | 390 | 400 | 410 | 430 |
| Mean density | $\rho_{mean}$ | 350 | 370 | 380 | 400 | 410 | 420 | 430 | 460 | 470 | 480 | 490 | 520 |

NOTE 1 Values given above for tension strength, compression strength, shear strength, char. modulus of elasticity in bending, mean modulus of elasticity perpendicular to grain and mean shear modulus have been calculated using the equations given in EN 384.

NOTE 2 The tension strength values are conservatively estimated since grading is done for bending strength.

NOTE 3 The tabulated properties are compatible with timber at moisture content consistent with a temperature of 20 °C and a relative humidity of 65 %, which corresponds to a moisture content of 12 % for most species.

NOTE 4 Characteristic values for shear strength are given for timber without fissures, according to EN 408.

NOTE 5 These classes may also be used for hardwoods with similar strength and density profiles such as e.g. poplar or chestnut.

NOTE 6 The edgewise bending strength may also be used in the case of flatwise bending.

Figure 5.22: Strength classes (based on bending tests) for rectangular cross-sectioned softwood as in EN338 [2]. In blue the values from the laboratory tests, corrected for moisture. The least optimistic value - the density - has been chosen for assignment of C22 to retrieve missing characteristics.

# 6

# MODELLING THE LOAD DISTRIBUTIONS

*CHAPTER 6 uses the found information on build-up, material state and safety philosophy to set up load combinations and a model to find the load distributions. Use has been made of PLAXIS 2D (2019) for the computation. The modelled section is section 4-1.*

## 6.1. LOAD CASES

The literature study of chapter 2 concludes with the need for assessment on 'rejection' or 'disapproval', a structure in consequence class 2 and a reference period of 15 years. Futher on, chapter 4.4 shows the possible loads that can be exerted on this specific case. The following cases can then be implemented in a finite element model. The final configuration (2003-2015) is the only case referring directly to the main research question on remaining capacity under the currently researched state and safety approach.

### 6.1.1. LAY OUT COMPARISON: SERVICEABILITY LIMIT STATE (SLS)

Nevertheless, the structure is modelled throughout its entire period in SLS under characteristic values representing the best estimate of the quay. The construction stages and renovations have an influence on the state of the soil that shows different loading and un-/reloading stiffnesses. This best estimate model also allows for a comparison of structure layout on the load distribution throughout the years. This not only shows if the past renovations had a positive influence on the load distribution, but can also be used for a damage accumulation model (not included in this thesis) that would show the influence the effect of permanent loads on the wood mechanical deterioration.
The final configuration (2003-2015) is also assessed on deformations in this limit state. The computations are then as follows:



1. SLS 1922: the best estimate model for the quay in the 1922 set up;
2. SLS 1982: an equal model for the set up in 1982;
3. SLS 2003: an equal model for the set up in 2003.

See See figures 6.1 to 6.2 for an overview of these cases.

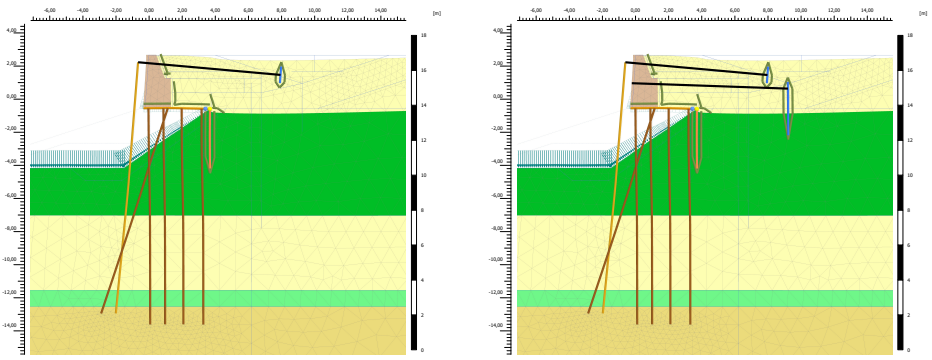

Figure 6.1: Left: SLS 1922, Right: SLS 1982.

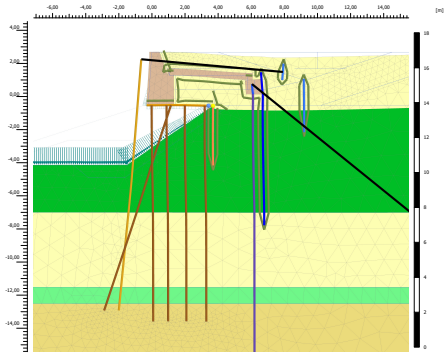

Figure 6.2: SLS 2003.

### 6.1.2. LOAD CASE COMPARISON: ULTIMATE LIMIT STATE (ULS)

The final configuration is modelled in ULS using the appropriate partial factors on the loads and soil strengths from NEN 8700 and NEN 8707. A few starting points are highlighted below.

Partial load factors for **permanent loads** are stated in NEN 8700 (appendix A.1, page 28 & 29) [32] to be the same as in new buildings. As the soil provides the resistance as well as the loading, the partial material factors on soil weight are 1.0 which results in no extra permanent loading in the 'selfweight governed' limit states. The partial factor for **variable loads** that are not of geotechnical origin is 1.15, the same as for buildings.
Water levels and retaining heights are to be adjusted according to NEN 8707. The guidelines for historical quay walls [10] however mention more conservative values that are also likely to occur.
**Water levels** are adjusted to 'LLWS' (lowest monthly measured level), which is lower than the average lowest level superimposed with the 15 cm deviation from NEN 8707. This norm also mentions a 5 cm increment on the inland waterlevel, while the 50 cm increment proposed by BiKa is not unlikely to occur in an area with tides and a possibly delayed backward waterflow from the island to the river.
Moreover, NEN 8707 mentions a 20 cm increase on the **retaining height** (appendix A, page 45). This is implemented for ULS case 1 as an extra surcharge. But also a lower pile embedment has been taken into account. An abrasion of 2 diameters is to be expected on the river bank [23], but the layer of slib above the riverbank protection layer (gravel and dirt) is slightly thicker for the outer pile and thinner for the inner pile. The entire slib layer is likely to be washed away or dredged in worst case and therefore is neglected in ULS.

The used load configurations are split into ones that push towards the river (land based) or ones that push the quay into the shore (water based) are as follows:

1. ULS Self weight (EB)- Land based loading with Embedded Beams;
2. ULS Self weight (A) - Land based loading with Anchors ;

3. ULS Surcharge (Parking spaces) - Land based loading;

4. ULS Ship berthing (non impact) - Water based loading;

5. ULS Ice - Water based loading;

6. ULS Wind (Mooring & Tree load) - Land based loading (Mooring anchor is attached inland).*

*The wind case is not of direct influence to the timber foundation do to the placement of the anchorage and trees far of the retaining wall and the steel sheet piles being placed in between the anchor and the concrete wall.
See figures 6.3 to 6.5 for an overview of these cases, and chapter 4 for the assumptions used for the load components.



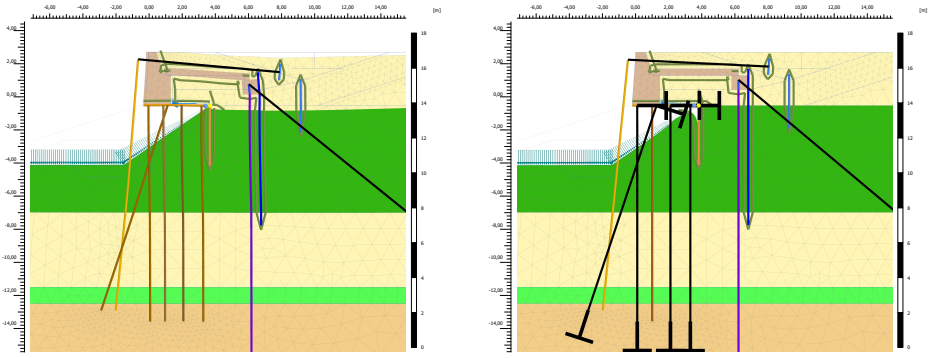

Figure 6.3: Left: ULS Self Weight (EB) with embedded beams, Right: ULS Self Weight (A) with note-to-node and fixed end anchors.

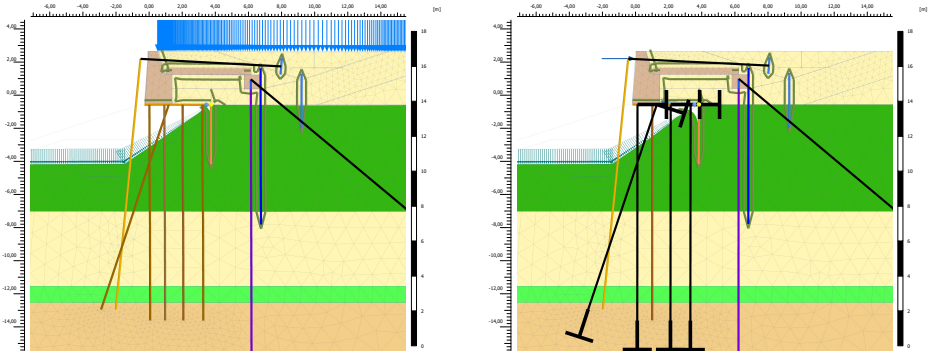

Figure 6.4: Left: ULS Surcharge, Right: ULS Ship.

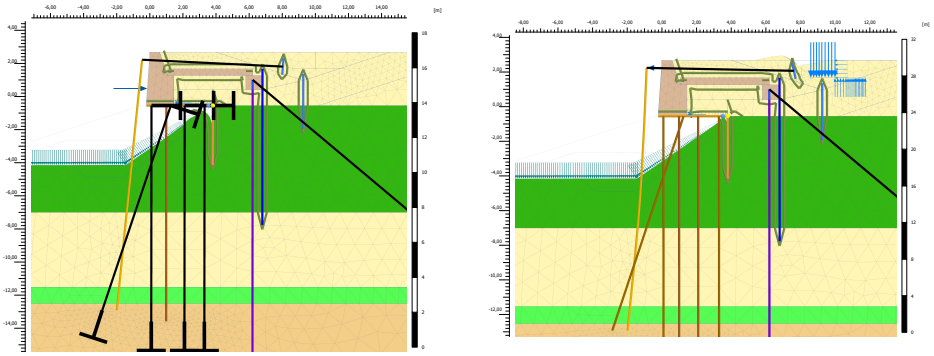

Figure 6.5: Left: ULS Ice, Right: ULS Wind. This combination is not used for further analysis on the timber.

## 6.2. COMPUTATIONAL MODEL SET UP

The model described is the main model used for computation of the load distribution in PLAXIS 2D.

### 6.2.1. ELEMENTS

An overview of the used elements is shown in figure 6.6 and 6.7.

The used elements for the **soil** are plane strain 15-noded triangular elements. The used soil model is the Hardening Strain model that gives a higher stiffness the higher the effective stresses. The **concrete wall** too is modelled as a soil, using the Mohr-Coulomb model and strength and stiffness values according to Dusko Ardiaca [71], matching concrete properties to a concrete with characteristic compressive strength of 25 MPa. **Interfaces** are modelled as soils in Plaxis as well. The used strength is obtained from literature (Potyondy for soil-structure interaction [72], Jaaranen & Fink [73] for wood-concrete and NEN 12812 for concrete-concrete and steel-concrete [74]. The use of 'soil' materials for interface modelling is possible due to the fact initial cohesion and friction coefficient (equal to the tangent of the friction angle) found in tests can directly be put in a Mohr Coulomb material model.

The timber **floor planks** are not modelled directly and are not thought of as a structural element in the cross section (2D situation). The **capping beam** instead takes its function of earth retainment. This element is modelled as an elastic plate, with equivalent depths for the centre-to-centre distance between each other. The timber sheetpile is modelled as a plate too and is connected with a hinge to the capping beam. The **piles** are modelled as embedded beams with hinged connections at the top. They too are elastic. Embedded beams offer the possibility of placing piles 'above' the mesh, connecting them with a continuous springs to the soil behind it. This way the soil can move through the pilerows, and the piles are not modelled as continuous sheets. The used material model for both plates and embedded beams are 5 noded beam elements according to the Mindlin theory, taking into account axial, bending and shear deformations. As these materials are modelled elastic, a post-analysis on failure is necessary.

Water is not modelled as elements but rather as a condition or state elements can be in. A global waterlevel is assigned for each phase. It is complemented by manually added pressures in case the level is higher above than underneath the platform (e.g. drainage issues).

The model overview shows all elements used for all stages, and therefore has overlapping elements. Plaxis element types are highlighted. See figures 6.6 and 6.7.

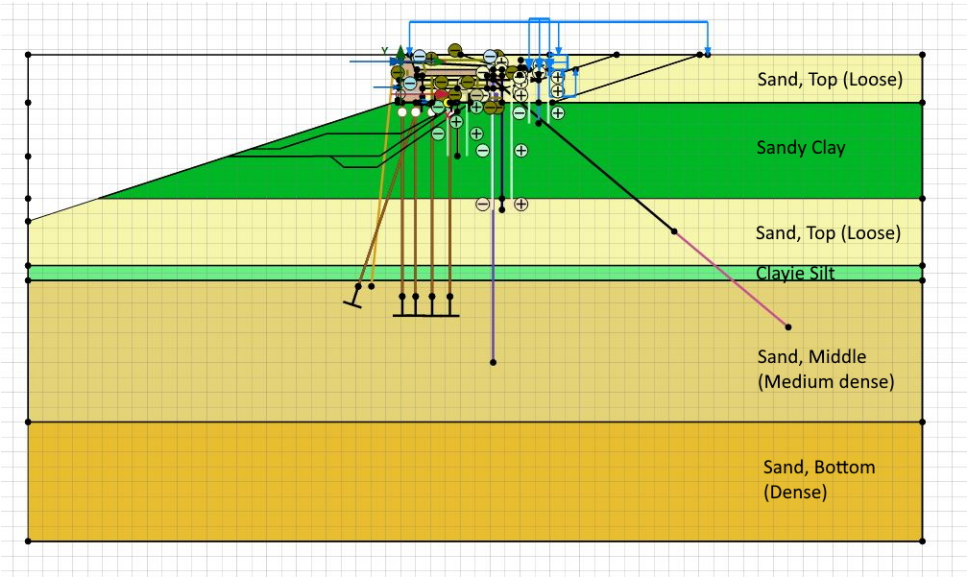


Figure 6.6: Zoomed out overall overview. Overall model size (hxwxd): 32.65x60x1 m.

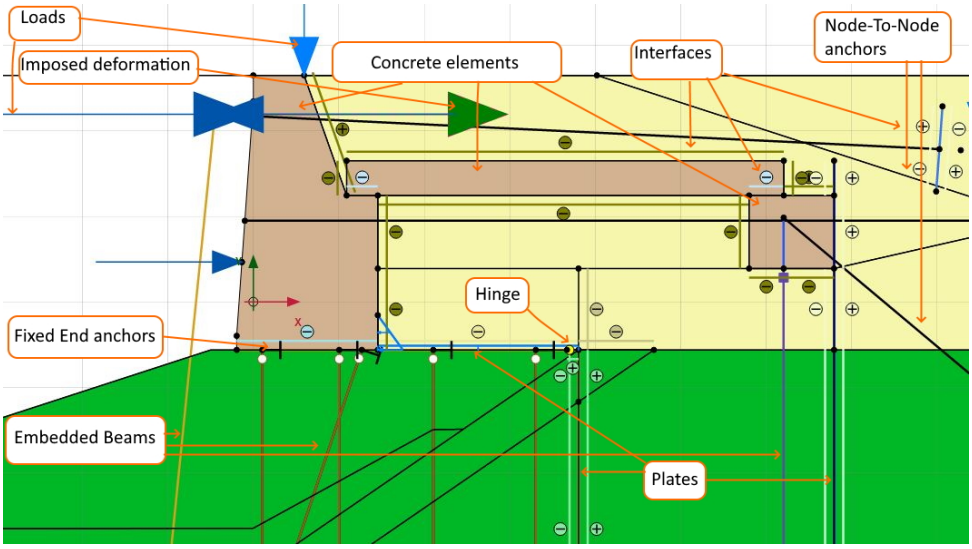


Figure 6.7: Pointed out element types in the model input view.

### 6.2.2. PROCEDURE

The procedure for calculating starts with a soil profile without structural elements. The soil is loaded on gravity to allow for formation of stress state in the soil. In the next phase, the 'plastic nil', the deformations are reset that give back the original groundlevel but the stresses are not reset. Following are the construction stages which are performed in a plastic, drained analysis.

All of these (SLS) stages are performed in series, with the best-estimate material characteristics. All the seperate ULS stages are then performed parallel to themselves, not influencing one another. Firstly, the materials are changed before the external loadings are applied. See figure 6.8.

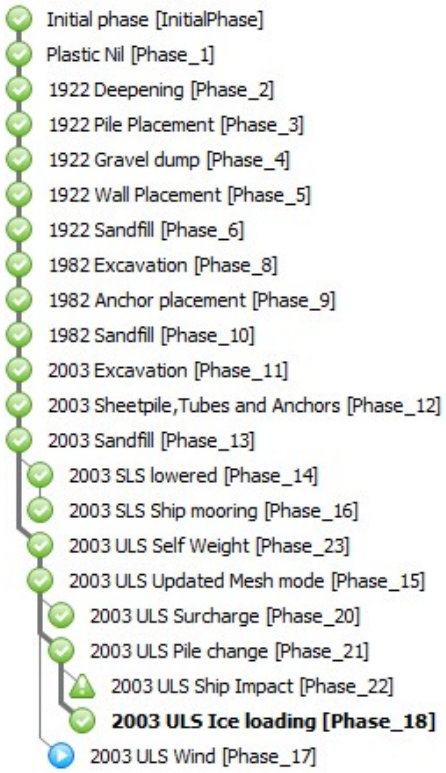


Figure 6.8: Stages of the Plaxis model.

### 6.2.3. LIMITATIONS

The model is not using the updated mesh function for the *SLS* cases, meaning geometrical non-linearity is not taken into account in theses stages. The updated mesh function is used for the *ULS* stages. This is particularly important for implementation of $2^{nd}$ order effects such as sliding.

The concrete is assigned with maximum tensile stresses and uses the mohr-coulomb criterion for compression and shear, but no further discrete or smeared cracking models are implemented. No reinforcement is implemented either: the section of the retaining wall is a solid block consisting of multiple elements. If maximum tensile stress occurs, the element will fail and the computation stop.

The latter holds for all soil-model implementing elements (soils, interfaces, concrete). If a percentage of the integration points reaches shear or tensile failure, the computation stops. This is due to Plaxis boundary conditions.

## 6.3. PREPARATION TESTS AND VALIDITY

The structure incorporates multiple embedments within different soil layers and cannot be easily calculated by hand due to the resulting statical indeterminacy. This holds for the resulting forces within the structure, but also on the forces acting on the structure, as soil pressures are dependant on the deformations caused by the reaction of the structure. The validity of the outcomes of the model can best be proven by comparison to real life tests, otherwise by checking of partial elements by hand calculations or by comparison to other proven software that uses different modelling approaches. Since no proof loading has been undertaken on the Maaskade itself, use has been made of the latter two options.

### 6.3.1. FRICTION TESTS

The sliding between the timber floor and concrete wall was modelled with the use of a Mohr-Coulomb interface.

The interface has been separately checked to see if it works as wished. It is seen that the numerical process is very stably for concrete on timber on concrete and less stable for concrete on a timber platform in soil. After discussion with a Plaxis expert [75], it is clear Plaxis is finetuned for soil-structure behaviour, not structure-structure. The advise is to use a smaller stiffness on the interface and to swap a friction angle dependant interface for a cohesion dependant interface.

This advise is partially taken into practice by means of a lower stiffness. As the interface has a low (virtual) thickness and a large stiffness when compared to the surrounding soil materials, the effects of lowering this stiffness are small. Furthermore, the strength is not adjusted and the question of whether the wall will slide off the plateau is not influenced (see figure 6.9).

The friction angle dependency could not be swapped for a cohesion dependency. As the amount of friction that can be taken depends on the amount of normal force on the interface, this approach works only if there is a constant normal force on the interface as the (input) cohesion property remains constant too. The numerical process is indeed more stable and the simple concrete-on-plateau models do what they are intended for even with the original stiffness, but with a beforehand unknown normal stress on the interface the friction angle approach is the only concept that catches the essence of friction and can be used for the original problem of the Maaskade quay.



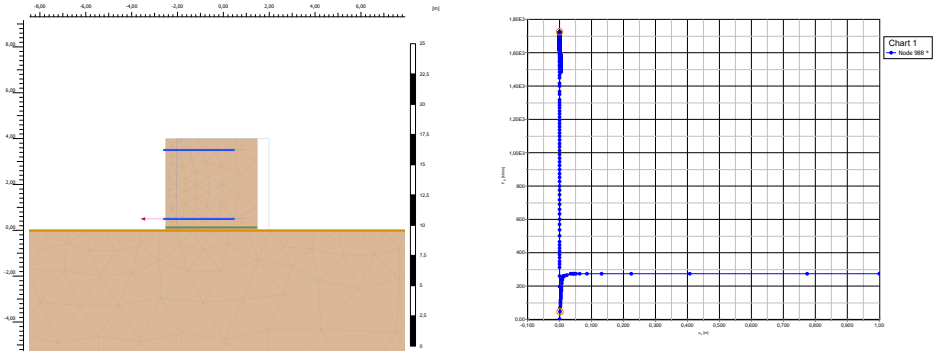


Figure 6.9: Left: overview of the test set up. Right: Force-displacement results. The tall curve gives the unstable solution for the best-estimate stiffness, the lower one with the stiffness reduced by $10^3$.

### 6.3.2. MOORING PILE

To find out if the mooring Pile and the beams coupling these piles together can stand a ship impact, or if the wall is touched on impact, two models are set up. There is not much known of this mooring piles other than the center to center spacing of 9.5 m. The assumed dimensions are an 0.4 x 0.4 $m^2$ cross section area for the piles and a 0.4 x 0.2 $m^2$ cross section area for the beam. The same length and E modulus have been used as deducted for the other piles.
The first model is a hand model by Davisson & Robinson [76]. An equivalent embedment depth makes it possible to model the piles as a column with a clamped base. This model can then be used to find the horizontal force that causes the necessary deflection for the mooring pile to touch the concrete wall and then to integrate the area underneath the force displacement curve to find the absorbed energy.
The second model is a Plaxis 3D model using a volume pile (instead of an embedded beam, a volume is present in the mesh with the timber properties). The same procedure is applied by using a prescribed deformation to find the force that is placed on the mooring pile and subsequently integrating the force displacement curve. See figure 6.10.

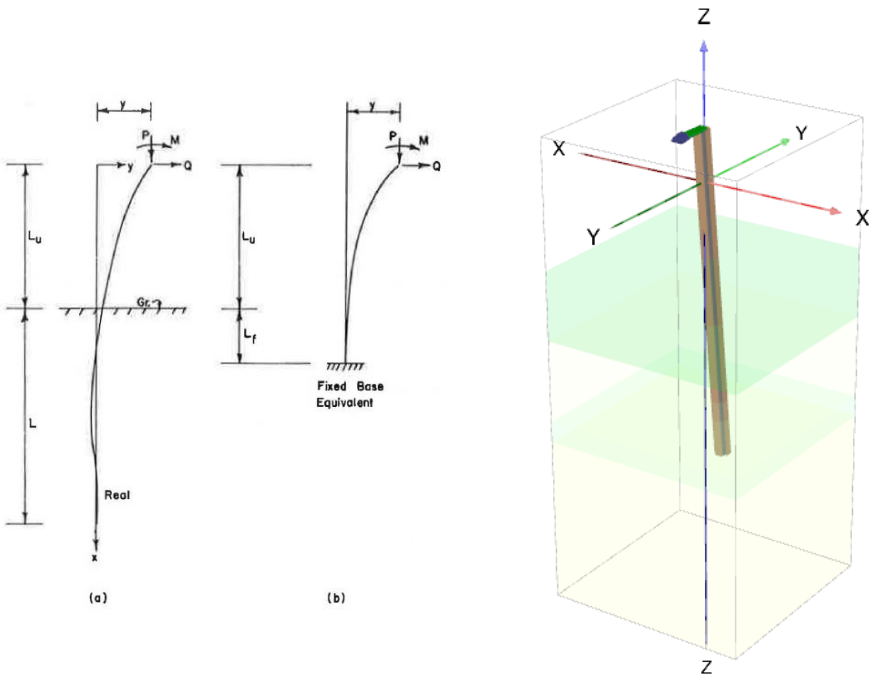


Figure 6.10: Left: Davisson's model, dependant on the subgrade modulus and on type of soil (cohesive/granular). Right: Plaxis 3D colume pile.

Both methods have a similar outcome, and it can be concluded that indeed the concrete wall will need to take a part of the ship impact if the ship hits the mooring pile directly. If the beams between the mooring piles are hit, the amount of energy absorbed is different and can be computed using the found stiffness on the single pile. Again, the ship impact will conclude in a force being applied on the quay wall behind the berthing structure. The energy absorbed in this 14 cm distance to the wall is 1610 Joule, the equivalent embedment in the soil 1.23 m, giving a total free length of 7.41 m.

### 6.3.3. COMPARISON TO HAND-BASED MODEL

For the loading under selfweight only, Plaxis 2D is used to calculate both the load itself and the reaction of the structure as a whole. Therefore it is quite a black box. Matrixframe (FEM for elastic calculations) has been used to check whether similar results where found if both the loads as the soil's bedding constants would be implemented by hand. For a realistic stress input on the sheetpile use has been made of the software D-sheetpiling. The outcome would also say something about the load predictability: whether a simpler load estimation would suffice or not.

Large differences were found. To find out the reason behind the differences, both models had to be simplified to a level the output would be equal. since both software have proven their reliability in practice, it was known at some point this would occur.

Three mayor differences were discovered. One of them on the reaction of the structure and two more on the loading of it.

- Firstly, the main curvature points of the piles after lateral loading were near the contact point with the clay in Matrixframe, while these were located between the clay and sand layers in Plaxis 2D. This indicated the depth independent bedding constants in Matrixframe were having a different effect than the depth dependant shear modulus in the interface stiffness factors in Plaxis. The 'looser' reaction of the clay in Plaxis also pushes the timber piles laterally. The loose reaction is at least partly explained by allowance of plasticity in the Plaxis soil models.
- Secondly, additional loading on the sheetpile is present in the form of (instantaneous) negative friction on the active side of this element.
- Lateral shear friction is present on the timber platform. It pushes the platform further towards the riverside.

### 6.3.4. ANNOTATIONS

It has to be mentioned that Matrixframe has the drawback in not being able to calculate plastically, and that a 1:1 comparison can only be made if no plasticity occurs in the Plaxis model either, which is doe snot hold for the soil elements.

Another important point to make is that tension occurs in two of the 4 vertical pilerows using this initial model.
However, the standard mortise and tenon connection in wall section 4-1 of the piles with

the capping beams is not to take tensile forces (author's judgement). For a tensile mortise and tenon joint, a glued or dovetailed tenon is expected.
Arguably, some friction can take place between the mortise and tenon due to prestressing by wedges, but the effect is most probably negligible. Especially in its final degraded state as seen in the 2019 pictures (see figure 6.11, left). This holds for pilerow 3. Pilerow 2 has a mortise and tenon joint with a bolted brace. This connections is assumed to be able to take tensile forces (through the bracing, not the tenon). See figure 6.11, right.


Figure 6.11: Left: Standard Mortise and Tenon joint (e.g. pile row 3). Right: Braced Mortise and Tenon joint (e.g. pile row 2).

From the comparison it became clear that the soil build up has a large influence on how the force transfer takes place. For example, the same structure in an all-clay environment in Plaxis proves to have smaller forces in every single pile row. The small stiffness differences within the clay mass make the entire structure settle when loaded. For the clay & sand environment in the Maaskade, the difference in stiffness between the clay and the sand layer makes the structure take up a larger portion of the lateral stresses in the soil as it is firmly embedded in the sand layer below. The foundation tends to resist the movements of the clay layer as opposed to settling with it.

## 6.4. ADAPTATIONS AND FINAL MODEL RESULTS

### 6.4.1. ADDITIONS TO SET UP

As mentioned in the previous section, connections other than the one of pilerow 2 are thought of as not being able to take tension. To incorporate this boundary condition, an additional procedure had to be incorporated. The options were as follows:

1. Iterative procedure using embedded beams: Firstly the model is calculated with all piles, then secondly the 'incorrect' tensile piles have their shaft and toe resistance

set to 0. The drawback is that stability is needed during self-weight loading in order to apply additional loading (not possible for stages ULS Ship and ULS Ice). The advantage is that the pile still gives lateral resistance and that the pile spacing effects are included;

2. Use of *node-to-node* and *fixed end anchors* as pile elements: The node-to-node anchor elements give the possibility to model with a maximum force. With the tensile resistance set to nearly 0, the piles 'deactivate' when loaded on tension. As they can only bear an axial force, additional fixed end anchors need to be placed laterally with an equivalent bending stiffness in axial direction perpendicular to the actual pile axis. The lateral anchors are set to a stiffness equivalent to that of a free pile embedded in the sand layer (6.5 m in length).
The drawback is that skin friction and lateral pile loading is not (fully) modelled; the node-to-node anchor connects the structure with a point further down in the soil mesh and only takes axial loads. The advantage is an instantaneous response without iterative procedure.

Stages ULS Ship and ULS Ice therefore incorporate anchor element instead of embedded beams and will not return information of bending moment, shear, friction and lateral pressures in/on the pile. Prestressing to previous stress level is necessary when changing piletype. Pilerow 2, the only pile that can take compression and tension, will remain an embedded beam as prestressing anchors in tension will result in a concentrated tensile load in the soil and thus failure at the piletoe. See figure 6.12.

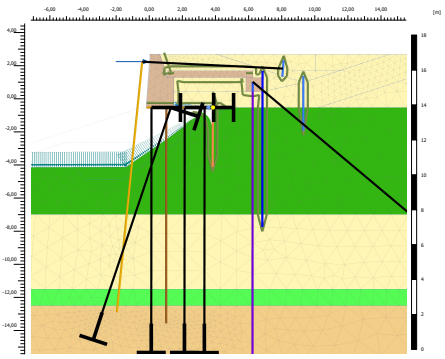

Figure 6.12: Anchor and Embedded beam lay out for ULS Ship.

### 6.4.2. SOIL RELATED STRENGTHS IN ULS

The characteristics of the soils are been downgraded for the ultimate limit state with a material factor of 1.1 on the tangent of $\phi'$ and on the cohesion. The ultimate vertical and lateral capacities based on Koppejan and Brinch-Hansen respectively are multiplied with factor $\xi_4$ = 0.96 for using the lowest value of 2 CPT's and $\gamma_b, \gamma_s$ = 1.2. For the tensile pile, the values are $\gamma_{MB4}, \gamma_{var,qc}$ = 1.35, 1.31.

### 6.4.3. COMPLETION OF STAGES

Since elastic elements are used for modelling timber, the moment of failure has to be deducted after post-processing the results. The calculation stages complete unless the soil fails. The only stages that failed in this way are ULS 3 (Ship berthing) and ULS 5 (wind). The former was expected to fail as a surplus of force (200 kN) is applied to find the moment of completion of the ship's energy absorption. The ship's energy is absorbed before the soil fails at 0.65 times the stage completion, resulting in a 130 kN equivalent static force, assuming the ship does not deform itself. At the completion of energy absorption, the $1^{st}$ pilerow almost becomes loose as the compression drops, with just 6.5 kN remaining.

### 6.4.4. RESULTS

In the results, the normative elements and sections reveal themselves in the raking pile (compression), pile row 2 (tension) and in the capping beam in the joint area where these two come together. In the model, the transverse beam that connects the raking pile with the capping beam is left out - this should be noted. Figure 6.13 shows this joint and the used cross section and $N_{c,90}$ effective area. Note that for the SLS comparisons, full sections are used for stress deduction, while for the ULS cases the eroded remaining dimensions are used. Figure 6.14 gives more details on this joint.



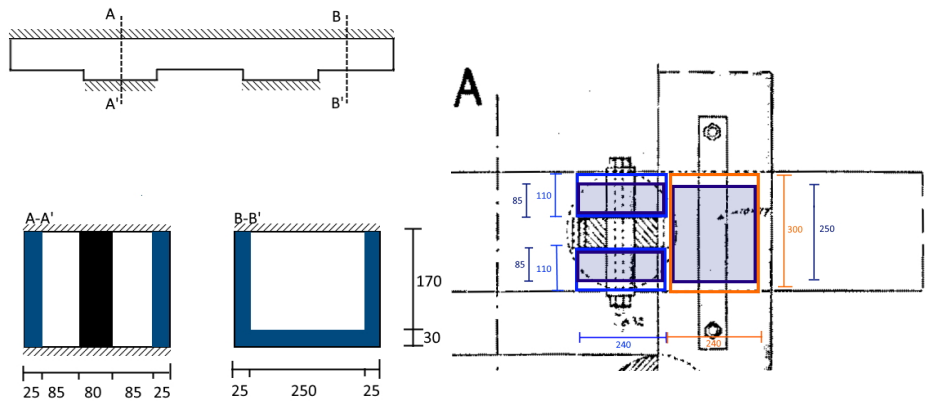


Figure 6.13: Left: Full and reduced cross sections. The mortise and tenon section on the left (pilerow 2 attachment) and the area used for the raking pilerow attachment on the right of this subfigure. Right: Effective areas for $N_{c,90}$ in plan view. In blue the connection pilerow 2 with the capping beam, in orange the connection with the transverse beam (raking pile). The dark blue tone shows the reduced areas. It has to be noted that these areas are based on the width of the steel strip that provides the contact.

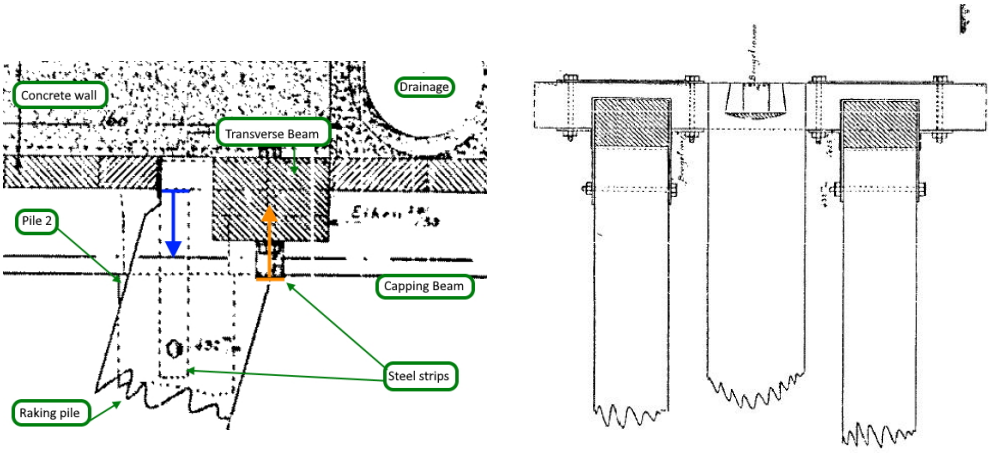


Figure 6.14: Sideviews of the joint.Right: The raking pile in between the two vertical piles has been found on site to be placed towards one of the two.

**SLS: Comparison of selfweight reactions throughout the years.**



This subsection gives the quantitative and qualitative results of the best-estimate models of the 1922, 1982 and 2003 build-ups. The deformation of the entire structure is indicated, then the pressures onto the structural elements, the axial forces on the piles and their deformation, and finally the shear forces in the capping beams. The latter is of interest for the compression perpendicular to the fibre at this spot, as the shear forces on either side of the contact point can be added to obtain this force. The corresponding figures are 6.15 to 6.23.

**1922**

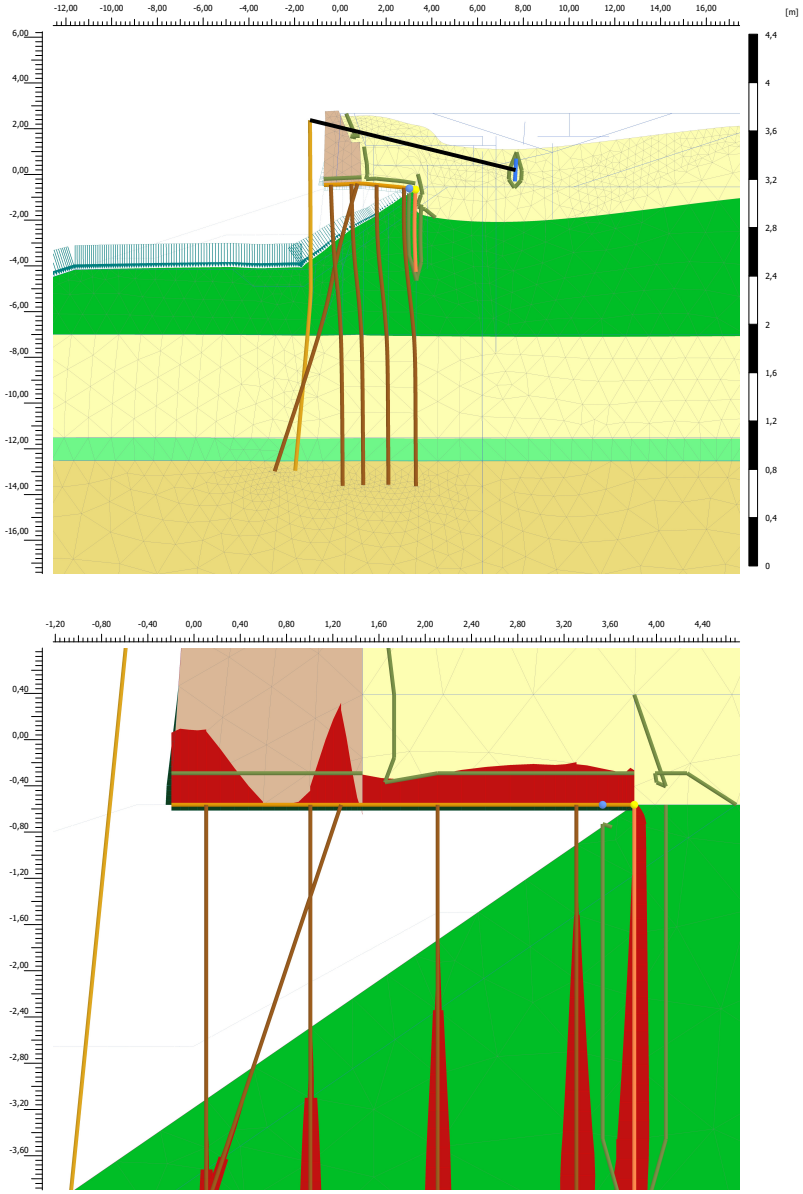


Figure 6.15: Top: Enlarged 1922 mesh deformations (factor 5). Bottom: The pressures acting on the soil-structure interface.

**1922**

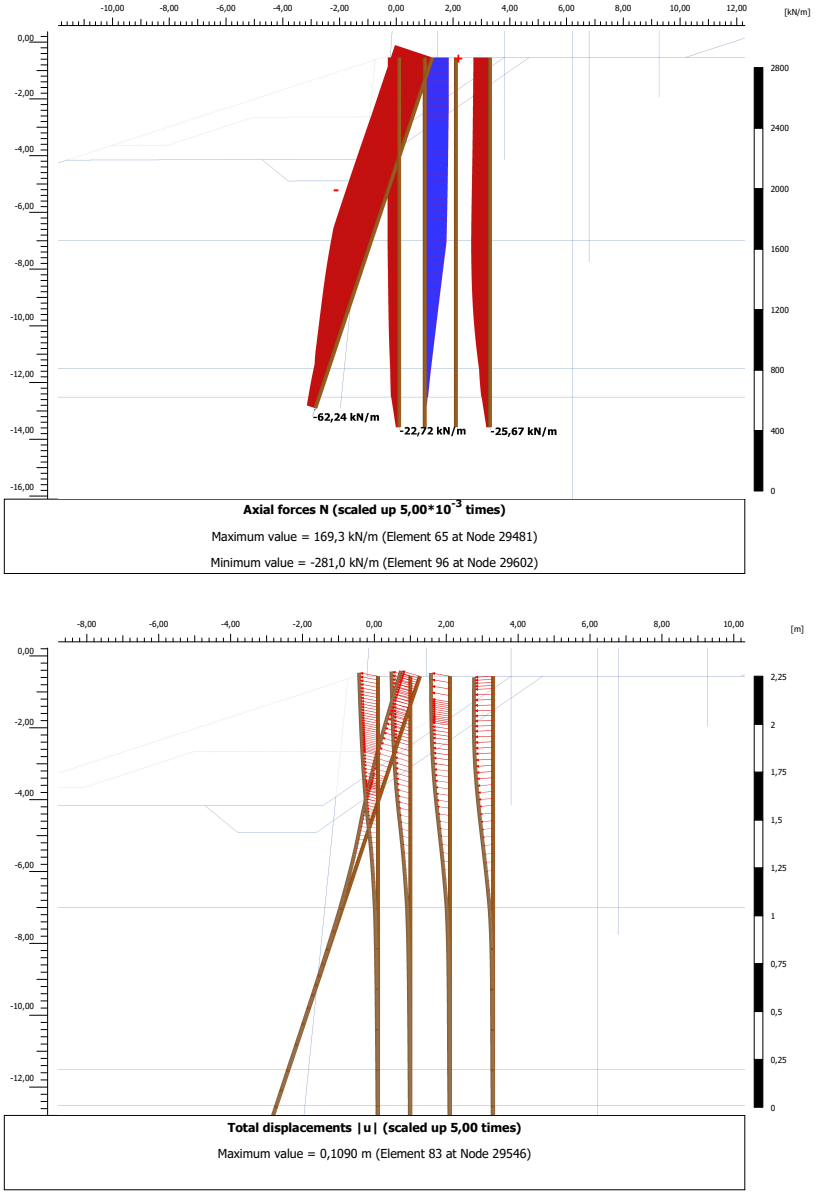


Figure 6.16: Top: Overview axial pile forces in the 1922 set up. Bottom: Deformations of the piles.

**1922**

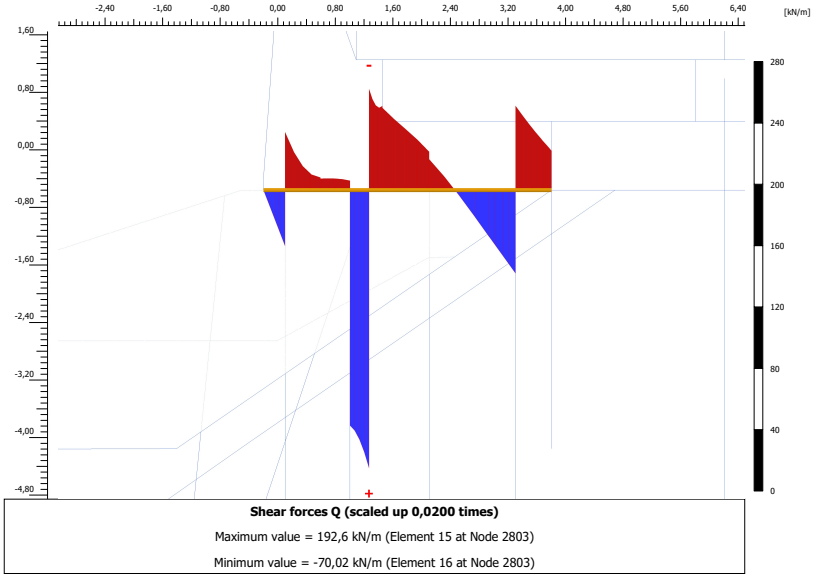


Figure 6.17: Shear forces in the capping beam for the 1922 set up.

**1982**

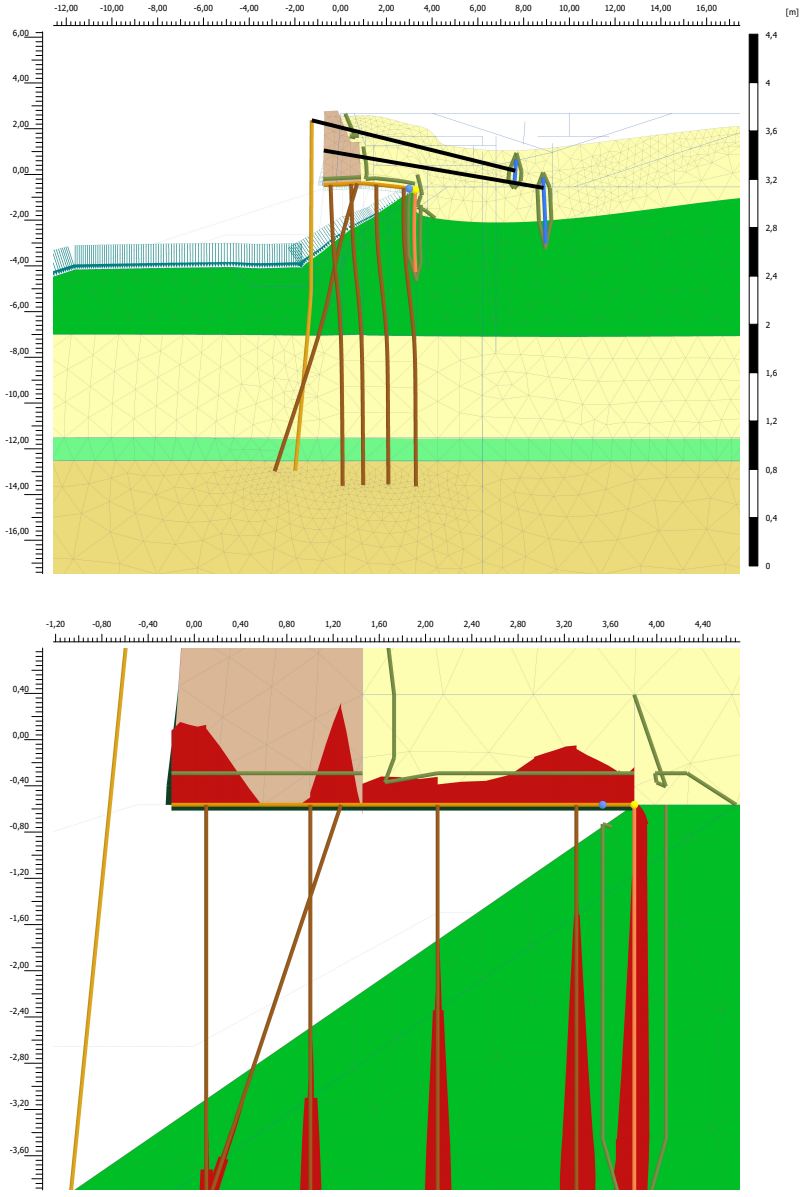


Figure 6.18: Top: Enlarged 1982 mesh deformations (factor 5). Bottom: The pressures acting on the soil-structure interface.

**1982**

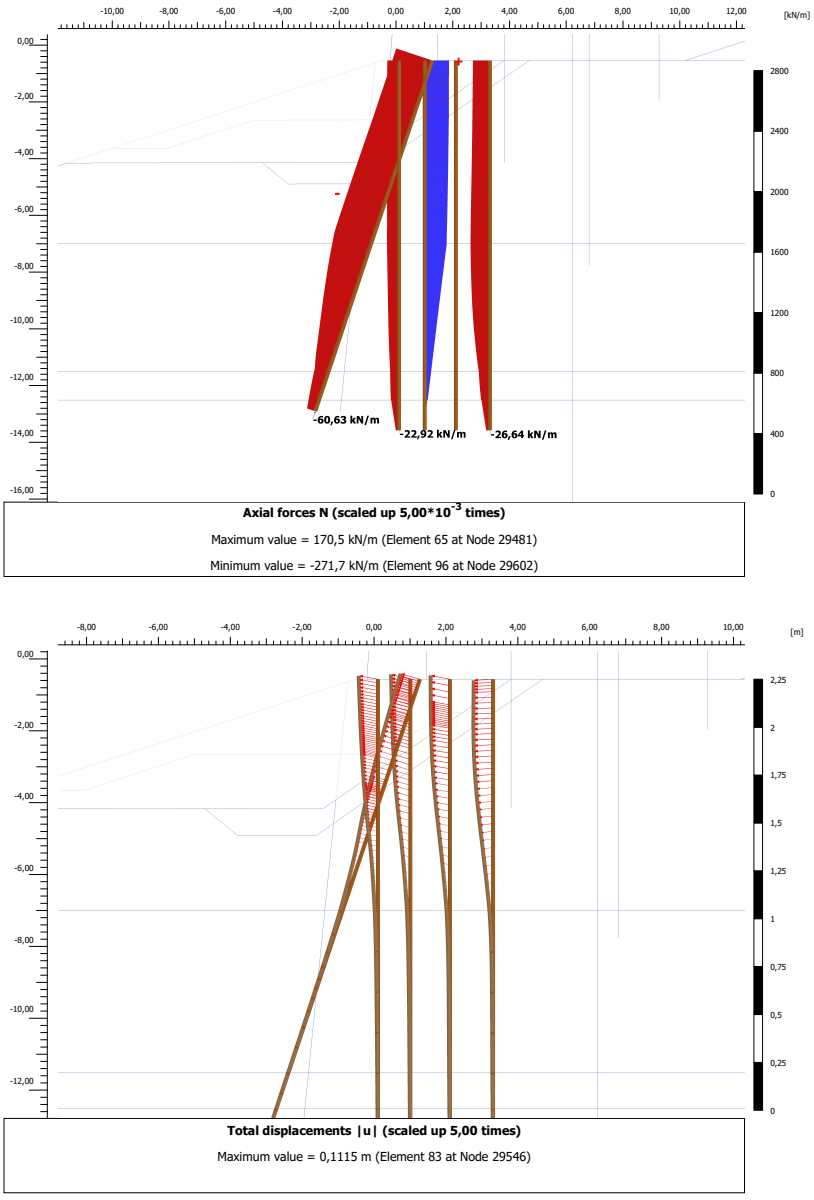


Figure 6.19: Top: Overview axial pile forces in the 1982 set up. Bottom: Deformations of the piles.

**1982**

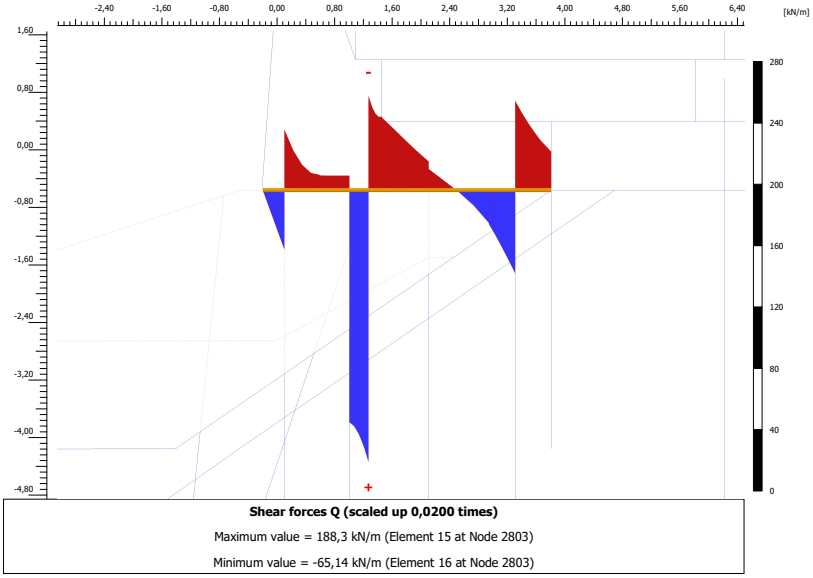


Figure 6.20: Shear forces in the capping beam for the 1982 set up.

**2003**

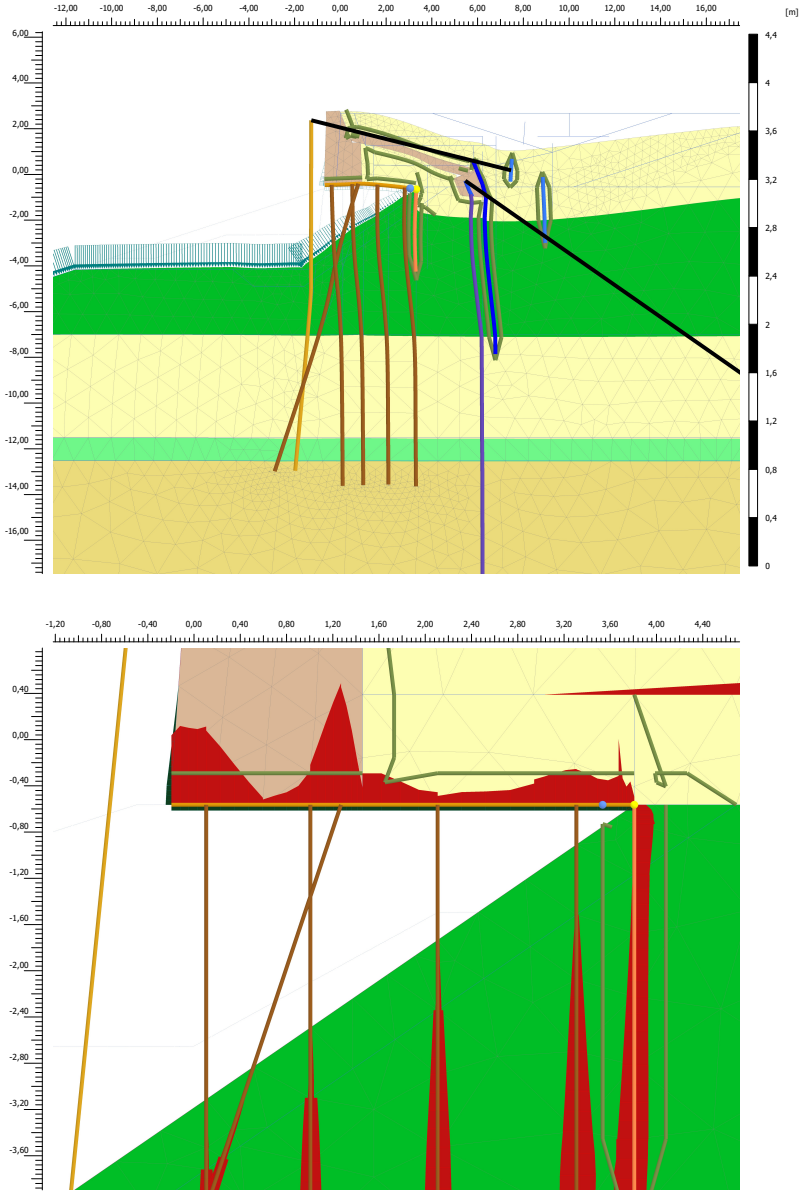


Figure 6.21: Top: Enlarged 2003 mesh deformations (factor 5). Bottom: The pressures acting on the soil-structure interface.

**2003**

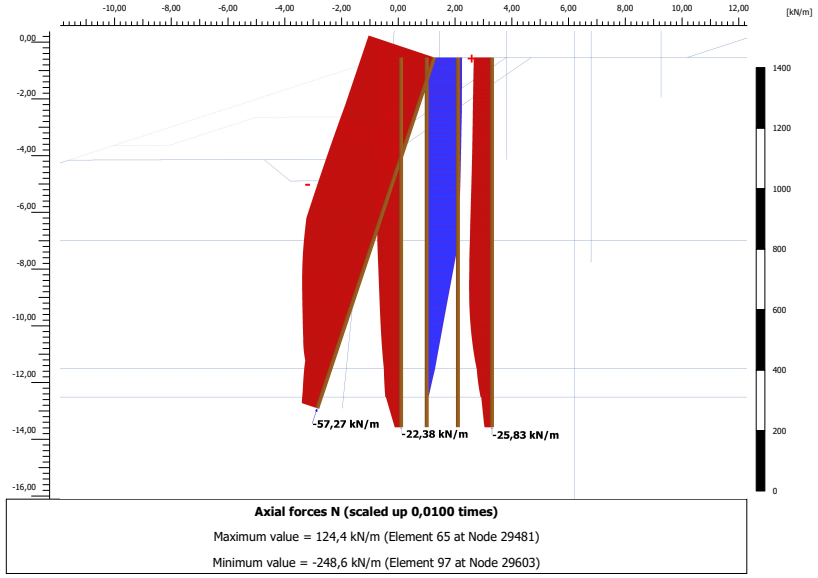


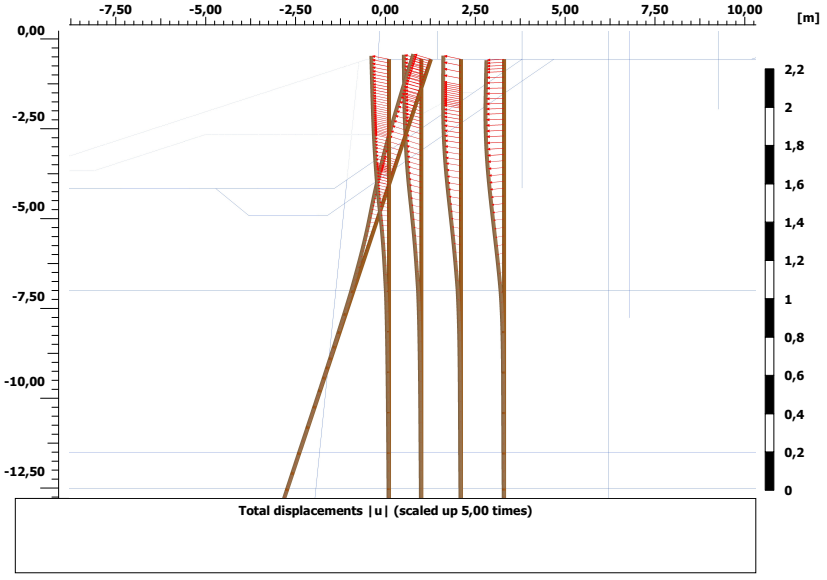


Figure 6.22: Top: Overview axial pile forces in the 2003 set up. Bottom: Deformations of the piles. Maximum value is 103 mm.

**2003**

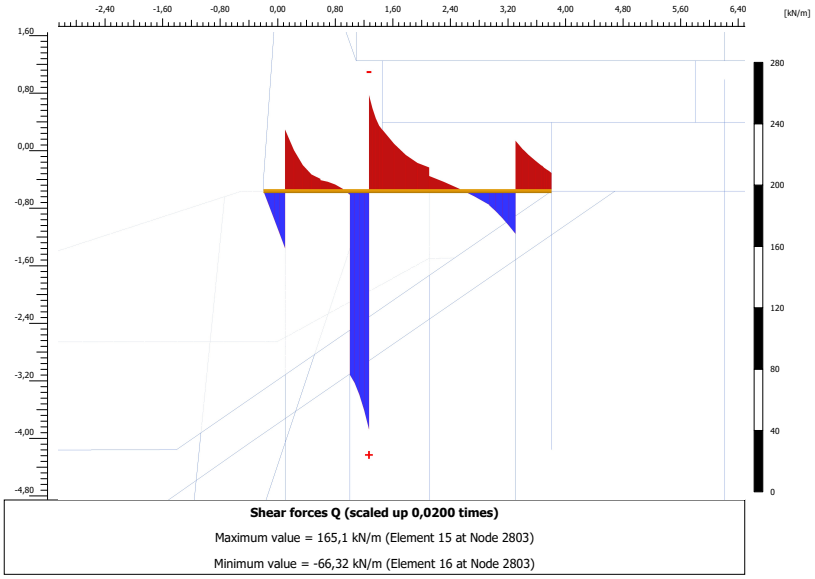


Figure 6.23: Shear forces in the capping beam for the 2003 set up.

**Stresses**

The capping beam has been checked at two locations: next to the raking piles (full section) and above pile row 2 at a mortise and tenon joint. These were the normative sections for this beam. The normal force next to the raking pilerow (R) is tensile on one side and compressive at the other. Hence indication of both forces on this location, and only of the tensile stress above pile 2. See figures 6.24 and 6.25.

The two most extreme piles (pile 2 in tension and pile R (raking pile) in compression) are further elaborated on stresses. The tapering of the piles has been taken into account in computing these numbers. Se figures 6.26 and 6.27.

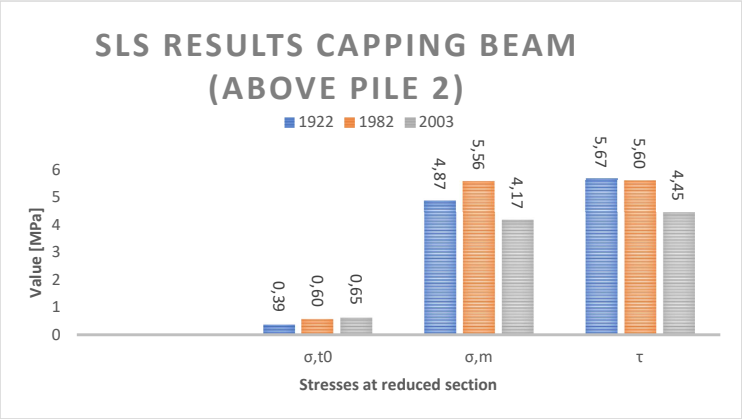


Figure 6.24: Non degraded sections are used for this comparison of stresses.

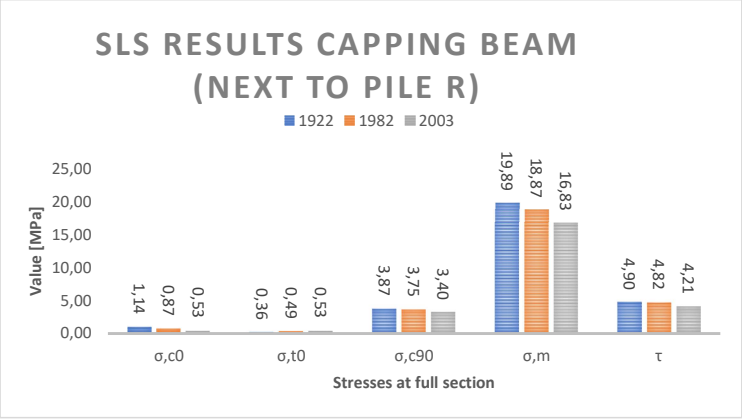


Figure 6.25: Non degraded sections are used for this comparison of stresses.

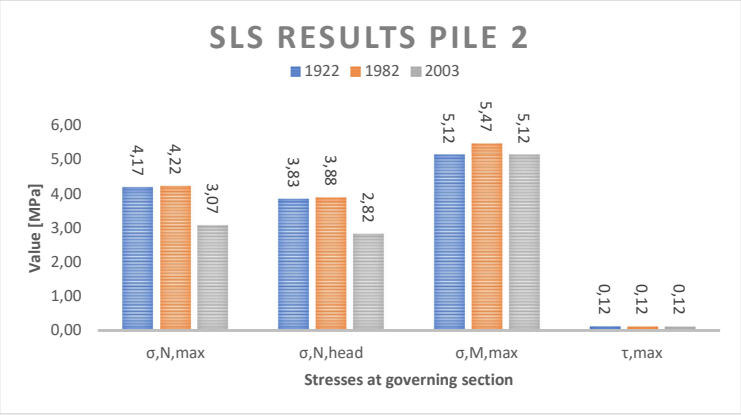


Figure 6.26

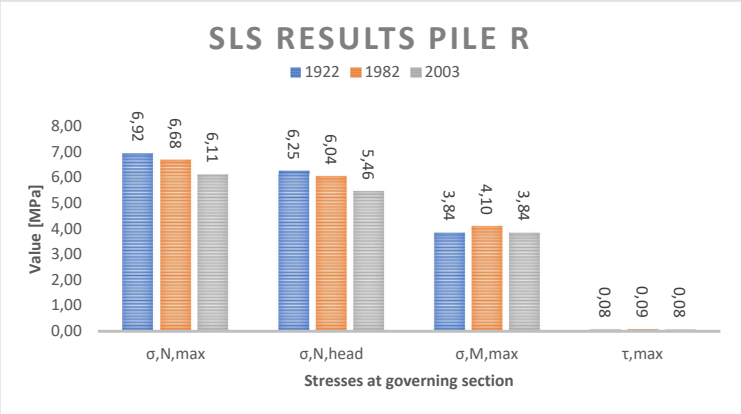


Figure 6.27

**ULS: Comparison of the load cases.**

The results under self weight (ULS1) are computed for the Embedded Beam (ULS selfweight (EB)) computation and the Anchor piles computation (ULS Selfweight (A)). Although the self weight load cases give different results from the SLS case due to changed material characteristics, they are not high lighted a second time. ULS Surcharge, ULS Ship and ULS Ice are. The deformations are reset at initiation of updated mesh calculations (geometrical nonlinearity) so mesh displacement figures are therefore not of interest. Shown are interface stresses on the platform, pile axial forces and capping beam shear and moment lines. Note the detachment of the clay against the sheetpile when the updated mesh mode is turned on.

### ULS surcharge

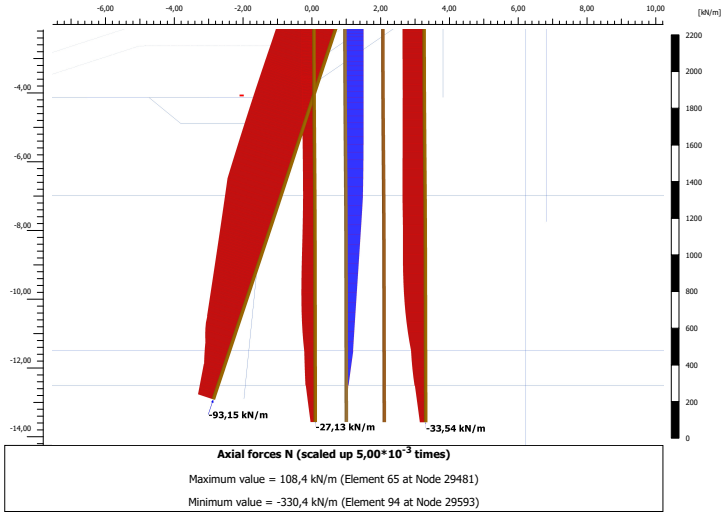


Figure 6.28: Top: Axial load out of the piles. Bottom: The pressures acting on the soil-structure interface.

### ULS surcharge

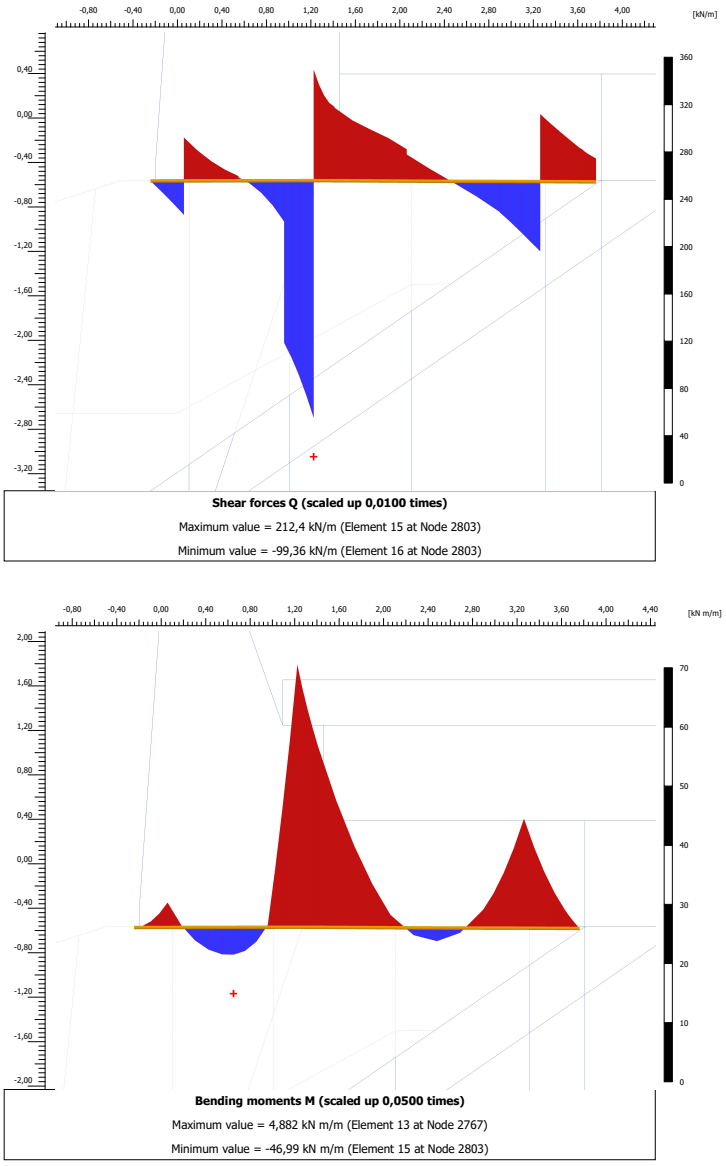


Figure 6.29: Top: Overview of the shear forces in ULS surcharge. Bottom: Idem for bending moments.

**ULS ship**

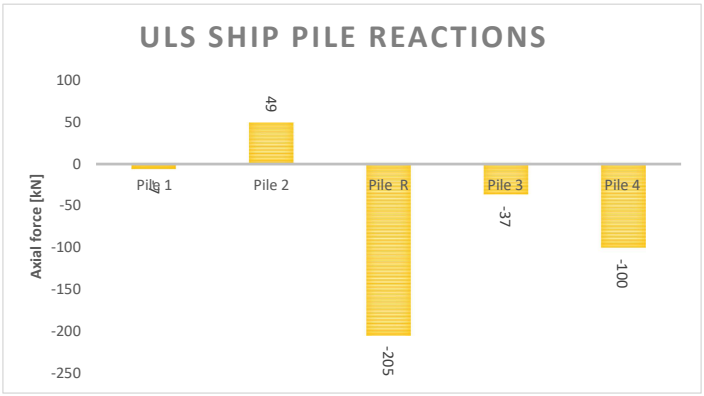


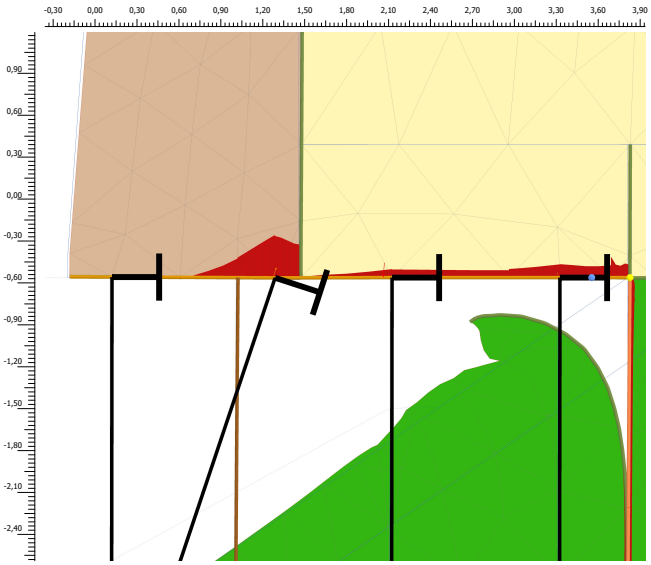

Figure 6.30: Top: Axial load out of the piles. The alternative graphics are used due to the absence of a graphical interpretation of forces in anchors in Plaxis. Bottom: The pressures acting on the soil-structure interface.

### ULS ship

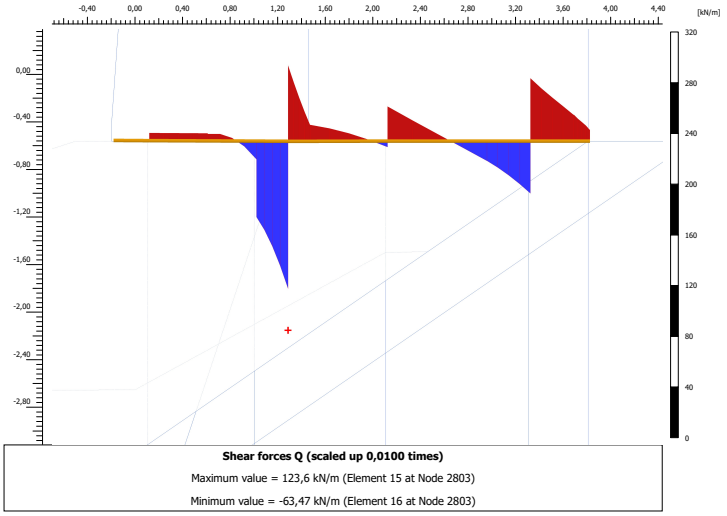


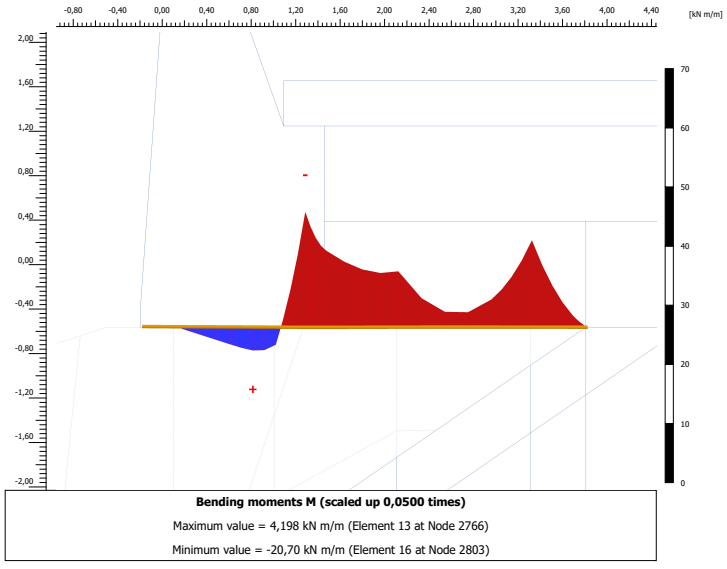


Figure 6.31: Top: Overview of the shear forces in ULS ship. Bottom: Idem for bending moments.

**ULS ice**

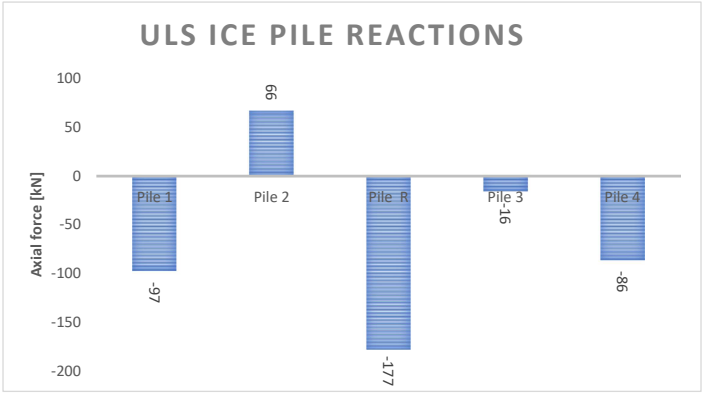


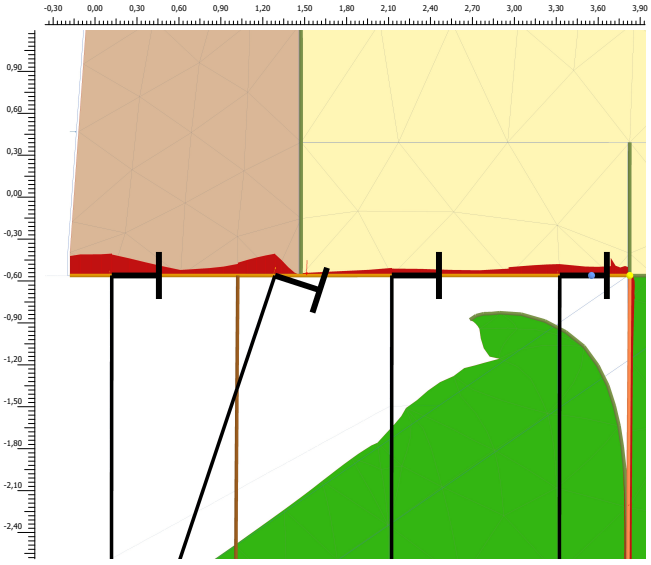

Figure 6.32: Top: Axial load out of the piles. The alternative graphics are used due to the absence of a graphical interpretation of forces in anchors in Plaxis. Bottom: The pressures acting on the soil-structure interface.

**ULS ice**

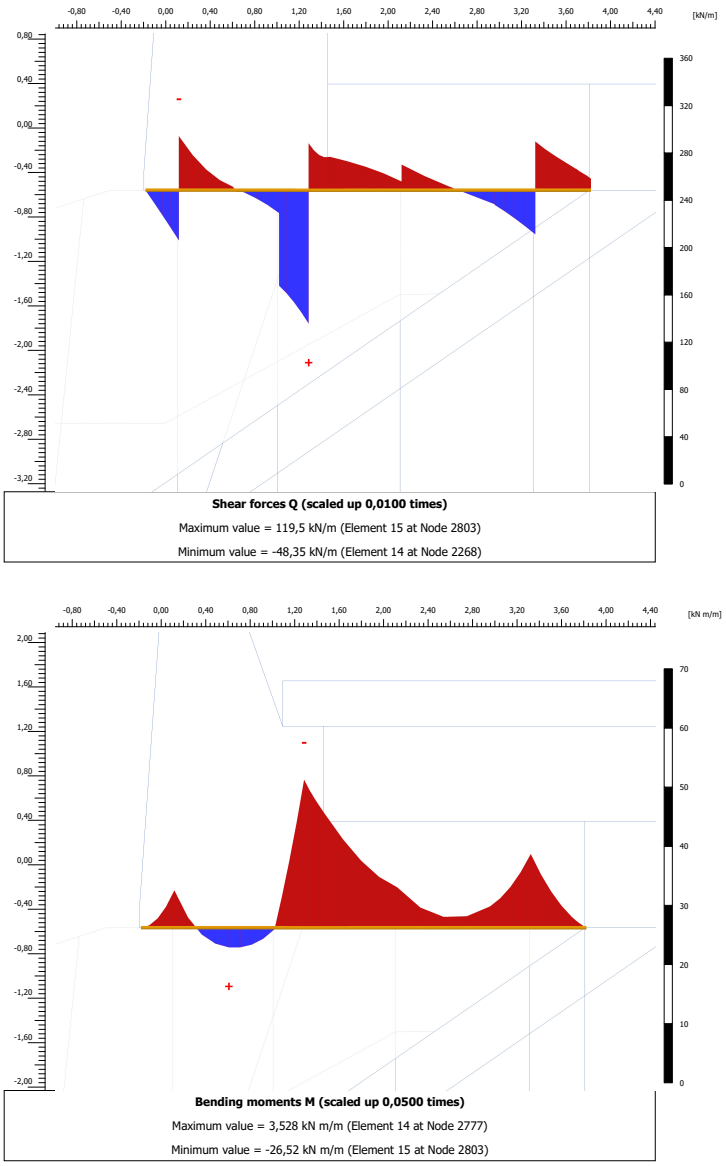


Figure 6.33: Top: Overview of the shear forces in ULS ice. Bottom: Idem for bending moments.

Resulting stresses in the two beam sections of the governing joint are presented in figure 6.34. Idem for pile row 2 and R in figure 6.35.

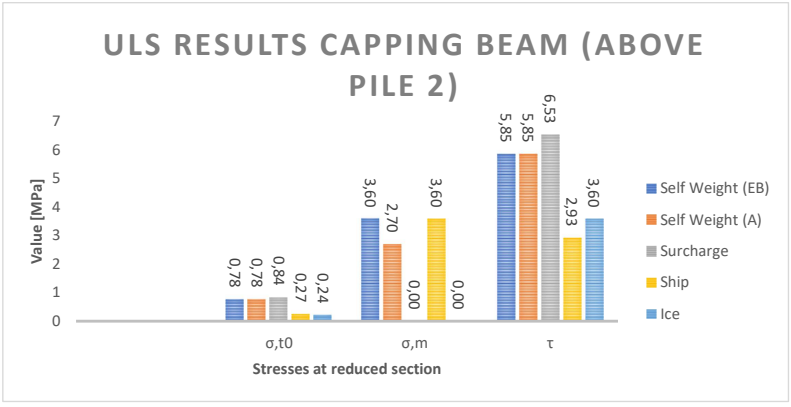


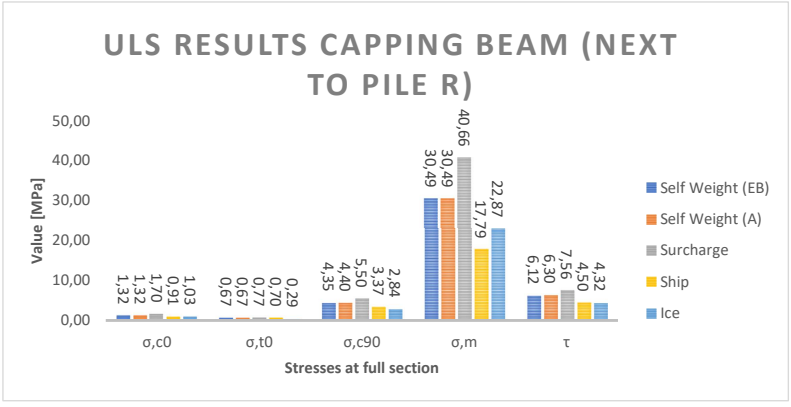


Figure 6.34: Resulting stresses in the capping beam taking into account erosion.

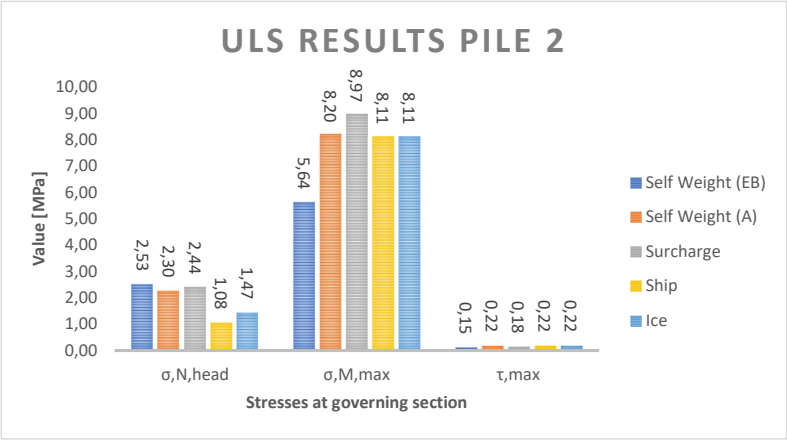


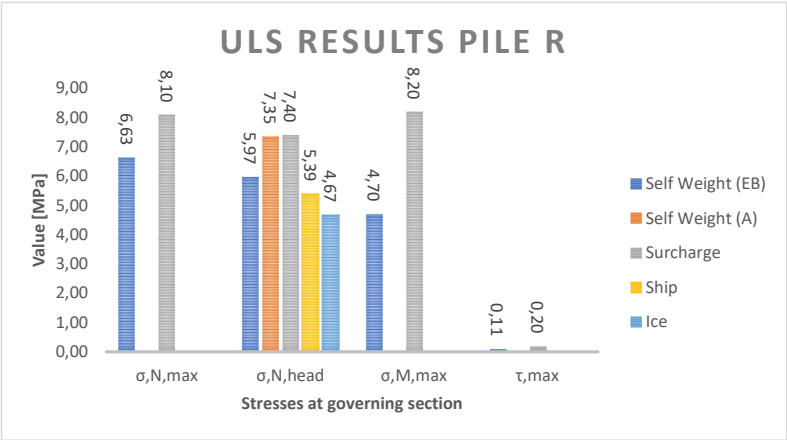


Figure 6.35: Resulting stresses in pile 2 and R (tensile for row 2).

It has to be noted that for pile row 2 the tensile force decreases by 10 kN (9%) during the 'swap' of embedded beams to node to node anchors. This affects on its turn the shear and compression perpendicular to the fibre in the capping beam by 3%. By being the only embedded beam pile in the structure, bending moments and shear in this pile rise significantly (45%) despite the addition of transverse anchors to the other pile rows. Concluding on the pilechange for the ULS ice and ULS ship phases, the changes in stresses in the capping beam are very small (internal force lines match very well), while in pile 2 itself the changes are large.

For both piles and the capping beam the surcharge load case is normative in terms of resulting design stress (Ed).

## 6.5. ASSESSMENT

Assessment of the quay will take place in SLS as a comparison between the three build ups (1922,1982,2003).

Assessment on the ULS situation of the quay will be made for the joint cross sections the capping beam and the governing piles (the raking pile row and pile row 2).

### 6.5.1. SLS CASE COMPARISON

The capping beam forces and axial pileforces have been plotted on a timeline to show the impact of the renovations (see figures 6.36 to 6.38).

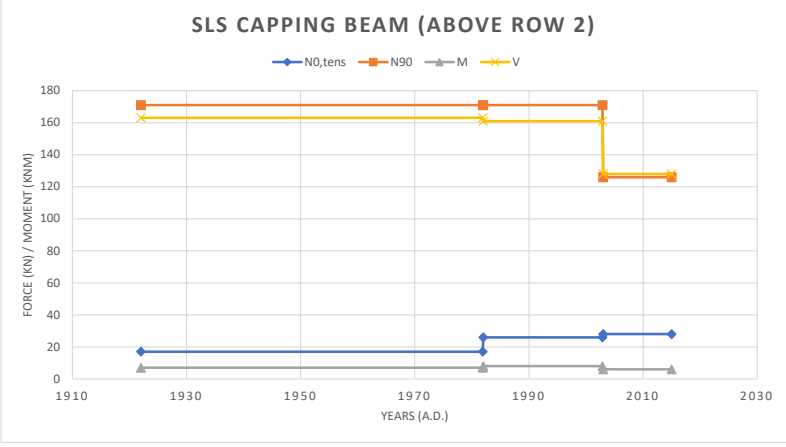


Figure 6.36: Overview of the forces over the years in the non eroded section in the mortise and tenon joint.

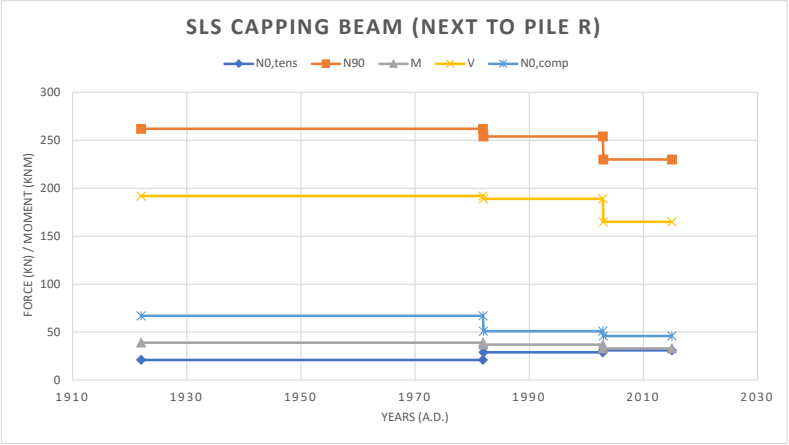


Figure 6.37: Overview of the forces in the non eroded section in full capping beam section.

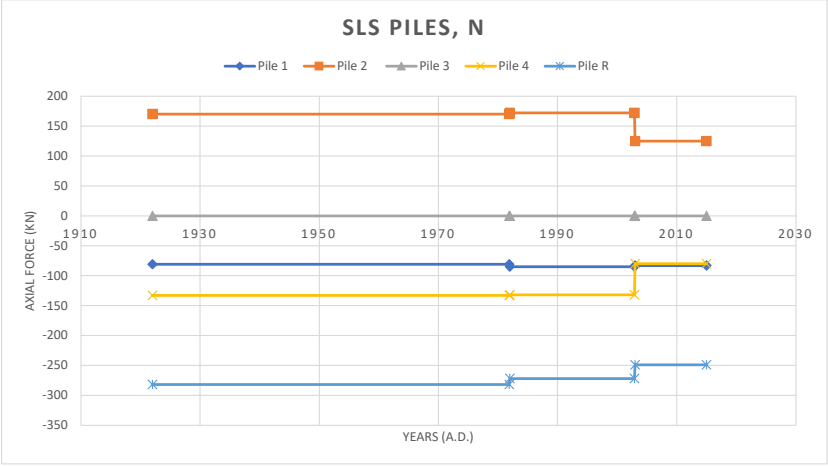


Figure 6.38: Overview of the axial pile forces over the years.

Apparent from the results in figures 6.36, 6.37, and 6.38 is that with every renovation, the forces and stresses in the normative elements decrease. The exceptions are the changes from 1922 to 1982 in the bending moments in the piles (see figures 6.26 and 6.26) and in the capping beam above pilerow 2 and, more interestingly, tension in the capping beam. This tension is present left of the raking pile joint and is caused by the friction with the wall. Having a larger horizontal interface force between the platform and the wall after addition of an anchor is counter-intuitive.

An annotation for the 1982 situation is that due to the unknown pre stress in the anchor rod the outcomes of this timestamp situation can differ from the actual situation.

The maximum deformations in the model can be found in the most upper tip of the concrete wall (horizontally) or on the street surface right next to the relieving platform (vertically), as it is not supported by a foundation and a three meter sand deposit is placed to fill the void behind the wall. More interestingly, the lateral displacement of the timber structure are 10.9 , 10.7 and 10.3 cm for the 1922, 1982 and 2003 build ups respectively. Vertically, the capping beam settles inland at the sheetpile connection (24/27/22 cm) and is raised underneath the wall (30/31/29 cm).

### 6.5.2. ULS STRESS TO STRENGTH RATIO'S

The timber strengths of the components can be found in three different ways.

1. Using the chosen C class in NEN 338 (C22) and the modification factor $k_{mod}$ (all strengths and stiffnesses);
2. Using the compression tests directly with a modification for moisture from literature (compression strength (//) and Young's modulus (//) only);
3. Using the advised values in NEN 8707 and NEN 1995-1-1 (national annex).

The strengths found in the laboratory tests and the C22 class are the strengths that will be used for assessment. Together with the used factors these are stated in table6.1: the used design strengths for the capping beam.
The design strength based on $f_{c,0,50,k}$ (Stevin test measurement changed to 50% moisture content) is downgraded with the material factor and upgraded with the system factor $k_{sys}$. Table 6.2 shows the used design strengths for the piles. The advised values from the codes are named for comparison.

The compressive strength given by the code NEN 8707 for long term loading is amazingly comparable to the one found in the lab (10.8 MPa versus 10.7 MPa). Since this code is newer than the 2013 national annex of 1995-1-1, a comparison with the latter is disregarded. The other strength difference often mentioned in literature and guidelines is the compressive strength perpendicular to the fibre. The differences with this one are immense; NEN 8707 and 1995 (National Annex) even mention strengths up to 6 MPa, whereas the strengths following C22 and the standard Eurocode approach go as low as 1.02 MPa.

The unity checks resulting from the compressive test strengths, adapted from moisture content and remaining strengths from the C22 class are to be found in figures 6.39 to 6.42.

| | kmod | ksys | kh | kc,90 | $\gamma_M$ | fc,0,d* | ft,0,d | fc,90,d** | f,m,d | f,v,d |
|---|---|---|---|---|---|---|---|---|---|---|
| ULS1 (EB) | 0.5 | 1.1 | 1 | 1 | 1.3 | 10.70 | 5.50 | 1.02 | 10.15 | 1.61 |
| ULS1 (A) | 0.5 | 1.1 | 1 | 1 | 1.3 | 10.70 | 5.50 | 1.02 | 10.15 | 1.61 |
| ULS2 | 0.65 | 1.1 | 1 | 1 | 1.3 | 10.70 | 7.15 | 1.32 | 13.20 | 2.09 |
| ULS3 | 0.9 | 1.1 | 1 | 1 | 1.3 | 10.70 | 9.90 | 1.83 | 18.28 | 2.89 |
| ULS4 | 0.65 | 1.1 | 1 | 1 | 1.3 | 10.70 | 7.15 | 1.32 | 13.20 | 2.09 |

Table 6.1: Used modification values, material factors and design strengths in MPa for the capping beam. * The fc,0,d is the only value in this table directly based on the Stevin test's $f_{c,0,50,k}$. **NEN 8707 mentions strengths of 4,5 MPa for cases where the amount of deformation is not of importance. A value of 6 MPa is named as maximum strength for capping beams in contact with <13 cm diameter piles and deformations of less than $\frac{1}{3}$ of the original thickness.

| | fc,0,d (Stevin, MC=50%) | f,c,0,d (NEN 8707) | f,c,0,d (NEN 1995-1-1:n.a.) | fm,d | fv,d |
|---|---|---|---|---|---|
| ULS1 (EB) | 10.70 | 10.8 | 9.8 | 10.15 | 1.61 |
| ULS1 (A) | 10.70 | 10.8 | 9.8 | 10.15 | 1.61 |
| ULS2 | 10.70 | 12.6 | 11.5 | 13.20 | 2.09 |
| ULS3 | 10.70 | 12.6 | 11.5 | 18.28 | 2.89 |
| ULS4 | 10.70 | 12.6 | 11.5 | 13.20 | 2.09 |

Table 6.2: Used strengths to compare the resulting stresses to for the piles. The shear and bending strength are from the C22 class and use the same factors as stated for the capping beam. Note that NEN8707 is from 2018 and NEN 1995-1-1:n.a. is from 2013.

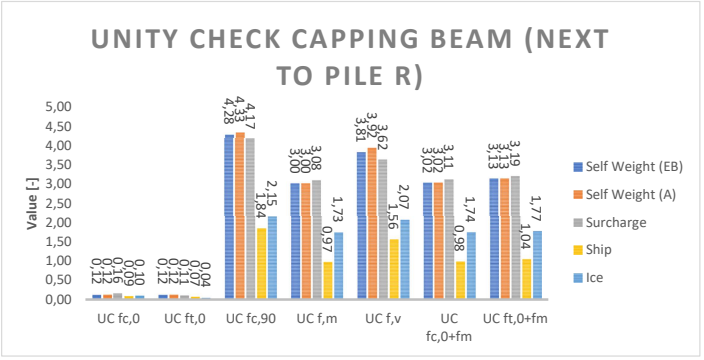


Figure 6.39

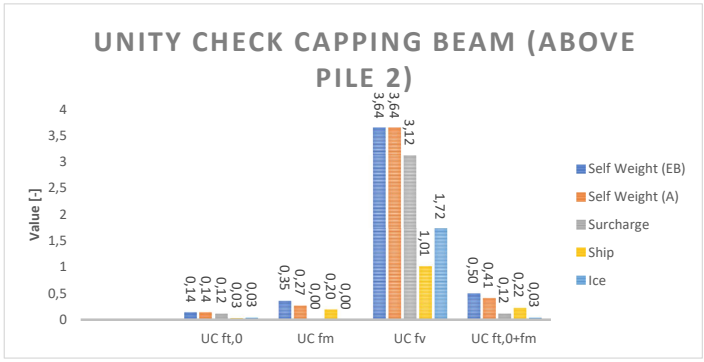


Figure 6.40

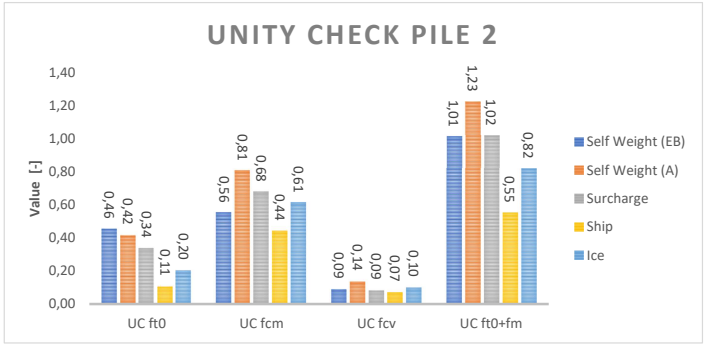


Figure 6.41: Unity check using the modified lab test strengths.

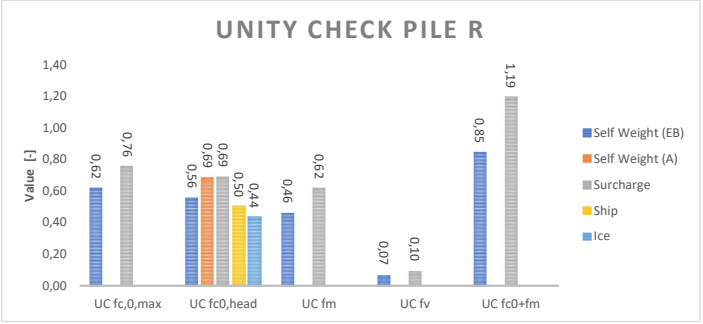


Figure 6.42: Unity check using the modified lab test strengths.

6

### 6.5.3. BUCKLING, TENSILE JOINT

**Buckling**

A hand calculation on buckling has been performed using Davisson's approach [76] (see figure 6.10) for piles with a free length above the ground. The approach gives an equivalent buckling length based on relative stiffnesses between the pile and the soil. For the mooring pile calculation (absorption of energy from a ship) this approach proved handy as an equivalent column length of 7.42 meter was found, comparable to the 7.65 m from the Plaxis 3D model. A group effect is named, and the reduction for the Maaskade foundation case would mean a factor 0.44 reduction in soil stiffness.

For the raking pile (largest compression value), the 3.23 m equivalent length together with a buckling length factor of 0.7 for a pinned connection on top and a clamped on bottom gives a reduction factor $k_c$ of 0.95 (hardly any) on buckling, resulting in 460 kN as a maximum capacity; less than the 330 kN present in the surcharge loadcase.

A sidenote is that the equivalent free standing column approach mentions that it can also be used for deflections due to lateral forces on the head. Following this approach reciprocally on the Plaxis model gives equivalent column lengths that reach into the sand layer. Moreover, a check on compression or buckling needs to be combined with present bending stresses. This would end in a negative verdict for the raking pile results.

A possible reason for a longer buckling length is the occurrence of plasticity in the soil around the piles. Depending on the plasticity development along the shaft, the solution to the pile buckling problem tends toward the Euler unsupported column, as mentioned by Lankreijer [77]. See figure 6.43 .

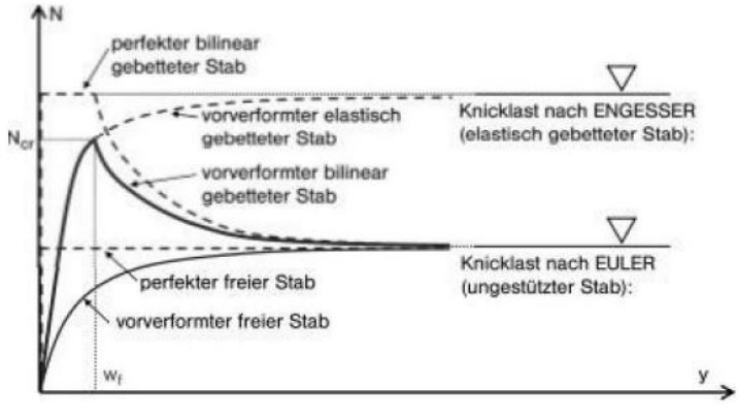


Figure 6.43: Buckling of continuously supported piles. Original from EA pfahle 2012 Anhang A, retreived from Lankreijer's thesis [77].

**Tensile joint**

The connection between pile 2 and the capping beam consists of a steel brace (10 x 77 mm) that wraps around the beam and is connected to the pile with a single, 32 mm bolt. The calculated strengths of different failure modes are presented in table 6.3. The characteristic density at 12 % moisture content is used for obtainment of the embedment strength. As the steel properties are unknown, the bolt strength is taken conservatively for modern standards.

| [kN] Governed by: | Embedment | Bolt* | Pull out (of which clay contributed)** | Soil weight |
|---|---|---|---|---|
| Rk | 147 | 114 | 556(123) | 256 |
| Rd | 56 | 62 | 302(70) | 233 |

Table 6.3: *Based on S235.**Factors f1*f2 are taken as 1.0 for the sand as well, as the tensile piles are surrounded by piles in compression.

With tensile forces reaching 170 kN in the original set up of 1922, it is very arguable if the connection can withstand this tensile force.
However, modelling the quay without the second pile (as if the connection is broken) showed another possible equilibrium. This is the quay that stands on three piles only: pilerow 1, pilerow R and pilerow 4. The results include smaller compressive forces in the piles, a factor 2.5 higher lateral deformations of the timber platform (25 cm) and differences in the capping beam internal force layout. The maximum shear is lower (maximum U.C. 2.95) but maximum bending moments are higher (maximum U.C. 6.08).

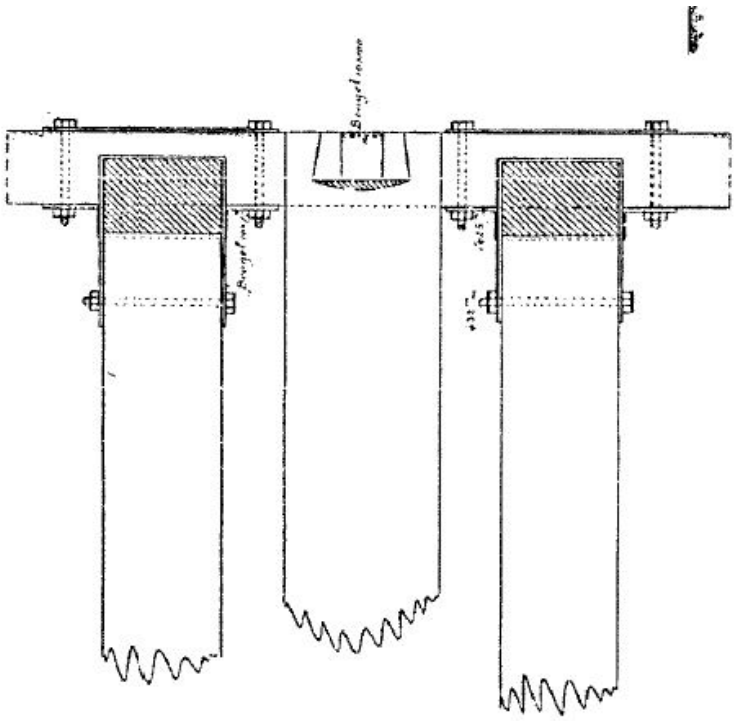

Figure 6.44: Sideview of the tensile joint in question. The raking pile is in the middle, the piles from the second pilerow on either side.

# 7

# DISCUSSION

The discussion gives a short summary of the found results concerning each research question. It mentions the similarity to expectations or literature, the implications of the methodology or outcome, the limitations of the analysis and suggestions for further work.

## CHAPTER 4: HISTORY, BUILD-UP AND LOADING

Chapter 4 is centred around *What is the build up of the Maaskade and what are the loads exerted on it?* The conclusions are that the western part of the quay is split in 7 different sections, of which some include raking piles and others do not. For means of slope stability some include fascine mattresses, others timber sheetpiles. Since most of the acquired timber material is from section 4-1, this section is analysed further in detail in this study. It consists of a timber platform on four vertical pile rows, a raking pile next to the second pile row, a sheetpile at the back and a concrete wall on top.
It is built in 1922 - 1923 and is believed to most likely be built in front of an older version. It saw an addition of an anchor attached to the wall in 1982 and a mayor renovation in 2003, when a steel sheetpile structure is placed behind the timber platform and concrete slabs were placed to span the space between the old concrete wall and the newly added sheetpile wall.
The structure implements mortise and tenon joints which are believed not to be able to take tension with the exception of the braced version at pile row 2. The piles are placed for 6.5 m in clay and for the remaining 6.5 m in a layer consisting mostly of loose sand. Load cases taken into account are surcharge (20 $\frac{kN}{m^2}$), ship loading by CEMT I class ships and ice loading for fresh water ((100 $\frac{kN}{m}$)).

This has shown the importance of an archive study for assessment of quays, especially when taking into account time effects. Since the age, build-up, used materials, connection types and soil build-up vary so much along 400 m of the western Maaskade quay it is very time consuming to assess it in its entirety and the chosen approach of de-

molition and renewal of the entirety by the curator is very understandable.
The large variety underlines the fact that any conclusions on the Maaskade using any build-up and geometry made in this report should be made on wall section 4-1, which is not the collapsed section. A suggestion for further research is analysis of an unbraced section.

The found material characteristics on piles are retrieved from both section 4-1 (71% of the requested timber) and 3-1 (29% of the requested timber). The former is placed in 1922, the latter in 1897 and therefore the deducted characteristics of the next chapter are based on mixed age specimens since not all piles could be traced back to their original location.

## CHAPTER 5: STATE AND STRENGTH OF THE TIMBER

Chapter 5 is meant to answer *What is the state and strength of the timber components?* After measuring the density, moisture content and dynamic Young's modulus on 45 piles, 21 pilepieces are selected on representability of the group and tested on compression in the Stevin II lab. The compressive strength to dynamic Young's modulus correlation is set up and the static Young's modulus is found using correlations from literature. These correlations are then used to find the values for the whole 45 piece strong pilegroup. This results in $f_{c,0,k}$ = 12.64 MPa and $E_{0,mean}$ = 11.3 GPa under 50% moisture content, the saturated state the wood is expected to be in in the quay.
The piles are documented as fir in the archives and have a slight taper from 24 cm diameter to 20. Cross sectional dimensions for the capping beam (b x h = 30 x 20 cm) and floor planks is taken from original drawings and one separate measurement per type. Since these are softwood as well (in contrast to transverse beams that attach to the raking pile), the found density of the piles (328 $\frac{kg}{m^3}$) is used to estimate a C22 class that is used for strengths that are not measured. Erosive deterioration is clearly present. Biological deterioration is mentioned without discriminating in measurement location in archival documents [60], but not analysed and taken into account in this study (other than the possible influence on the compressive tests).

The used assignment to bending class C22 comes with a sidenote. The bending classes in NEN 338 are to be used for sawn timber; the correlations on which the classes are based are not meant for logs on which this assignment is based. The same goes for the used correlation between dynamic and static Young's moduli. Therefore, the bending and shear strengths of the piles have not been computed according to proper procedures. The class assignment is based on the lowest of found values on characteristic density, compressive strength (//) and mean Young's modulus (//) under the standard 12% moisture content. This lowest value is the characteristic density (328 kg/m$^3$). Would the base of the assignment be the compressive strength, the class could be as high as C40. However, literature mentions the only slightly stronger C24 as an often used strength class for the *horizontal* timber (F3O guideline [37]) which means the C22 could be a fair assumption on the beam. Direct measurements in the laboratory would give a definite answer.

The characteristics based on 12% M.C. values and which are scaled afterwards with a $k_{mod}$ factor (for moisture and time dependant effects) take time-dependant mechanical damage - if present - into account twice because the C-class assignment has been done by using test outcomes on historical elements from the quay.
Lastly, more measurements on the horizontal timber would give a more reliable dimension that can be used for modelling stress distributions, like the ones in the following chapter. Another suggestion for future work is the installation of an angle measuring sensor during compression tests to follow possible bending effects in the timber as used during bending property testing described by Yoshihara & Oka [78]. This was an issue during execution of the compressive testing.

## CHAPTER 6: MODELLING THE LOAD DISTRIBUTIONS

Chapter 6 answers the question *What are the load distribution, resulting stresses and weakpoints in the quay?* This has been analysed using 2D FEM software called Plaxis on a large scale model of 65 x 33 m that takes into account construction sequence. Compared are the three build ups of 1922, 1982 and 2003 under best-estimate material characteristics under pure self weight. Results include a declining force in both the piles and the capping beam towards and including the last build up. Exception is the tension in the capping beam that originates from the concrete wall horizontal forces. The results show that due to horizontal loading and the triangular set up of pile 2 in combination with the raking pile tension occurs in row 2 and 3. Due to its connection, tension in pile 3 is not accepted and eliminated from the model. Furthermore, the piles act as embedded in the sand layer and deflect only in the clay layer. Because of the large stiffness differences between the clay and the sand layer, the piles offer the quay a way of retaining the clay's lateral movement.
Under ULS (Ultimate Limit State), four load cases are compared (self weight, surcharge, ship impact and ice) for the final 2003 build up only. Load case *Ship* and *Ice* are modelled with different elements as the load distribution is unknown beforehand, and only anchor elements allow for deactivation under tension. The approach followed in sectional force assessment is the one of Eurocode 5. The four sections of notice during analysis were the raking pile and row 2 at clay-sand layer interface (maximum bending moment) and the capping beam connecting these two piles. This joint is the place with normative stresses and can be regarded as the weakspot of the structure. Results show that the surcharge load case is normative for effecting stress, but not anymore after taking into account diminishing strength of timber under different load durations. Permanent loading (self weight) wins here. The piles are withstanding their axial loads but in combination with bending just surpass the unity check (U.C.) of 1.0. The unity check on the capping beam sectional forces reveal U.C.>3 on shear, bending and compression perpendicular to the fibre for the section right next to the raking pile, which normally results in a negative assessment. A possible breaking of the braced connection in tension with pile row 2 is mentioned as well.

Results of chapter 6 proved to be heavily reliant on soil stiffness and stiffness differences between the layers and the weaker top soil layer's ability to expand sidewards. A

model with clay only showed smaller forces in every single timber element for the price of larger deformations. The used difference between the stiffness of sandy clay and the loose sand is 10 following NEN 9997 advised values [9](see appendix C for the material specifications). In the author's opinion, proving a lower stiffness difference could significantly change the results. A sensitivity analysis of the ratio of the two soil layers would be advised.

Another important factor in the FEM model outcome is the simplification from 3D to 2D. The placement of the raking pile underneath the capping beam is not according to reality. Any compressive forces on this pilerow could have a more direct interaction with the concrete wall above it and its forces do not need to be passed necessarily through the transverse beam into the capping beam.
Modelling piles in 2D is physically not possible either. The use of embedded beams is a good approach for piles placed under this centre to centre distance. However, it is known and specifically pointed out that these elements are not meant to be used for lateral loading by a point load on the pile head, which is definitely the case for this set up [30]. The reliability of modelling with these elements for this case is not separately proved in this thesis.

Changing the embedded beam elements to node-to-node anchors proved partially successful. The capping beam internal forces are spot on between the phases ULS self weight (EB) and ULS self weight (A). Next to the obvious differences in the changed piles, pile row 2 (the only one that stayed an embedded beam) shows large differences in internal forces (10% axially but 45% in bending moments) between the two phases that both represent the same situation. This has to be kept in mind for the assessment of this pile in phases ULS ship and ULS ice. See appendix C for the exact alignment of the forces. Deactivation of embedded beam rows in Plaxis would be preferred to the mentioned process and is a suggestion for the software developers.

The assessment in chapter 6 is based on a model that uses linear plate and beam elements that connect in nodes without dimensions. A check of the capping beam in two sections (mortise and tenon section and full beam section) results in very high unity checks and thus a negative assessment. But in reality the beams and piles have a volume which allows for redistribution of forces. The spans in between the piles in the model are 0.9 to 1.2 meter, but in reality the diameter of the pile (0.24 m) has to be deducted. Smaller spans result in smaller bending moments. In the beam directly above a pile the peaks in the moment line would flatten. Next, shear forces due to point loads near supports have been found to result in lower stresses than expected following mechanics[17]. This reduced shear force effect is also not implemented in the model. Since the compressive force perpendicular to the grain is deducted from the difference in shear force line left and right of the connection, this would reduce this compressive load as well. In the case of the Maaskade, point loads in the beam are only present as a result of the supports but arguably the tensile load on pile row 2 that transfers into the beam on top by means of the steel brace could be seen as such a load.
The compressive strength perpendicular to the grain is set in the codes according to an

acceptable deformation, as the strength continues to rise if the area is sufficiently supported. Both NEN8707 [1] and the national annex of eurocode 5 suggest a value of 4.5 MPa for this strength if deformations do not matter, and up to 6 MPa for small diameter piles and a low registered deformation. If these strengths are to be implemented, the negative ordeal on this element would disappear instantly.
For all these effects it is necessary to perform an analysis on a different scale and material models than the Plaxis model used. For example, a FEM model of 1 x 1 meter with correct volumes and orthotropy material models. To find out if the quay suffices, this is highly recommended.

Last but not least is the mention of the connection to pile row 2. It is expected not to be able to withstand the tensile loads in ultimate limit state (the normative strength is 56 kN). A different equilibrium would then be possible with the structure standing on just pile row 1, 4 and the raking piles. The price for this force redistributions are a factor 2.5 larger deformations but the unity checks are of the same order of magnitude.

# 8

# CONCLUSION

The answer to the main research question *"What is the (remaining) capacity of the timber foundation of a historical quay wall with relieving platform?"* could doubtfully be answered in means of 'resistance to vertical loading' or 'resistance to lateral loading' but in practice these load states will never take place separately. Instead, it is more useful to mention the amount of times the structure is able to resist the given load situation. Before the study was made, the answer to the research question was expected to be that the quay was at least able to take on its own weight together with a part or a multitude of subjected loads.

The approach in this thesis of following NEN 1995 with NEN 8707 and NEN 9997 and basing the outcomes solely on cross sections results in unity checks for safety of over 3 for multiple strengths, with 4.33 being the extreme value for compression parallel to the fibre on the capping beam at the transverse beam attachment. And this is because of self weight, a load case that becomes governing due to application of the lowest $k_{mod}$ factor, not because of highest resulting stresses.

It is known that assessing historical quays can result in a negative verdict, but this result is still extreme. Inspections of the quay in 2016 did show broken capping beams all along the westside of the Maaskade, but the structure was still standing with the exception of the one spot that had collapsed. Nothing is mentioned on the integrity connections to pile row 2.

As mentioned in the discussion, the Finite Element Model has serious drawbacks in geometry and material models applied to correctly represent the actual force distribution or possible redistributions after local failures. Important strengths such as the compression perpendicular to the fibre are mentioned in guidelines to be higher for certain situations and deformations that cannot be deducted properly with this model either. And on top of that, uncertainty remains in the actual strengths present other than compression parallel to the fibre as they have not been measured.

All in all, a sensible conclusion on the capacity of the quay can not be given based on this study solely since the quay did not collapse on self weight. Useful results during the study have been summarised in the discussion section.

# 9

# RECOMMENDATIONS

**Model**
The main recommendation on further research is specific for this quay. A realistic load distribution has not been concluded on in the dissertation. A simulation in 3D, taking away the restrictions of modelling in two dimensions. These restrictions are the use of pile-approaching elements such as the embedded beam rows, the incorrect modelling of the connection between the raking pile and the capping beam (inclusion of the transverse beam) and importantly: correct volumes and contact surfaces of the elements in joints.
Since the loads in the piles are reliant on the ratio of stiffness between the loose sand and the sandy clay, a further analysis varying this ratio and documenting the outcome is of interest.

**Inspection**
An assumption made in this study is that the mortise and tenon joint cannot take tension, especially in its final degraded state. For connections that can take tension such as the mortise and tenon joint with external brace, the integrity is of interest as it influences force distribution. For quays under inspection that are yet to be analysed, it is therefore important to find out what type of connection is present and if it is intact, though it is questionable of how much detail divers could provide on this matter.

**Material tests**
For the testing of the left timber in the Delft laboratory, it is advised to test the compressive strength perpendicular to the fibre to see in what way it matches the advised EC5 national annex numbers on foundation beam strengths. As biological deterioration is measured in 2002 during laboratory tests, it makes sense to reanalyse the beam on this aspect as well or at least to find the document that describes these tests in more detail.
If further compression tests are to be made on piles, it is advised to install an extra sensor that measures rotations of the testes specimen to prevent ambiguity on the Young's modulus.

# REFERENCES


[1] Koninklijk Nederlands Normalisatie-Instituut, *NEN8707 (nl) Assessment of an existing structure in case of reconstruction and disapproval – Geotechnical constructions,* (2018).

[2] Nederlands Normalisatie-instituut, *NEN EN 388: Structural timber - Strength classes,* (2013).

[3] SBRCURnet, Municipality Rotterdam, and Port of Rotterdam, *Handbook Quay Walls*, edited by J. de Gijt and M. Broeken (SBRCURnet, Rotterdam, 2005).

[4] V. V. Hamme, *Over de werking van het dieselheiblok*, Ph.D. thesis, Technische Hogeschool Eindhoven (1981).

[5] R. K. Klaassen and J. G. Creemers, *Wooden foundation piles and its underestimated relevance for cultural heritage,* Journal of Cultural Heritage **13**, S123 (2012).

[6] J. D. de Jong, *TNO 2016 R10731-2 : Onderzoek naar de huidige toestand van de houtconstructie onder de kademuur van de Maaskade te Rotterdam*, Tech. Rep. (TNO, 2016).

[7] W. Gard, N. Montaruli, and J. W. Van De Kuilen, *End-of-life wood quality of mooring poles,* in *World Conference on Timber Engineering 2012, WCTE 2012*, July (Auckland, 2012) pp. 51–52.

[8] R. K. Klaassen, *Life expectation of wooden foundations - A non-destructive approach,* in *Proceedings of the 10th International Conference on Structural Analysis of Historical Constructions, SAHC 2016* (Berlin, 2015) pp. 694–700.

[9] Nederlands Normalisatie Instituut, *NEN 9997-1 + C2. Geotechnical design of structures - Part 1: General rules,* (2016).

[10] J. De Gijt, A. Roubos, D. Grotegoed, and SBRCURnet, *Handboek Binnenstedelijke Kademuren* (SBRCURnet, Rotterdam, 2014).

[11] UNESCO, *Prehistoric Pile Dwellings around the Alps - UNESCO World Heritage Centre,* (2019).

[12] F. Keller and J. E. Lee, *The lake dwellings of Switzerland and other parts of Europe* (Longmans, London, 1878) pp. 3,4.

[13] E. Wennekes and L. P. Grijp, *De hele dag maar op en neer. Over heien, heiliedjes en hoofdstedelijke muziekgebouwen,* (2002).

[14] M. Crossman and J. Simm, *Manual on the use of rock in coastal and shoreline engineering* (Thomas Telford, London, 2004).

[15] R. K. Klaassen, *Speed of bacterial decay in waterlogged wood in soil and open water,* International Biodeterioration & Biodegradation **86**, 129 (2014).

[16] H. Blass and C. Sandhaas, *Journal of Chemical Information and Modeling*, Vol. 53 (KIT Scientific Publishing, Karlsruhe, 2017) arXiv:arXiv:1011.1669v3 .

[17] H. Blass, *Timber Engineering - STEP: 2* (Centrum Hout, Almere, 1995).

[18] D. Ridley-Ellis, P. Stapel, and V. Baño, *Strength grading of sawn timber in Europe: an explanation for engineers and researchers,* European Journal of Wood and Wood Products **74**, 291 (2016).

[19] Nederlands Normalisatie-instituut, *NEN EN 408: Timber structures - Structural timber and glued laminated timber - Determination of some physical and mechanical properties,* (2012).

[20] G. Daniel, *Fungal Degradation of Wood Cell Walls,* in *Secondary Xylem Biology: Origins, Functions, and Applications* (Elsevier, 2016) Chap. 8, pp. 131–150.

[21] M. Humar, C. Brischke, and W. Unger, *Protection of the bio-based material,* in *Performance of Bio-based Building Materials* (Elsevier Ltd, 2017) Chap. 4, pp. 187–247.

[22] A. J. Baker, *Degradation of Wood By Products of Metal Corrosion.* US Forest Products Laboratory Research Paper (1974).

[23] M. Voorendt and W. Molenaar, *Manual Hydraulic structures* (Delft, 2019) p. 961.

[24] A. van Tol, *CTB1410* (Delft, 2006).

[25] B. Das, *Geotechnical Engineering Handbook* (J Ross Publishing, 2010) p. 4.64.

[26] J. M. Abbas Al-Shamary, Z. Chik, and M. R. Taha, *Modeling the lateral response of pile groups in cohesionless and cohesive soils,* International Journal of GeoEngineering **9**, 1 (2018).

[27] J. Brinch-Hansen, *The Ultimate Resistance of Rigid Piles Against Transversal Forces,* Bulletin No. 12, Geoteknisk Institut (The Danish Geotechnical Institute) , pp. 5 (1961).

[28] J. Bijnagte, *Interaction lectures 2019 Laterally loaded piles Part 1,* (2019).

[29] R. B. J. Brinkgreve, Bentley, Plaxis, and TU Delft, *Modelling piles and pile groups in FEM,* (2019).

[30] J. Sluis, *Validation of Embedded Pile Row in PLAXIS 2D,* Ph.D. thesis, TU Delft (2012).

[31] *Plaxis 2D 2019 Reference Manual* (2019).

[32] Nederlands Normalisatie-instituut, *NEN 8700 (nl): Assessment of existing structures in case of reconstruction and disapproval - Basic Rules,* (2011).

[33] J. van de Kuilen, *Service life modelling of timber structures,* Materials and Structures (RILEM) (2006), 10.1617/s11527-006-9158-0.

[34] J. van de Kuilen and W. Gard, *Damage assessment and residual service life estimation of cracked timber beams,* Advanced Materials Research **778**, 402 (2013).

[35] C. Gerhards, *Time related effects on wood strength,* Wood and Fibre Science **23**, 89 (1992).

[36] J. van de Kuilen and W. Gard, *Mechanical performance modelling,* in *Performance of bio based building materials*, edited by D. Jones and C. Brischke (Elsevier: Woodhead publishing, Duxford, 2017) Chap. 8.6, pp. 522 – 538.

[37] F3O and SBRCURnet, *Richtlijn Houten Paalfunderingen onder gebouwen*, 3rd ed. (SBRCURnet, Delft, 2016).

[38] Nederlands Normalisatie-instituut, *NEN 5491 (nl) Quality requirements for timber - Piles - Coniferous timber [Withdrawn],* (2010).

[39] B. openstreetmap, *Openstreetmaps,* (2020).

[40] R. Stoute, *Geschiedenis Rotterdam en 't Noordereiland,* .

[41] J. Rademaker, *VERKENNEND (NULSITUATIE) BODEMONDERZOEK*, Tech. Rep. (atkb, 2017).

[42] Stadsarchief Rotterdam, *Brandgrens,* (1940).

[43] RET, *RET Historie,* .

[44] *Archief Rotterdam: Objectkaarten,* (2020).

[45] J. Cillen, *Motorschip Noordereiland (2000),* .

[46] Nederlands Organisatie voor Toegepast-natuurwetenschappelijk Onderzoek TNO, *DINOloket,* .

[47] M. grondmechanica, *Waterzijde Sonderingen - 08*, Tech. Rep. (MOS Grondmechanica, 2016).

[48] R. Schonewille, *HYDROLOGISCH ADVIES Maaskade Rotterdam*, Tech. Rep. 1 (atkb, 2017).

[49] Gemeentewerken Rotterdam, *Archival drawing: 865-043 dl2,* (2003).

[50] Royal Haskoning DHV, *Vervanging Maaskade BE8466-603*, Tech. Rep. (2018).

[51] Port of Rotterdam, *Maaskade vernieuwing 500 meter kade,* (2019).

[52] I. Stikvoort, *Old Quay Walls*, Ph.D. thesis, TU Delft (2014).

[53] Rijkswaterstaat, *Tienjarig overzicht 1981-1990* (1994) p. 237.

[54] Unknown, *Archival report: Kaaimuurbouw linker maasoever,* (Tekeningen archief gemeentewerken Rotterdam, Rotterdam, 1850).

[55] *Archival drawing: XI_9,* .

[56] *Archival drawing: Maaskade Westzijde, Vernieuwd,* (1922).

[57] J. De Gijt, *Discussion on the Maaskade,* (2020).

[58] *Archival Drawing: Maaskade westzijde verankering +- 100m kademuur.* (1947).

[59] Gemeentewerken Rotterdam, *Archival report: Maaskade w.z. Herberekening 1982*, Tech. Rep. (1982).

[60] R. van der Valk, *Archival report: Rapport indicatief onderzoek houten odnerdelen kademuren Nieuwe Maas*, Tech. Rep. (Gemeentewerken Rotterdam, Rotterdam, 2005).

[61] R. Limon, *Archival drawing: Noordereiland Maaskade WZ, details overkluizingsconstructie,* (2003).

[62] F. Knibbeler, *Discussion on the Maaskade,* .

[63] *Archival Drawing: Revisie van de vernieuwing Maaskade WZ 1923,* (1923).

[64] Koninklijk Nederlands Normalisatie-Instituut, *NEN 1991-1-7 Actions on Structures,* (2011).

[65] G. Mayhead, *Some drag coefficients for British forest trees derived from wind tunnel studies,* Agricultural Meteorology **12**, 123 (1973).

[66] Royal Haskoning DHV, *Vervanging Maaskade Doorsneden sloopwerk BE8466-606*, Tech. Rep. (2018).

[67] D. Wilschut, *Archival report: Maaskade Westzijde. Draagvermogen van bestaande paalfundering*, Tech. Rep. (Gemeentewerken Rotterdam, Rotterdam, 2003).

[68] S. Aicher and G. Stapf, *Compressive strength parallel to the fiber of spruce with high moisture content,* European Journal of Wood and Wood Products **74**, 527 (2016).

[69] G. Ravenshorst, *TU Delft University*, Ph.D. thesis (2015).

[70] Koninklijk Nederlands Normalisatie-Instituut, *NEN EN 14358: Timber structures - Calculation and verification of characteristic values,* (2016).

[71] D. H. Ardiaca, *Mohr-Coulomb parameters for modelling of concrete structures,* Plaxis Bulletin , 12 (2009).

[72] J. Potyondy, *Skin Friction Between Various Soils and,* Géotechnique **11**, 339 (1961).

[73] J. Jaaranen and G. Fink, *Frictional behaviour of timber-concrete contact pairs,* Construction and Building Materials **243**, 118273 (2020).

[74] Koninklijk Nederlands Normalisatie-Instituut, *NEN-EN 12812: Falsework, performance requirements and general Design,* (2004).

[75] R. Brinkgreve, *Discussion on Plaxis,* (2020).

[76] Davisson, *Lateral Load Capacity of Piles,* Highw Res Rec , 104 (1970).

[77] T. Lankreijer, *Buigingsknik van ankerpalen*, Ph.D. thesis, TU Delft (2014).

[78] H. Yoshihara and S. Oka, *Measurement of bending properties of wood by compression bending tests,* Journal of Wood Science **47**, 262 (2001).

[79] Nederlands Normalisatie-instituut, *NEN EN 13183-1: Moisture content of a piece of sawn timber - Part 1: Determination by oven dry method,* (2019).

[80] Zono, *Numpy Trendline,* (2017).

[81] J. Pošta, P. Ptáček, R. Jára, M. Terebesyová, P. Kuklík, and J. Dolejš, *Correlations and differences between methods for non-destructive evaluation of timber elements,* Wood Research **61**, 129 (2016).

[82] G. Ravenshorst, *Compression Test instructions,* (2019).

# A

# STORAGE SITE MEASUREMENTS

Appendix of Chapter 5

## A.1. AIM AND CONTENT

APPENDIX A holds information on the measurements done at the storage site (being the dimensions, density, dynamic $E_0$ modulus) as well as choice of the acquired material and its naming for later reference.

## A.2. STANDARDS

The standards used during measurements was NEN EN 13183-1 for determining the moisture content of each specimen.[79]

## A.3. EQUIPMENT

Various equipment has been used for cutting and measuring on the storage site. Details are found below:

- Tracked material handler with grappler;
- Chainsaw, angle grinder;
- Permanent marker, wax crayons;
- Measuring tape;
- Cely RW 2 Piece scale; 0,5 kg accuracy;
- Brookhuis Timber Grader MTG, accuracy 1 Hz;
- Binder FD oven, 1 $^{o}$C accuracy.

## A.4. EXECUTION OF STORAGE SITE WORK

The execution of work can be split in two as piles were handled separate of the horizontal timber parts. All lifting has been done by the tracked material handler, which resulted in damage occurring to the material. Worst case, the element would brake (some floor planks).
For the piles, the workflow went as follows (see figure A.1):

1. Placement of 6 piles next to each other on flat ground;
2. Cut-off of the heads, including connection (approximately 50 cm);
3. Marking of the pileheads and piles by permanent marker;
4. Dimension measurements of the piles: perimeters at both ends and the middle, length of the whole;
5. Weighing the total pile by placement on the two-support scale;
6. Response frequency measurement by the Timber Grader MTG, making use of an external hammer;
7. Cut at half-span to obtain a 3 cm disc, for moisture content measurement. Marking of the disc and the unmarked half;
8. Ordering of the 12 pile halves, heads and discs to make place for the next batch of 6 piles.

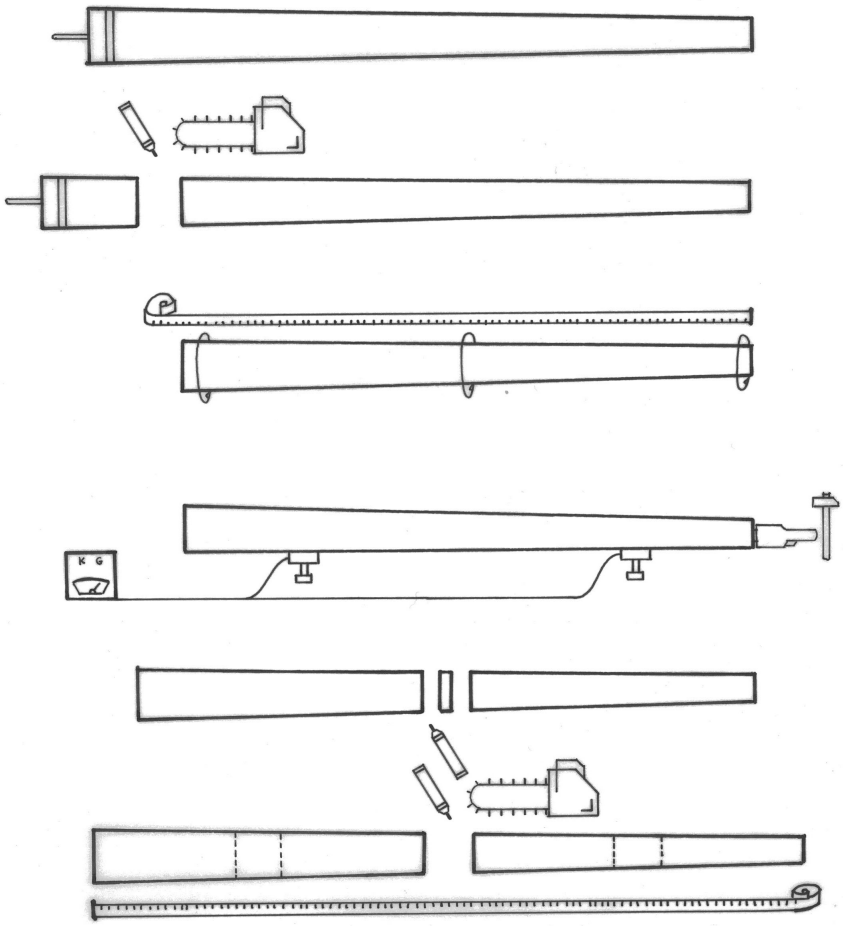


Figure A.1: Procedure illustrated.

For horizontal foundation elements, the next steps have been applied:

1. Placement of 5 elements on flat ground;
2. Marking all elements
3. Dimensioning 1 element per type (see figure A.2);
4. Cut-down into pieces of approximately 2 m.
5. Ordering of the timber and preparation of the next batch.

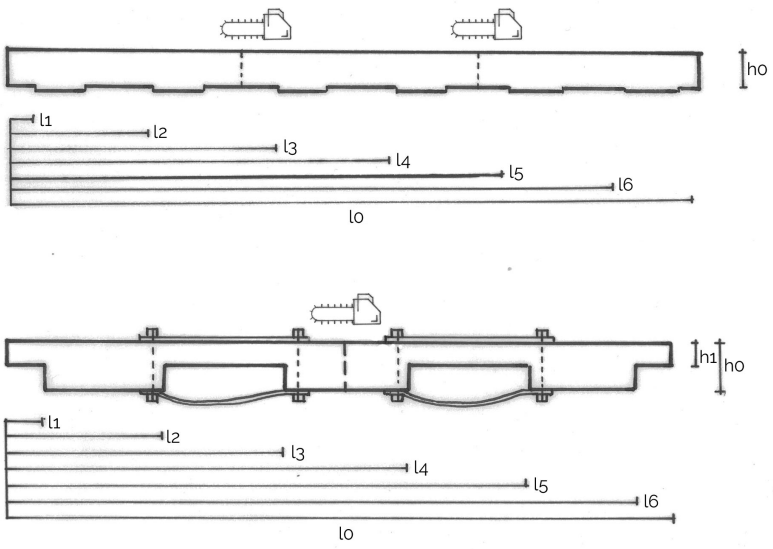


Figure A.2: Naming and placement of cuts in horizontal parts. Capping beams and plancks (top), primary transverse beams (bottom). Lengths measured till former attachment points.

With all marking procedures, it was of great importance to have a consistent naming system. See table A.1. Next to the above mentioned measurements, moisture content of the pile discs was determined by the oven dry method ([79]). A second and/or third measurement was made for control.

Table A.1: Naming of all acquired pieces. These are put on the piece with either a permanent marker or wax crayon. The naming of the type is after the Dutch translation (P-Paal, S-Schoorpaal, K-Kesp, D-Dwarsbalk, V-Vloerplank).

| Element | Type | Group | Connectiontype | Elementnumber | Piecenumber | Example |
|---|---|---|---|---|---|---|
| Pile | P | A-K;<br>O if unknown;<br>'EO'if un-expectedly added (in the lab) | A: Dowel<br>B: Dowel with brace<br>C: Mortice-and-Tenon joint<br>D: Mortice-and-Tenon joint with brace<br>or O if unknown | 01 and ongoing | 1st number for first cutting cycle<br>2nd number for further down-sizing<br>00 for whole pile | POA0150<br>PFC0341 |
| Raking pile | S | I-K or<br>O if unknown | A: with brace<br>or O if unknown | 01 and ongoing | 1st number for first cutting cycle<br>2nd number for further down-sizing<br>00 for whole pile | SOB0222<br>SKA0100 |
| Capping beam | K | G-K or<br>O if unknwon | - | 01 and ongoing | 1st number for first cutting cycle<br>2nd number for further down-sizing<br>00 for whole beam | KG0104 |
| Primary transverse beam | D | I-K or<br>O if unknwon | - | 01 and ongoing | 1st number for first cutting cycle<br>2nd number for further down-sizing<br>00 for whole beam | DK0201 |
| Plank | V | G-K or<br>O if unknwon | - | 01 and ongoing | 1st number for first cutting cycle<br>2nd number for further down-sizing<br>00 for whole plank | VO0100 |

## A.5. RESULTS AND ANALYSIS

**Processing of the storage site measurements** Dynamic E modulus has been obtained making use of the density and length, see equation A.1 [16].

$$E_{dyn} = 4 * \rho * f * l^2 \tag{A.1}$$

with
$E_{dyn}$ = dynamic Young's modulus parallel to the grain $[Pa]$
$\rho$ = density $[kg/m^3]$
$f$ = frequency $[Hz]$
$l$ = specimen length $[m]$

For determination of the volume, use is made of the open cone formula.

$$V = \frac{1}{3}\pi(r_1^2 + r_1 r_2 + r_2^2)h \tag{A.2}$$

with
$V$ = volume of the pile piece [$m^3$]
$r_1$ = bottom radius [$m$]
$r_2$ = top radius [$m$]
$h$ = specimen length [$m$]

The moisture content is calculated according to formula A.3. The dry mass has been determined according to NEN 13183-1 [79] with control measurements stating no more than 0.1 % difference should occur between two measurements.

$$\omega = 100 * \frac{m_{wet} - m_{dry}}{m_{dry}} \tag{A.3}$$

with
$\omega$ = moisture content [%]
$m_{wet}$ = wet mass [$kg$]
$m_{dry}$ = dry mass [$kg$]

Using the obtained moisture contents, the densities could then be adapted using equation A.4. The formula uses a 0.5% volume change untill saturation point [69].

$$\rho_{12} = \frac{(1 + \frac{\Delta V}{100})}{(1 + \frac{\Delta G}{100})} * \rho_{\omega} \tag{A.4}$$

with

$\rho_{12}$ = density under 12% moisture content [$kg/m^3$]
$\rho_{\omega}$ = density under current moisture content [$kg/m^3$]
$\omega$ = moisture content [%]
$\Delta V = \beta * (\omega - 12)$ = change in volume [%]
until $\omega$ = 30% at most (fibre saturation corresponding to used borders for the E modulus). $\beta$ =0.5 [%]
$\Delta G$ = change in weight [%]

For the $E_0$ modulus, the conversion factor of 0.89 has been used for green (>30% M.C.) to dry (12% M.C.) state, as named by Aicher & al. [68], as the conversion formula of EN 408 only holds for a moisture content between 8 and 18%.

**Outcomes**

From all piles, the dimensions noted down are stated in table A.2. Table A.3 shows the found E moduli and moisture contents. Further on, retrieved dimensions from the horizontal timber can be found in table A.4.

Table A.2: Measurement results from all acquired piles

| Pile | Length (m) | Perimeter P1 (m) | P2 (m) | P3 (m) | m (kg) | f (Hz) | $D_{head}$ (m) | $D_{tip}$ (m) |
|---|---|---|---|---|---|---|---|---|
| PAA0100 | 16.3 | 0.72 | 0.67 | 0.57 | 280 | 278 | 0.23 | 0.18 |
| PCA0100 | 15.1 | 0.79 | 0.72 | 0.6 | 322.5 | 303 | 0.25 | 0.19 |
| PDC0100 | 11.04 | 0.75 | 0.74 | 0.6 | 236.5 | 220 | 0.24 | 0.19 |
| PDO0100 | 10.96 | 0.74 | 0.65 | 0.55 | 208.5 | 229 | 0.24 | 0.18 |
| PDO0200 | 10.68 | 0.84 | 0.82 | 0.78 | 264 | 234 | 0.27 | 0.25 |
| PEC0100 | 14.37 | 0.7 | 0.69 | 0.6 | 244 | 337 | 0.22 | 0.19 |
| PFC0100 | 9.58 | 0.69 | 0.67 | 0.59 | 183 | 259 | 0.22 | 0.19 |
| PFC0200 | 14.6 | 0.72 | 0.69 | 0.6 | 282.5 | 181 | 0.23 | 0.19 |
| PFC0300 | 15 | 0.78 | 0.7 | 0.53 | 363 | 161 | 0.25 | 0.17 |
| PGC0100 | 9.56 | 0.71 | 0.75 | 0.65 | 195.5 | 278 | 0.24 | 0.21 |
| PGC0200 | 14.85 | 0.7 | 0.68 | 0.56 | 266.5 | 190 | 0.22 | 0.18 |
| PGC0300 | 13.7 | 0.75 | 0.73 | 0.57 | 280.5 | 166 | 0.24 | 0.18 |
| PIA0100 | 12.8 | 0.8 | 0.7 | 0.6 | 259 | 190 | 0.25 | 0.19 |
| PJC0100 | 13.55 | 0.67 | 0.68 | 0.6 | 211.5 | 176 | 0.22 | 0.19 |
| PKO0100 | 11.5 | 0.7 | 0.77 | 0.8 | 283 | 234 | 0.25 | 0.22 |
| POA0100 | 12.74 | 0.75 | 0.75 | 0.62 | 260 | 205 | 0.24 | 0.20 |
| POA0200 | 15.36 | 0.8 | 0.75 | 0.69 | 300 | 176 | 0.25 | 0.22 |
| POA0300 | 11.66 | 0.77 | 0.67 | 0.64 | 307 | 215 | 0.25 | 0.20 |
| POA0400 | 12.98 | 0.8 | 0.69 | 0.64 | 252.5 | 185 | 0.25 | 0.20 |
| POA0500 | 12.6 | 0.8 | 0.8 | 0.7 | 288 | 200 | 0.25 | 0.22 |
| POA0500 | 15 | 0.79 | 0.65 | 0.5 | 216 | 190 | 0.25 | 0.16 |
| POA0600 | 16.55 | 0.78 | 0.69 | 0.53 | 356 | 166 | 0.25 | 0.17 |
| POC0100 | 14.25 | 0.68 | 0.73 | 0.6 | 222 | 161 | 0.23 | 0.19 |
| POC0200 | 12.04 | 0.81 | 0.79 | 0.7 | 288 | 215 | 0.26 | 0.22 |
| POC0300 | 14.14 | 0.74 | 0.71 | 0.6 | 266 | 195 | 0.24 | 0.19 |
| POC0400 | 10.6 | 0.72 | 0.72 | 0.59 | 197.5 | 239 | 0.23 | 0.19 |
| POC0500 | 11.88 | 0.67 | 0.7 | 0.61 | 195 | 249 | 0.22 | 0.19 |
| POC0600 | 8.56 | 0.6 | 0.69 | 0.7 | 158 | 293 | 0.22 | 0.19 |
| POC0700 | 9.6 | 0.75 | 0.69 | 0.62 | 216.5 | 249 | 0.24 | 0.20 |
| POC0800 | 15 | 0.85 | 0.78 | 0.59 | 332 | 166 | 0.27 | 0.19 |
| POC0900 | 13.2 | 0.7 | 0.68 | 0.6 | 226.5 | 185 | 0.22 | 0.19 |
| POC1000 | 7.48 | 0.68 | 0.74 | 0.75 | 167.5 | 190 | 0.24 | 0.22 |
| POC1100 | 11.8 | 0.7 | 0.71 | 0.59 | 238 | 234 | 0.23 | 0.19 |
| POC1200 | 14.56 | 0.67 | 0.68 | 0.6 | 241.5 | 181 | 0.22 | 0.19 |
| POC1300 | 12.6 | 0.68 | 0.68 | 0.45 | 210.5 | 195 | 0.22 | 0.14 |
| POC1400 | 14.9 | 0.74 | 0.7 | 0.59 | 249.9 | 239 | 0.24 | 0.19 |
| POC1500 | 10.95 | 0.72 | 0.84 | 0.85 | 342 | 210 | 0.27 | 0.23 |
| POO0100 | 8.72 | 0.64 | 0.72 | 0.77 | 190.5 | 259 | 0.25 | 0.20 |
| POO0200 | 10 | 0.7 | 0.75 | 0.76 | 227 | 254 | 0.24 | 0.22 |
| POO0300 | 9.85 | 0.72 | 0.68 | 0.65 | 184.5 | 273 | 0.23 | 0.21 |
| SFA0100 | 10.96 | 0.83 | 0.8 | 0.71 | 306 | 234 | 0.26 | 0.23 |
| SOA0100 | 12.45 | 0.79 | 0.77 | 0.64 | 299 | 234 | 0.25 | 0.20 |
| SOA0200 | 11.2 | 0.67 | 0.75 | 0.8 | 225.5 | 239 | 0.25 | 0.21 |
| SOA0300 | 11.3 | 0.85 | 0.8 | 0.8 | 264.5 | 244 | 0.27 | 0.25 |
| SOA0400 | 14.9 | 0.76 | 0.71 | 0.53 | 324 | 185 | 0.24 | 0.17 |

Table A.3: Processed results from all acquired piles. Outliers in gray.

| Pile | V ($m^3$) | $\rho_\omega$ ($kg/m^3$) | $E_{0,dyn}$ (MPa) | M.C.(%) | $\rho_{12}$ ($kg/m^3$) | $E_{0,dyn,12}$(MPa) |
|---|---|---|---|---|---|---|
| PAA0100 | 0,56 | 501 | 41184 | 58,1 | 374 | 46274 |
| PCA0100 | 0,57 | 561 | 46988 | 71,5 | 383 | 52796 |
| PDC0100 | 0,45 | 529 | 12488 | 33,4 | 475 | 14032 |
| PDO0100 | 0,37 | 558 | 14056 | 31,6 | 509 | 15793 |
| PDO0200 | 0,57 | 466 | 11639 | 37,3 | 405 | 13077 |
| PEC0100 | 0,51 | 478 | 44882 | 44,7 | 393 | 50429 |
| PFC0100 | 0,38 | 486 | 11975 | 36,4 | 426 | 13455 |
| PFC0200 | 0,55 | 518 | 14469 | 41,8 | 435 | 16257 |
| PFC0300 | 0,54 | 677 | 15804 | 40,5 | 575 | 17757 |
| PGC0100 | 0,39 | 507 | 14332 | 39,8 | 433 | 16104 |
| PGC0200 | 0,49 | 547 | 17430 | 40,8 | 463 | 19584 |
| PGC0300 | 0,56 | 500 | 10345 | 44,6 | 411 | 11624 |
| PIA0100 | 0,50 | 515 | 12194 | 46,4 | 418 | 13701 |
| PJC0100 | 0,46 | 458 | 10423 | 34,6 | 407 | 11712 |
| PKO0100 | 0,48 | 586 | 16960 | 36,8 | 511 | 19056 |
| POA0100 | 0,52 | 501 | 13656 | 38,1 | 433 | 15344 |
| POA0200 | 0,65 | 458 | 13393 | 41,1 | 387 | 15048 |
| POA0300 | 0,40 | 765 | 19222 | 45,3 | 625 | 21598 |
| POA0400 | 0,45 | 563 | 12996 | 32,2 | 511 | 14602 |
| POA0500 | 0,61 | 470 | 11937 | 32,2 | 426 | 13412 |
| POA0500 | 0,48 | 448 | 14569 | 44,6 | 369 | 16370 |
| POA0600 | 0,54 | 661 | 19944 | 33,1 | 594 | 22409 |
| POC0100 | 0,53 | 420 | 8845 | 31,7 | 383 | 9938 |
| POC0200 | 0,57 | 504 | 13512 | 42,6 | 421 | 15182 |
| POC0300 | 0,53 | 498 | 15147 | 34,2 | 444 | 17019 |
| POC0400 | 0,42 | 476 | 12209 | 42,3 | 398 | 13718 |
| POC0500 | 0,40 | 482 | 16886 | 36,4 | 423 | 18973 |
| POC0600 | 0,28 | 560 | 14093 | 38,0 | 484 | 15835 |
| POC0700 | 0,38 | 574 | 13117 | 44,9 | 471 | 14738 |
| POC0800 | 0,62 | 532 | 13190 | 35,3 | 470 | 14820 |
| POC0900 | 0,47 | 487 | 11607 | 30,4 | 448 | 13042 |
| POC1000 | 0,30 | 552 | 4459 | 28,9 | 515 | 5010 |
| POC1100 | 0,43 | 551 | 16790 | 33,9 | 492 | 18865 |
| POC1200 | 0,48 | 504 | 14011 | 33,3 | 453 | 15743 |
| POC1300 | 0,43 | 495 | 11952 | 35,8 | 436 | 13429 |
| POC1400 | 0,54 | 466 | 23648 | 32,9 | 420 | 26571 |
| POC1500 | 0,56 | 613 | 12957 | 38,1 | 529 | 14559 |
| POO0100 | 0,36 | 537 | 10948 | 42,7 | 447 | 12301 |
| POO0200 | 0,44 | 521 | 13435 | 42,4 | 435 | 15095 |
| POO0300 | 0,38 | 488 | 14102 | 45,4 | 398 | 15845 |
| SFA0100 | 0,50 | 615 | 16174 | 31,2 | 562 | 18173 |
| SOA0100 | 0,49 | 605 | 20556 | 42,5 | 506 | 23096 |
| SOA0200 | 0,54 | 421 | 12069 | 36,5 | 369 | 13561 |
| SOA0300 | 0,58 | 460 | 13976 | 38,3 | 397 | 15703 |
| SOA0400 | 0,46 | 706 | 21455 | 41,4 | 594 | 24106 |

| Name | l0 (m) | h0(m) | b0 (m) | l1 (m) | l2 (m) | l3 (m) | l4 (m) | l5 (m) | l6 (m) | h1 (m) |
|---|---|---|---|---|---|---|---|---|---|---|
| KO0200 | 6.48 | 0.25 | 0.17 | 1.95 | 3.15 | 4.4 | 5.5 | 6.15 | N/A | N/A |
| DH0100 | 4.95* | 1.63 | 0.3 | 0.16 | 0.77 | 1.07 | 1.75 | 2.13 | 2.49 | 1.05 |
| VO0300 | 6.38 | 0.07 | 0.25 | 0.83 | 1.92 | 2.95 | 4.1 | 5.1 | N/A | N/A |

Table A.4: Dimensions retrieved from horizontal timber example pieces.*DH0100 has been broken in two during transport. Measured length is approximately 2/3 of the total length.

## A.6. CONCLUSION

The measurements were primarily made for inventory and selection purposes. The investigated elements, the piles and raking piles, were compared on density but selected on E modulus.

The measure dynamic modulus measurements are corresponding with the higher C-classes in the Eurocode (NEN EN 338 [2]), but this is not because of the wood quality. It is because the small vibration of the hammer that sends the signal does not reach sufficient strain for acquiring the E modulus as presented in this norm; further up in the stress-strain curve the stiffness goes down. Thus the two are not comparable directly.

For further testing, 6 piles were picked. To show the range of strengths present 2 piles with low stiffness, 2 with medium and 2 with high stiffness were selected. These are POC0100 & PJC0100, POC0700 & PGC0100 and PKO0100 & POA0600 respectively. Due to difficulty on site, pile POA0600 was abandoned, while the average-stiff pile POA0100 was picked. In the choice, no distinction is made between raking piles and ordinary piles since no difference between the two is found, assuming the same timber batch has been used for both.

The average and deviation values for $\rho_{12}$ are 451 and 60 kg/m$^3$. Excluding the outliers the average and deviation values for $E_{dyn,12}$ are 16128 and 3547 MPa. Find the distributions in figure A.3.

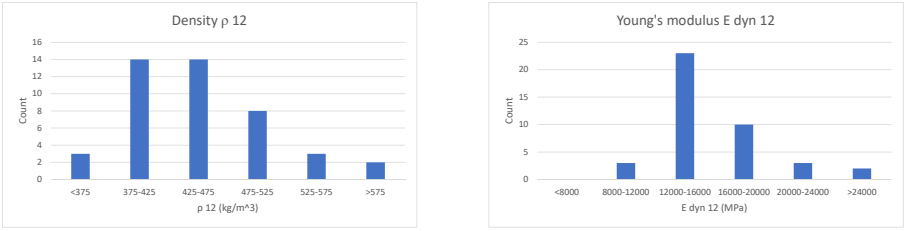


Figure A.3: Distributions of the modified density and dynamic Young's modulus.

## A.7. DISCUSSION

Due to use of new equipment, some dynamic E modulus measurements could have been read wrongly from the screen of the Brooker device. PEC0100, PAA0100 and PCA0100 are most probably too high for this reason, especially because they end on 0100 - meaning they are the first measurement of their piletype.

For later similar measurements a recommendation would be to obtain the moisture content without cutting the disc in the middle, as it is hard to find the corresponding pile halves together for further processing after selection.

# B

# COMPRESSION TEST PILES

Appendix of Chapter 5

## B.1. AIM AND CONTENT

THIS appendix holds a detailed description of the set up and steps taken preceding and occurring during the compression test of the piles. The aim of the experiment is to determine compressive strength parallel to the grain, $f_{c,0}$, and the Young's modulus parallel to the grain, $E_0$. It has to be noted that three unidentified pilepieces arrived from the harbour. They have been used in all results (PEO01, PEO02 and PEO03).

## B.2. STANDARDS

The standards used during and around the test were:

1. NEN EN 13183-1 for determining the moisture content of each specimen.[79]
2. NEN EN 408, chapter 14 & 15 for test set up and determination of $f_{c,0}$ and $E_0$ respectively. [19]

## B.3. EQUIPMENT

During storage, use has been made of the climatised room. The room is kept at a constant temperature of 19.1 $^o$ C and a moisture content of 30.6 % RH.

During precedenting measurements, use has been made of the following equipment:

- Sauter scale, type EB60, 1 gram accuracy;
- Mettler Toledo scale, type BBK422-3DXS, 0,01 gram accuracy;
- Binder FD oven, 1$^o$ C accuracy;

- Brookhuis Timber Grader MTG, 1 Hz accuracy;
- Measuring tape.



During the compression test, these pieces of equipment have been used:

- Losen Hausenwerk hydraulic Universal Testing Machine (UTM) (building year 1950), maximum load 500 000 kg;
- ONO Sokki Gs-551 Linear Variable Differential Transformers, accuracy 1$\mu$m;
- Hottinger Baldwin Messtechnik load cell, including SP 3540A, DA3417 and KWS3073 elements;
- MP3 data logging software, version 1.1.1.97;
- Hoisting crane, electronic screw driver and measuring tape.

## B.4. PRECEDENTING MEASUREMENTS

Before the actual compression test was carried out, some measurements had to be made and actions taken. The aim is to determine moisture content, as well as $E_{0,dyn}$, to compare it afterwards with the $E_{0,stat}$ from the compressive test. This was the moment the elements were taken out of the climatised room. In chronological order:

1. Measuring of the weight and volume, to find the density. Use is made of the Sauter scale and a tape measure. Measured dimensions are lower and upper perimeter and length.
2. Response frequency measurement. $1^{st}$ peak is noted down. Use is made of the Timber Grader MTG.
3. Size downgrade of the pile pieces by circular saw on both sides.*
4. Cutting off of two 2 cm discs at both ends for moisture content determination.
5. Weighing of the discs on the Mettler Toledo scale.
6. Drying of the discs in the Binder oven at $103^{o}$C for 2 days.
7. Weighing of the discs.
8. Repetition of the drying and weighing as a control measurement.

* NEN EN 408 states the compression test can be done on an element 6 times its smaller cross-sectional dimension. With an average diameter found in the stock of 211 mm, a dimension is chosen of 1500 mm. Due to installation ease reasons in the machine, the actual cut-down aimed size has been 1495 mm. The specimen was placed in a U-shaped mould, after which both ends are adapted in height to ensure parallel cutting. The specimen was then screwed into the mould, and cut at each end. Due to a restricted

height of the circular saw, the specimen needed to be rotated 180 degrees around its length axis to ensure a full cut.

Afterwards, the measurement of weight, dimensions and response frequency would be repeated, following exactly the same steps as before the cutting operation (step 1 and 2). No replacement into the climate room took place until commence of the compression test, lasting up to 10 days afterwards.



During the precedenting measurements it becomes clear that pilepart POA0750 is not measured at the storage site at the Rotterdam harbour. The marking has been misread; the pile is actually POA01 and corresponding dynamic e moduli are indeed similar. Pileparts PEO01,PEO02 and PEO03 have lost their original marking and are tested 'anonymously' being denoted as extra piles.

## B.5. COMPRESSION TEST EXECUTION

The compression test took place in a deformation controlled manner and according to NEN EN 408 [NEN408]. Using the LVDT measurement devices as well as the force appliance during compression, live action could be followed in the MP3 software. Measured were: time (MP3), displacements (5 LVDT's), force (Universal Testing Machine). See figure B.1 for the set-up.

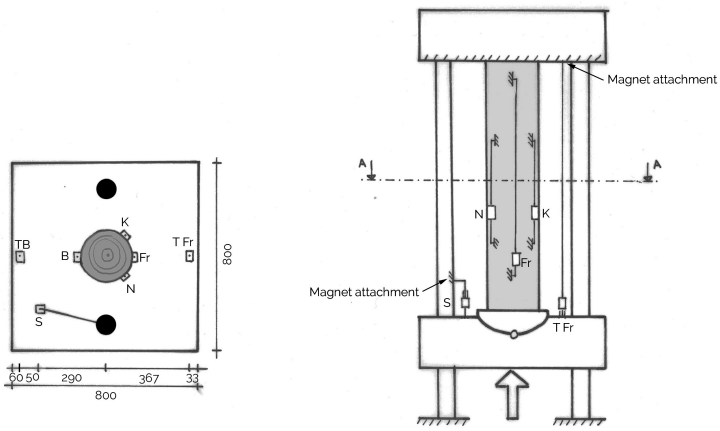


Figure B.1: Set up and placement of the measurement devices. Left: vertical section A-A' (exact placement of the LVDTs). Right: side view (TFr sensor has been put aside for the overview).

The test sequence consists of the following steps:

1. Placement of the pile element between the top and bottom compression plate. This was done using a crane and a hammer, for adjustment of the bottom hinge.
2. Fixation of the timber. The bottom plate is pushed upwards until the pile touches the top plate.
3. Placement of the LVDT's (see figure B.1). 3 Are attached to the machine: 1 in the middle (touching the threaded column and the bottom plate; **'S'**), 2 on the front and back (touching the top plate and the bottom plate; **'TFr'& 'TB'**). These are attached with magnets. The remaining 4 LVDT's are placed on the timber: 2 spanning approximately 4 diameters (front and back, 800-1000 mm; **'Fr'& 'B'**), 1 spanning a knot (300 mm span; **'K'**), 1 spanning a piece of clear wood (300 mm span; **'N'**). These are attached with screws directly into the specimen. The spans between the screws differ with every pile and are therefore noted down.
4. Photography of the specimen before starting the loading.
5. Start of the experiment and data logging. Initiation speed is not registered, as it is used to firmly grip the specimen until a force of 10 kN. The force is measured by the compression press itself; the sensor is named **'F'**.
6. Deformation controlled loading. Reset of the displacement in sensor **S** after having reached 10 kN (main LVDT in middle of the table) (step 1), then setting the deformation inducement to 0.5 mm/s (step 2). This speed is continued until maximum compressive strength is reached.
7. Photography of the specimen at maximum load.
8. Choice of continuation speed. After clear plasticity and maximum compression indication, the force-displacement curve is closely watched. If no sudden drop occurs, indicating failure, the speed is turned up to 3.0 mm/s (step 3).
9. Unloading after steep drop of the Force-Deformation curve indicating failure of the timber (step 4).
10. Detachment of the LVDT's on the timber and removal of the pile element. Exportation of the logged data (step, time, displacement and force) in XML format.

# B.6. RESULTS AND ANALYSIS

## B.6.1. PRECEDENTING MEASUREMENTS

### PROCESSING

Like at the storage site, a dynamic E modulus could be found using formula B.1 [16].

$$E_{dyn} = 4 * \rho * f * l^2 \tag{B.1}$$

with
$E_{dyn}$ = Dynamic Youung's modulus parallel to the grain $[Pa]$
$\rho_{test}$ = density at current moisture content $[kg/m^3]$
$f$ = frequency $[Hz]$
$l$ = specimen length $[m]$

For determination of the volume, use is made of the open cone formula.

$$V = \frac{1}{3}\pi(r_1^2 + r_1 r_2 + r_2^2)h \tag{B.2}$$

with
$V$ = nolume of the pile piece $[m^3]$
$r_1$ = Bottom radius $[m]$
$r_2$ = Top radius $[m]$
$h$ = specimen length $[m]$

The moisture content is calculated according to formula B.3. The dry mass has been determined according to NEN 13183-1 [79] with control measurements stating no more than 0.1 % difference should occur between two measurements.

$$\omega = 100 * \frac{m_{wet} - m_{dry}}{m_{dry}} \tag{B.3}$$

with
$\omega$ = moisture content %
$m_{wet}$ = Wet mass $[kg]$
$m_{dry}$ = Dry mass $[kg]$

The found $E_0$ moduli and compressive strengths $f_{c,0}$ can be post-processed to 12% moisture content state using NEN EN 384, paragraph 5.4.2. if the moisture content is between 8 and 18 %. As all moisture contents of the tested log elements surpassed these values, use has been made for the compressive strengths of the findings by Ros,Kuhne & al, Glos and Kollman, which have been summarised in the graph as presented in Aicher's and Stapf's paper on compressive strength [68]. See figure B.2.

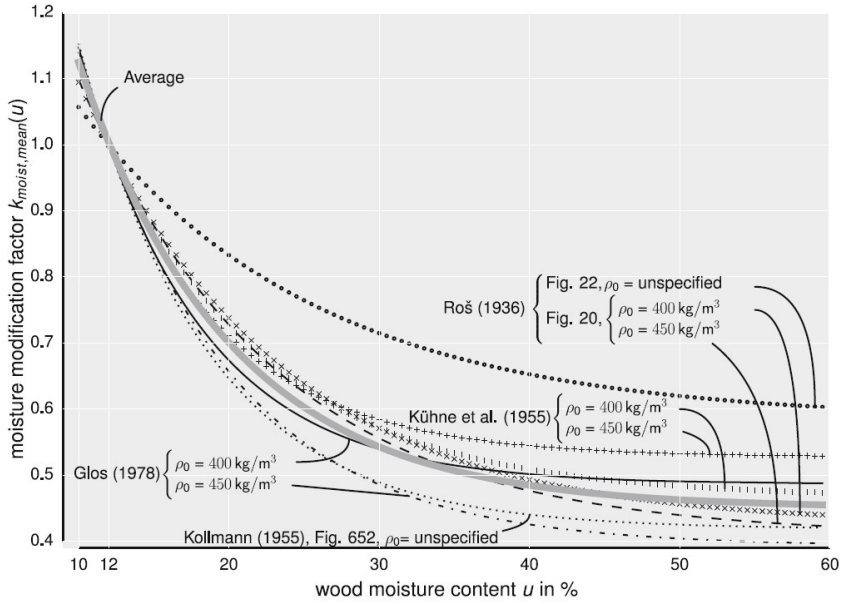


Figure B.2: The literature review of Aicher & al show us a clear drop in compressive strength parallel to the fibre with increasing moisture content. Graph from [68].

For deriving the $E_{0,12}$ modulus, the stated modification factor of 0.89 from wet to dry state has been interpolated between dry ($\omega$= 12%) and green ($\omega$=30%) state [68].

Regarding the density, as for the Rotterdam Harbour measurements use has been made of equation B.4. This simplified formula is not accounting for volume changes.

$$\rho_{12} = \frac{(1 + \frac{\Delta V}{100})}{(1 + \frac{\Delta G}{100})} * \rho_\omega \tag{B.4}$$

with

$\rho_{12}$ = density under 12% moisture content $[kg/m^3]$
$\rho_\omega$ = density under current moisture content $[kg/m^3]$
$\omega$ = moisture content [%]
$\Delta V = \beta * (\omega - 12)$ = change in volume [%]
until $\omega$ = 30% at most (fibre saturation corresponding to used borders for the E modulus). $\beta$ =0.5 [%]
$\Delta G$ = change in weight [%]

### RESULTS

Table B.1 and B.2 show the sizes and dynamic E moduli found before the size adaptation, while table B.3 and B.4 show the ones after the size adaptation.

Table B.1: Measurement results before the cut - part 1.

| Pilepiece | Perimeter P1 (mm) | P2 (mm) | l (mm) | m (kg) | f (Hz) | $D_{ave}$ (mm) |
|---|---|---|---|---|---|---|
| PEO01 | 580 | 595 | 2120 | 23.95 | 1279 | 187 |
| PEO02 | 402 | 482 | 2118 | 17.34 | 898 | 141 |
| PEO03 | 688 | 698 | 1927 | 34.72 | 1371 | 221 |
| PGC0120 | 680 | 680 | 1940 | 36.58 | 1298 | 216 |
| PGC0122 | 725 | 750 | 1825 | 38.6 | 1415 | 235 |
| PGC0140 | 710 | 691 | 2026 | 40.24 | 1279 | 223 |
| PGC0150 | 660 | 615 | 2080 | 34.26 | 1225 | 203 |
| PJC0120 | 660 | 704 | 2081 | 34.88 | 1230 | 217 |
| PJC0121 | 668 | 632 | 1978 | 32.14 | 1337 | 207 |
| PJC0142 | 618 | 633 | 1962 | 28.04 | 1298 | 199 |
| PKO0120 | 742 | 780 | 2028 | 45.76 | 1293 | 242 |
| PKO0142 | 552 | 514 | 2196 | 21.79 | 1166 | 170 |
| POA0140 | 704 | 668 | 2038 | 39.62 | 1249 | 218 |
| POA0750 | 608 | 772 | 2020 | 26.61 | 1230 | 220 |
| POC0120 | 620 | 730 | 2030 | 35.76 | 1078 | 215 |
| POC0140 | 795 | 668 | 2720 | 31.6 | 1191 | 233 |
| POC0150 | 510 | 578 | 2030 | 18.62 | 1254 | 173 |
| POC0720 | 780 | 755 | 2820 | 48.39 | 1186 | 244 |
| POC0721 | 730 | 773 | 2255 | 53.6 | 1118 | 239 |
| POC0740 | 705 | 700 | 2880 | 46.06 | 976 | 224 |
| POC0742 | 632 | 598 | 1800 | 29.31 | 1425 | 196 |

Table B.2: Measurement results before the cut - part 2. Outliers in gray.

| Pilepiece | V ($m^3$) | $\rho_\omega$ (kg/$m^3$) | $E_{dyn,\omega}$ (MPa) | M.C. (%) | $rho_{12}$ | $E_{dyn,12}$ (MPa) |
|---|---|---|---|---|---|---|
| PEO01 | 0,0582 | 411 | 12096 | 22,6 | 392 | 11551 |
| PEO02 | 0,0330 | 525 | 7620 | 31,2 | 469 | 7620 |
| PEO03 | 0,0736 | 471 | 13163 | 24,1 | 446 | 12688 |
| PGC0120 | 0,0714 | 512 | 12997 | 25,6 | 481 | 12646 |
| PGC0122 | 0,0790 | 489 | 13035 | 24,8 | 461 | 12619 |
| PGC0140 | 0,0791 | 509 | 13661 | 27,3 | 470 | 13435 |
| PGC0150 | 0,0673 | 509 | 13226 | 27,2 | 471 | 12998 |
| PJC0120 | 0,0771 | 453 | 11868 | 25,3 | 425 | 11529 |
| PJC0121 | 0,0665 | 483 | 13520 | 22,2 | 461 | 12875 |
| PJC0142 | 0,0611 | 459 | 11908 | 22,9 | 436 | 11395 |
| PKO0120 | 0,0935 | 490 | 13466 | 24,4 | 463 | 13003 |
| PKO0142 | 0,0497 | 439 | 11511 | 23,1 | 417 | 11028 |
| POA0140 | 0,0763 | 519 | 13454 | 29,9 | 469 | 13447 |
| POA0750 | 0,0769 | 346 | 8586 | 22,7 | 329 | 8205 |
| POC0120 | 0,0738 | 485 | 9307 | 18,5 | 470 | 8653 |
| POC0140 | 0,1161 | 272 | 11453 | 23,7 | 258 | 11014 |
| POC0150 | 0,0479 | 389 | 10096 | 20,7 | 373 | 9521 |
| POC0720 | 0,1322 | 366 | 16379 | 28,8 | 334 | 16260 |
| POC0721 | 0,1014 | 529 | 13446 | 29,5 | 479 | 13406 |
| POC0740 | 0,1131 | 407 | 12870 | 29,1 | 370 | 12797 |
| POC0742 | 0,0542 | 541 | 14238 | 21,6 | 517 | 13504 |

Table B.3: Measurument results after the cut - part 1.

| Pilepiece | Perimeter P1 (mm) | P2 (mm) | l (mm) | m (kg) | f (Hz) | $D_{ave}$ (mm) |
|---|---|---|---|---|---|---|
| PEO01 | 600 | 570 | 1495 | 17.74 | 1713 | 186 |
| PEO02 | 424 | 460 | 1495 | 12.425 | 1167 | 141 |
| PEO03 | 697 | 681 | 1495 | 27.23 | 1732 | 219 |
| PGC0120 | 680 | 680 | 1492 | 29.25 | 1679 | 216 |
| PGC0122 | 734 | 714 | 1495 | 31.96 | 1703 | 230 |
| PGC0140 | 703 | 695 | 1495 | 24.43 | 1713 | 222 |
| PGC0150 | 650 | 638 | 1500 | 25.26 | 1664 | 205 |
| PJC0120 | 676 | 656 | 1495 | 25.07 | 1698 | 212 |
| PJC0121 | 677 | 648 | 1495 | 24.56 | 1732 | 211 |
| PJC0142 | 632 | 620 | 1495 | 21.1 | 1708 | 199 |
| PKO0120 | 746 | 771 | 1495 | 33.74 | 1767 | 241 |
| PKO0142 | 545 | 530 | 1495 | 15.12 | 1664 | 171 |
| POA0140 | 680 | 705 | 1495 | 24.78 | 1688 | 220 |
| POA0750 | 605 | 582 | 1497 | 20.06 | 1596 | 189 |
| POC0120 | 660 | 740 | 1500 | 24.53 | 1610 | 223 |
| POC0140 | 705 | 662 | 1495 | 22.77 | 1649 | 218 |
| POC0150 | 520 | 662 | 1495 | 14.265 | 1625 | 188 |
| POC0720 | 795 | 750 | 1495 | 35.14 | 1625 | 246 |
| POC0721 | 743 | 769 | 1495 | 35.84 | 1669 | 241 |
| POC0740 | 713 | 695 | 1495 | 31.60 | 1484 | 224 |
| POC0742 | 649 | 592 | 1495 | 24.68 | 1684 | 198 |

Table B.4: Measurement results after the cut - part 2. Outliers in gray.

| Pilepiece | V ($m^3$) | $\rho_\omega$ (kg/$m^3$) | $E_{dyn,\omega}$ (MPa) | M.C. (%) | $rho_{12}$ | $E_{dyn,12}$ (MPa) |
|---|---|---|---|---|---|---|
| PEO01 | 0,0407 | 436 | 11428 | 22,6 | 415 | 10914 |
| PEO02 | 0,0233 | 534 | 6505 | 31,2 | 478 | 6505 |
| PEO03 | 0,0565 | 482 | 12930 | 24,1 | 456 | 12464 |
| PGC0120 | 0,0549 | 533 | 13374 | 25,6 | 500 | 13012 |
| PGC0122 | 0,0624 | 512 | 13287 | 24,8 | 483 | 12863 |
| PGC0140 | 0,0581 | 420 | 11025 | 27,3 | 388 | 10843 |
| PGC0150 | 0,0495 | 510 | 12715 | 27,2 | 472 | 12496 |
| PJC0120 | 0,0528 | 475 | 12245 | 25,3 | 446 | 11896 |
| PJC0121 | 0,0522 | 470 | 12612 | 22,2 | 449 | 12010 |
| PJC0142 | 0,0466 | 453 | 11803 | 22,9 | 430 | 11295 |
| PKO0120 | 0,0685 | 493 | 13759 | 24,4 | 466 | 13285 |
| PKO0142 | 0,0344 | 440 | 10889 | 23,1 | 418 | 10432 |
| POA0140 | 0,0571 | 434 | 11063 | 29,9 | 392 | 11057 |
| POA0750 | 0,0420 | 478 | 10914 | 22,7 | 455 | 10430 |
| POC0120 | 0,0586 | 419 | 9773 | 18,5 | 406 | 9087 |
| POC0140 | 0,0556 | 410 | 9956 | 23,7 | 388 | 9575 |
| POC0150 | 0,0418 | 342 | 8065 | 20,7 | 328 | 7606 |
| POC0720 | 0,0710 | 495 | 11682 | 28,8 | 451 | 11597 |
| POC0721 | 0,0680 | 527 | 13125 | 29,5 | 478 | 13086 |
| POC0740 | 0,0590 | 536 | 10551 | 29,1 | 488 | 10491 |
| POC0742 | 0,0458 | 538 | 13651 | 21,6 | 515 | 12947 |

Outlier PEO02 shows a similarly low E modulus value for the measurement before the cut and is therefore seen as a reliable measurement. Leaving out the $2^{nd}$ outlier in the Young's modulus adaptation to a 12 % M.C., we find a mean and deviation of $E_{0,dyn,12,2000}$ (before the cut) of 11911 MPa and 1622 MPa respectively.

After the cut, the mean and deviation values of $E_{0,dyn,12,1500}$ become 11567 and 1248 MPa respectively after leaving out outliers.

The mean density values on 12% M.C. are 437 and 442 kg/m$^3$ before and after the cut respectively.



## B.6.2. COMPRESSION TEST

### PROCESSING

After all piles were tested, the XML data were loaded into a Python script to compute force-displacement diagrams and stress-strain diagrams . Formula B.5, B.6 and B.7 were used for the latter.

$$\sigma = \frac{F}{A_{ave}} \tag{B.5}$$

with
$\sigma$ = stress $[N/mm^2]$
$F$ = Force $[N]$
$A_{ave}$ = Average area $[mm^2]$

$$\epsilon = \frac{\Delta l}{l} \tag{B.6}$$

with
$\epsilon$ = strain [‰]
$\Delta l$ = displacement $[m]$
$l$ = LVDT attachment span $[mm]$

$$E = \frac{\sigma}{\epsilon} \tag{B.7}$$

with
$E$ = Young's modulus or Modulus of Elasticity $[N/mm^2]$
$\sigma$ = stress $[N/mm^2]$
$\epsilon$ = strain $[-]$

NEN EN 408 [19] states equations and borders to be used for $f_{c,0}$ and $E_{c,0,stat}$ respectively (see equation 10 and 11 on page 21 and 22). The maximum compressive stress parallel to the grain is thus simply obtained by observing the output of sensor F, and marking the stress at the point of maximum force application. The computation of the E modulus values have been made using a python code which makes a first order polynomial fit on

the stress-strain graph [80]. As stated in NEN 408, the values for the Young's moduli have been taken between 0.1* $f_{c,0}$ and 0.4* $f_{c,0}$; if the coefficient of correlation was lower than 0.99 another attempt is made for between the borders of 0.11* $f_{c,0}$ and 0.39* $f_{c,0}$ with 10 iterations maximum (ending between 0.2 and 0.3* $f_{c,0}$). The trendline approach follows Hooke's law (equation B.7). If this would not give a satisfying R-value, the fit of the E modulus would be discarded. This was often the case for incorrect measurements, e.g. a non-activated LVDT (vertical stress-strain graph up to a certain point).

As all LVDT sensors gave a different output (see subsection *Discussion*), a further filtering of the data had to be made. First of all, all measurements where the stress-strain graph would go backwards and resulted into a negative or very high E modulus on the fit were disregarded. This was done by setting the rule that the strain on the upper border (0.4*$f_{c,0}$ on the first iteration) had to be higher than the first one.
Secondly, outlier measurements were discarded too, where an outlier is recognised by the 1.5 Inter Quartile Range rule: Percentile 25-1.5*IQR and Percentile 75+1.5*IQR are the limits. A form of reliability of the sensor is now apparent; it is clear for how many measurements a good fit could be given that is not out of range in comparison with the other measurements.
Thirdly, the borders of the fit-measurement were adjusted to 0.05 and 0.10*$f_{c,0}$. Now, the measurements could better be compared with the dynamic measurements of the precedenting tests.

Both the reliability of the sensor and the comparison with the dynamic modulus would be the base for choice of a sensor for E modulus selection.

### RESULTS: SENSOR SPECIFIC

Results of the measurements are presented in this subsection.

#### Compressive strength



Table B.5: Found compressive strengths under current moisture content and for the 12 % M.C.. Outliers in gray. The outlier POC0720 actually is a pilepart that has not been tested till yielding, and had to be discarded anyway.

| Pilename | $fc_{0,\omega}$ (MPa) | M.C. - $\omega$ (%) | $fc_{0,12}$ |
|---|---|---|---|
| PEO01 | 20.82 | 22.6 | 30.13 |
| PEO02 | 10.06 | 31.2 | 19.09 |
| PEO03 | 20.76 | 24.1 | 31.33 |
| PGC0120 | 13.62 | 25.6 | 21.47 |
| PGC0122 | 19.41 | 24.8 | 29.87 |
| PGC0140 | 20.09 | 27.3 | 33.40 |
| PGC0150 | 17.1 | 27.2 | 28.34 |
| PJC0120 | 13.61 | 25.3 | 21.30 |
| PJC0121 | 20.35 | 22.2 | 29.09 |
| PJC0142 | 19.24 | 22.9 | 28.09 |
| PKO0120 | 21.87 | 24.4 | 33.26 |
| PKO0142 | 18.83 | 23.1 | 27.64 |
| POA0140 | 17.44 | 29.9 | 31.65 |
| POA0750 | 15.26 | 22.7 | 22.16 |
| POC0120 | 16.22 | 18.5 | 21.06 |
| POC0140 | 20.81 | 23.7 | 31.07 |
| POC0150 | 15.62 | 20.7 | 21.44 |
| POC0720 | 7.23 | 28.8 | |
| POC0721 | 18.74 | 29.5 | 33.54 |
| POC0740 | 10.69 | 29.1 | 18.85 |
| POC0742 | 19.82 | 21.6 | 27.86 |

#### Static E modulus

The next tables will show the filtering and comparison of the static and dynamic moduli.

Table B.6: Filtering of results and comparing to the dynamic counterparts, for the NEN EN 408 borders of 0.1 and 0.4 times the compressive strength. Rejects: R (fit) <0.99, Outliers: < q25-1.5 IQR or > q75+1.5 IQR. N remaining equals the number of approved tests.

| Sensor | N rejects | N Outliers | N Remaining | Mean ($\frac{E_{stat}}{E_{dyn1500}}$) | StDev ($\frac{E_{stat}}{E_{dyn1500}}$) | $E_{0,\omega,mean}$ [MPa] |
|---|---|---|---|---|---|---|
| Fr | 0 | 1 | 20 | 0.63 | 0.19 | 7624 |
| B | 5 | 0 | 16 | 1.82 | 0.60 | 22757 |
| K | 0 | 0 | 21 | 0.65 | 0.29 | 8013 |
| N | 3 | 2 | 16 | 0.80 | 0.19 | 10038 |
| TFr | 7 | 2 | 12 | 0.47 | 0.13 | 5550 |
| TB | 2 | 0 | 19 | 0.68 | 0.26 | 8407 |
| S | 0 | 0 | **21** | 0.51 | 0.17 | 6216 |
| Fr-B_ave | 0 | 2 | 19 | 0.97 | 0.21 | 11975 |
| TFr-TB_ave | 2 | 3 | 16 | 0.57 | 0.18 | 6760 |

Table B.7: Filtering of results and comparing to the dynamic counterparts, for the borders of 0.05 and 0.10 times the compressive strength. These are borders that allow better comparison with the dynamic moduli.

| Sensor | N rejects | N Outliers | N Remaining | Mean ($\frac{E_{stat}}{E_{dyn1500}}$) | StDev ($\frac{E_{stat}}{E_{dyn1500}}$) | $E_{0,\omega,mean}$ [MPa] |
|---|---|---|---|---|---|---|
| Fr | 2 | 0 | 19 | 0.60 | 0.22 | 7483 |
| B | 10 | 0 | 11 | 2.51 | 1.01 | 31918 |
| K | 1 | 1 | 19 | 0.65 | 0.24 | 7971 |
| N | 5 | 1 | 15 | 0.82 | 0.22 | 10430 |
| TFr | 14 | 0 | 7 | 0.40 | 0.12 | 4907 |
| TB | 5 | 0 | 16 | 0.59 | 0.35 | 7247 |
| S | 8 | 0 | 13 | 0.24 | 0.11 | 2813 |
| Fr-B_ave | 2 | 4 | 15 | **1.08** | 0.17 | 13527 |
| TFr-TB_ave | 2 | 3 | 16 | 0.52 | 0.24 | 6082 |

### RESULTS: ELEMENT SPECIFIC

The following graphs show the stress strain curves and fits for the test of each specimen. The first graph shows the measurements of the LVDTs on the timber, while the second one shows the LVDT output of the table located sensors. These graphs do not show the full measurement: whenever maximum strain is achieved no more is plotted. This does mean some LVDT output that went into reverse to show a negative strain increment is not visible.

Pictures (if available) show the specimen before the test and during maximum stress. Close-ups are taken off the failing spot. If the picture is not available this is indicated (e.g. when it was chosen to make only a zoomed in picture instead of an overview).

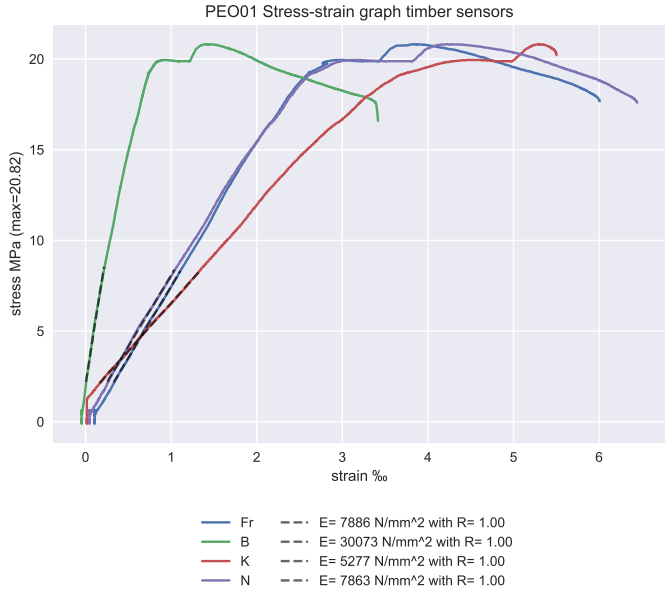


Figure B.3

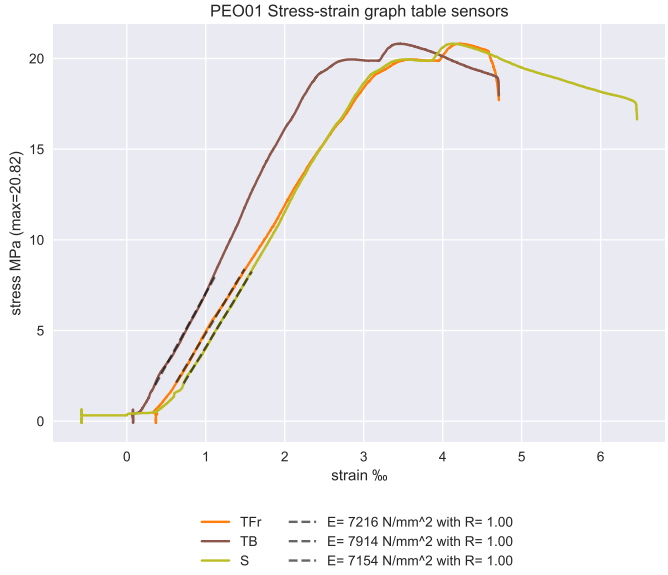


Figure B.4

Figure B.5: Overview of the testpiece PEO01 before testing.

Figure B.6: Close-ups of the failuring testpiece PEO01.

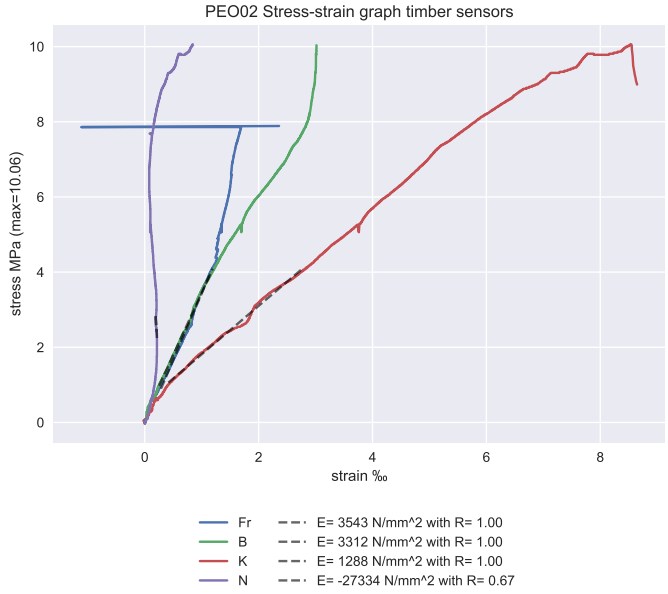


Figure B.7

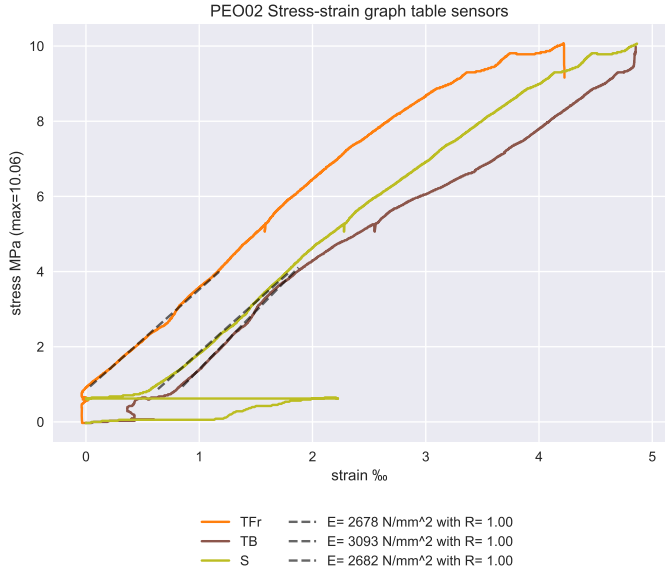


Figure B.8


Figure B.9: Overview of the testpiece PEO02 before testing.

Figure B.10: Close-ups of the failuring testpiece PEO02.

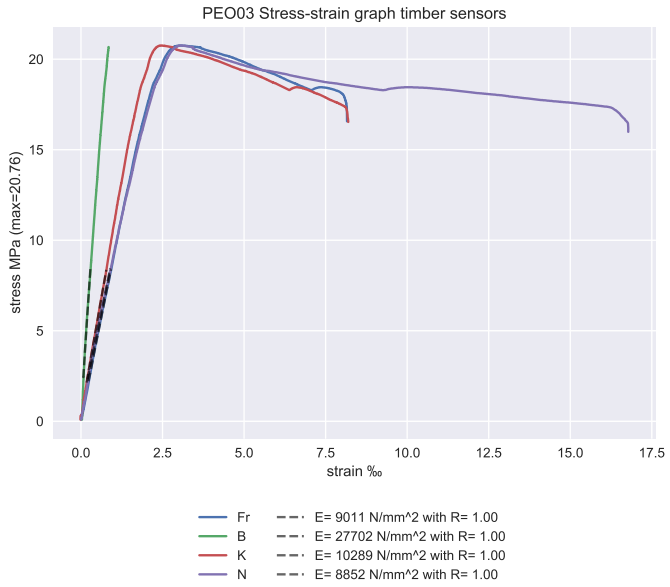


Figure B.11

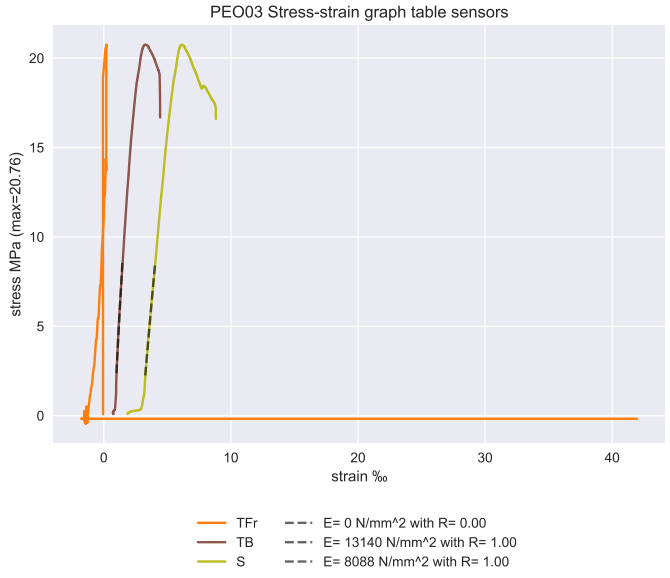


Figure B.12


Figure B.13: Overview of the testpiece PEO03 before testing.


Figure B.14: Close-ups of the failuring testpiece PEO03.

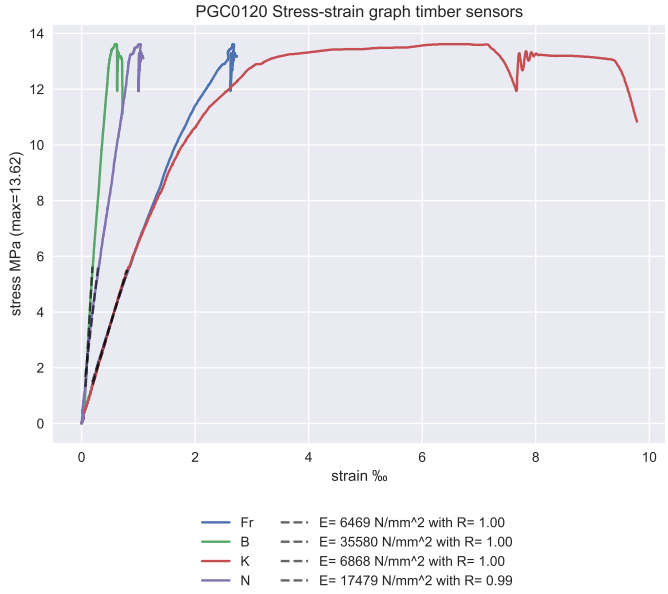


Figure B.15

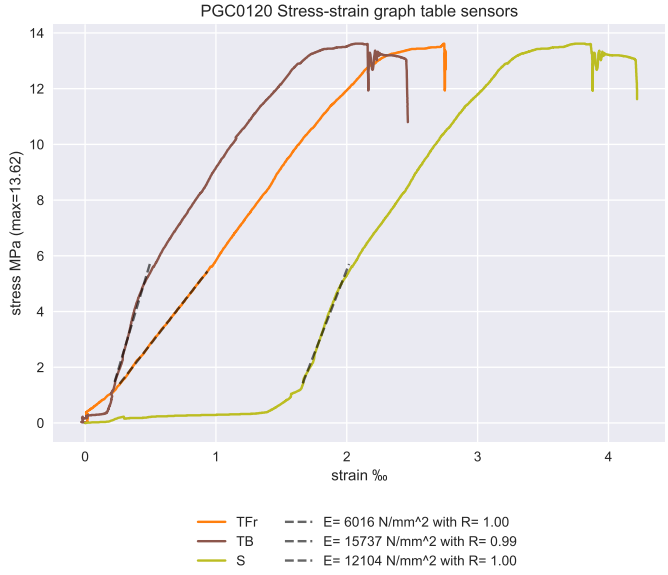


Figure B.16

Figure B.17: Overview of the testpiece PGC0120 before testing (left), and during plasticity (right).

Figure B.18: Close-ups of the failuring testpiece PGC0120.

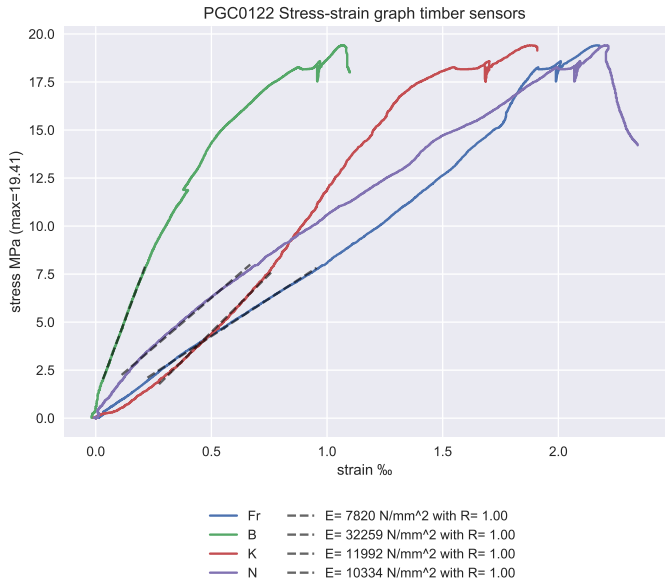


Figure B.19

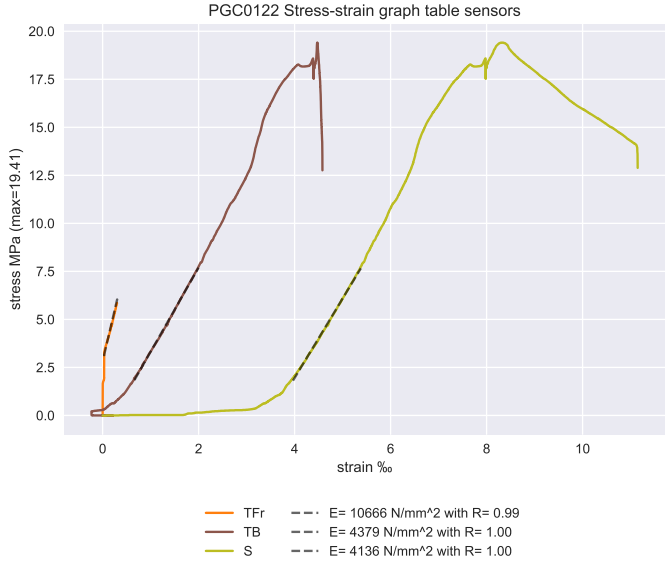


Figure B.20

Figure B.21: Overview of the testpiece PGC0122 during plasticity

Figure B.22: Close-ups of the failuring testpiece PGC0122.

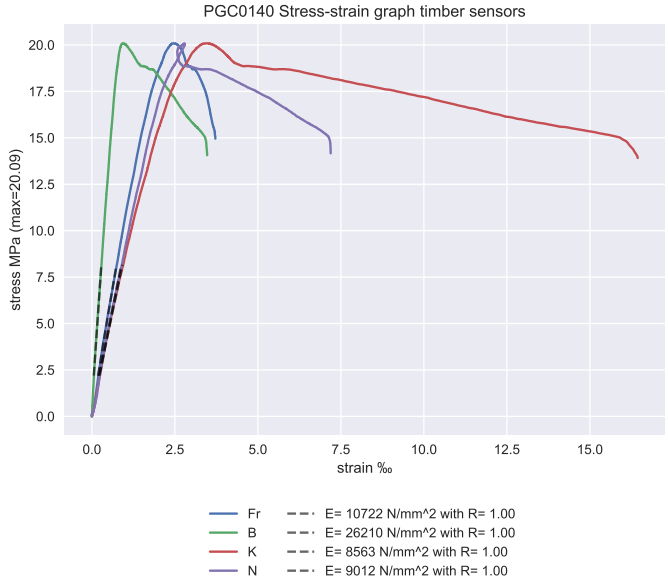


Figure B.23

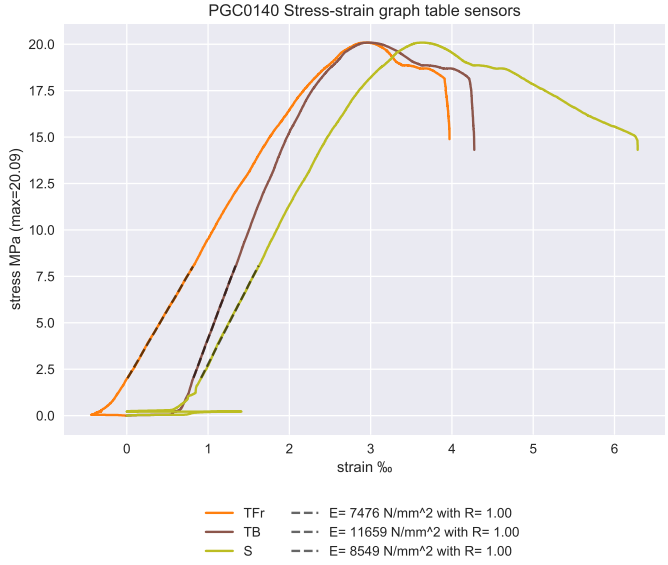


Figure B.24

Figure B.25: Overview of the testpiece PGC0140 before testing.

Figure B.26: Close-ups of the failuring testpiece PGC0140.

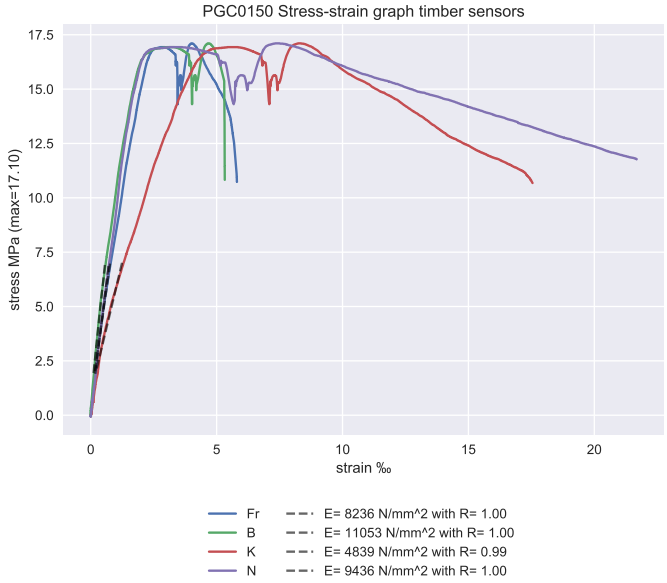


Figure B.27

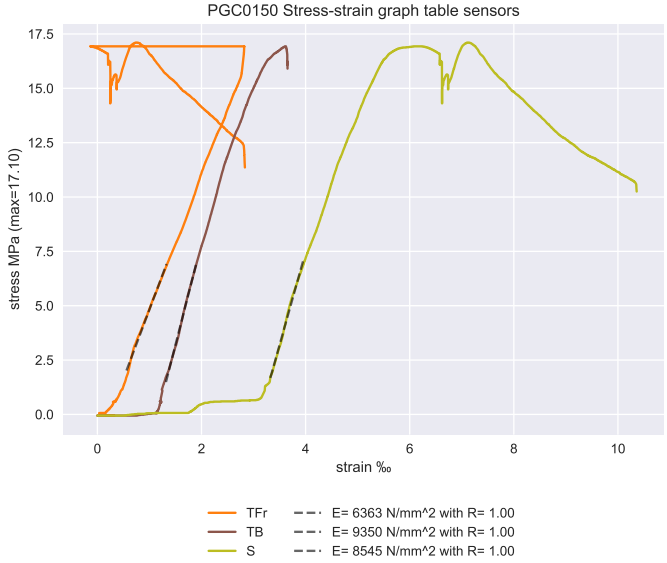


Figure B.28

There are no pictures available of the testing of pilepiece PGC0150.

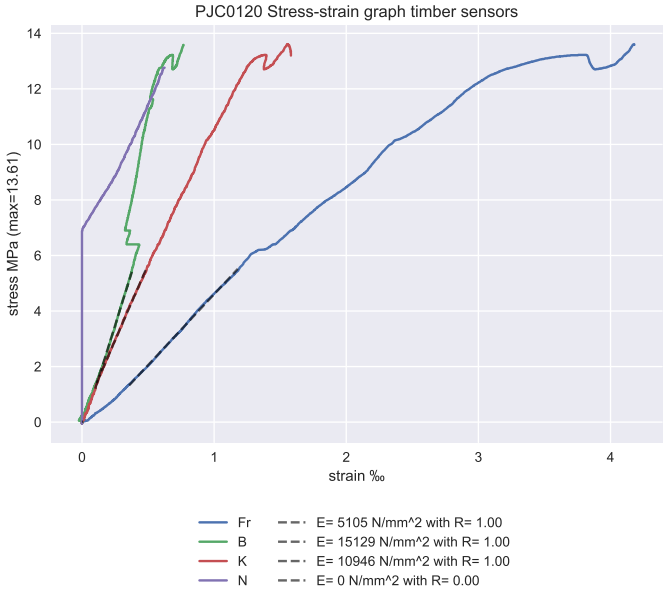


Figure B.29

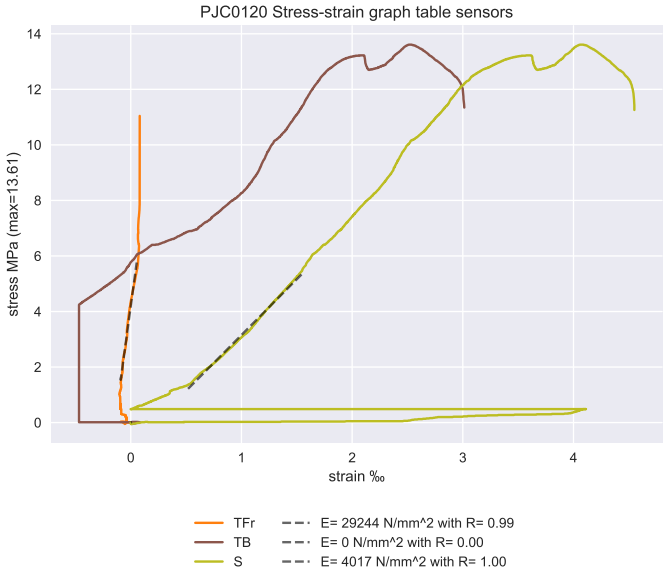


Figure B.30

Figure B.31: Overview of the testpiece PJC0120 during plasticity (right).

Figure B.32: Close-ups of the failuring testpiece PJC0120.

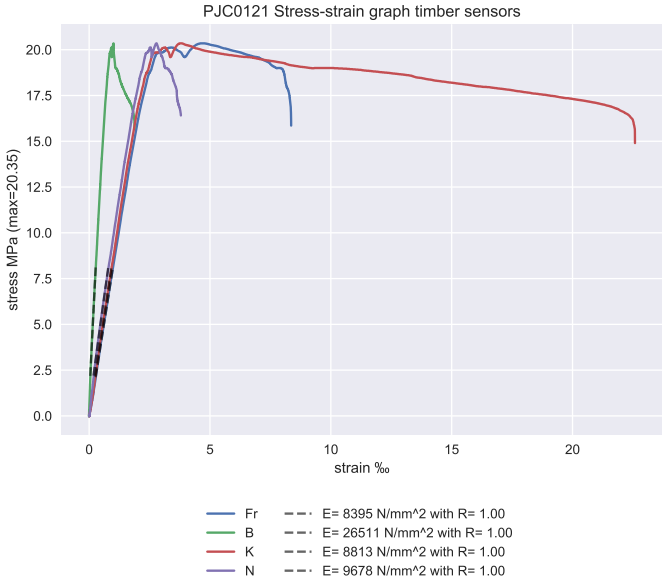


Figure B.33

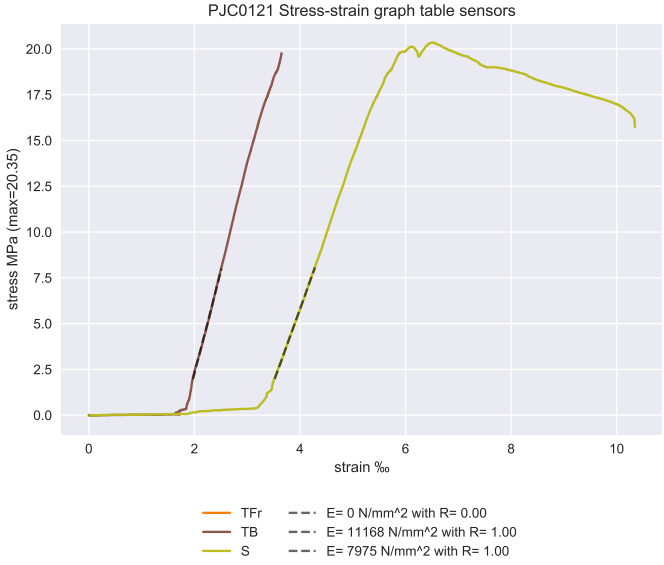


Figure B.34

Figure B.35: Overview of the testpiece PJC0121 during plasticity (right).

Figure B.36: Close-ups of the failuring testpiece PJC0121.

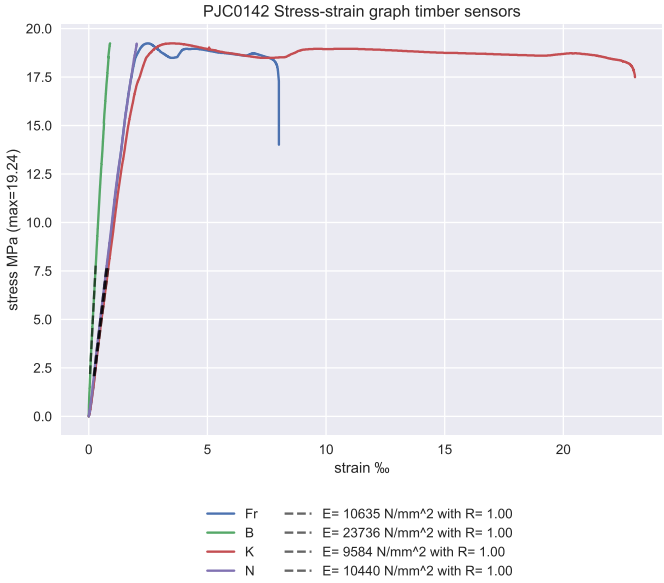


Figure B.37

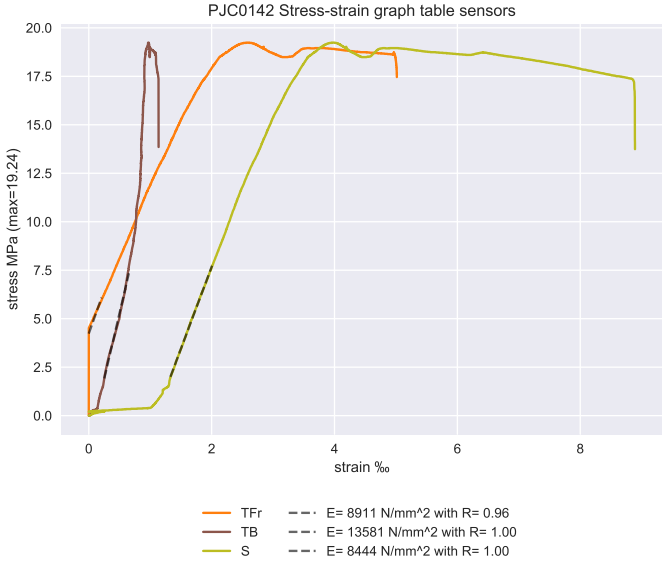


Figure B.38

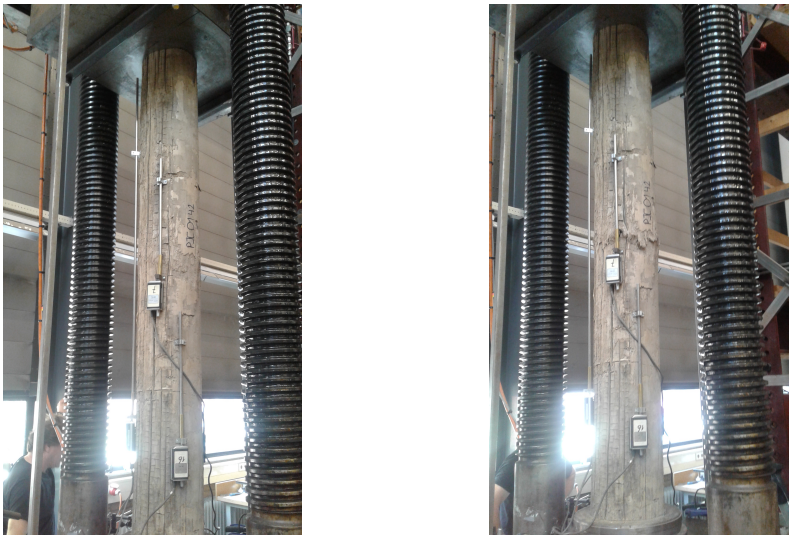

Figure B.39: Overview of the testpiece PJC0142 before testing (left), and during plasticity (right).

Figure B.40: Close-ups of the failuring testpiece PJC0142.

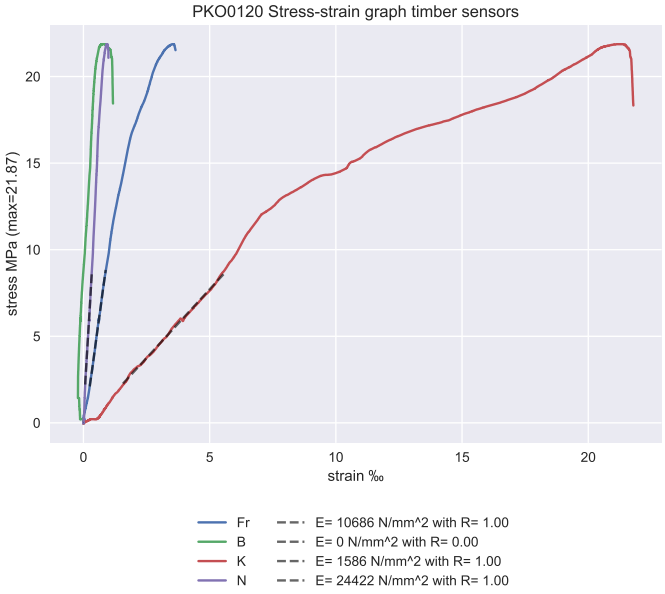


Figure B.41

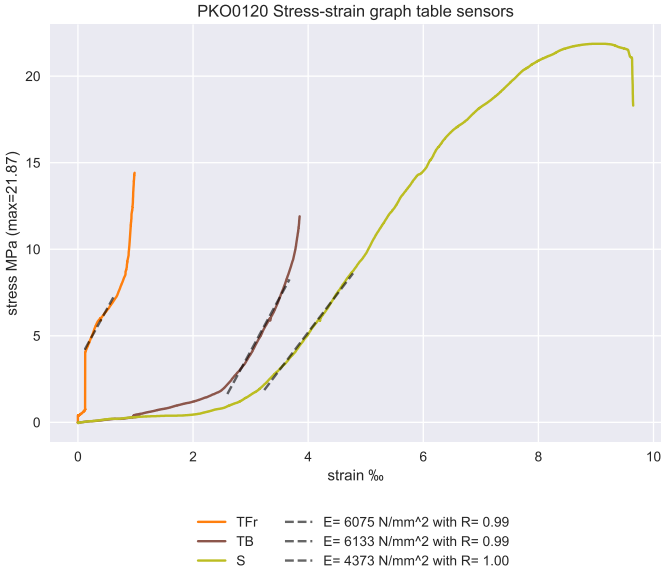


Figure B.42

Figure B.43: Overview of the testpiece PKO0120 before testing (left), and during plasticity (right).

Figure B.44: Close-ups of the failuring testpiece PKO0120 (left), after testing (right).

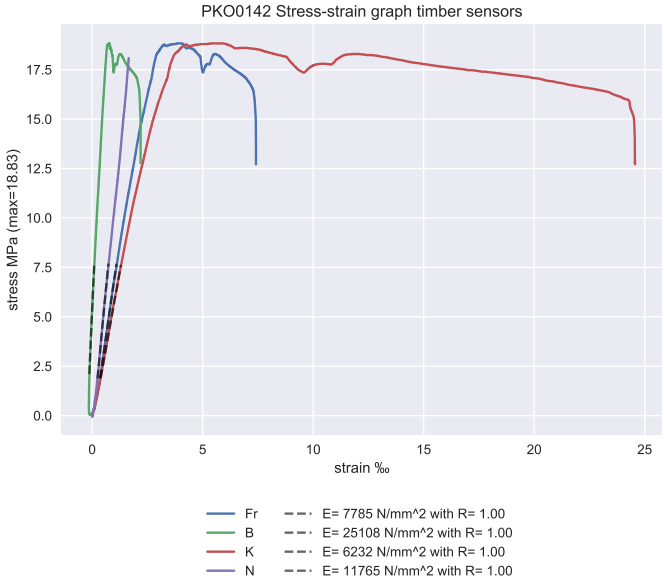


Figure B.45

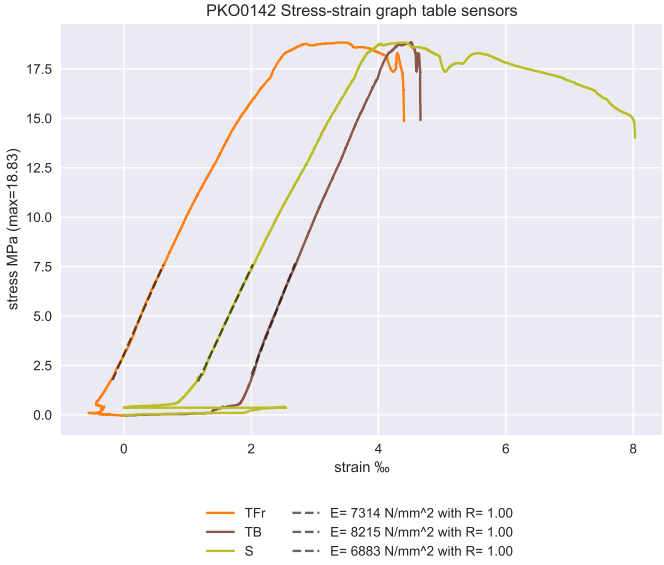


Figure B.46

Figure B.47: Overview of the testpiece PKO0142 before testing.

Figure B.48: Close-ups of the failuring testpiece PKO0142.

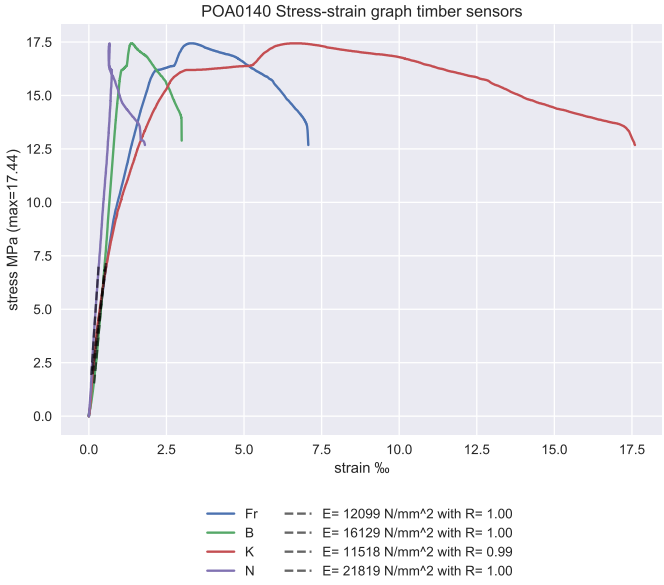


Figure B.49

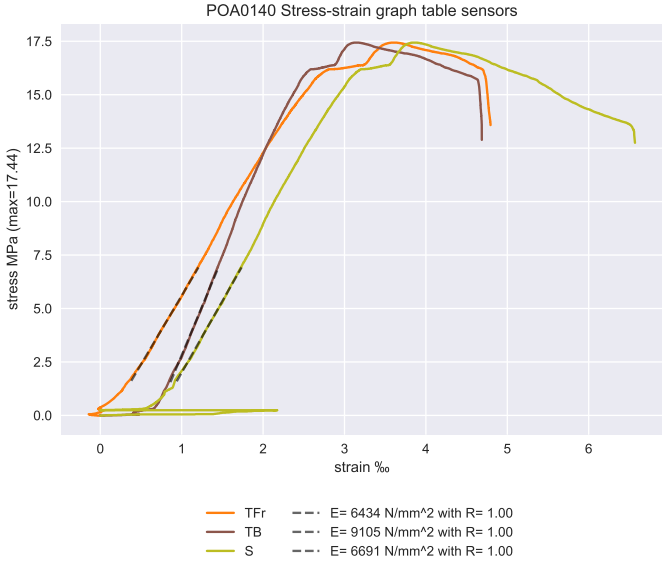


Figure B.50

Figure B.51: Overview of the testpiece POA0140 before testing.

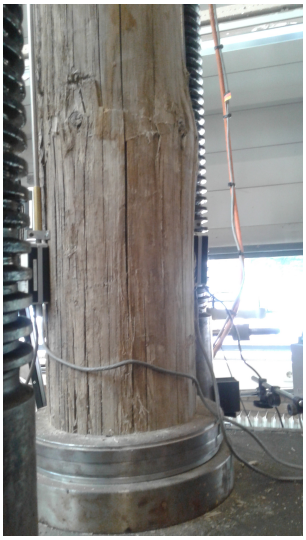

Figure B.52: Close-ups of the failuring testpiece POA0140.

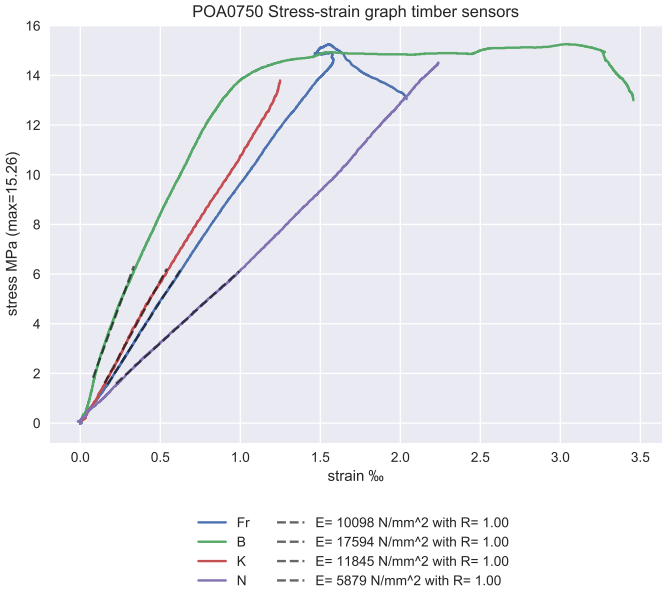


Figure B.53

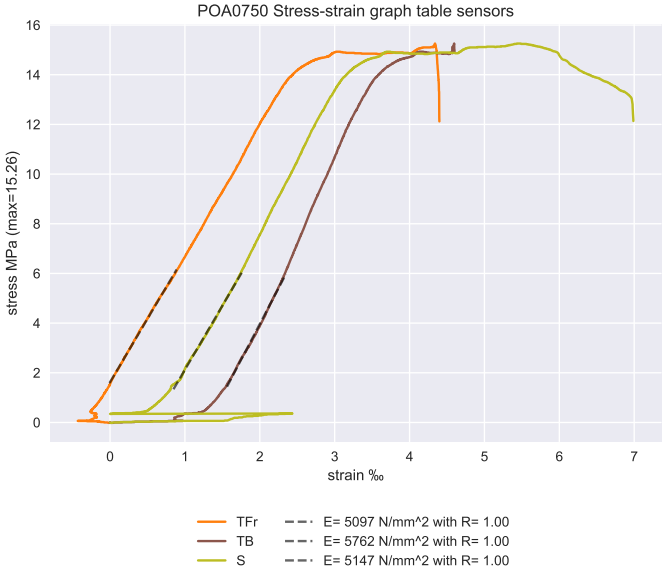


Figure B.54

There are no pictures available of POA0750 before the test commence.

Figure B.55: Close-ups of the failuring testpiece POA0750.

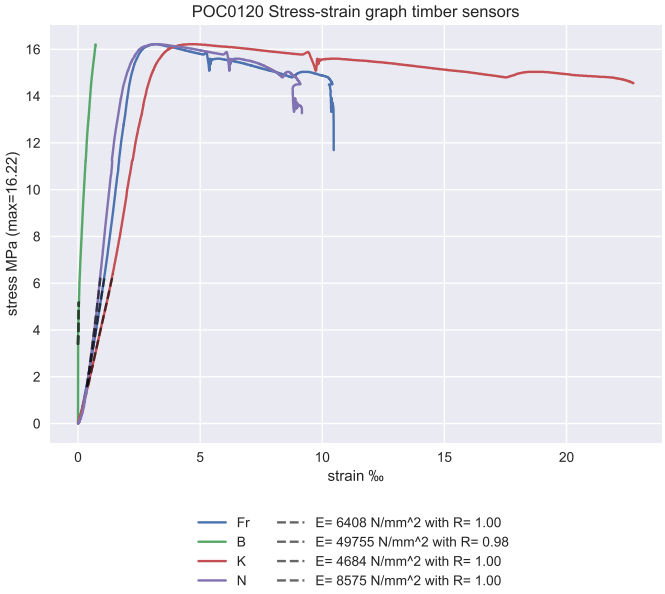


Figure B.56

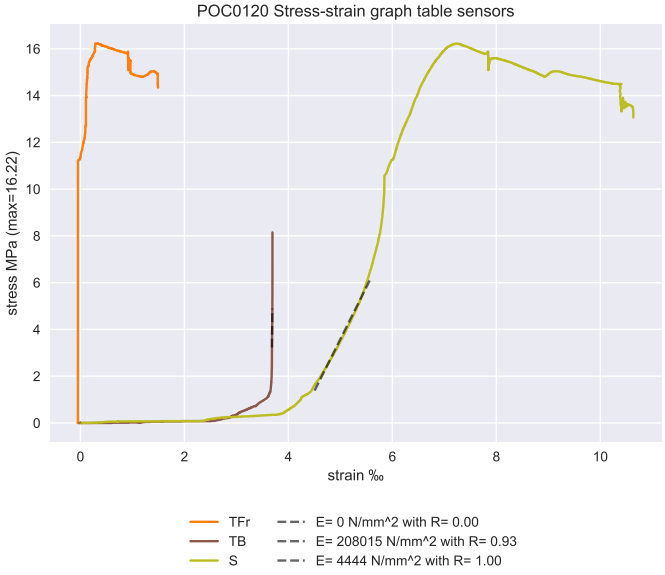


Figure B.57

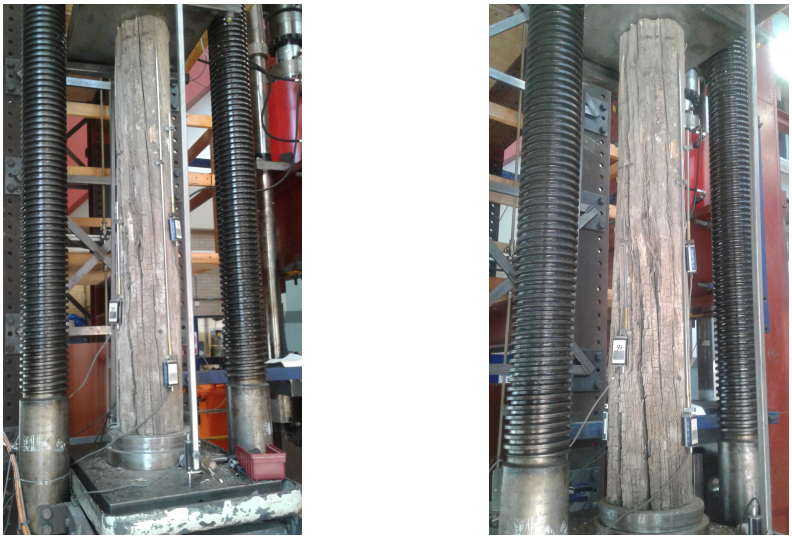

Figure B.58: Overview of the testpiece POC0120 before testing (left), and during plasticity (right).

Figure B.59: Close-ups of the failuring testpiece POC0120. Note the eroded top.

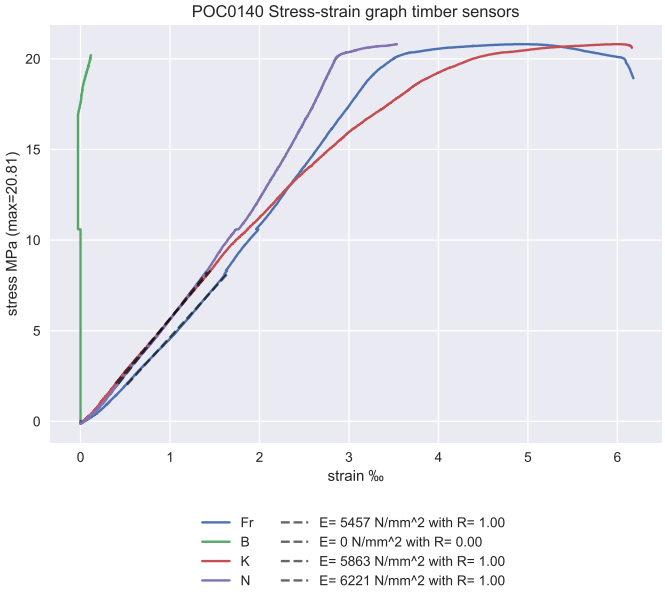


Figure B.60

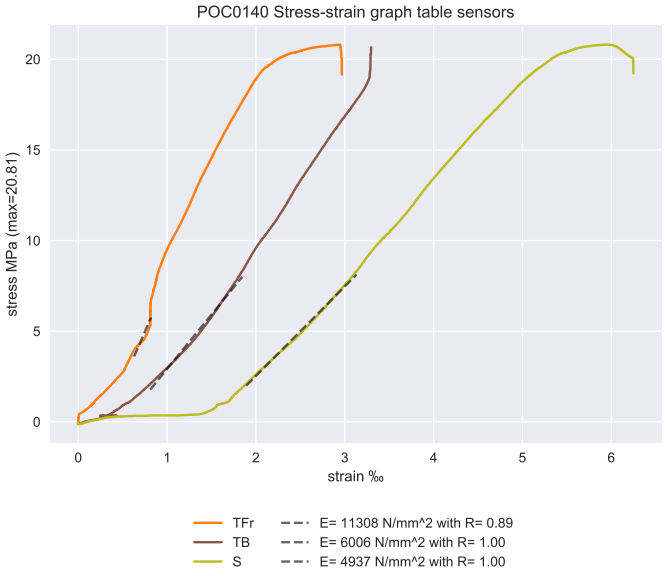


Figure B.61

Figure B.62: Overview of the testpiece POC0140 before testing (left), and during plasticity (right).

Figure B.63: Close-ups of the failuring testpiece POC0140.

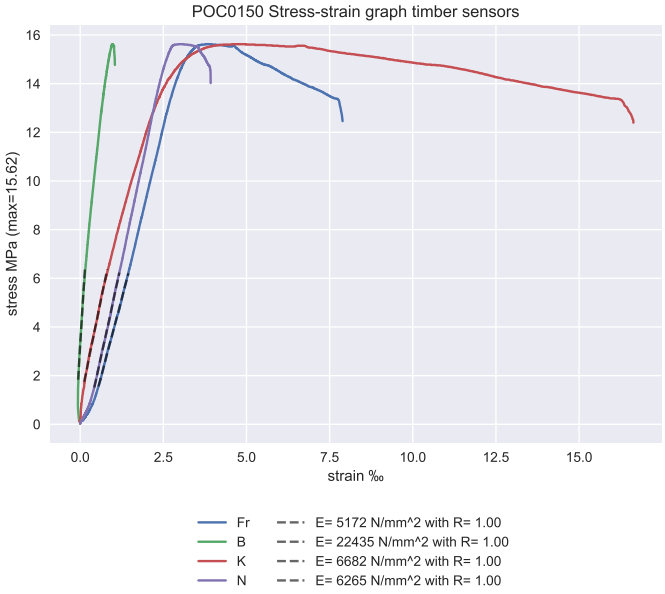


Figure B.64

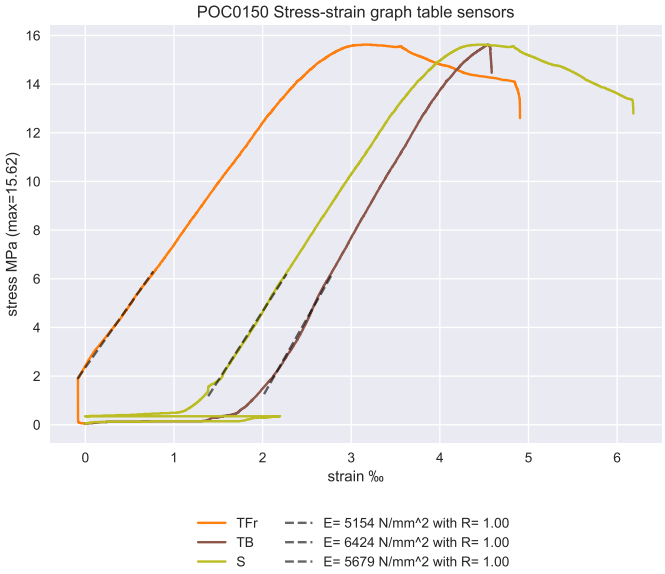


Figure B.65

Figure B.66: Overview of the testpiece POC0150 before testing.

Figure B.67: Close-ups of the failuring testpiece POC0150.

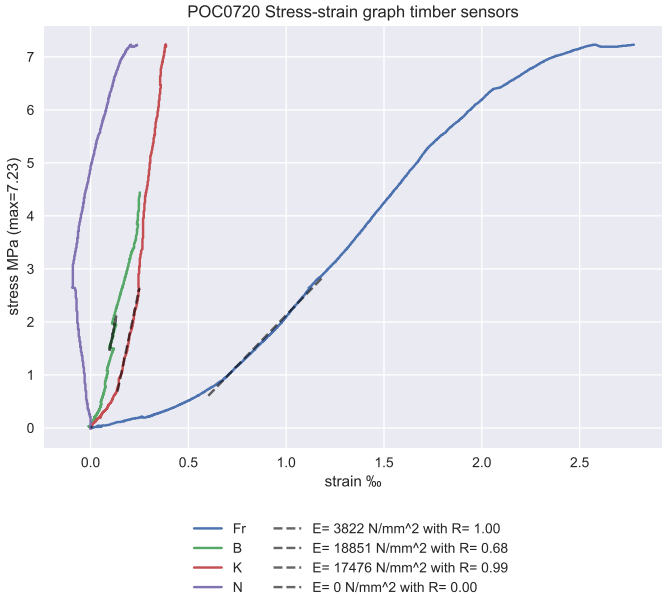


Figure B.68

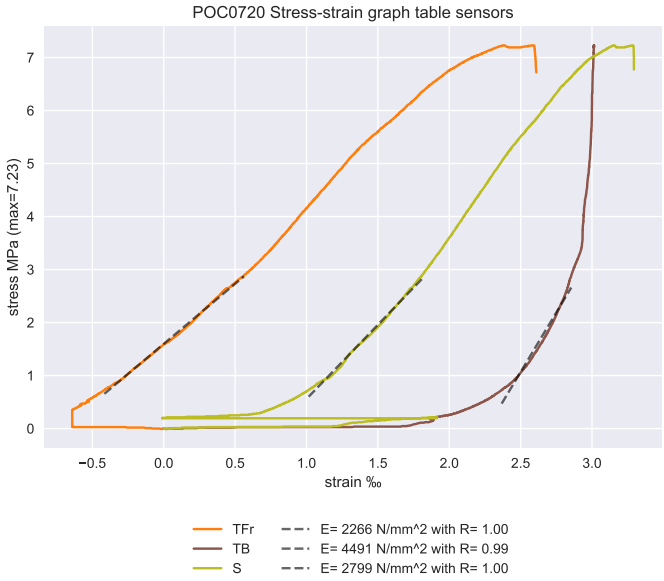


Figure B.69

There are no pictures available of pilepart POC0720 during testing. Due to its severely

damaged base (loose strands instead of a firm log), testing has been stopped before reaching ultimate stress.

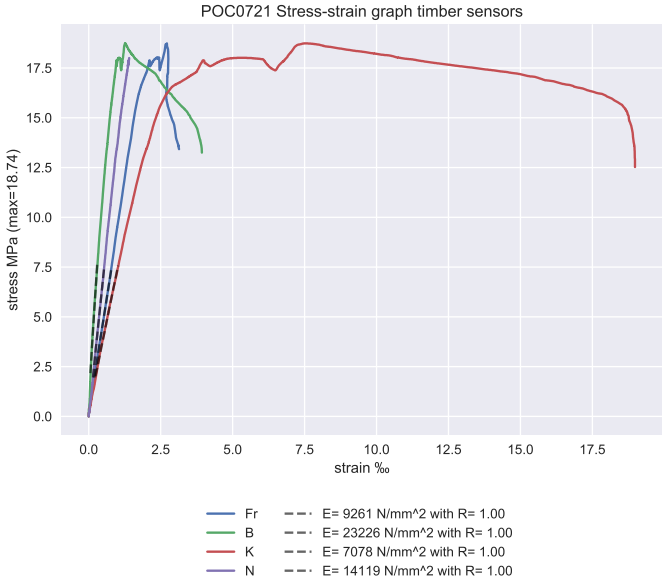


Figure B.70

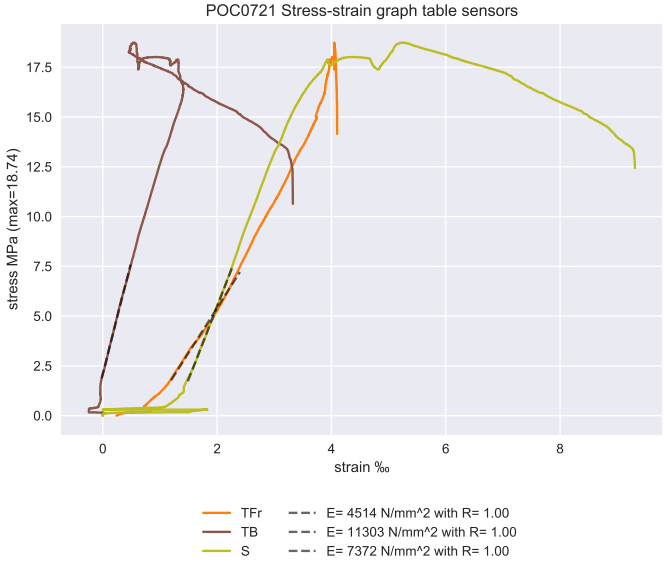


Figure B.71

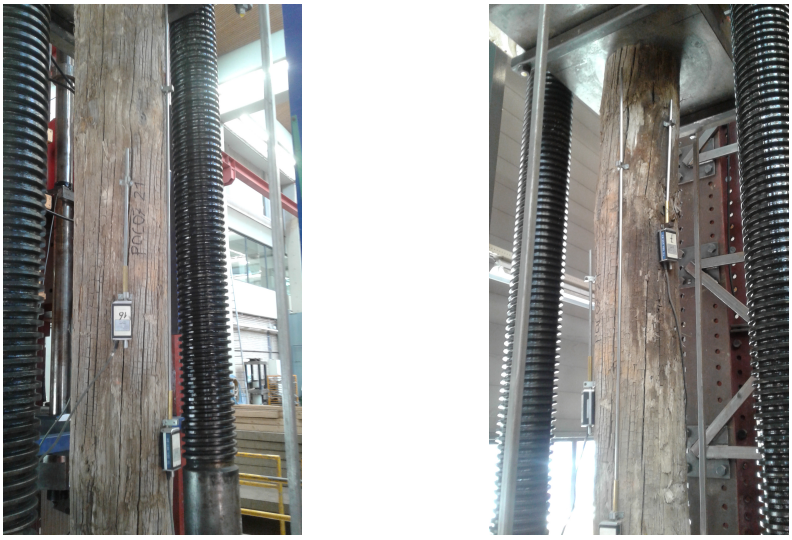

Figure B.72: Overview of the testpiece POC0721 before testing (left), and during plasticity (right).

Figure B.73: Close-ups of the failuring testpiece POC0721.

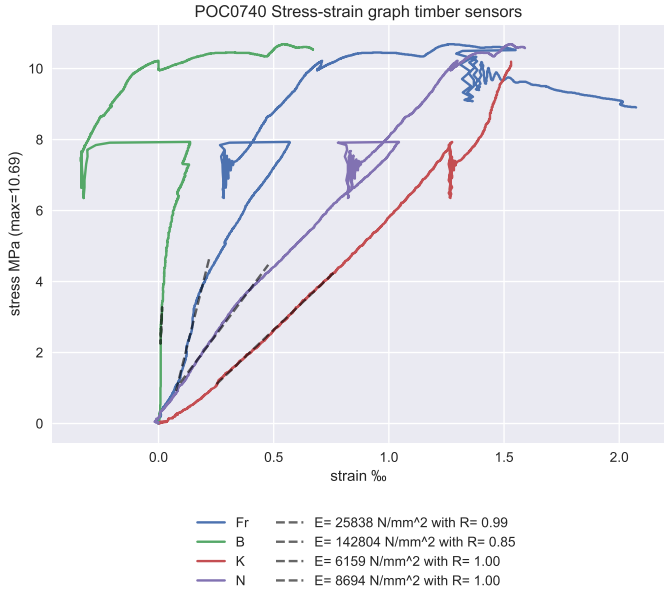


Figure B.74

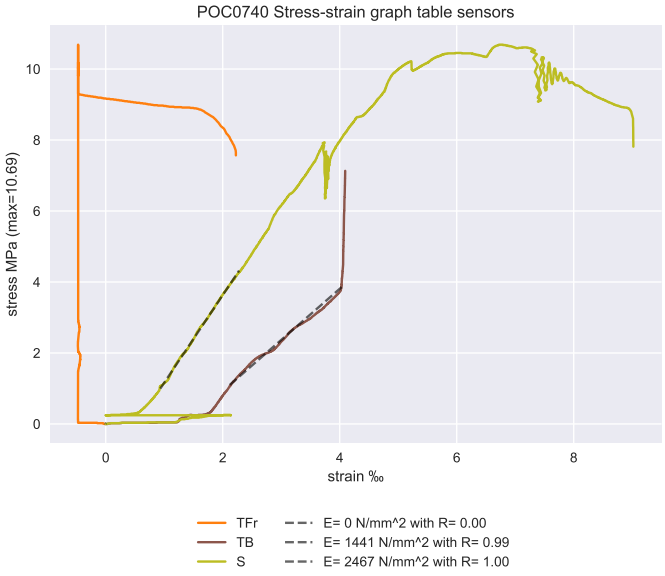


Figure B.75

Figure B.76: Overview of the testpiece POC0740 before testing.

Figure B.77: Close-ups of the failuring testpiece POC0740.

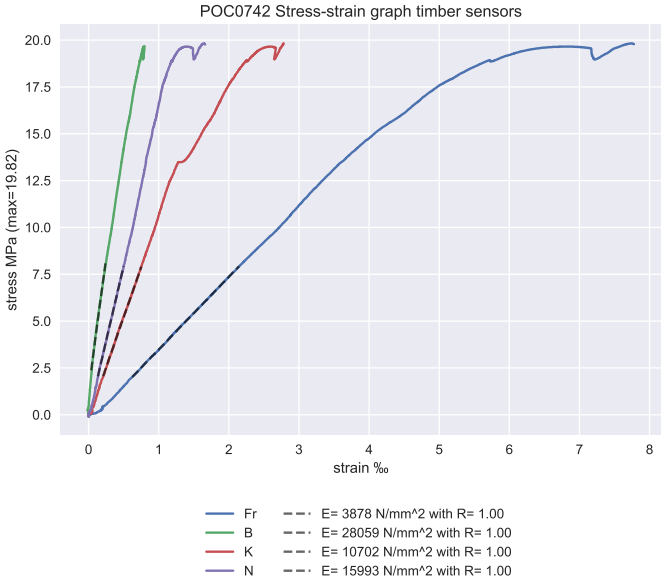


Figure B.78

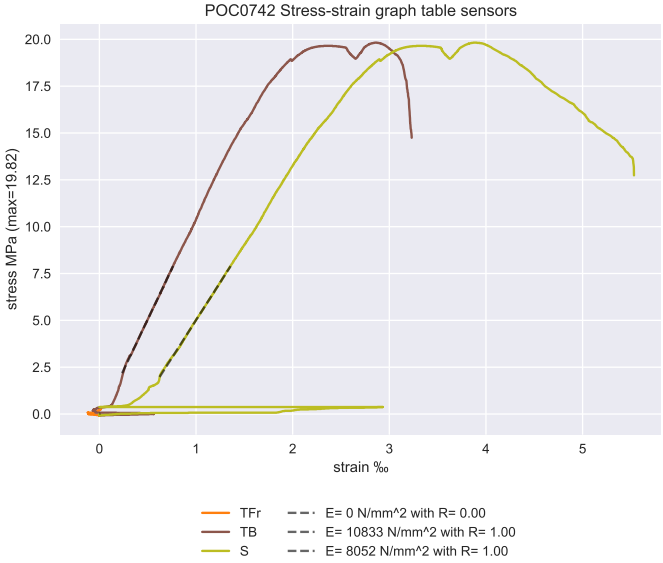


Figure B.79

Figure B.80: Overview of the testpiece POC0742 before testing.

Figure B.81: Close-ups of the failuring testpiece POC0742.

## B.7. CONCLUSION

### B.7.1. COMPRESSIVE STRENGTH

The compressive strength is measured by one LVDT only and the results are straight forward. The bar graph can be seen in figure B.82. Mean and standard deviation are 17.52 and 3.43 MPa respectively.

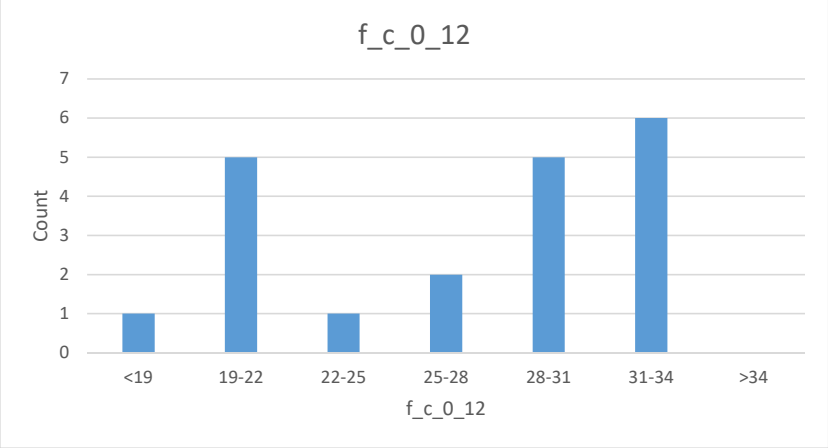


Figure B.82: Bar graph of the resulting compression forces after change to 12 % moisture content.

To find out the compressive strengths of the whole group of piles tested in the Charlois harbour, it is necessary to correlate it with the dynamic E modulus measurement. This has been done in figure B.83.

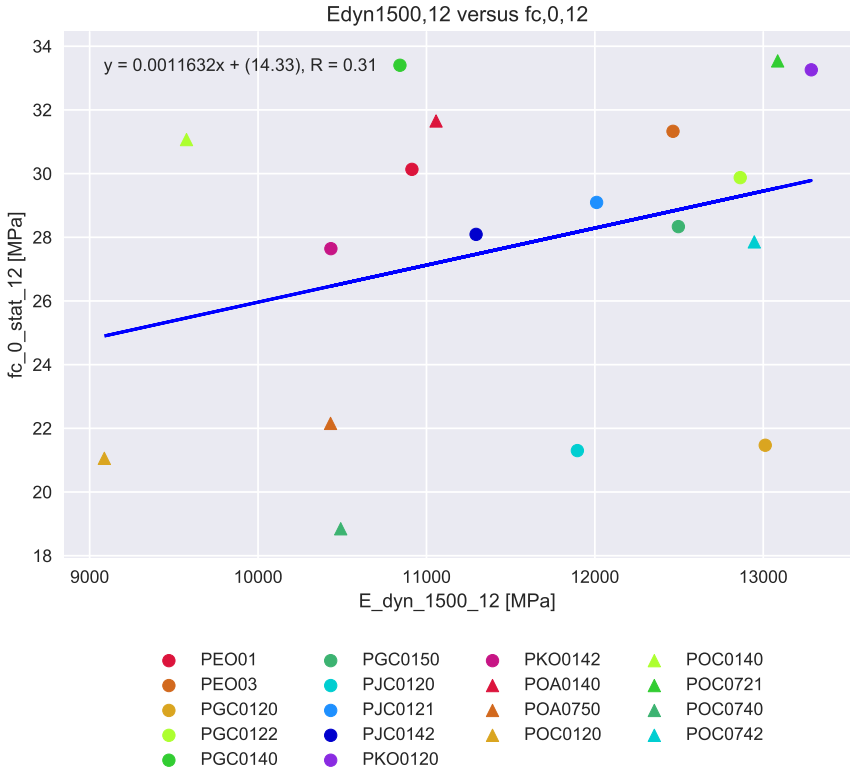


Figure B.83: Formula for obtaining fc0 out of Edyn. Two outliers from the Edyn1500 series have been excluded, as has the prematurely terminated fc,0 strength, resulting in 3 missing pile elements. The coefficient of correlation is 0.31.

### B.7.2. YOUNG'S MODULUS

As seen in table B.6, for the regular borders needed for determining an Young's modulus sensor 'S' gives the highest reliability. No outliers and no rejects are to be found here. The outcome is a rather low average of 6216 MPa under the average moisture content of 25 %.

As seen in table B.7, for the lower boundaries, the average signal of Fr and B gives the factor closest to 1.0 in comparison with $E_{0,dyn,1500}$, namely 1.08. The outcome of its average under the *regular* borders gives a modulus of 11975 under 25 % M.C..

To find what is to be expected, literature is consulted. We find the graph by Ravenshorst [69] in figure B.84 and the graph by Posta & al (Norway spruce) in figure B.85 [81].

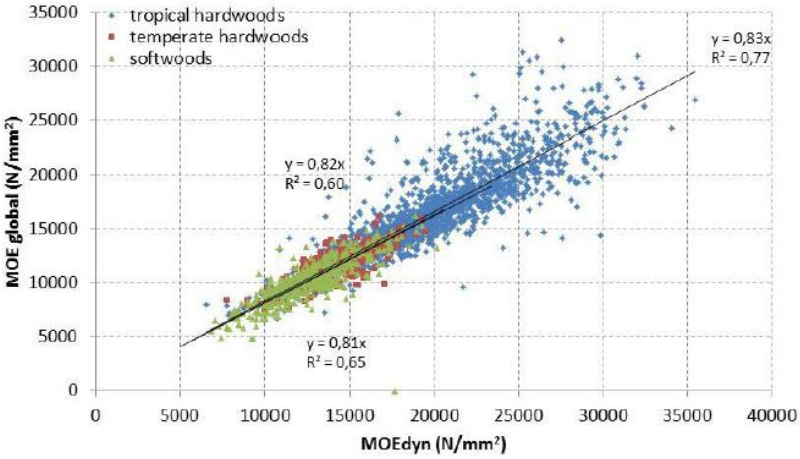


Figure B.84: Comparison of static to dynamic E moduli for different wood species, measurement by a Brookhuys timber grader [69].

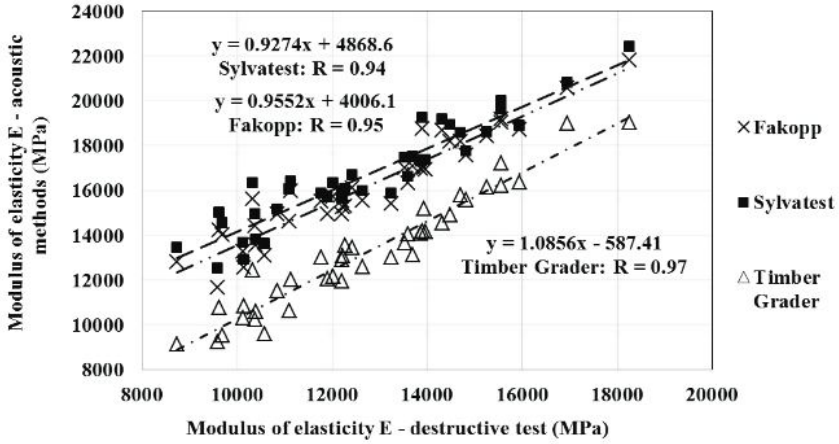


Figure B.85: Comparison of static to dynamic E moduli for Norwegian spruce, measurement by a timber grader [81].

The slightly lower outcome of the static moduli of the combined signal Fr and B is to be expected and probably indeed the best estimate after comparing the different outcomes. The final results for the E moduli can be seen in table B.8 and figures B.86 and B.87. The mean and standard deviations are 11570 and 2465 MPa respectively.

| Pilename | $E_{0,stat,\omega}$ (MPa) | R fit | Outlier? | M.C. (%) | $E_{0,stat,12}$ (MPa) |
|---|---|---|---|---|---|
| PEO01 | 12472 | 1.00 | | 22.6 | 11911 |
| PEO02 | 3428 | 1.00 | Outlier | 31.2 | |
| PEO03 | 13688 | 1.00 | | 24.1 | 13195 |
| PGC0120 | 11912 | 1.00 | | 25.6 | 11590 |
| PGC0122 | 12677 | 1.00 | | 24.8 | 12272 |
| PGC0140 | 15305 | 1.00 | | 27.3 | 15051 |
| PGC0150 | 9442 | 1.00 | | 27.2 | 9279 |
| PJC0120 | 7677 | 1.00 | | 25.3 | 7458 |
| PJC0121 | 12840 | 1.00 | | 22.2 | 12227 |
| PJC0142 | 14626 | 1.00 | | 22.9 | 13996 |
| PKO0120 | 15797 | 1.00 | | 24.4 | 15253 |
| PKO0142 | 11840 | 1.00 | | 23.1 | 11344 |
| POA0140 | 13872 | 1.00 | | 29.9 | 13865 |
| POA0750 | 12845 | 1.00 | | 22.7 | 12276 |
| POC0120 | 12903 | 1.00 | | 18.5 | 11997 |
| POC0140 | 10934 | 1.00 | | 23.7 | 10515 |
| POC0150 | 8451 | 1.00 | | 20.7 | 7970 |
| POC0720 | 6503 | 1.00 | | 28.8 | 6456 |
| POC0721 | 13320 | 1.00 | | 29.5 | 13280 |
| POC0740 | 51085 | 0.99 | Outlier | 29.1 | |
| POC0742 | 10426 | 1.00 | | 21.6 | 9889 |

Table B.8: Resulting static E moduli from the Fr/B sensors combined outcome.

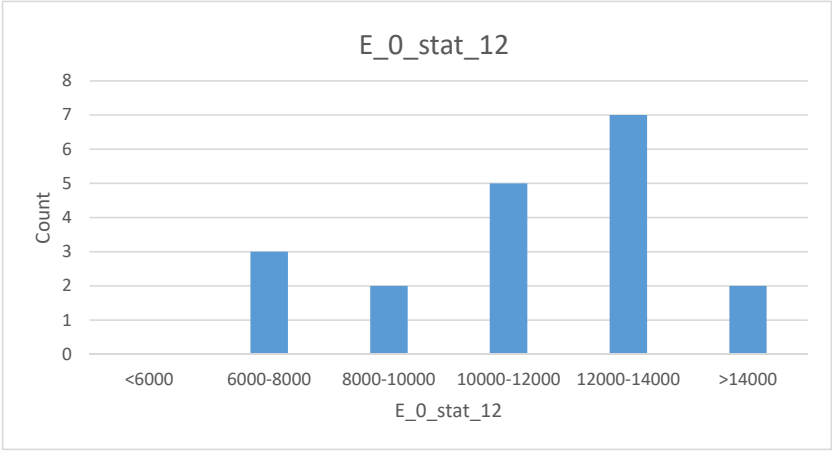


Figure B.86: Bar graph of the static E modulus results in MPa or N/mm$^2$.

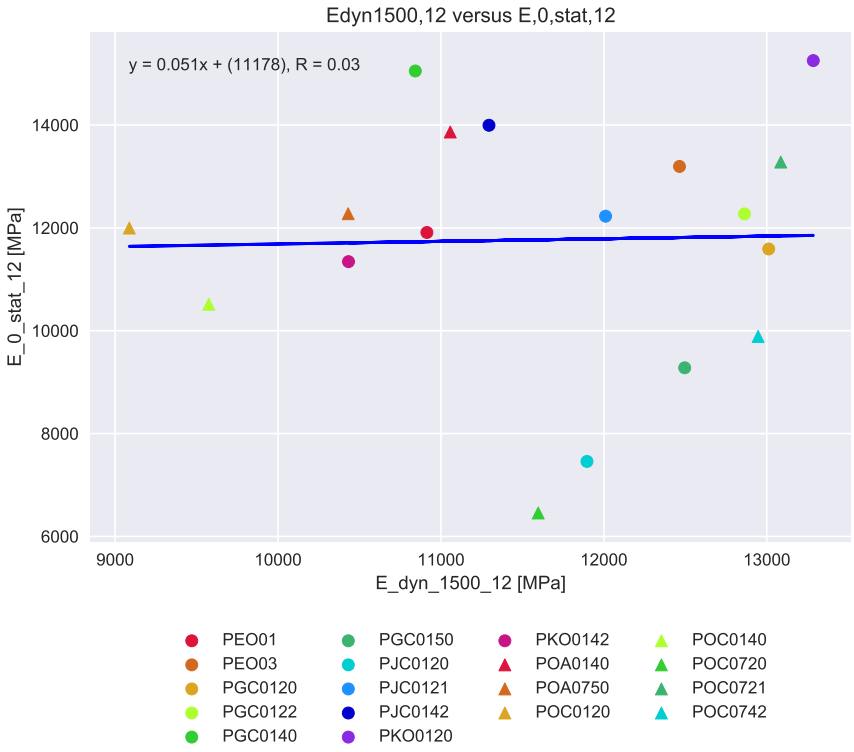


Figure B.87: Comparison of static to dynamic E moduli for the Fr/B signal, after conversion to 12% M.C.. All outliers and rejects are excluded. Note the low coefficient of correlation R = 0.03. The number of elements tested do not give a good base for the formulation of a formula.

### B.7.3. FAILURE

Failure of the pilepieces took place in several ways.

- Either by local buckling of a substantial piece of outer shell (e.g. PJC0120 or PKO0120);
- Crushing of the entire cross section - possibly a kink band formation as described by Aicher & al. [68] (e.g. PGC0122 or PJC0142);
- By formation of a plastic hinge and bending (PEO02).

The latter form should have been prevented, but this pilepiece was exceptionally thin and without adjusting the machine was most probably inevitable.

## B.8. DISCUSSION

### B.8.1. HANDLING THE MATERIAL

In hindsight, a different logistical approach to the sequence of handling the logs could have given higher certainty of the moisture content. As it happened now, first all the

down-sizing was made after which the piles were tested one by one. During this time (up to 10 days in the most extreme case) drying could occur, especially since the temperature outside rose up to 38$^{o}$C, influencing the inside lab temperatures and relative humidities.



### B.8.2. STRAIN MEASUREMENT BY DIFFERENT LVDTS

Very different output has been found for the different sensors (see B.88, left). Since the TB and TFr sensors are attached by magnets and show most irregular graphs, their output was expected to be the least consistent (high deviations). Some of their output numbers are also very extreme (see figure B.88, right). The Fr and S sensors give the most stable data resulting in similarly shaped curves when comparing tests with each other, while it seems a rule that sensor B measures a stiffer reaction than sensor Fr. From the visuals during the test, fracture often occurred at one spot. With 1 specimen being tested to larger strains (PEO02) a clear buckling with plastic hinge occurred. It is therefore suspected that bending does occur and could have an influence on the found E moduli of the differently placed sensors.

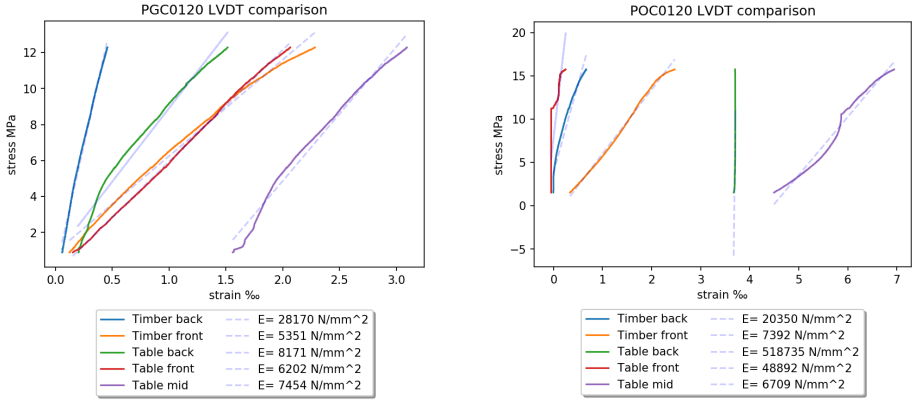


Figure B.88: Sensor output comparison. Typical difference (left) and extreme difference (right). The E moduli here have not been taken with the NEN 408 limits in mind and are purely shown for comparison.

Because the different LVDT outputs show such different numbers and such different graphs, it has been checked if difference in measurement show a rotation of the table. Rotations are computed according to figure B.89. The same pilepieces are shown again in figure B.90. It is clear that some sensors clearly give wrong output (TFr and TB for POC0120). However, the rotation output of the timber measurement (in purple) is also often in the other direction in comparison to the table. This is possible because of the hinge between the table and the specimen. Table rotation output differs between one sensor and the other as well.

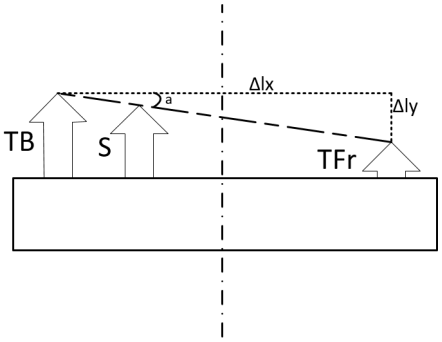


Figure B.89: Computing the angle $\alpha$ in degrees: $a = tan^{-1}(\frac{180}{\pi} * \frac{\Delta l_x}{\Delta l_y})$. Clockwise positive.

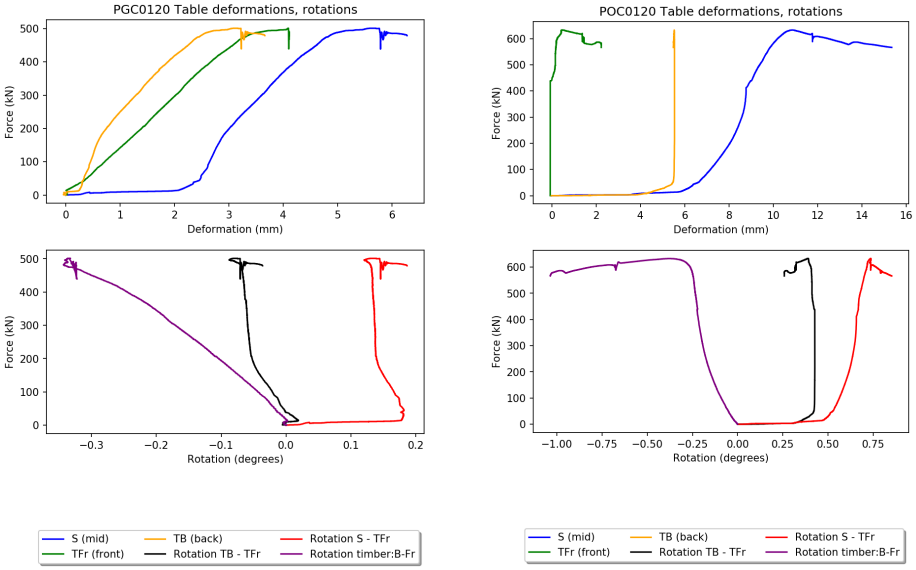


Figure B.90: Sensor output comparison. Typical difference (left) and extreme difference (right).

It seems bending could be present in the test specimens. It is the question if the tests are of a good base to determine compression strength or the E modulus using a formula that assumes pure compression. Comparison of the static with the dynamic Young's moduli have shown however that averaging the front and back sensors B and Fr gives an outcome that could be expected.

### B.8.3. PREMATURE STOP OF THE TEST

By fear of timber shrapnel flying through the lab the compression test was hold after a steep drop in the force-displacement curve that could be followed live on the screen.

This does mean a post-yield plateau is often not measured. This further measurements could also have given more insights whether one of the ends was not locked and thus whether bending was taking place in every pile.



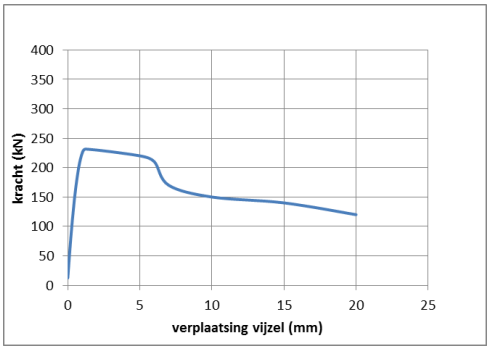


Figure B.91: A stress-strain graph with more elaborate yielding course. Original provided by the TU Delft [82].

### B.8.4. SPECIFIC SPECIMENS

Four tests are noticeable.

First of all, Specimen POC0120 was visually the only one where decay was present. A part of its shell seen in figure B.58 on the top was smoothed and on first sight looked mostly eroded. However, soft parts in the cross section were also noticed on touch. The ultimate stress is however only slightly below average.

Secondly, pilepart POC0720 ws so heavily damaged at its bottom, that the element was not tested until maximum stress (yielding). During the test the damages worsened too much. The entire bottom was reduced to loose strands from the beginning.

Thirdly, during the test of pilepart POC0740 the hinge of the machine shifted twice during testing. This was accompanied by a loud bang and can clearly be seen in the stress strain graphs (B.74).

Last but not least is PEO02, which started bending sidewards during failure (B.6).

# C

# COMPUTATIONAL MODEL IN- & OUTPUT

Appendix of Chapter 6

## C.1. AIM AND CONTENT

APPENDIX C Shows input and output of the computational model of wall section 4-1 in FEM software Plaxis 2D 2019. The aim is to provide the reader with information on the input: used materials, set ups and stages, as well as on the output: more detailed graphs on the governing spots in the timber structures.

## C.2. INPUT

### C.2.1. MATERIALS

The timber elements are prismatic. The E modulus is 11 324 MPa. Piles have a diameter of 0.22 and the capping beam is hxb = 0.2 x 0.3 m.

| Interface | $\phi$' reduction | $\phi$' soil | $\phi$' new | $\mu$,stat | c' reduction | c' soil | c' new |
|---|---|---|---|---|---|---|---|
| Wood90-Concrete | N/A | 35 | 35 | 0.7 | | 5530 | 0 |
| Wood0-Sandy Clay | 0.8 | 25 | 20 | 0.36 | 0.2 | 5 | 1 |
| Wood0-Clayie Silt | 0.8 | 32 | 25.6 | 0.35 | 0.2 | 1 | 0.2 |
| Wood90 -Sand,top | 0.8 | 33 | 26.4 | 0.5 | | 0.01 | |
| Steel-SandyClay | 0.65 | 25 | 16.3 | 0.29 | 0.35 | 5 | 1.75 |
| Steel-Sand,Middle | 0.76 | 34.6 | 26.3 | 0.49 | | 0.01 | |
| Steel-Sand,Top | 0.76 | 33 | 25 | 0.47 | | 0.01 | |
| Steel- Clayie Silt | 0.65 | 32 | 18.2 | 0.38 | 0.35 | 1 | 0.35 |
| Concrete-Sand,top | 0.88 | 33 | 29 | 0.55 | | 0.01 | |
| Concrete-Concrete | N/A | 35 | 36.9 | 0.75 | | 0.01 | |

Table C.1: Used Interface materials. The structure-structure interfaces (Concrete-Concrete, Timber-Concrete) are based on the static friction coefficients, not from friction angle reductions. Structure-structure interfaces have a residual interface strength of 0.99, making sliding without failure possible and an E modulus $10^3$ times lower than their original for the same reason (see chapter 6.3.1). The structure-sand interfaces have the soil's stiffness.

| Soil | $\gamma_{dry}$ | $\gamma_{sat}$ | $\phi'$ | $\phi'$ | c' | E50 | Eoed | Eur | m (power) | Rinter |
|---|---|---|---|---|---|---|---|---|---|---|
| Sand,Top | 18 | 19 | 33 | 3 | 0.01 | 25000 | 20000 | 100000 | 0.5 | 0.7* |
| Sand, Middle | 18 | 20 | 34.6 | 4,6 | 0.01 | 37500 | 30000 | 150000 | 0.5 | 1 |
| Sand,Bottom | 19 | 21 | 39.3 | 9.3 | 0.01 | 75700 | 60500 | 302500 | 0.5 | 1 |
| Gravel, river | 17 | 19 | 35 | 5 | 0.01 | 62500 | 50000 | 250000 | 0.5 | 1 |
| Clayie Silt | 20 | 20 | 32 | 0 | 1 | 5600 | 4500 | 22500 | 1 | 1 |
| Sandy Clay | 18 | 19 | 25 | 0 | 5 | 2500 | 2000 | 10000 | 1 | 1 |

Table C.2: Used soil characteristics for the hardening soil elements. * This is for the interface between concrete and sand.

| Plate | E [kN/m2] | EI eq. [kNm2] | EA eq. [kN] | w eq. [kN/m] | $\nu$ [-] |
|---|---|---|---|---|---|
| 1982 Larssen II neu | 2.10E8 | 10395 | 1092000 | 0.399 | 0.30 |
| 2003 PU8 | 2.10E8 | 24402 | 2436000 | 0.893 | 0.30 |
| 1922 Timber Sheetpile | 1.13E7 | 2447 | 1305000 | 1.650 | 0.35 |
| 1922 Timber Floor/Beam | 1.13E7 | 512 | 153529 | 0.194 | 0.35 |

Table C.3: Used plate materials.

| Embedded beam | Thickness [m] | Diameter [m] | $L_{spacing}$ [m] | E [kN/m2] | $\gamma$ [kN/m$\hat{3}$] |
|---|---|---|---|---|---|
| 2003 open tube | 0.0095 | 0.609 | 4.88 | 2.10E8 | 79 |
| 1922 Timber pile | N/A | 0.22 | 1.02 | 1.13E8 | 11 |
| 2003 groutbody | N/A | 0.25 | 4.88 | 2.40E8 | 25 |

Table C.4: Used embedded beams.

| Anchor rod | EA [kN] | $L_{spacing}$ [m] | $F_{t,max}$ [kN] | $F_{c,max}$ [kN] |
|---|---|---|---|---|
| 1982 | 333991 | 3,00 | 374 | 10 |
| 2003 | 599713 | 4,88 | 671 | 10 |

Table C.5: Used anchor rods.

### C.2.2. LOADS

| Load | Ek | Ed |
|---|---|---|
| Surcharge [kN] | 20 | 26.6* |
| Ship [Joule] | 1600 | 2072** |
| Ice [kN] | 100 | 115 |

Table C.6: Loads in the ULS models. *This load includes 0.2 m extra sand (geometrical uncertainty). **The characteristic value of the energy absorbed by the mooring pile has been deducted from the design load of the ship. The energy absorption by the quay translates in a 130 kN equivalent static load.



## C.3. OUTPUT

The output on the raking pile row and capping beam, on which the conclusions are based are presented below.

The capping beam has piles attached to it at x=0.3 (pilerow 1), x=1.2 (pilerow2), x=1.465 (raking pile row - or rather: transverse beam), x=2 .3 (pilerow 3), x=3.5 (pilerow 4), x=4 (sheeptile).

### C.3.1. PLAXIS GRAPHS

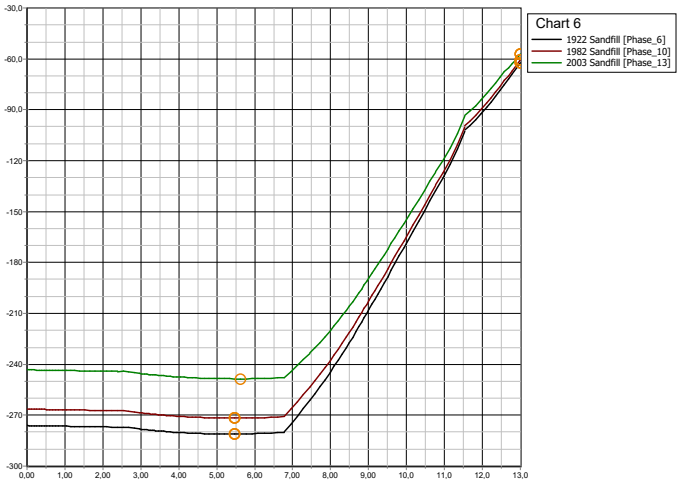


Figure C.1: Axial forces under SLS in pile row R

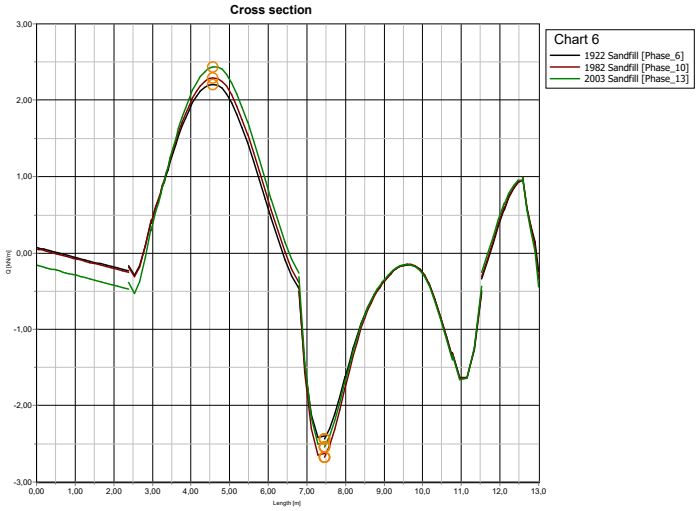


Figure C.2: Shear forces under SLS in pile row R

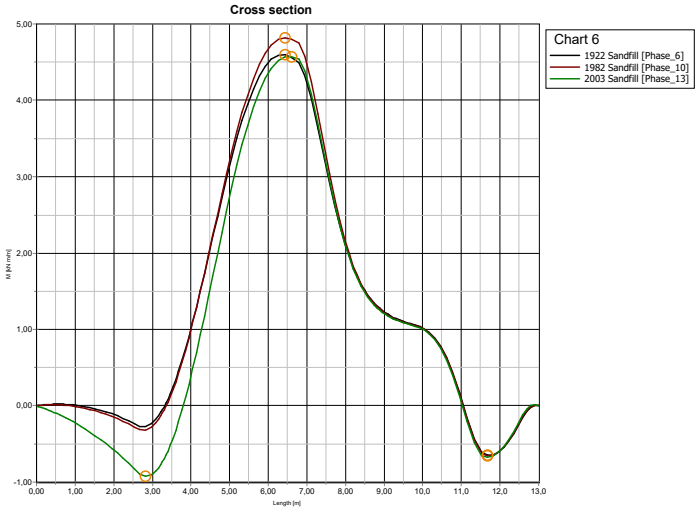


Figure C.3: Bending moments under SLS in pile row R

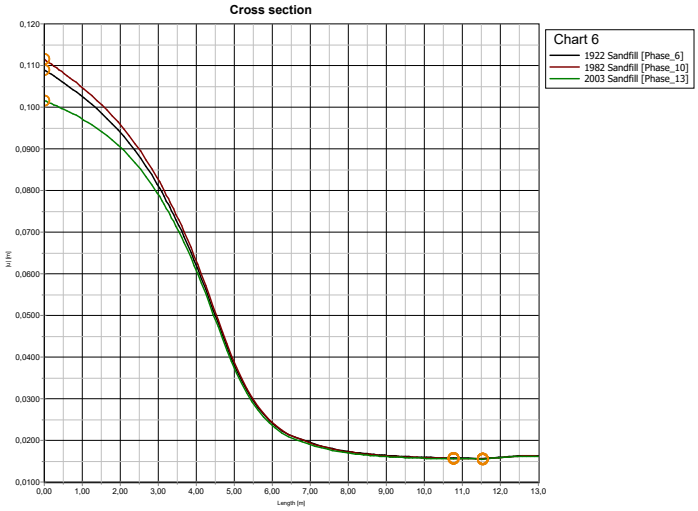


Figure C.4: Deflections under SLS in pile row R. Deflections under ULS in pile row R .The equivalent column length estimated of 3.23 m is not matching the displacement field.

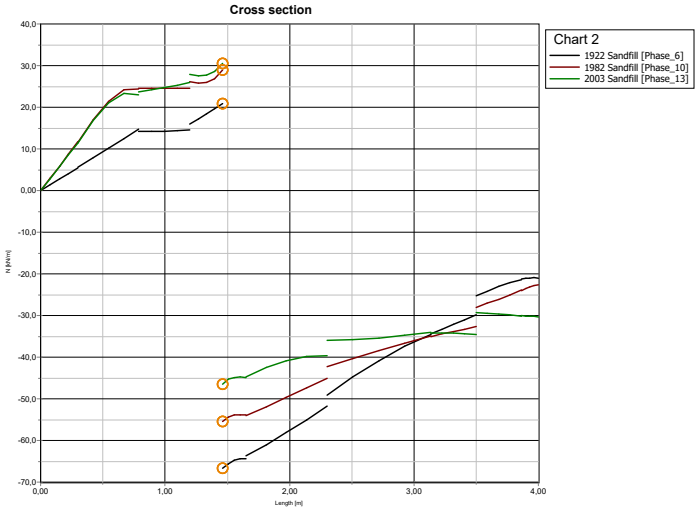


Figure C.5: Axial forces under SLS in the capping beam

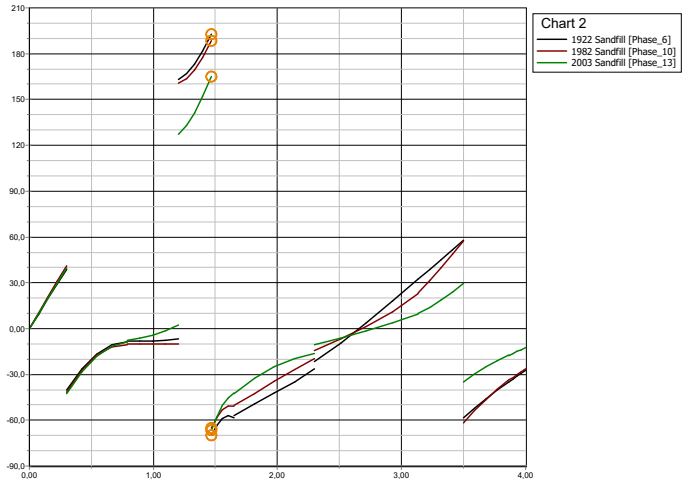


Figure C.6: Shear forces under SLS in the capping beam

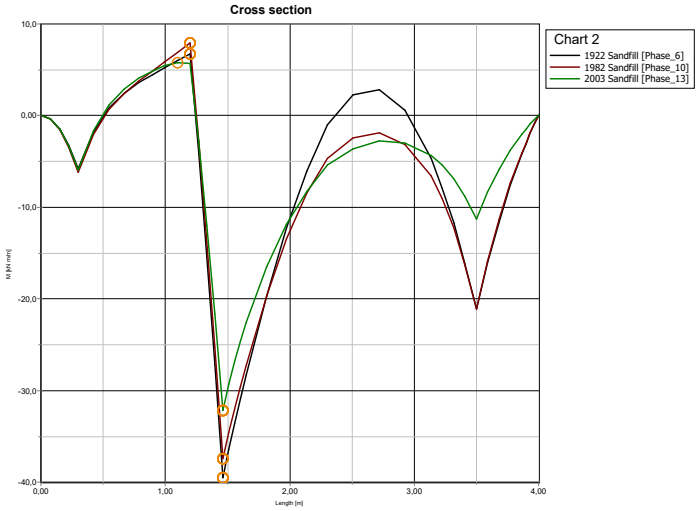


Figure C.7: Bending moments under SLS in the capping beam

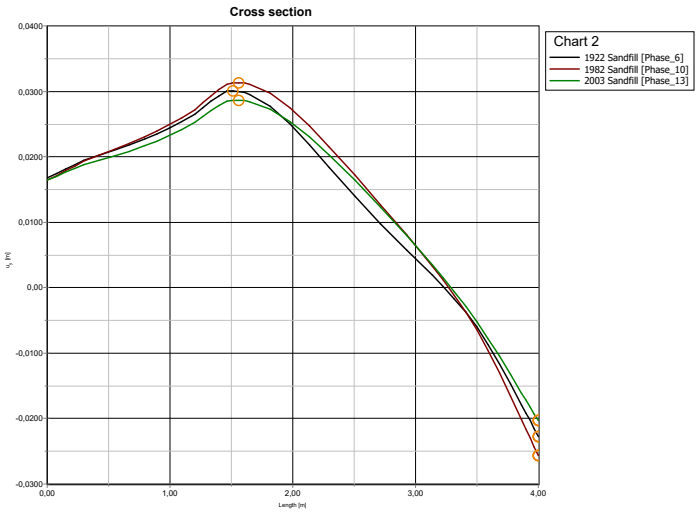


Figure C.8: Deformations under SLS in the capping beam

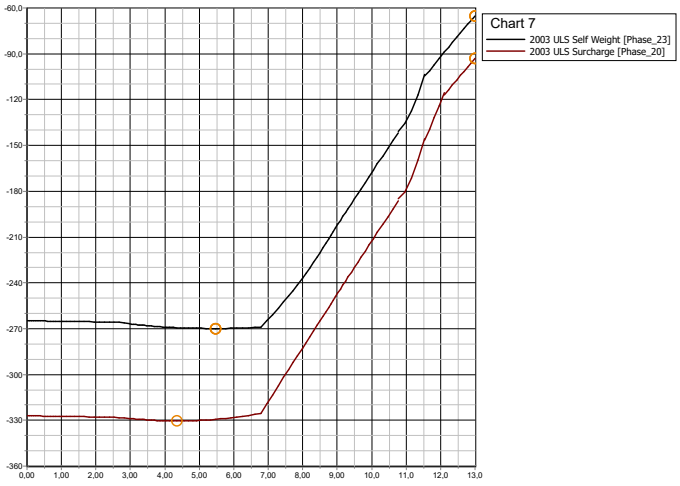


Figure C.9: Axial forces under ULS in pile row R

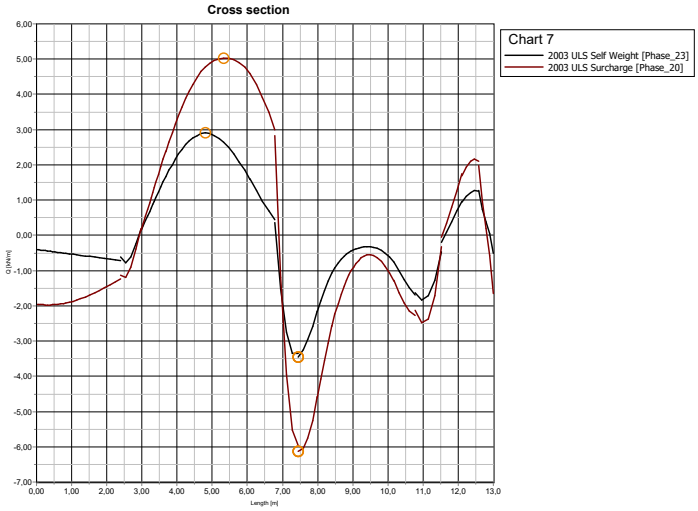


Figure C.10: Shear forces under ULS in pile row R

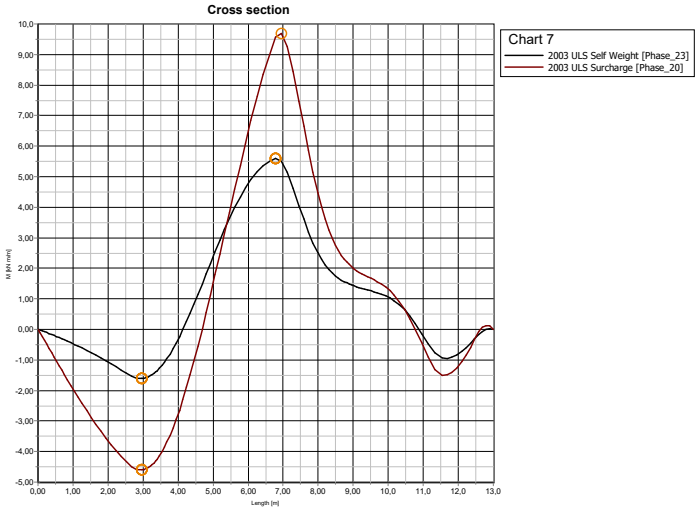


Figure C.11: Bending moments under ULS in pile row R

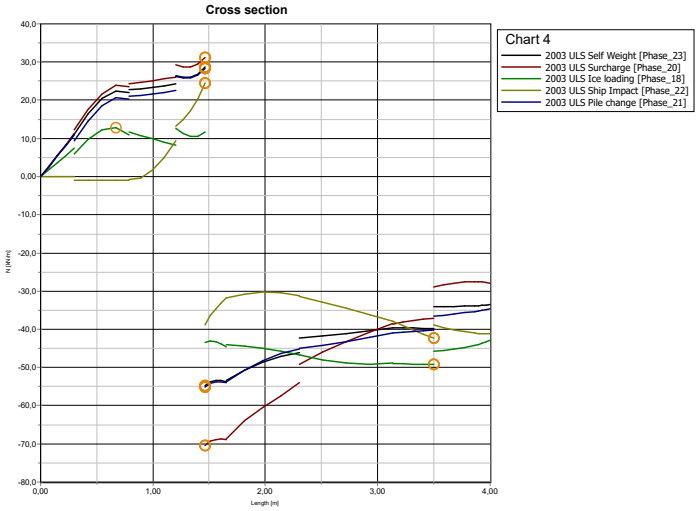


Figure C.12: Axial forces under ULS in the capping beam

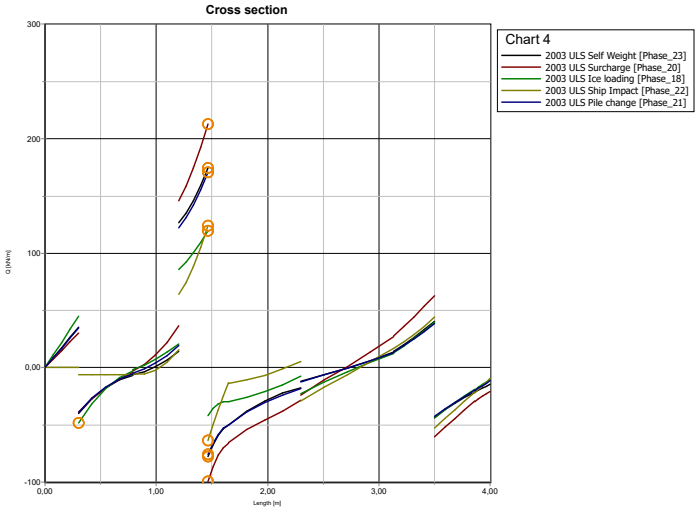


Figure C.13: Shear forces under ULS in the capping beam

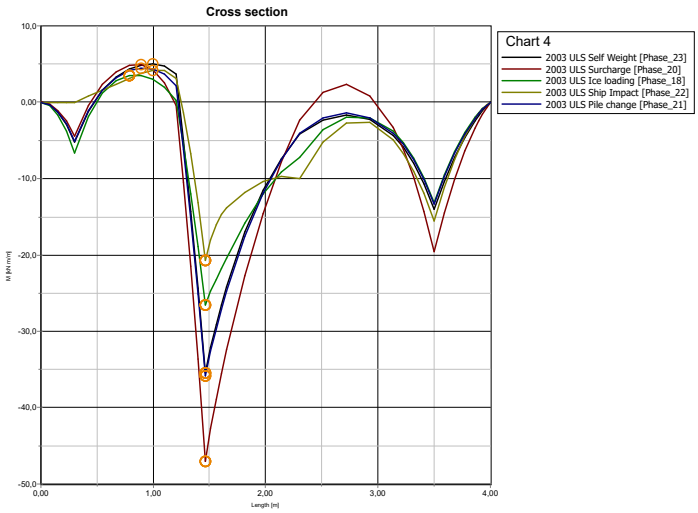


Figure C.14: Bending moments under ULS in the capping beam

SPOORWEGHAVEN XI^A

SPUIKANAAL-1876

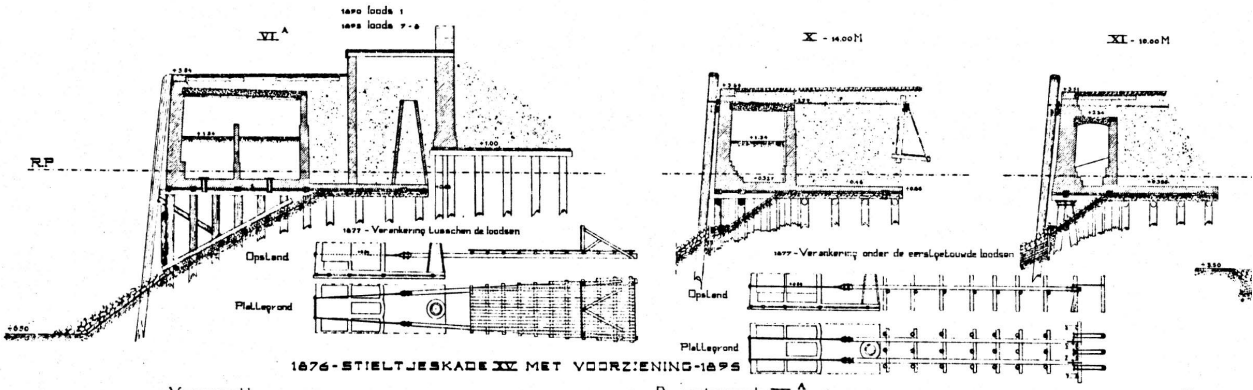


1876-STIELTJESKADE XX MET VOORZIENING-1895

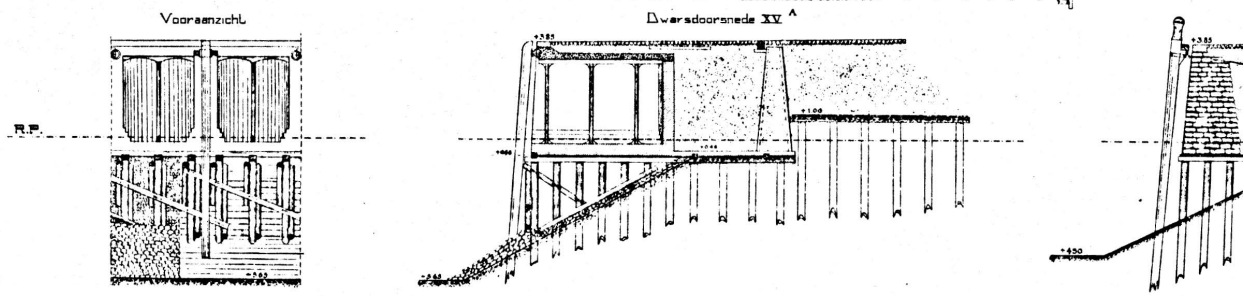


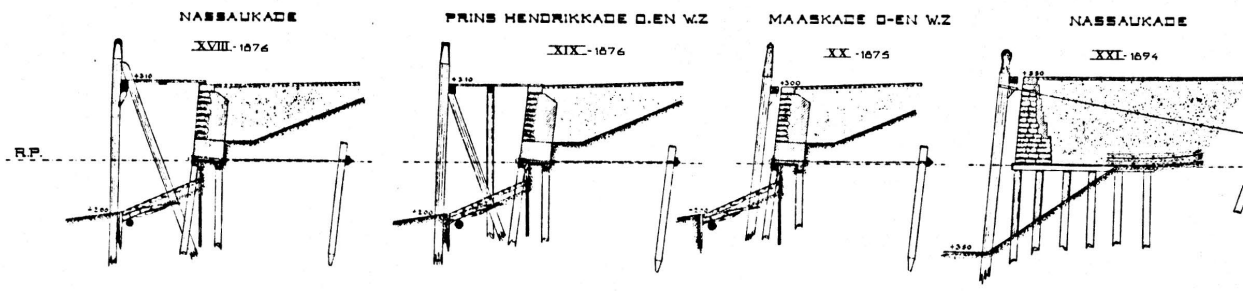


MAASKADE-WESTZIJDE-PRINSENHOOFD-PRINS-HENDRIKKADE-WESTZIJDE